Атомная энергия

Number 2, 1956

The Soviet Journal of

ATOMIC ENERGY

IN ENGLISH TRANSLATION

CONSULTANTS BUREAU, INC.

227 WEST 17TH STREET, NEW YORK 11, N. Y. ALGONQUIN 5-0713

ATOMNAYA ENERGIYA

Academy of Sciences of the USSR

Number 2, 1956

The Soviet Journal

of

ATOMIC ENERGY

IN ENGLISH TRANSLATION

CONSULTANTS BUREAU, INC.
227 West 17th Street
New York 11, N. Y.

Printed in the United States

Annual Subscription $ 75.00
Single Issue 20.00

THE STUDY OF THE PHYSICAL CHARACTERISTICS OF THE REACTOR OF THE ATOMIC ELECTRIC POWER STATION

A. K. Krasin, B. G. Dubovsky, E. Ya. Doilnitsyn, L. A. Matalin, E. I. Inyutin, A. V. Kamaev and M. N. Lantsov

In this article a description is given of experiments on the study of physical characteristics of the reactor of the atomic electric power station of the Academy of Sciences of the USSR. The data obtained may be utilized both in connection with the starting up and operation of other similar reactors, and also in the further improvement of the methods of engineering design calculations for the heterogeneous energy producing water-cooled reactors operating on thermal neutrons.

INTRODUCTION

The calculation of the physical parameters of the reactor of the atomic power station [1-3] was carried out by methods which had been earlier checked experimentally only on uranium-graphite lattices with a low content of water or steel. Therefore before the reactor was put into operation it was necessary to check the calculations on a reactor the construction of whose lattice cells would be close to that of the cells of the reactor of the atomic electric power station. For this purpose there was assembled and put into operation a graphite uranium physical reactor (GWP) which was constructed of square graphite bars of density 1.67 gm/cm^3. This reactor was in the form of a cylinder of 260 cm diameter and 190 cm in height. The lower reflector was 40 cm thick, while the upper reflector was 54 cm thick.

In the active zone and in the upper reflector there were 85 vertical openings of 44 mm diameter which formed the square reactor lattice with 140 mm pitch. In the side reflector there were horizontal openings into which neutron counters and ionization chambers were placed. Mixed oxide of uranium was used as the fissionable material (Uranium with a 10% content of U^{235} was used). The mixed oxide powder was placed in the circular gap between two stainless steel tubes (mark IX18N9T) of diameter 9×0.4 mm and 13.4×0.2 mm. The tubes were filled with the uranium oxide powder to a height of 960 mm. A heat generating element constructed in this manner contained on the average 214 g of powder. The amount of steel in a single element was ~152 grams. The inner tube was filled with water. Seven such uranium elements were assembled into a single unit which simulated the working channel of the reactor. The units were loaded into the vertical openings of the graphite pile. When the minimal critical loading with uranium was being determined, the remaining openings were filled with graphite plugs. Before the uranium units were loaded into the assembly, a neutron source of intensity $2 \cdot 10^6$ neutrons/sec was placed at the center of the graphite pile, then the whole registering apparatus was checked and the rate of counting of the counters and of the chambers was determined. As the uranium loading proceeded the rate of counting increased in all the registering equipment. If one graphically plots the variation of the reciprocal of the relative increase in number of counts ($^1/_N$) as a function of uranium loading, then the extrapolation of such a graph (the graph of reciprocal multiplication) until it intersects the horizontal axis will determine to a certain degree of accuracy the value of the critical loading. By successive extrapolation of graphs (obtained on the basis of data provided by different registering devices) one may determine in advance with sufficient accuracy the value of the critical loading of the reactor. The necessity for knowing the exact value of the critical mass (M_{cr}) is determined by the hazard which may arise as a result of an uncontrolled rapid increase in the power of such a reactor in the case of even a relatively small excess of reactivity.

It should be noted that starting with a loading of ~70% (estimated from early extrapolations) it is useful

to utilize not only the graphs of reciprocal multiplication, but also the so-called difference curve of reciprocal multiplication – the reciprocal value of the difference in the counting rate at a given loading and the counting rate at 70% loading $\frac{1}{N-N_{70}}$. Such a method for extrapolating the critical mass leads more smoothly to the actual value of the critical loading from the direction of smaller loadings which increases the safety of conducting the experiment. Figure 1 gives graphs of reciprocal multiplication plotted on the basis of readings of various registering devices. For purposes of comparison the difference curve is also plotted in the same figure.

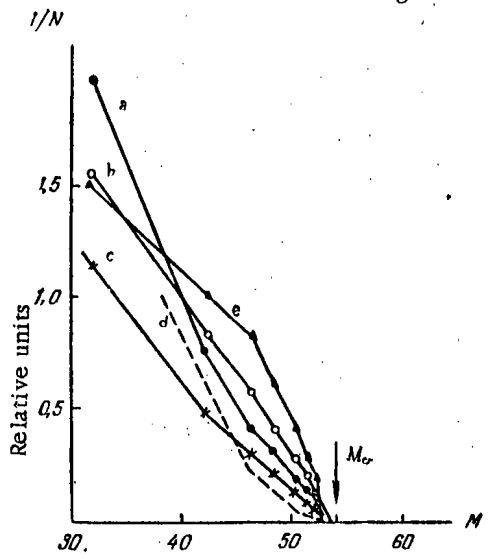

Figure 1. Curves of reciprocal multiplication. a) Counter No. 1 on the boundary between the active zone and the reflector; b) counter No. 2 on the boundary between the active zone and the reflector; c) ionization chamber on the boundary between the active zone and the reflector; d) counter No. 3 in paraffin at the outer wall of the reflector; e) difference curve.

The loading of the reactor proceeded from the center outwards toward the periphery. The reactor became critical when 54 units were loaded into it. When the openings in the reflector were filled with graphite plugs and uranium units were inserted into openings intended for safety rods and control rods, the minimum critical loading of the GWP reactor was determined, and turned out to be equal to 50 units or 6.3 kg of U^{235} which corresponds to an active zone radius of 60 cm.

The theoretical calculations which had been made by M. E. Minashin, Yu. A. Sergeev, V. Ya. Sviridenko, and G. Ya. Rumyantsev gave (within the limits of accuracy of the calculation) values of M_{cr} (5.35 - 7.40 kg of U^{235} or 42-58 units) which agreed well with the experimental data. On the same reactor a study was made of the effect of an annular layer of water (4 mm thick) on the compensating ability of a boron control rod (26 mm in diameter) of the reactor of the atomic electric power station. It was determined that a 4 mm layer of water around the rod decreases its compensating ability by 10%. Calculations carried out by D. F. Zaretsky indicated that a 15% decrease should be expected. The other experiments carried out on the reactor of the atomic electric station are described below.

Determination of the Critical Loading of the Reactor of the Atomic Electric Power Station

On the diagram of the lattice (Figure 2) is shown the placing of the start-up registering equipment used in the course of achieving the critical loading of the reactor. Three neutron proportional counters and three ionization chambers were placed in the vertical channels of the reactor. In view of the fact that equipment designed to control the power level of the reactor of the atomic electric power station under normal operating conditions does not have the sensitivity required to determine the degree of approach of the reactor to its critical condition, special radiotechnical equipment of high sensitivity was constructed. At the output of one of the circuits a dynamic speaker was placed which enabled one to determine changes in the neutron flux by a change in the frequency of clicks.

After the insertion into the center of the reactor of a neutron source of intensity $2 \cdot 10^6$ neutrons/sec, the loading of the reactor with working channels (WC) was begun. To decrease the loss of neutrons from the unloaded cells of the reactor graphite plugs were inserted into them. The curves of reciprocal multiplication were plotted from the readings of all the registering devices; in addition difference curves were also plotted. The working channels were loaded progressively from the center out toward the periphery. In the course of loading, measurements were made of the effectiveness of the action of manual control rods (MC) and of the safety rods (SR). After 60 working channels filled with water had been loaded, a self-sustaining chain reaction was achieved.

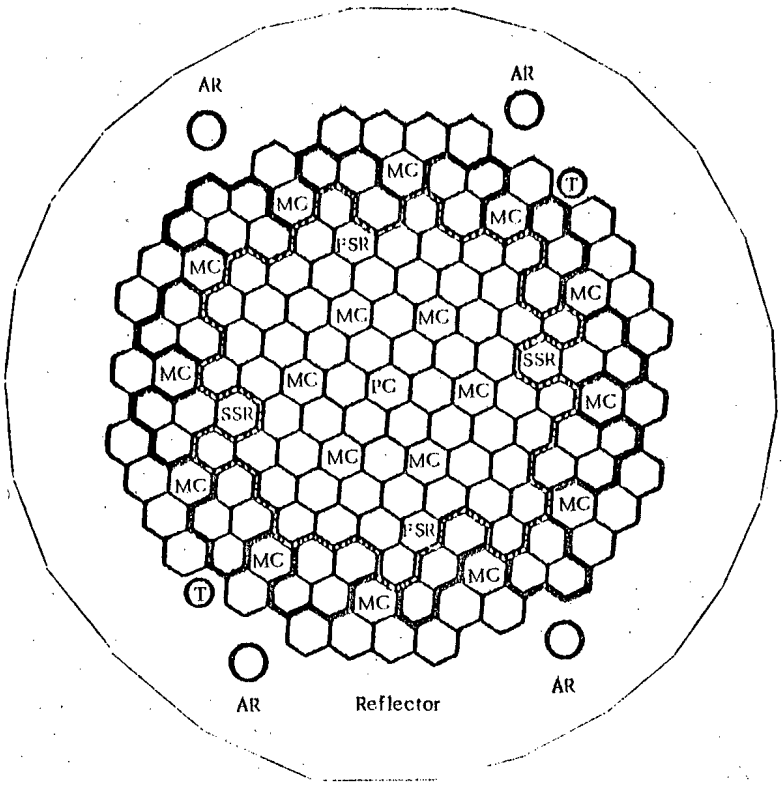

Figure 2. Diagram of the lattice of the reactor of the atomic electric power station. PC) cell of a physical experimental channel; MC) cell of a manual control rod; AC) cell of an automatic control rod; SSR) cell of a slow safety rod; FSR) cell of a fast safety rod; T) cell of a channel for continuous control of the temperature of the moderator ;) boundary of the critical loading of the reactor with water in the working channels;) boundary of the critical loading of the reactor without water in the working channels.

For practical design calculations of energy-producing reactors it is necessary to know the value of critical loading not only when water is present in the working channels, but also in its absence. An experiment made without water in the working channels showed that the critical condition in this case is attained when 101 working channels are loaded. In the diagram (Figure 2) the critical loadings are marked in both cases.

Calibration of the Boron Rods and the Determination of the Available Reserve Reactivity of the Atomic Power Station

The considerable excess of the technological loading of the reactor (128 WC) compared to the critical loading (60 WC) is due to the necessity of having a sufficient reserve of reactivity which is required to compensate for the burn-up of U^{235} in the course of operation during ~ 100 days at a power level of 30,000 kw, to compensate for the decrease of reactivity by the waste and poisoning uranium fission products and by the negative temperature effect.

When all the working channels were loaded the excess reactivity was compensated by the complete insertion of six boron rods of the inner circle, four symmetrically situated rods of the outer circle, and one automatic control rod. The eight manual control rods (MC) of the outer circle which remained not inserted, the two safety rods (SR) and the three automatic control rods (AC) formed the reserve for stopping the chain reaction in case of an unforeseen building up of the activity of the reactor.

The available reserve reactivity is one of the most important characteristics describing the state of operation of the reactor, and it is therefore necessary to control its magnitude continually. To determine the available reserve of reactivity (in relative units) a comparison was made of the effctiveness of the influence of various portions of the control rods and of the safety rods on the reactivity of the reactor. As a calibration unit of reactivity that reactivity was chosen which arises as a result of displacing a pair of auto-

matic control rods by 1 cm in the middle portion of the height of the active zone of the reactor. Because the influence of the rod on the reactivity is in this region directly proportional to its displacement, this unit is called a lineal centimeter. To convert lineal centimeters into absolute reactivity the time of doubling of the power level of the reactor was measured when a super-critical condition corresponding to 10, 20 and 30 lineal centimeters was produced. The time of doubling of the power level of a reactor determines the excess reactivity (ΔK); thus it was determined that in the initial stages of operation of the reactor of the atomic electric power station 10 lineal centimeters corresponded to $\Delta K = (4.5 \pm 0.2) \cdot 10^{-4}$.

The influence on the reactivity of the displacement of the rod under investigation depends significantly on the position of the other inserted rods, and therefore it is more useful to carry out, not an individual calibration of each rod, but rather the calibration of a group of similar rods after first having checked that they are identical by comparing them under similar conditions.

Within $\pm$ 10% accuracy the rods turned out to be identical in their effectiveness. After the rods were checked and found to be identical, they were calibrated. The rod being calibrated was set as zero (fully removed from the reactor). The reactor was compensated at a low power level in such a way that the automatic control rods would be inserted to 80 cm (to about the middle of the rod). The neighboring manual control rods (MC) of the outer ring were removed completely. The rod being studied was inserted to such a depth as to cause the automatic withdrawal of the AC rods through 10 lineal cm (from 80 cm to 70 cm). By means of withdrawing a rod far removed both from the rod under investigation and from the AC rods, the automatic control rods were returned to their initial position (80 cm). Then the next segment of the rod being studied was inserted in such a way as to again produce a withdrawal of the AC rods through 10 cm. etc., until the rod under investigation had been inserted completely. As a result of this the dependence of the effectiveness of the rod being studied on its depth of insertion was established.

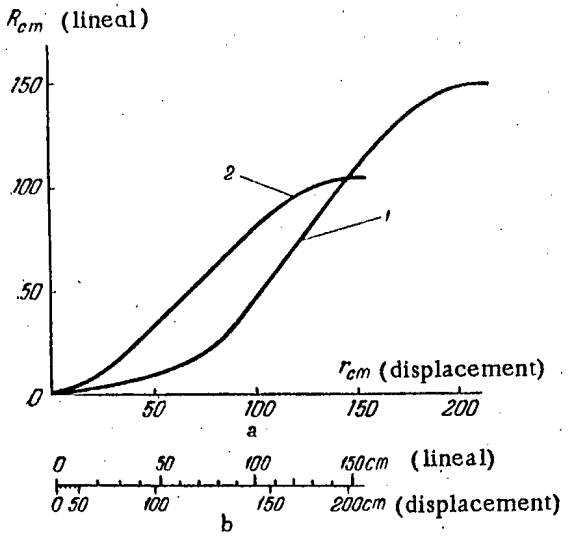

Figure 3. Calibration curves for automatic and manual control rods (a) and a nomogram for a manual control rod (b).
1) Automatic control rod; 2) manual control rod.

Figure 3 shows calibration curves for automatic and manual control rods and also an example is given of the method of construction of a calibration nomogram. The linearity of the graph in the region of medium depth of insertion of the rods confirms the appropriateness of our choice of the relative unit for measurement of reactivity. The depth of insertion of the rod into the reactor is expressed in terms of displacement cm as distinct from lineal cm.

In the region of the lineal portion of the graphs the rod has the greatest effect on the reactivity. The fact that the linear portions of the graphs for the AC and the MC rods do not coincide is explained by the fact that at zero position the lower end of the MC rod is 60 cm above the active zone, while the lower end of the AC rod in its zero position is level with the upper boundary of the active zone.

The effectiveness of an absorbing rod depends significantly on the position of the neighboring rods. For example, the effectiveness of the action of an MC rod of the outer ring is decreased from 150 lineal cm in the case of removal of neighboring rods to 120 and 90 lineal cm in the case of insertion of one or two neighboring rods respectively. The results of the determination of the effectiveness of the action of absorbing rods are given in Table 1.

From Table 1 it follows that the total available reserve reactivity in the initial stages of operation is $\Delta K = 0.11 \pm 0.005$. The error in the determination of the value of ΔK is made up of errors in the determination of the identical nature of the rods, of error in the determination of the "value" of 10 lineal cm. ($\Delta K = 4.5 \cdot 10^{-4}$) and of error introduced by the possible small fluctuations in the reactivity of the reactor during measurements.

TABLE 1

Type of rod	One MC rod of the inner circle	One MC rod of the outer circle	Two SR rods	Two AC rods
Effectiveness of rods in ΔK . .	0.013 ± 0.001	0.007 ± 0.001	0.018 ± 0.002	0.0054 ± 0.001

For a supercritical state of the reactor not only is the effectiveness of SR rods important, but also the speed with which they can be introduced into the active zone. This is particularly important in the case of a rapid increase in reactivity caused by the rupture of the thin-walled tubes which are under high water pressure. To investigate the operating time of the safety rods a study was made of the nature of the falling off of the power level with time as a result of an emergency shut-down of the reactor. The study was conducted by means of recording oscillograms with the aid of an ionization chamber and an oscillograph. The ionization chamber with boron-coated internal electrodes was placed into the neutron beam emerging from the reactor and was well shielded against γ-rays by a layer of lead 250 mm thick. The oscillogram showing the falling off of the power level (Figure 4) after prolonged operation of the reactor at a power level of 22,500 kw shows that during approximately 1 second the power level of the reactor falls to approximately 50%. In the case of the reactor operating at a low power level (0.01%) this time decreases to 0.5 seconds. The apparent decrease in the effectiveness of the action of the safety rods in the former case is related to the increase of the reactor reactivity at the time of release of rods due to the cooling down of the uranium and the water.

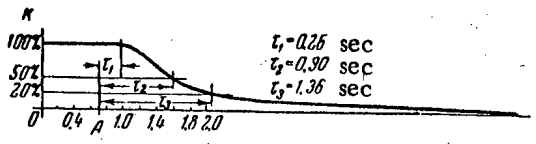

Figure 4. Oscillogram showing the falling off of the power level.
A) The instant at which the button releasing the safety rods is pressed.

The Influence of Water on the Reactor Reactivity

As has been pointed out already, the critical loading of the reactor in the case that the working channels are filled with water is considerably smaller than in the case of the absence of water (60 and 101 working channels respectively). This demonstrates the considerable positive influence of the water on the reactor reactivity which had been predicted by means of calculations [3]. As a result of this it became necessary to study the possible consequences of water entering the graphite moderator. The investigation of the influence of water on the reactivity was carried out by means of measuring the time required for the doubling of the power level of the reactor, and consequently of ΔK as the amount of water in the reactor was varied. If a column of water in a tube (62 mm in diameter) is introduced into the central cell of the reactor its reactivity is decreased by an amount $\Delta K = -(18 \pm 2)\ 10^{-4}$. The introduction of thin cylindrical layers of water (4 mm thick) into four safety rod channels slightly increased the reactivity by $\Delta K = +0.5\ 10^{-4}$.

To obtain data required for an estimate of the increase of reactivity in the case of complete flooding of the moderator an experimental simulating channel (SC) was used with an increased water content. One cm. of height of a standard working channel contains 3.6 cm^3 of water, in the case of a complete flooding of the reactor 1 cm of height of a cell could contain 6.6 cm^3 of water, while 1 cm of height of a simulating channel can hold 8.6 cm^3 of water, which enabled one to estimate the increase in the reactivity of the reactor in the most unfavorable case when all of the "accidental" water is concentrated close to the uranium.

A comparison of the effectiveness of a working channel (with the normal amount of water) and a simulating channel with an "accidental" amount of water was made in the various cells of the reactor with 101 working channels being loaded and for the two cases: without and with water.

In the first case the addition of water had a greater effect on the reactivity than in the second case. As the distance from the center increased, the effect of the water decreased to zero and even became negative.

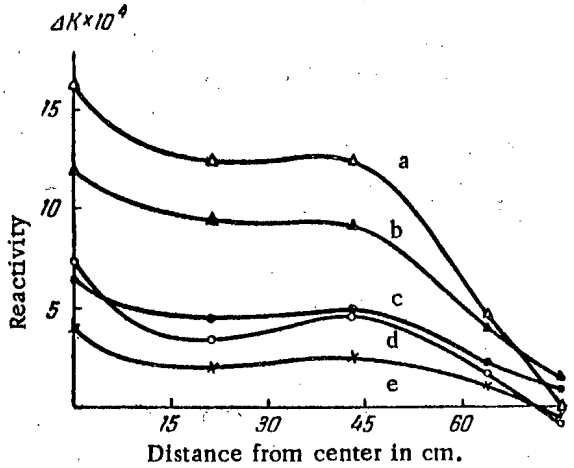

Figure 5. Curves showing effect on reactivity. a) One SC (100 WC without water); b) one WC with water (100 WC without water); c) one WC with water (100 WC with water); d) one SC (100 WC with water); e) recalculation of the effect of SC in one cell (the case of accidental flooding of the reactor).

The accuracy of the compensation of reactivity in these experiments was $\Delta K = \pm 3 \cdot 10^{-5}$. Figure 5 shows the results of these measurements. In order to obtain the increment in the reactivity obtained as a result of replacing a working channel without water by a simulating channel the ordinates of the corresponding graphs should be added.

It is interesting to note the positive essentially heterogeneous effect of water situated close to the uranium. Comparison of curves a and d and also of b and c permits one to draw the conclusion that in the case of flooding of the moderator of the reactor there will be a decrease in the effect of the excess water in the cells of the reactor in comparison with that described by case d. In the first approximation one may assume that the ordinates of the curve d will be diminished in the same ratio as that of the ordinates of curves c and b. The curve e of this figure obtained as a result of such a recalculation characterizes the possible effect of the water on the reactivity of the reactor in the case of the moderator being flooded.

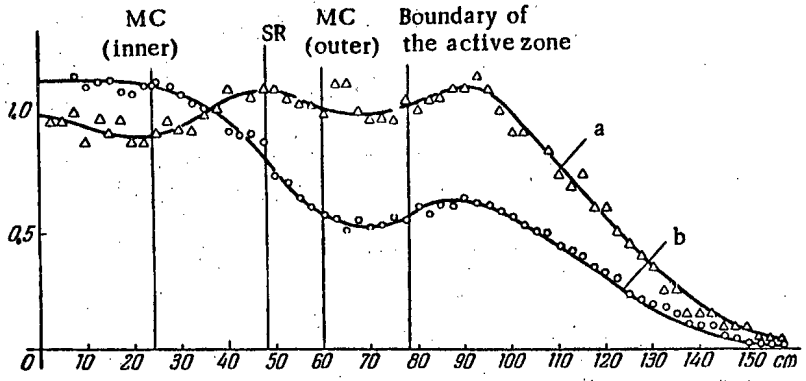

Figure 6. Thermal neutron density distribution along the reactor radius. a) Measured when six inner and three outer manual control rods are fully inserted; b) measured when one inner and twelve outer manual control rods are fully inserted.

Using this curve and knowing the number of working channels at each radius one may estimate the probable total increase in reactivity under accidental flooding which turned out to be $\Delta K = 0.016$. Calculation on the basis of curve d of the excess reactivity under accidental flooding of the moderator gives a maximal estimate which is equal to $\Delta K_{max} = 0.030$. It may seem from Table 1 that the safety control rods and the reserve control rods can more than compensate this increase in reactivity.

Measurement of the Probability of Resonance Neutron Capture.

As is well known, the curve for the cross-section for absorption of neutrons by U^{238} has sharp resonance peaks in the epithermal region of neutron energies. An exact knowledge of the probability of resonance capture of neutrons ($1 - \varphi$) is needed for the proper design of a reactor.

The measurements were carried out using the methods described in reference [4].

As a result of ten series of measurements the average value

$$\varphi = 0.906 \pm 0.015$$

was obtained.

The indicated error in the determination of φ was principally determined by our inaccurate knowledge of the constants ordinarily used for reactor design calculation.

A Study of the Parameters of the Neutron Distribution

The thermal neutron density distribution was studied by means of the activation of thin gold and copper foils placed into horizontal and vertical experimental channels in the reactor with a subsequent measurement of their β activity. The activation was carried out with a cadmium filter and without it. The results of these measurements are shown in Figure 6. From the curves it may be seen that the neutron density is lowered at the absorber positions. As a result of analysis of such curves, the optimal depth of insertion of the absorbing rods was chosen for various regimes of reactor operation.

For the measurement of the radial distribution of neutrons of intermediate energies the following indicators were used: indium, gold, cobalt, and manganese which show resonance neutron capture at energies of 1.45, 4.91, 130 and 346 ev respectively. The weight of these indicators did not exceed 3 mg so that the introduction of resonance neutron absorbers did not lead to a distortion of the resonance neutron distribution. Figure 7 shows the results of measurements with gold and manganese indicators. Analogous results of measurements with indium and cobalt indicators are not shown here. As should be expected the decrease in the neutron density in the region of operation of MC rods is more noticeable in the case of measurements made with gold and indium indicators.

Since the U^{235} concentration is very high in the reactor of the atomic electric power station and the quantities of water and of iron are also high it was necessary to study the spectrum of thermal neutrons. The spectrum was studied by means of a mechanical neutron selector in a vertical neutron beam emerging from the center of the reactor operating at a power level of 1500 kw at which the moderator temperature was equal to 420°K. The velocity distribution of thermal neutrons obtained in this manner is shown in Figure 8. For comparison (dotted curve) the Maxwellian distribution of neutrons (the one most nearly corresponding to the given spectrum) is given corresponding to a temperature of 500°K. From Figure 8 it may be seen that

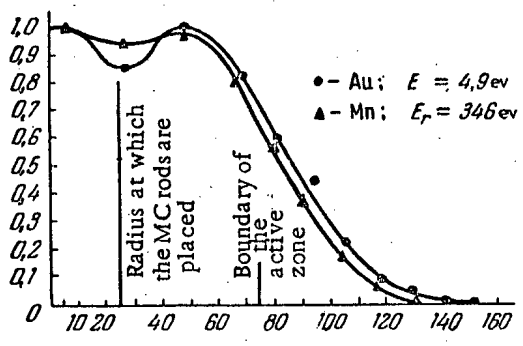

Figure 7. Radial density distribution of resonance neutrons in the reactor.

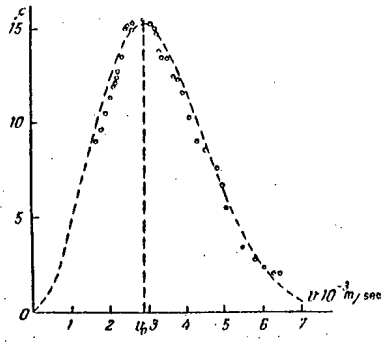

Figure 8. Spectrum of thermal neutrons in the beam.

the temperature of the neutron gas is slightly above 500°K. The small difference between the experimental and the calculated curves is related to the preferential absorption of neutrons by uranium and by iron in the soft portion of the spectrum. It is possible that there is a small increase in the effective temperature of the neutron gas in the beam connected with the escape of neutrons from the graphite surface in the experimental channel. The deviation of the observed neutron distribution from the Maxwellian one amounts to not more than 10% with the measurements being accurate to not better than ± 5%.

For comparison, the effective temperature of the neutron gas was determined by the method of boron filters previously calibrated on the mechanical selector. Satisfactory agreement was obtained with the selector measurements. Similar measurements of the spectrum and the temperature of the neutron gas were also carried out for the edge of the active zone. In this case the neutron beam was taken out along the horizontal experimental channel. It was established that the temperature of the neutron gas at the edge of the active zone exceeds the temperature of the moderator by 70-100°C, with the difference becoming less within the indicated temperature range as the moderator temperature increases.

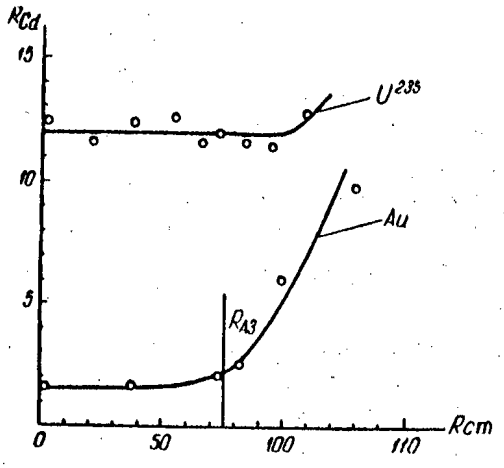

Figure 9. Cadmium ratios for U^{235} and Au.

In order to determine the magnitude of the relative contribution of resonance neutrons to the energy released in the reactor the cadmium ratios (R_{Cd}) were measured for gold and for U^{235}:

$$R_{Cd} = \frac{\text{activation without cadmium}}{\text{activation with cadmium}}$$

The thickness of cadmium in these experiments was 0.25 mm. The cadmium ratio for U^{235} determines the relative number of fissions in the thermal and resonance regions. From the cadmium ratio for gold, the ratio of fluxes of thermal and resonance neutrons in the reactor was determined. At the center of the reactor the cadmium ratios for Au and for U^{235} are respectively equal to 1.5 and 12. From the curves giving the dependence of the cadmium ratios on the reactor radius (Figure 9) it may be seen that 8.3% of the U^{235} fissions take place in the epicadmium region.

TABLE 2

Characteristic	Experimental value	Calc. value
1. Critical loading in the presence of water in working channels, expressed as a number of WC.	60	59
2. Critical loading in the absence of water in working channels, expressed as a number of WC.	101	99
3. Reserve of excess reactivity at the beginning of operation.	0.11 ± 0.005	0.122
4. Compensating ability of:		
one MC rod of the inner ring	0.013 ± 0.001	0.12
one MC rod of the outer ring	0.007 ± 0.001	0.007
two SR rods	0.018 ± 0.002	0.02
5. Probability of escaping resonance capture	$\varphi = 0.906 \pm 0.015$	—
6. Fraction of U^{235} fissions in the epicadmium region.	8.3%	—
7. Temperature of the neutron gas.	At the nominal power level exceeds the temperature of the medium by 70° C.	—

CONCLUSION

The experimental data obtained above permitted us to check the results of design calculations for the reactor of the atomic-electric power station. The heterogeneous effect has been demonstrated of the influence of water on the reactor reactivity which increases noticeably as the amount of water close to the uranium is increased. Water which is situated far from the reactor decreases reactor reactivity. In the most unfavorable case of the complete flooding of the reactor moderator with water, excess reactivity appears for the compensation of which two safety rods and the reserve control rods are sufficient. Experimental investigation of the neutron density distribution along the radius and along the height of the reactor for various rod positions per-

mitted us to select the optimal system for the compensation of excess reactivity by control rods. In Table 2 are given the principal results of the investigation of the physical characteristics of the reactor of the atomic electric power station. For comparison calculated values [3] are also given.

The following persons participated in the present work in addition to the authors: M. V. Bakhtina, Yu. Yu. Glazkov, V. Ya. Kitaev, Yu. I. Koryakin, E. F. Makarov, V. A. Parfenov, L. P. Khatyanov, V. R. Trubnikov and Yu. Yu. Shuvalov.

The authors consider it their duty to express their deep gratitude to Professor D. I. Blokhintsev for the general scientific direction and for the valuable advice given in the course of carrying out the present work, and also to academicians I. V. Kurchatov, A. P. Aleksandrov, A. I. Alikhanov, corresponding member of the Academy of Sciences of the USSR N. A. Dollezhal' and to Professor V. S. Fursov for taking part in the discussion of the planning of experiments at the time of starting up the reactor. The authors also wish to thank the personnel of the atomic electric power station for aid in carrying out experiments, and in particular their thanks go to N. A. Nikolaev, A. N. Grigoryants, G. N. Ushakov and V. A. Konovalov.

LITERATURE CITED

[1] D. I. Blokhintsev, N. A. Nikolaev, Reactor Construction and Reactor Theory. (Reports of the Soviet delegation at the International Conference on the Peaceful Uses of Atomic Energy) USSR Acad. Sci. Press 1955, p. 3.

[2] D. I. Blokhintsev, N. A. Dollezhal', A. K. Krasin, Atomic Energy 1956, No. 1, 10 (T.p. 7)*.

[3] D. I. Blokhintsev, M. E. Minashin, Yu. A. Sergeev, Atomic Energy 1956, No. 1, 24 (T.p. 21)*.

[4] M. B. Egiazarov, V. S. Dikarev, V. G. Madeev. Measurement of the Resonance Absorption of Neutrons in a Uranium-graphite Lattice. (Report at the session of the Academy of Sciences of the USSR devoted to the peaceful utilization of atomic energy, July 1-5, 1955).

---

* T. p. = Consultants Bureau Translation pagination.

MULTIGROUP METHOD OF CALCULATIONS USED IN THE DESIGN OF THE REACTOR FOR THE ATOMIC ELECTRIC POWER STATION

G. I. Marchuk

In reference [1] a survey is given of the methods and of the results of the physical design calculations for the reactor of the APS which are closely related to the well known two-group method. The design calculations for the APS reactor were also performed by means of the multigroup method. Some of the results of these calculations obtained on the basis of an extensive use of the method of finite differences are given in the present article.

1. Statement of the Problem

The principal problems of the physical design of a reactor are the determination of its critical size and the determination of the spatial and energy distribution of the neutron flux and of the neutron weighting function.

A more or less satisfactory solution of these problems is possible within the framework of the well-developed age-velocity theory which, as is well known, agrees sufficiently well with experiment only in that case when the elastic slowing down of the neutrons takes place on nuclei whose mass is considerably larger than the mass of the neutron.

If in the moderator mixture, nuclei of hydrogen-containing materials are present then the use of age-velocity theory may lead to significant errors in the determination of the spectrum and of the neutron weighting-function and consequently of the critical size of the reactor.

In uranium-graphite-water reactors, water is usually the principal heat transfer medium and it is placed near the heat producing elements forming together with them and with the surrounding graphite moderator the basic cell of the heterogeneous reactor.

The reactor of the atomic electric power station belongs exactly to this type of thermal neutron heterogeneous reactors [2].

It is evident that the closer the water in the cell is situated to the uranium lumps, the greater number of neutrons will be slowed down in the water and consequently the water will be more effective in its role as moderator. This essentially determines the basic heterogeneous effect of the water on the slowing down of neutrons in the cell of the reactor.

As regards the region of diffusion of thermal neutrons, here it is very important to note the fact that at thermal energies water has a very considerable capture cross section. However, in spite of the existence of considerable absorption of neutrons by water in the region of thermal neutron diffusion estimates, confirmed by experiment, show that its total effect on the reactivity of the reactor of the atomic electric power station is positive. At the same time one should also note that the effect of water situated far from the uranium lumps may turn out to be negative because of the strong capture by water of neutrons in the region of thermal neutron diffusion.

A proper method of taking into account all the competing factors allows one to choose in the most advantageous manner the construction of the cell of a heterogeneous reactor.

Consequently, one of the main problems that must be solved prior to the calculation of critical size, is the design of the cell of the heterogeneous reactor. These calculations allow one at a later stage to determine physical constants averaged over the neutron spectrum in the cell, the effective age of neutrons as a function of their energy, and the probability of escaping resonance capture in the course of the slowing down process. One should note, however, that particular difficulties arise in the solution of just this last problem.

After all the effects indicated above have been estimated on the basis of considering a single cell and after all the effective constants averaged over the spectrum of the cell have been obtained, the heterogeneous reactor may be replaced by a homogeneous one * calculations on which represent a much simpler problem, and may be carried out by several different methods.

2. The Averaging of the Physical Constants for the Reactor of the Atomic Electric Power Station

In this section we must first of all solve the problem of the spatial and energetic distribution of neutrons (over the cell of a heterogeneous reactor).

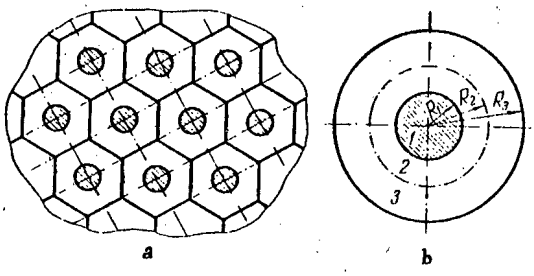

Figure 1. The reactor cell used for the calculation. a) The reactor lattice; b) the equivalent cell.

In view of the fact that the geometry of the cell of the active zone of the reactor turned out to be quite complicated it was decided for purposes of calculation to replace the actual geometry by a certain effective one possessing axial symmetry (Figure 1). Thus, it was assumed that zone 1 of the cell is filled with water, zone 2 contains a mixture of uranium, water, graphite and structural materials, and finally that zone 3 is filled with graphite.

In order to calculate the neutron spectrum in the cell the well known kinetic equation was used in the P_1-approximation.

$$\left.\begin{aligned} \frac{1}{\Sigma_s}\cdot\frac{1}{r}\frac{\partial}{\partial r}r\psi_1+\psi_0(r,u)&=\sum_i\int_{u-q_i}^{u}du'f_{0i}(u-u')\,\psi_0(r,u')+S(r,u),\\ \frac{1}{3\Sigma_s}\frac{\partial\psi_0}{\partial r}+\psi_1(r,u)&=\sum_i\int_{u-q_i}^{u}du'f_{1i}(u-u')\,\psi_1(r,u'),\end{aligned}\right\}\qquad(2.1)$$

where ψ_0 and ψ_1 are the coefficients of the first two terms in the expansion of the collision density function $\psi(r, u, \mu) = nv\Sigma_s$ in terms of Legendre polynomials:

$$\psi(r,u,\mu)=\psi_0(r,u)+\psi_1(r,u)\,P_1(\mu)+\ldots$$

$$f_{li}(u)=\frac{(M_i+1)^2}{4M_i}e^{-u}\cdot P_l\left[\frac{M_i+1}{2}e^{-\frac{u}{2}}-\frac{M_i-1}{2}e^{\frac{u}{2}}\right],\qquad(A)$$

q_i is the maximum logarithmic energy loss for a neutron colliding elastically with a nucleus of mass M_i; $S(r, u)$ are the monochromatic sources of neutrons of energy 2 Mev ($u = 0$) which uniformly fill zone 2 of the cell.

For all the elements i with the exception of hydrogen the well known hypotheses and methods of the age-velocity theory were used for the evaluation of the integrals in the right-hand sides of equations (2.1).

The system of the integers-differential equations so obtained was then reduced to a system of multiple-group diffusion equations. In doing this it was assumed that within each group the collision density $\psi(r, u, \mu)$

* With regard to a more accurate method of taking into account the heterogeneous nature of the installation see reference [3].

may at a fixed value of r be represented as a linear function of u.

$$\psi(r, u, \mu) = \psi^j(r, \mu) + \frac{\psi^{j+1}(r, \mu) - \psi^j(r, \mu)}{\Delta u}(u - u_j). \qquad (B)$$

where $\psi^j(r, \mu) = \psi(r, u_j, \mu)$ and u_j are certain representative points over the whole range of lethargy selected for the purposes of calculation.

In order to be able to take into account certain conditions at the zone boundaries inside the cell, the system of diffusion equations referred to above was replaced by a finite difference system which it is not difficult to solve.

The results of calculations of the neutron spectrum nv(r) over the reactor cell are given in Figure 2.

After the neutron spectrum in the reactor cell has been found, the averaging of the physical constants does not present any difficulties and may be carried out for any logarithmic energy u by means of the formula

$$\chi(u) = \frac{\int_{(D)} \chi(r, u)\, nv\, dv}{\int_{(D)} nv\, dv}, \qquad (2.2)$$

where (D) is the total volume of the cell, while $\xi\Sigma_s$, Σ_c, Σ_f and $\frac{1}{3\Sigma_{tr}} = D$ should be used in turn for the quantity $\chi(r, u)$. After the neutron spectrum in the cell had been found, the calculation of the effective age of the neutrons was carried out with the aid of the formula

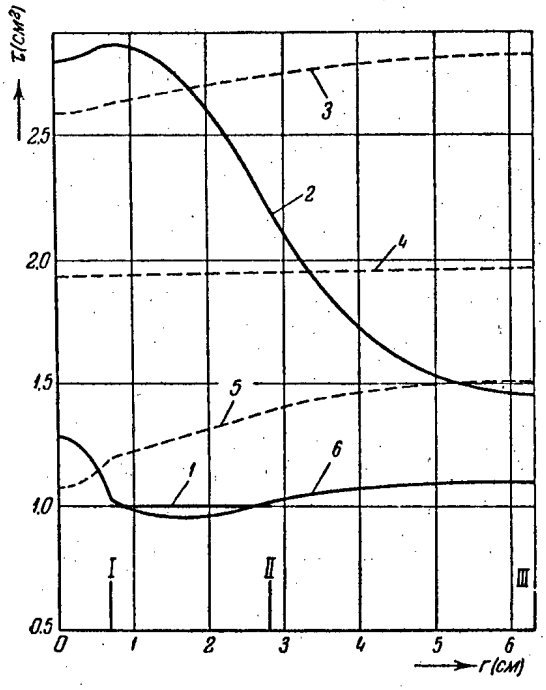

Figure 2. Spatial and energetic neutron distribution over the reactor cell.
1) Q(r); 2) Nv(r); 3, 4, 5) nv(r, u) for u = 2.5; u = 14.0; u = 17.5 respectively; 6) $10^{-1}\Phi(r)$;
I, II, III) zone boundaries within the cell.

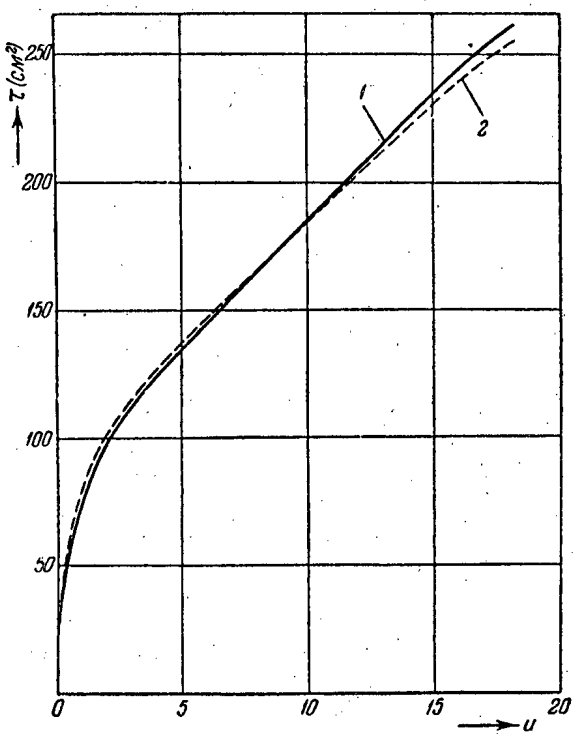

Figure 3. Effective neutron age.
1) $\tau(u)$ for a homogeneous mixture; 2) $\tau(u)$ taking into account the spatial and energetic neutron distribution in the cell.

$$\tau(u)=\frac{\int\limits_{(D)}\frac{Nv\,dv}{3\Sigma_s^2(r,0)}}{\int\limits_{(D)}Nv\,dv}+\int\limits_0^u du'\,\frac{\int\limits_{(D)}\frac{nv}{3\xi\Sigma_s\Sigma_{tr}}dv}{\int\limits_{(D)}nv\,dv}, \tag{2.3}$$

where Nv is the neutron flux before slowing down, ξ is the mean logarithmic energy loss per collision.

On comparing results of calculations carried out with the aid of (2.3) with the value of $\tau(u)$ obtained from the formula for a homogeneous mixture:

$$\tau_g(u)=\frac{1}{3\Sigma_{s0}^2}+\int\limits_0^u\frac{du}{3\xi\Sigma_s\Sigma_{tr}}, \tag{2.4}$$

where $\Sigma_{s0}=\Sigma_s(0)$ and $\frac{1}{3\xi\,\Sigma_s\Sigma_{tr}}$ are quantities calculated taking into account the formal replacement of the cell by a homogeneous one, it becomes evident that the effect of heterogeneity in the slowing down process is sufficiently small, and it may be entirely neglected (Figure 3).

This circumstance shows in particular that it is possible to use the age-velocity slowing down theory for the calculation of the critical size of the reactor.

We now proceed to one of the most essential characteristics of a heterogeneous reactor – the probability that a neutron escapes resonance capture by U^{238} nuclei in the course of the slowing down process. This quantity is denoted by φ.

In view of the weak mutual shielding of uranium lumps in an actual reactor cell, the calculation of φ reduces to the investigation of a single annular block cooled on the inside by water, and surrounded on the outside by moderator 3 of infinite extent (Figure 4).

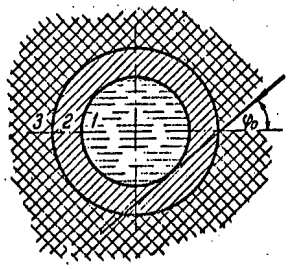

Figure 4. Annular block of a single cell.
1) Water; 2) fuel; 3) moderator.

Let us assume that the flux of neutrons with energies above resonance is essentially determined by the slowing-down spectrum and varies but little from point to point.

Then, in accordance with the work of Gurevich and Pomeranchuk [4], it is not difficult to determine the total number of those neutrons being absorbed which come from moderators 1 and 3 towards the uranium block, and in order to do this it is necessary to calculate the attenuation of their flux along various directions of their motion.

The calculation of the attenuation of the neutron flux along all possible directions and the subsequent integration over all these directions gives us the possibility of obtaining the total number of neutrons of a given energy being absorbed in the uranium block.

The subsequent summation of the number of absorbed neutrons over all the energies taking into account the shape of the resonance leads to a formula which holds when the thickness of the uranium blocks is much smaller than the mean free path for scattering in the material of the block.*

$$\ln\varphi=-n_0\frac{A\left[S_1\sqrt{l_1}+S_2\sqrt{l_2}\right]\sqrt{\varepsilon}+BV_{u\varepsilon}}{\xi V_3\cdot\Sigma_s}, \tag{2.5}$$

* Formula (2.5) for the cell of the reactor of the atomic electric power station was obtained by V. V. Orlov.

where n_0 is the number of uranium blocks per cell; V_u is the volume of a uranium block; ϵ is the porosity of the uranium; S_1 and S_2 are the inner and outer surfaces of the block; V_s is the volume of the moderator in the cell; ξ is the mean logarithmic energy loss; $\sqrt{l_1} = \sqrt{D}F_1\left(\frac{d}{D}\right)$; $\sqrt{l_2} = \sqrt{d}F_2\left(\frac{d}{D}\right)$ where d and D are respectively the inner and outer diameters of the block and $F_1\left(\frac{d}{D}\right)$ and $F_2\left(\frac{d}{D}\right)$ are certain functions whose graphs are shown in Figures 5a and 5b.

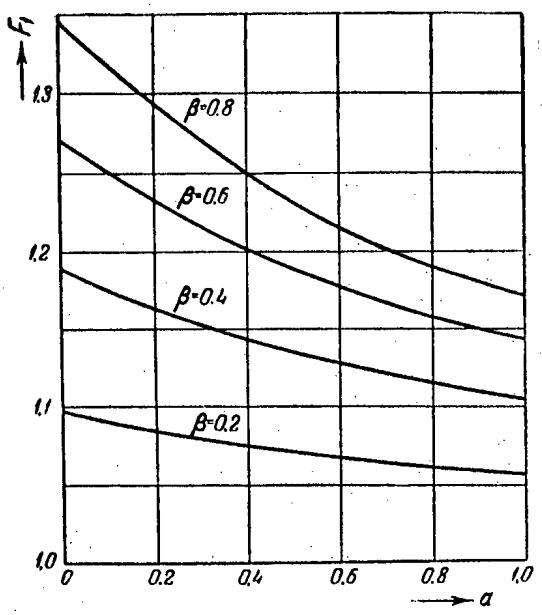

Figure 5a. Graph of the function $F_1(\alpha, \beta)$ where $\alpha = d(\Sigma_s)_{H_2O}$ for a resonance energy $\beta = \frac{d}{D}$.

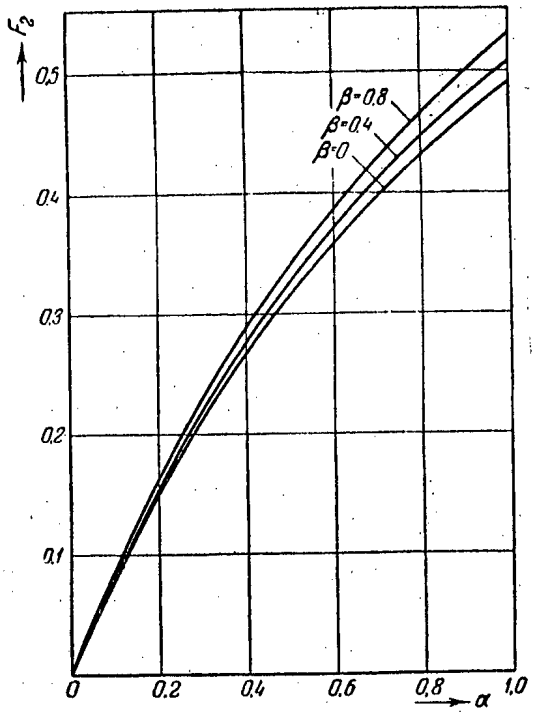

Figure 5b. Graph of the function $F_2(\alpha, \beta)$.

A and B are constants evaluated from formulae:

$$A = \sum_j \frac{\sqrt{\sigma_0^j \Gamma_j^2}}{E_j}, \quad B = \int \sigma(E)\frac{dE}{E}, \tag{D}$$

where σ_0^j is the absorption cross section at the peak of the j'th resonance, and E_j is the energy of this resonance, the summation over j being extended to all the resonances above the energy E.

To determine the values of the constants A and B over the whole spectrum theoretically it is necessary to have an accurate knowledge of all the parameters for all the resonances of U^{238}. In view of the inadequate knowledge of these parameters, V. V. Orlov used the experimental data on the total absorption of neutrons by nuclei of U^{238} obtained for solid uranium blocks of various diameters [5].

In reference [5], constants A and B for the formula of Gurevich and Pomeranchuk [4]

$$\ln\varphi = -\frac{AS\sqrt{l}\sqrt{\varepsilon} + BV_{u^2}}{\xi\Sigma_s V_s}, \tag{2.6}$$

where $\sqrt{l} = \sqrt{D}\cdot F_1(0)$. are found for solid uranium blocks of diameter D placed inside a moderator.

It is evident that as $d \to 0$, Formula (2.5) goes over into (2.6). Consequently, the values of the constants A and B in (2.5) and (2.6) must coincide. Thus Formula (2.5) allows us to determine the magnitude of the probability of escaping resonance capture by U^{238} nuclei in the reactor cell. For practical calculation it is useful to effectively distribute in energy the quantity so obtained among the strongest absorption resonances of U^{238}.

By a similar method, but taking geometry into account, one may calculate the quantity μ – the fast neutron multiplication factor. Since for the reactor of the atomic electric power station μ is close to 1, we shall not take it into account in the following for the calculation of critical masses.

3. Basic Equations

We consider the system of basic equations for the homogeneous reactor equivalent to the reactor of the atomic electric power station:

$$\left.\begin{aligned} &\nabla D_0 \cdot \nabla N v - \Sigma_{s0} \cdot N v = \\ &\quad = -\nu_f \left\{ \int_0^{u_T} n v \Sigma_f \, du + \Phi \Sigma_{fT} \right\}, \\ &\Sigma_{s0} N v = q(\mathbf{r}, 0), \\ &\nabla D \cdot \nabla n v - \Sigma_c \cdot n v(\mathbf{r}, u) = \frac{\partial q}{\partial u}, \\ &\nabla D_T \cdot \nabla \Phi - \Sigma_{cT} \Phi(\mathbf{r}) = -q(\mathbf{r}, u_T), \end{aligned}\right\} \qquad (3.1)$$

where $q = nvE_c$ is the slowing down density; $\Phi(\mathbf{r})$ is the thermal neutron flux; $\nu_f = 2.46$.

Quantities relating to the thermal energy region are denoted by the index "t".

As is well known, Equations (3.1) hold in the case when the absorption cross section does not depend strongly on the energy.

If Σ_c has a resonance at energy u, then the slowing down density $q(\mathbf{r}, u)$ changes discontinuously on passing from energy $u + 0$ to $u - 0$ by the amount

$$q(\mathbf{r}, u + 0) = \varphi(u) q(\mathbf{r}, u - 0), \qquad (E)$$

where φ is the probability of escaping resonance capture at the given point.

Together with the boundary condition, which in this case must be taken to require the vanishing of the solution at the extrapolated boundary, the eigenvalue problem becomes closed.

The solution of the system (3.1) is found as a rule by the method of successive approximations which consists of assuming a certain source distribution $Q(\mathbf{r})$ and of finding its new value in a better approximation by means of solving the system of Equations (3.1).

This process should be continued until the ratios of two consecutive values of the function $Q(\mathbf{r})$ become equal within the prescribed limits of accuracy to the same constant for all points of the active zone. The ratio found by this procedure will be the desired eigenvalue of the system, i.e.,

$$k_{eff.} = \frac{Q^{(n)}(\mathbf{r})}{Q^{(n-1)}(\mathbf{r})} \qquad (3.2)$$

where the index n is the order of the successive approximation.

Thus the solution of the eigenvalue problem has been reduced to the successive solution of Cauchy problems which are much simpler from the point of view of actual specific calculations.

In addition to the determination of the neutron spectrum, the calculation of the spatial and energy distribution of the neutron weighting function in the reactor is also of considerable interest.

In this case, as is well known, the mathematical problem reduces to the solution of the following system of differential equations

$$\left.\begin{aligned}
&\nabla D_{s0}\cdot\nabla Nv^*-\Sigma_{s0}\cdot Nv^*(\mathbf{r})=-\Sigma_{s0}\cdot nv^*(\mathbf{r},0),\\
&\nabla D\nabla nv^*-\Sigma_r\cdot nv^*(\mathbf{r},u)=-\xi\Sigma_s\frac{\partial nv^*}{\partial u}-\nu_f\Sigma_f\cdot Nv^*(\mathbf{r}),\\
&nv^*(\mathbf{r},u_T)=\psi^*(\mathbf{r}),\\
&\nabla D_T\cdot\nabla\Phi^*-\Sigma_{cT}\Phi^*(\mathbf{r})=-\nu_f\Sigma_{fT}Nv^*(\mathbf{r}).
\end{aligned}\right\}\qquad(3.3)$$

there, just as in the case of the basic reactor Equations (3.1), it is necessary to assume that the solution will be bounded inside the reactor and equal to zero at the extrapolated boundary.

The method of successive approximations for the solution of the system of Equations (3.3) consists of the following. In the right hand sides of Equations (3.3) the function $Nv^*(\mathbf{r})$ is given, and then a new value of $Nv^*(\mathbf{r})$ is found as a result of solving the system (3.3) etc. In this procedure k_{eff} is defined as the ratio of two successive values of $Nu^*(\mathbf{r})$ which have become established after several interactions:

$$k_{eff.}=\frac{Nv^{*(n)}(\mathbf{r})}{Nv^{*(n-1)}(\mathbf{r})}\qquad(3.4)$$

It is naturally understood that the eigenvalues of the basic Equations (3.1) must coincide with those of the conjugate Equations (3.3). It is useful to keep this circumstance in mind when estimating the accuracy of the calculations performed.

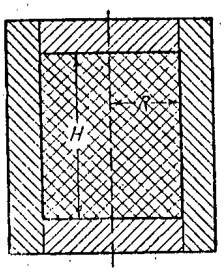

Figure 6. Diagram of the reactor.

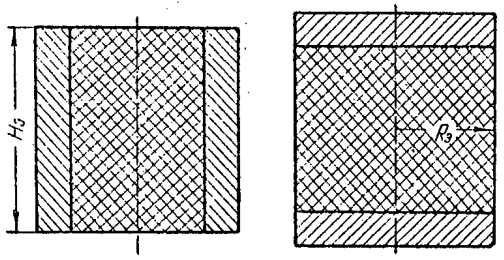

Figure 7. Reactor types used for calculations.

The system of Equations (3.1) as well as the system (3.2) may be solved by means of various approximate methods. But before proceeding to the solution of these systems one should note one important circumstance.

Because the reactor of the atomic electric power station has a complicated geometry (Figure 6), the direct solution of systems (3.1) and (3.3) is very difficult. Therefore, in order to simplify the solution of these systems of equations usually the reactor of cylindrical shape is replaced by a certain spherical one of an appropriate effective size. However, in our case this method may lead to considerable error.

It turned out that the most flexible method for the solution of problems was the method of successive approximations, which consists of the following.

Let us consider a cylindrical reactor without end reflectors which has the same radius as the real one (Figure 7). Assuming a certain effective height H_{eq} of this reactor and determining $k_{eff.}$, we can then find the extrapolated boundary of the equivalent reactor without side reflectors.

$$R_{eq}=R+\delta R$$

where δR is the equivalent increment.

Let us then consider another one - dimensional reactor whose height corresponds to the actual one and whose side reflectors are replaced by the equivalent increment found above (Figure 7). Having determined

$k_{eff.}$ for this reactor we can then calculate the equivalent increment of height, etc.

These calculations should be continued until a limiting value of $k_{eff.}$ has been established which will be the required approximate eigenvalue of the system. In order to find the critical mass of the reactor, one must carry out a series of analogous calculations either for different dimensions of the active zone and a fixed concentration of U^{235}, or for different concentrations of U^{235} and fixed reactor dimensions. The desired value of the critical mass will be obtained for that uranium concentration which gives $k_{eff.} = 1$.

4. The Multigroup Method of Solving the Equations

In the preceding section it was shown how the problem of calculating the critical mass of the reactor can be reduced to the successive solution of one-dimensional plane and cylindrical problems.

Since the system (3.1) as well as (3.3) consists of equations of the diffusion and age-velocity type, let us investigate the approximate methods available for their solution.

For the active zone of one-dimensional reactors with plane and cylindrical geometry, the age-velocity equation of the system (3.1) has, as is well known, the form

$$\frac{D}{\xi\Sigma_s}\nabla^2 q - \frac{\Sigma_c}{\xi\Sigma_s} q = \frac{\partial q}{\partial u}, \tag{4.1}$$

where

$$\nabla^2 = \frac{1}{r^\alpha}\cdot\frac{\partial}{\partial r}\cdot r^\alpha \frac{\partial}{\partial r}$$

and $\alpha = \begin{matrix} 0 \text{ for plane geometry} \\ 1 \text{ for cylindrical geometry.} \end{matrix}$

In solving Equation (4.1) for the various zones of the reactor, the following boundary conditions must be used at the boundaries separating the different media

$$\frac{1}{\xi\Sigma_s} q = \frac{1}{\xi'\Sigma_s'} q';$$
$$\frac{D}{\xi\Sigma_s}\nabla q = \frac{D'}{\xi'\Sigma_s'}\nabla q' \tag{4.2}$$

(primes denote quantities referring to adjoining zones in the reactor).

At the same time one must assume that the solution should remain bounded within the reactor volume, and must vanish over the outer extrapolated boundary of the reactor.

We shall seek the solution of Equation (4.1) by means of the method of nets.* In order to do this we shall superimpose on the semi-infinite strip ($R_1 \le r \le R_2$; $u > 0$) within which the function $q(r, u)$ is defined as a rectangular net with a pitch Δr along the r axis, and a pitch Δu along the u axis.

It is well known that a differential operator may be replaced by a number of approximate methods. However, for making calculations for thermal neutron reactors or other similar ones a triangular scheme is the most convenient one, which may be represented in the case of weak absorption during the slowing down process in the form

* The multigroup method of reactor calculations described in this article was developed by the author in 1953 [6].

$$q_k^{j+1} = \frac{1 - \frac{\Delta\tau}{2l^2}}{1 + \frac{\Delta\tau}{2L_c^2}} q_k^j + \frac{\mu}{1 + \frac{\Delta\tau}{2L_c^2}} M(q_k^j), \tag{4.3}$$

where

$$\frac{1}{L_c^2} = \frac{\Sigma_c}{D}, \qquad \Delta\tau = \int_{u_j}^{u_{j+1}} \frac{D\,du}{\xi\Sigma_s}, \qquad \mu = \frac{\Delta\tau}{\Delta r^2},$$

$$M(q_k^j) = \begin{cases} q_{k+1}^j - 2q_k^j + q_{k-1}^j & \text{for } \alpha = 0 \\ q_{k+1}^j - 2q_k^j + q_{k-1}^j + \frac{\Delta r}{2r_k}(q_{k+1}^j - q_{k-1}^j) & \end{cases}$$

for $\alpha = 1$.

We must now formulate the subsidiary relationships which will enable us to obtain in a similar way the solution at the zone boundaries and at the center of the reactor. For this, the radius of the active zone must be divided up into segments of length Δr in such a way that the point $r = 0$ should fall in the center of the first interval Δr, the boundary between the active zone and the reflector $r = R_1$ should fall in the center of the last interval, while the reflector must be broken up into segments $\Delta r'$ in such a way that the boundary between the active zone and the reflector, and also between it and the second adjacent reflector, must fall at the center of the first (or the last) interval $\Delta r'$.

Thus it is assumed that the solution of the problem for each zone may be continued analytically by half of a Δr step in the direction of the adjacent zones. This well known method [7] turned out to be convenient for specifying the conditions at the zone boundaries in the finite difference formulation.

Indeed, if we assume that X^{j+1} and Y^{j+1} are the desired functions at a fictitious point, then we may obtain without difficulty that

$$X^{j+1} = K^j q_s^{j+1} + L^j q_{s+1}^{j+1},$$

$$Y^{j+1} = \frac{1}{\lambda_1}[X^{j+1} + q_s^{j+1}] - q_{s+1}^j, \tag{4.4}$$

where

$$K^j = \frac{1 - \frac{\lambda_2}{\lambda_1}}{1 + \frac{\lambda_2}{\lambda_1}}, \qquad L^j = \frac{2\lambda_2}{1 + \frac{\lambda_2}{\lambda_1}},$$

$$\lambda_1 = \frac{\xi\Sigma_s}{\xi'\Sigma_s'}, \qquad \lambda_2 = \frac{\Delta r}{\Delta r'} \cdot \frac{D'}{D} \cdot \frac{\xi\Sigma_s}{\xi'\Sigma_s'}, \tag{F}$$

and the index "s" is the number of the last point in the active zone of the reactor (the primes on the function q_k^j have been omitted).

For the boundary condition at $r = 0$ it is necessary to take

$$q_{-1}^{j+1} = q_1^{j+1},$$

where

$$q_1^{j+1} = q^{j+1}\left(\frac{\Delta r}{2}\right), \tag{G}$$

and

$$q_{-1}^{j+1} = q^{j+1}\left(-\frac{\Delta r}{2}\right).$$

Assuming further that $q_n^j = 0$ (where $q_n^j = q^j(R)$ and R is the extrapolated reactor boundary) we arrive at a closed system of difference equations with the aid of which one may find the values of the functions at all the

fundamental and fictitious points of the reactor. Since the difference Equation (4.3) has already been solved with respect to the unknown function q_k^{j+1} the system may be solved in terms of the simplest arithmetical operations.

The successive solution of the system referred to above for all $j = 1, 2, \ldots m$ leads us to the desired solution of the slowing down problem.

The diffusion equations of the system (3.3) are solved in an analogous manner.

Let us consider one of the diffusion equations

$$\nabla^2\Phi - \frac{1}{L_{cr}^2}\Phi = -f(r), \tag{4.5}$$

where $f(r)$ is a given function; $1/L_{st}^2$ is a constant which has different values in different reactor zones.

As before, let us assume that

$$\left.\frac{d\Phi}{dr}\right|_{r=0} = 0, \quad \Phi(R_0) = 0, \tag{4.6}$$

and at the zone boundaries

$$\Phi = \Phi'$$
$$D_T \frac{d\Phi}{dr} = D_T' \frac{d\Phi'}{dr}. \tag{4.7}$$

In the finite difference form the problem (4.5, 4.7) in analogy with the earlier case takes the form

$$M(\Phi_k) - \frac{\Delta r^2}{L_{cr}^2}\Phi_k = -\Delta r^2 f_k \tag{4.8}$$
$$(k = 1, 2, \ldots, s-1),$$
$$\Phi_{-1} = \Phi_1, \quad \Phi_n = 0, \tag{4.9}$$
$$X = K\Phi_s + L\Phi_{s+1}, \quad Y = X + \Phi - \Phi_{s+1}, \tag{4.10}$$

where

$$K = \frac{1-\lambda}{1+\lambda}, \quad L = \frac{2\lambda}{1+\lambda}, \quad \lambda = \frac{D_T'}{D_T}\cdot\frac{\Delta r}{\Delta r'}. \tag{4.10a}$$

For convenience in solving equations (4.5-4.7) we eliminate from systems of the form (4.8) the unknowns X and Y with the aid of (4.10). As a result we obtain for all points of the reactor the following equations:

$$a_k\Phi_{k+1} - b_k\Phi_k + c_k\Phi_{k-1} = -\Delta r_k^2 f_k. \tag{4.11}$$

Dividing equation (4.11) by a_k we shall obtain the difference system of diffusion equations in the final form

$$\Phi_{k+1} - B_k\Phi_k + C_k\Phi_{k-1} = -\varepsilon_k f_k, \tag{4.12}$$

with the condition that

$$\Phi_{-1} = \Phi_1, \quad \Phi_n = 0. \tag{4.13}$$

In (4.12) the following notation has been adopted

$$B_k = \frac{b_k}{a_k}, \quad C_k = \frac{c_k}{a_k}, \quad e_k = \frac{\Delta r_k^2}{a_k}. \tag{4.14}$$

We now go to the solution of the system (4.12-4.13). In this connection it is useful to examine basically two methods which are the most applicable from a computational point of view. The first of these amounts to a method of reducing the boundary value problem to two Cauchy problems. For this it is sufficient to specify two different values of the unknown function Φ at the junction point $k = -1$ under the condition $\Phi_{-1} = \Phi_1$.

As a result of the successive solution of the system (4.12) we shall correspondingly obtain two linearly independent solutions. Constructing a linear combination of these two results which is a solution of Equation (4.12) and which satisfies condition (4.13) we arrive at the desired solution of the problem.

This method turns out to be very convenient in a number of cases. But for a large number of computational points the rounding-off error which increases exponentially from point to point leads to a significant loss of accuracy, and this leads to the necessity of carrying out the calculation to a larger number of significant figures.

In such cases it is useful to utilize a method proposed by I. M. Gelfand and O. V. Lokutsevsky [10] and independently by Stark [8] which may be called the method of difference factorization. It consists of writing the second order difference equation (4.12) in the form of a system of three first order difference equations. Thus in addition to (4.12) let us also consider the following:

$$(\nabla + \mu_{k+1})(I_{k+1} + \sigma_{k+1}\Phi_{k+1}) = -\varepsilon_k f_k, \tag{H}$$

where

$$\left.\begin{aligned} I_{k+1} &= \Phi_{k+1} - C_{k+1}\Phi_k, \\ \nabla\psi_k &= \psi_k - \psi_{k-1}. \end{aligned}\right\} \tag{4.15}$$

and the constants μ_k and σ_k are so far arbitrary; they must be so chosen that equation (4.13) becomes identically the same as (4.12). Fairly simple manipulations lead to the system of first order difference equations:

$$\left.\begin{aligned} \beta_{k+1} &= \frac{C_{k+1}}{B_k - \beta_k}, \\ Z_{k+1} &= \beta_{k+1}[Z_k + \varepsilon_k f_k], \\ \Phi_k &= \frac{\beta_{k+1}\Phi_{k+1} + Z_{k+1}}{C_{k+1}}. \end{aligned}\right\} \tag{4.16}$$

The new quantities β_k and Z_k are related to μ_k and σ_k by the relations:

$$\beta_k = \frac{1}{1+\sigma_k},$$
$$Z_k = -I_k + (1-\beta_k)\Phi_k. \tag{4.17}$$

The computation of β_k and Z_k from Formulas (4.16) is carried out from left to right, and the computation of Φ_k from right to left. Such computations do not lead to an exponential increase in the rounding-off error and therefore this method is free of disadvantages inherent in other methods.

With respect to the boundary conditions at the center of the reactor and at the outer extrapolated boundary, it may be easily seen that they will be satisfied if one assumes

$$\beta_1 = C_1, \quad Z_1 = 0, \quad \Phi_N = 0. \tag{4.18}$$

In conclusion it should be noted that in certain cases it is useful to reduce the age-velocity equation to a

system of equations of the diffusion type and to carry out the solution by the method of difference factorization which possesses exceptional universality and applicability. This method may be easily programmed on the majority of computing machines.

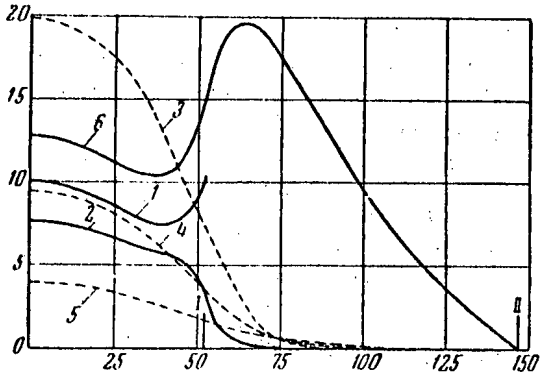

Figure 8. Spatial and energy distribution of neutrons in a critical reactor.
1) 10 Q(r); 2) nv(r); 3, 4, 5) nv(r, u); 6) Φ(r) for u = = 1.0; u = 5.0; and u = 17.75 respectively; I and II) boundaries of reactor zones.

Figure 8 shows the results of the determination of the neutron spectrum for the critical state of the reactor of the atomic electric power station.

Figure 9 shows the results of calculating the neutron weighting function in the reactor.

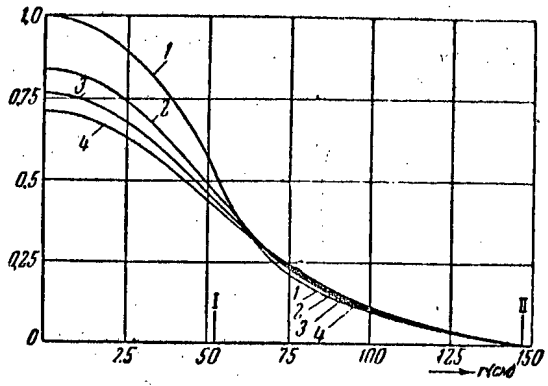

Figure 9. The spatial and energy distribution of the conjugate function in the reactor.
1) $\Phi^*(r)$; 2, 3) $nv^*(r, u)$ at energies u = 8.0; u = 1.0 respectively; 4) $Nv^*(r)$.

The value of $k_{eff.}$ computed with the aid of the fundamental reactor equations is equal to 1.023, while the same value is computed with the aid of the conjugate equations is 1.021. Thus, $k_{eff.}$ computed with the aid of the fundamental and the conjugate reactor equations differs by 0.2%. This circumstance points to the fact that the mathematical problem has been solved with good accuracy. The total error in the determination of the critical parameter of the system $k_{eff.}$ amounts to 2.3%. The calculated value of the cadmium ratio is in good agreement with the experimental value.

The data required as the point of departure for the multigroup calculations came from reference [1].

The author expresses his deep gratitude to D. I. Blokhintsev and also to E. S. Kuznetsov for discussions of this work and for valuable remarks. The author is also indebted to V. V. Smelov who performed all the computations and who carried out the design calculations on a reactor cell.

LITERATURE CITED

[1] D. I. Blokhintsev, M. E. Minashin, Yu. A. Sergeev, Atomic Energy 1956, No. 1, 24 (T.p. 21)*.

[2] D. I. Blokhintsev, N. A. Nikolaev, "Reactor construction and reactor theory." (Reports of the Soviet Delegation at the International Conference on the Peaceful Uses of Atomic Energy). Acad. Sci. USSR Press, 1955, p. 3.

[3] S. M. Feinberg, "Heterogeneous methods of reactor calculations. Survey of results and comparison with experiment.", Ibid., p. 152.

[4] I. I. Gurevich, I. Ya. Pomeranchuk, "The theory of resonance absorption in heterogeneous systems.", Ibid., p. 220.

[5] N. B. Egiazarov, V. S. Dikarev, V. G. Madeev, "Measurements on resonance neutron absorption in uranium-graphite lattices." (Report at a session of the Acad. Sci. USSR, 1955).

[6] G. I. Marchuk, "On approximate methods of nuclear reactor calculations.", (Presentation at a session of the Acad. Sci. USSR, 1955).

[7] L. Kollats, "Numerical methods of solving differential equations." Foreign Lit. Press, 1953.

* T. p. = Consultants Bureau Translation pagination.

[8] R. Erlich, H. Hurwitz, Nucleonics 12, 2, 23 (1954).

[9] S. Glasstone and M. Edlund, The Elements of Nuclear Reactor Theory, Foreigh Lit. Press, 1954.

[10] O. V. Lokutsievsky, Report at a Conference of Functional Analysis, Moscow, 1956.

MASSES OF THE H, D, He^4 AND C^{12} ISOTOPES

R. A. Demirkhanov, T. I. Gutkin, V. V. Dorokhov, A. D. Rudenko

Results are given of the measurements of the masses of the H, D, He^4 and C^{12} isotopes carried out by means of a mass-spectrograph with a resolving power of 70,000-100,000. The data obtained agree well with the corresponding mass values obtained from the energy balance of nuclear reactions.

Introduction

A careful measurement of isotopic masses is one of the best means for determining such an important property of the nucleus as the binding energy of the nucleons in the nucleus. The masses of the isotopes of medium and heavy elements are in most cases not known with sufficient accuracy, or have not been measured at all. Therefore their measurement is of considerable interest in connection with the necessity of the experimental determination of the binding energy of the nucleons in the nucleus, particularly in the region of the "magic numbers" for medium and heavy nuclei.

The mass spectrographic determination of the masses of the medium and heavy elements is carried out by means of utilizing intermediate doublets connecting the isotope being measured with O^{16}.

In most cases the intermediate doublets are made up of ions of the various combinations of the isotopes H, D, C^{12} ($C^{12}_m H_n$ or $C^{12}_m D_n$), and therefore the accuracy of measurement of the masses of the isotopes of medium and heavy elements is determined first of all by the experimental error in the measurement of the masses of the H, D, C^{12} isotopes.

During the last few years a number of articles have appeared devoted to the precision measurements of the masses of the isotopes of the light elements by means of mass-spectrographs [1-5]. Moreover, on the basis of data on the total energies of nuclear reactions isotopic masses have been calculated with considerable accuracy [6, 7].

The values of the masses of H and D obtained by various authors agree well with each other, while values obtained for the mass of C^{12} have a spread far outside the limits of the quoted experimental errors (see Table 3).

The lack of reliable data for the mass of the C^{12} isotope excludes the possibility of using ions of the group $C^{12}_m H_n$ for a precise calibration of the mass spectrographic scale in the region of medium and large masses.

This fact led us to make new measurements of the masses of the H, D, He^4 and C^{12} isotopes.

Description of the Apparatus

A schematic diagram of the mass-spectrographic equipment which was used for the measurement of the masses is given in Fig. 1. The apparatus was designed and constructed by M. Ardenne with the collaboration of G. Jaeger and the authors of the present article. The ion-optical arrangement is a variant of the Bainbridge-Jordan system.

The ion beam was produced in the following manner: the ions are generated in a plasma source with ordinary charge contraction. The voltage of the discharge arc was 50-200 volts with the arc current equal to 0.25-0.75 amps. The ions are removed through a circular (0.15 mm diameter) emission opening S_0 in the anode. The magnitude of the accelerating voltage is 35-45 kv. The entrance slit S_1 of width

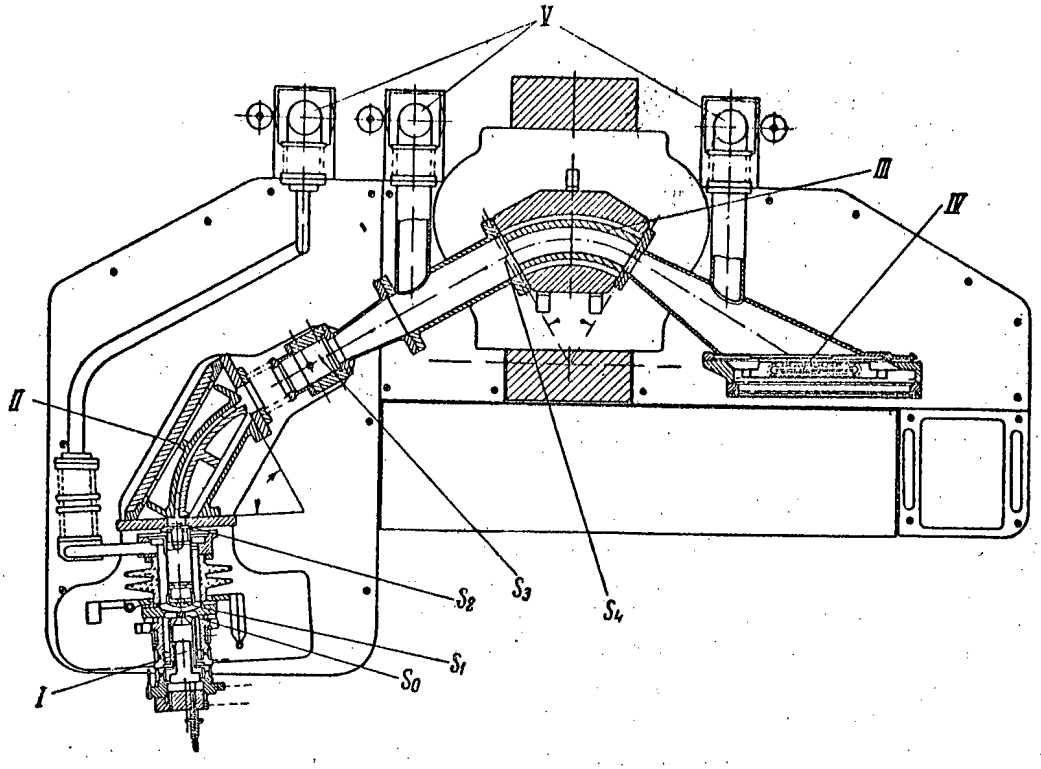

Fig. 1. Schematic drawing of the mass-spectrograph.
I) Plasma ion source; II) cylindrical electrostatic lens; III) magnetic analyzer; IV) photographic camera with an ion-optical converter; V) diffusion pumps; S_0-emitting slit; S_1- principal entrance slit; S_2- aperture slit; S_3- intermediate slit; S_4-entrance slit into the magnetic analyzer.

5-10μ is at a distance of 10 mm from the emitting slit (S_0). At a distance of 212 mm from the exit slit is situated the aperture slit S_2 of dimensions 30 x 1000 μ. Thus the aperture of the beam was $\sim 7 \times 10^{-5}$. The mean radius of curvature of the cylindrical condenser is equal to 300 mm, the angle of bending is $\Phi_1 = 63°38'$.

In the plane of the image of the cylindrical lens there is a diaphragm with a slit S_3 of dimensions 200 to 500μ. The entrance slit S_4 of the ion beam in the magnetic analyzer has the dimensions 500 x 1000μ. The gap between the magnetic poles is 3 mm. The radius of curvature for the principal mass m_0 in the magnetic field is equal to 300 mm. The bending angle is $\Phi_m = 60°$. The cardinal points of the electric and the magnetic lenses are situated symmetrically. The plane of the photographic plate is at an angle of 30° to the optical axis.

The source of high voltage for the acceleration of the ions is a half-wave rectifier with a large time-constant. The potential is applied to the plates of the cylindrical condenser from dry "B" batteries BAS-G-80-L-2.1 specially selected and periodically checked for stability. The voltage of the order of 2000-3000 volts is applied symmetrically so that the surface of zero potential passes in the middle between the condenser plates. The electromagnetic windings are fed from storage batteries of 135 ampere-hour capacity. The operating pressure in the region of the cylindrical condenser is $5-6 \times 10^{-6}$ mm of mercury.

The average resolving power determined from the line half-width measured on a comparator is 70,000. The maximum resolving power obtained for the $C^{12}H_2$-N^{14} doublet as a result both of comparator and of microphotometric measurements amounts to 100,000 for the $C^{12}H_2$ line, and to 120,000 for the N^{14} line. The lines were recorded on "Schumann" photographic plates ofdimensions 6 x 18 cm. 14 spectra were photographed on each plate.

The use of a plasma source with a high current density of emitted ions ($\sim$50 mm/cm^2) and with a small spread in the velocity of the ions ($\sim$ 2 v) allows one to make measurements with a small beam aperture, and

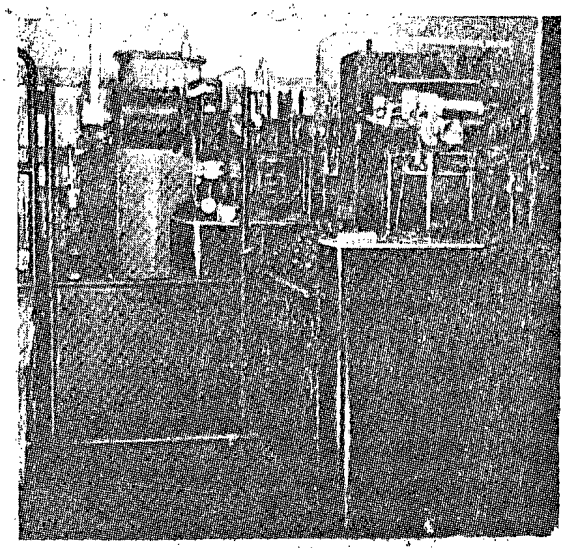

Fig. 2. External view of the equipment.

with relatively short exposures (0.1-5 sec). With such short exposures the requirements on the stability of the equipment supplying voltage to the magnet and to the cylindrical condenser are reduced, while the small value of the aperture and the small velocity spread of the ions ($\Delta u/u \sim 5 \times 10^{-5}$) ensure a small value for errors of the second order and a good sharpness of the image.

The ion optical converter which is situated very close to the plane of the photographic plate enables one to observe visually the mass-spectrum, to adjust the group of lines being observed in the center of the focal plane, and to monitor the quality of the spectrum during exposure by observing the outer lines. Special provisions for adjusting the ion-optical system (quartz plates with a fluorescent layer, observation windows, means for regulating the width and position of the slits in the pumped-out system), and also vacuum locks for changing the photoplates and for separating the source from the vacuum system of the apparatus permit one to prepare the mass spectrograph for operation in a relatively short time.

Dispersion and the Mass Scale

A mass spectrum always contains lines whose ions differ from each other in mass by the magnitude of the mass of the hydrogen atom M(H) = 1.008142 $\pm$ 2 x 10^{-6} a.m.u., e. g. $N^{14+} - N^{14}H^{+} - N^{14}H_2^{+} - N^{14}H_3^{+}$.

Having selected certain of these lines as "base-lines" one may experimentally calibrate the mass scale, i.e., for a given region of the photographic plate one may determine $\Delta M(\Delta x, x)$ in the following approximate form:

$$\Delta M = A(\Delta x) + B(\Delta x)^2 + \qquad (1)$$

If the spectrogram contains "base-lines" with a known mass difference M_1 and M_2 situated at positions x_1 and x_2 (Fig. 3), then the constants A and B may be found from the following relations:

$$A = \frac{M_1 x_2^2 - M_2 x_1^2}{x_1 x_2^2 - x_2 x_1^2}, \qquad (2)$$

$$B = \frac{M_2 x_1^2 - M_1 x_2^2}{x_1^2 x_2 - x_1 x_2^2}. \qquad (3)$$

In practice if the doublet being investigated is photographed near the center of the plate the deviations from linearity turn out to be so small that there is no need for quadratic interpolation, and then

$$\Delta M = A(\Delta x), \qquad (4)$$

where the value of A may be computed with sufficient accuracy from the formula

$$A = \frac{2M_H}{x_1 + x_2}. \qquad (5)$$

In photographing doublets formed by ions of small masses (M < 13) the "base-lines" turn out to lie outside the limits of the plate and therefore for the determination of the dependence of $\Delta M(\Delta x, x)$ in this case one must use lines of an auxiliary spectrum (for example $C_4H_3 - C_4H_4 - C_4H_5$ or $O - OH - OH_2$) registured on the same plate as the doublet under investigation with the same ion-optical parameters of the apparatus. It is expedient to use ions of the OH_n group for the auxiliary spectrum since the mass of the O^{16} oxygen isotope is assumed to be equal to 16, and the values for the mass of the hydrogen atom obtained by different methods agree reasonably well

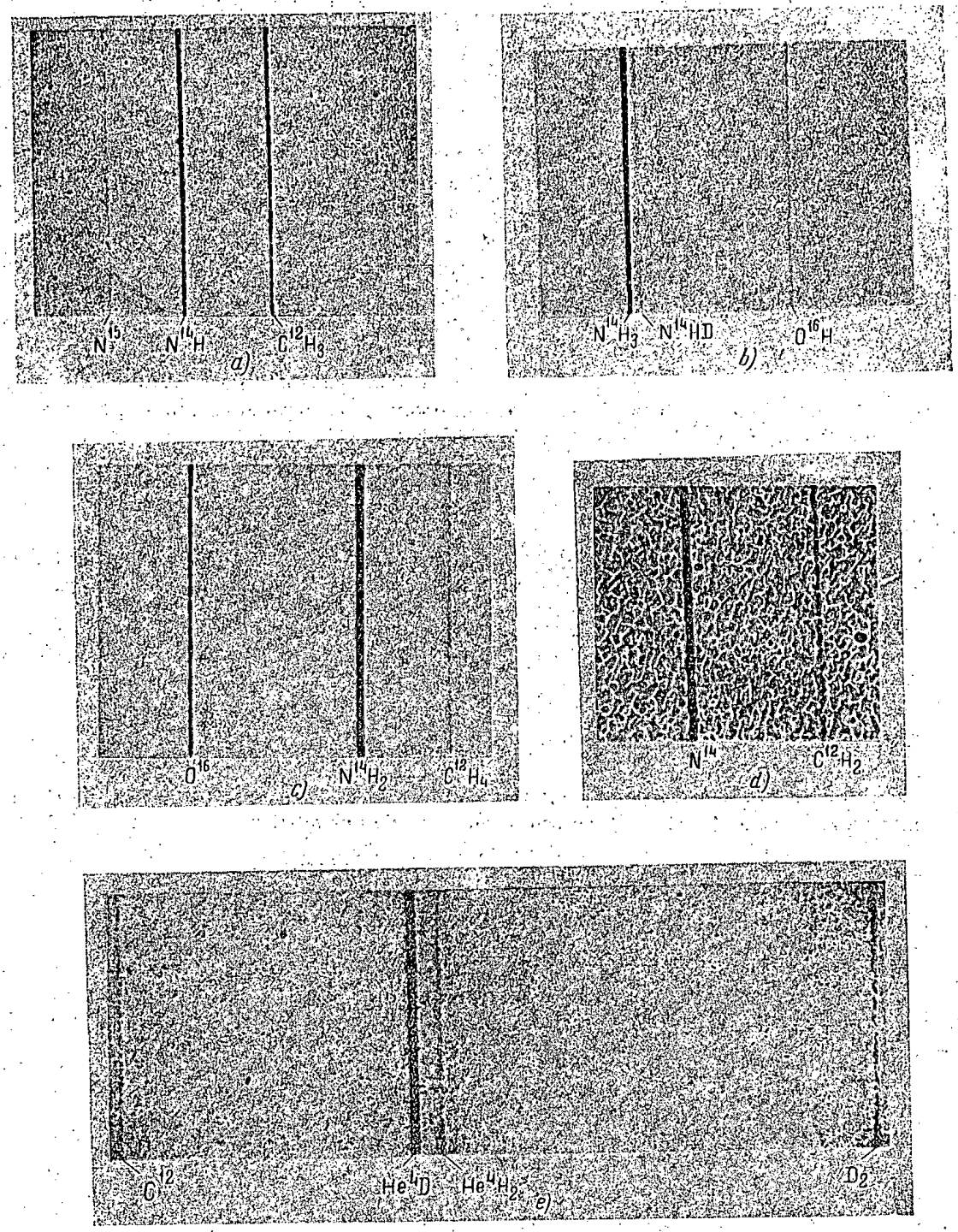

Fig. 3. Photographs of mass-spectrographic doublets. a) The triplet $N^{15}-N^{14}H-C^{12}H_3$ (×40); b) the triplet $N^{14}H_3-N^{14}HD-O^{16}H$ (×40); c) the triplet $O^{16}-N^{14}H_2-C^{12}H_4$ (×40); d) the doublet $N^{14}-C^{12}H_2$ (×60); e) the quartet $1/2\ C^{12}-He^4D-He^4H_2-D_2$ (×40).

among themselves. The lines of the auxiliary mass-spectrum are brought to the photoplate by means of changing the strength of the magnetic field. In our experiments in view of the absence of a strict linearity in the variation of the dispersion along the photoplate the magnetic field strength was varied so that the central "base line" of the auxiliary spectrum would fall directly below the doublet under investigation at the center of the plate. In this case the relationship between ΔM and the corresponding distance Δx between the doublet lines is determined by the expression

$$\Delta M = \Delta x \frac{M_{av}}{D} \tag{6}$$

where M_{av} is the average value of the masses of the ions constituting the doublet being investigated, and D is the dispersion constant determined from the relation

$$D = \frac{M_1}{A} \tag{7}$$

in accordance with the data for the auxiliary spectrum (M_1 is the mass corresponding to the central "base-line" with an accuracy of 10^{-5}).

For the determination of ΔM with an accuracy of 10^{-6} a.m.u. the value of M_{av} may be computed using data on the masses of the isotopes of the light elements. As may be easily seen, for this it is sufficient to know the value of M_{av} with an accuracy of 10^{-4}. The values available at present for the masses of the isotopes of the lightest elements agree among themselves with the required limits of accuracy (10^{-4}). For example, Table 1 gives values of M_{av} obtained by various authors for the doublet $D-He^4$.

TABLE 1

Investigator	Value in a.m.u.
Ewald [1]	$4.01662 \pm 10 \cdot 10^{-6}$
Nier [4]	$4.016674 \pm 14 \cdot 10^{-6}$
Ogata and Matsuda [3]	$4.016680 \pm 12 \cdot 10^{-6}$
Li, Whaling et al. [6]	$4.016672 \pm 14 \cdot 10^{-6}$

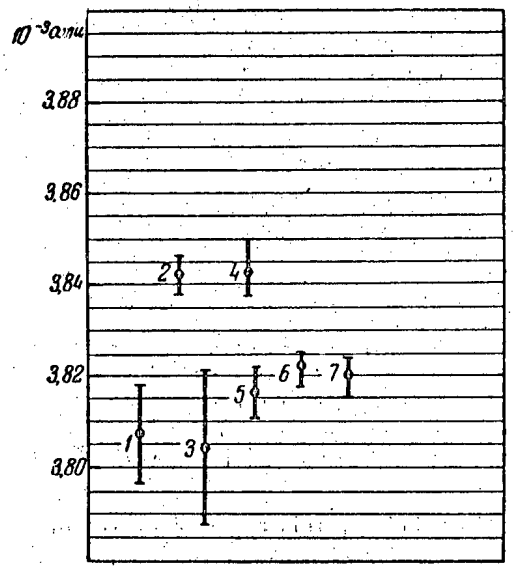

Fig. 4. Mass defect M−A of the C^{12} isotope according to the data of: 1) Ewald, 1951 [1]; 2) Nier, 1951 [4]; 3) Li, Whaling et al., 1951 [6]; 4) Ogata and Matsuda, 1953 [3]; 5) Dzhelepov and Zyryanova, 1952 [7]; 6) Mattauch and Bieri, 1954 [2]; 7) the present work.

The influence of the leakage flux of the magnetic analyzer was taken into account by introducing an additional "magnetic correction" coefficient into expression (6).

In all cases the distance between the lines of the doublet was determined by means of measuring it ten times on a comparator with an optical magnitification of the image by a factor of 140 or 280. To exclude subjective errors the measurement of Δx for any one doublet was repeated by three or four operators. The final value of Δx was obtained as the average value of 10-12 doublets taken from 3-4 different photographs.

Experimental Results

The masses of the H, D, He^4 and C^{12} isotopes were found from the following relations:

$$H = \frac{1}{16}O + \frac{3}{8}\alpha + \frac{1}{8}\beta + \frac{1}{16}\gamma,$$

$$D = \frac{1}{8}O - \frac{1}{4}\alpha + \frac{1}{4}\beta + \frac{1}{8}\gamma,$$

$$He^4 = \frac{1}{4}O - \frac{1}{2}\alpha + \frac{1}{2}\beta + \frac{1}{4}\gamma - \delta,$$

$$C^{12} = \frac{3}{4}O - \frac{3}{2}\alpha - \frac{1}{2}\beta + \frac{3}{4}\gamma,$$

where

$$\alpha = \Delta M(H_2 - D),$$

$$\beta = \Delta M\left(D_3 - \frac{1}{2}C^{12}\right),$$

$$\gamma = \Delta M(C^{12}H_4 - O),$$

$$\delta = \Delta M(D_2 - He^4),$$

are respectively the mass differences for the doublets $H_2 - D$, $D_3 - 1/2C^{12}$, $C^{12}H_4 - O$, $D_2 - He^4$.

TABLE 2

Mass Differences of the Doublets in 10^{-3} a.m.u.

Investigator	$H_2 - D$	$D_2 - He^4$	$D_3 - {}^1/_2C^{12}$	$C^{12}H_4 - O^{16}$
Data of present work	1.5483±0,001	25.600±0,002	42.298±0,007	36.388±0,004
Ewald (1951) [1]	1.5503±0,0015	25.604±0,008	42.292±0,012	36,371±0,012
Nier (1951) [4,5]	1.5519±0,00172	25.612±0,009	—	36,427±0,008 *
Ogata and Matsuda(1953) [3]	1.5492±0.0008	25.603±0,006	42.301±0,009	36,419±0,006
Li, Whaling et al. (1951) [6]	1.5494±0,0024	25.596±0,008	42.302±0,016	36,372±0,019
Mattauch and Bieri (1954) [2]	1.5473±0,0076	25.6060±0,0047	42.3254±0,0052	36.4086±0,0038

*) Collins, Nier and Johnson, Phys. Rev. 84, 717 (1951).

TABLE 3

Masses of the H, D, He^4 and C^{12} Isotopes*

Investigator	M (H)	M (D)	M (He^4)	M (C^{12})
Ewald (1951) [1]	1,008141±2	2,014732±4	4.003860±12	12.003807±11
Li, Whaling et al. (1951) [6]	1,008142±3	2,014735±6	4.003873±15	12.003804±17
Ogata and Matsuda (1953) [3]	1.008145±2	2,014741±3	4.003879±9	12.003844±6
Nier (1951) [4,5]	1,008146±3 **	2,014778±8	4.003944±19	12.003842±4 **
Mattauch and Bieri (1954) [2]	1,0081459±0,5	2.01474444±0,9	4.0038797±1,6	12.003823±3,3
Data of the present work	1.008142±1	2.014736±2	4.003872±4	12.003820±5

*) Experimental errors are given in μa.m.u.
**) Collins, Nier and Johnson, Phys. Rev. 84, 717 (1951).

The final results of the measurement ΔM of these doublets are given in Table 2. (The values for the mass differences of the ions are given in thousandths of a.m.u.). The calculated values of the masses of H, D, He^4 and C^{12} are given in Table 3. In the same tables are given corresponding data obtained in recent years by other workers.

Conclusion

The values of the isotopic masses of H and D obtained in this work agree sufficiently well with the data obtained by Li, Whaling et al. [6] from nuclear reactions, and by Ewald [1] with a mass-spectrograph. The deviations of our values of the masses of H and D from the data obtained by Ogata and Matsuda [3], by Mattauch and Bieri [2], and by Nier and collaborators [4, 5] do not exceed the possible errors. The value for the mass of the He^4 isotope obtained by us agrees with the value obtained from nuclear reactions, and within the limits of experimental error agrees with the data of Ewald, Nier, Ogata and Matsuda. The values of the mass of the C^{12} isotope as may be seen from Table 3 may be divided into two groups (Fig. 4). The values for the mass of C^{12} obtained by Nier [4, 5] and by Ogata and Matsuda [3], differ from the corresponding data of Ewald [1], Mattauch, Bieri [2], Li, Whaling et al. [6] and Dzhelepov and Zyryanova [7] by about 3×10^{-5} a.m.u. with an experimental error of less than 10^{-5} a.m.u.

The value obtained by us for the mass of C^{12} almost coincides with the data of Mattauch and Bieri and within experimental error agrees well with the values obtained by Li, Whaling et al. [6] and by Ewald [1]. Such a good agreement of the values of the mass of C^{12} obtained by different independent methods indicates that the data for the mass of C^{12} in this group of measurements are the more reliable ones.

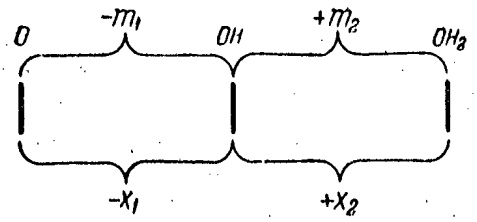

Fig. 5. Spectrum for the determination of the dispersion of the scale.

At the same time the existence of such a discrepancy between the data of this group of measurements, and the data of Nier [4, 5] and Ogata and Matsuda [3] points to the presence of still investigated systematic errors due most likely to the ion-optical peculiarities of the mass-spectrographs.

The author consider it to be their duty to express their gratitude to M. Ardenne for valuable advice and for his interest in this work, and also to G. Jaeger, I. A. Chukhin, and V. Roggenbuk for the help given by them in adjusting the equipment.

Note: After the present article was completed a communication by Nier and collaborators [10] appeared giving new preliminary values of masses obtained on a new mass-spectrometer with a maximum resolving power of approximately 100,000: H = 1.0081439 ± 5; D = 2.0147380 ± 10; C^{12} = 12.0038174 ± 18.

LITERATURE CITED

[1] H. Ewald, Z. Naturforsch, 6a, 293 (1951).

[2] J. Mattauch and R. Bieri, Z. Naturforsch, 9a, 303 (1954).

[3] K. Ogata and H. Matsuda, Phys. Rev. 89, 27 (1953).

[4] A. Nier and T. Roberts, Phys. Rev. 81, 507 (1951).

[5] A. Nier, Phys. Rev. 81, 624 (1951).

[6] C. Li, W. Whaling, W. Fowler and C. Lauritsen, Phys. Rev. 83, 512 (1951).

[7] B. S. Dzhelepov and L. N. Zyryanova, Uspekhi Fiz. Nauk 48, 4651 (1952).

[8] Drummond, Phys. Rev. 97, 1004 (1955).

[9] A. H. Wapstra, Physica 21, 367 (1955).

[10] A. Nier et al., Bull. Amer. Phys. Soc. No. 7, 18 (1955).

INVESTIGATION OF GAMMA-RAYS EMITTED BY NUCLEI OF CALCIUM, NICKEL AND POTASSIUM ON CAPTURING THERMAL NEUTRONS

B. P. Adyasevich, L. V. Groshev, A. M. Demidov, V. N. Lutsenko

The energies and intensities of γ-rays emitted by nuclei of calcium, nickel and potassium when they capture thermal neutrons were measured by a magnetic spectrometer which analyzes the compton-electrons. The γ-ray spectra were studied in the energy interval 0.25-12 Mev. The intensities of γ-rays are expressed in terms of the number of γ-quanta emitted per 100 neutrons captured. Possible γ-transition diagrams have been constructed for Ca^{41}, Ni^{59}, Ni^{61} and K^{40} nuclei.

The present work is a continuation of the investigation of γ-rays emitted by nuclei on capturing thermal neutrons which is being carried out with the RFT reactor of the Academy of Sciences of the USSR. The experimental conditions, the method of measurement and the spectrometer have all been described before [1]. Below results are given on the investigation of γ-rays from the nuclei of calcium, nickel and potassium.

Calcium

For the measurement of γ-rays emitted on neutron capture by calcium of natural isotopic composition a sample of CaF_2 of 1.7 kg weight was used. In addition the γ-spectrum was investigated for a sample enriched in the Ca^{40} isotope. In this case the salt $CaCO_3$ was used in the amount of 360 g. Before measurements were made the samples were specially purified from small chlorine impurities which, as was shown by preliminary measurements, could make an appreciable contribution to the spectrum because of the large neutron absorption cross section for chlorine.

TABLE 1

Isotope	Composition of natural mixture in %	Composition of enriched sample in %	Isotopic σ in barns	Atomic σ in barns	Neutron binding energy in the product nucleus in Mev
Ca^{40}	96.82	99.9	0.22	0.21	8.367 ± 0.01
Ca^{42}	0.64	~ 0.03	39.7	0.25	7.93 ± 0.02
Ca^{43}	0.129	< 0.005	—	—	—
Ca^{44}	2.13	~ 0.05	0.63*)	0.013	11.3 ± 0.07
Ca^{46}	0.0032	< 0.005	0.25*)	0.0008	—
Ca^{48}	0.178	< 0.03	1.1 *)	0.002	—

* Activation cross section.

Table 1 gives the isotopic compositions for the samples investigated, and also the thermal neutron capture cross sections by the different calcium isotopes as found in the literature, and also the neutron binding energies [2, 4].

The thermal neutron capture cross section is not known for Ca^{43}. On the basis of the data given in the table one may expect that the γ-ray spectrum emitted when neutrons are captured by the natural mixture of the isotopes of calcium will consist principally of the γ-rays of Ca^{41} and Ca^{43} since the capture cross section for the natural mixture is equal to 0.43 ± 0.02 barns.

The γ-ray spectrum of Ca was studied in the energy range 0.25-8.5 Mev. The intensity of γ-rays with an energy > 6.6 Mev does not exceed 0.5 γ-quantum per 100 neutrons captured.

Fig. 1 and 2 show the directly observed γ-ray spectra for the samples of CaF_2 and $Ca^{40}CO_3$. Values of $H\rho$ in oersted-cm are plotted along the horizontal axis along the lower edge of the figures, and values of the γ-ray energy in Mev along the upper edge. The numbers of coincidences observed in 10 minutes are plotted along the vertical axis. They are obtained after subtracting the background determined by the number of coincidences in

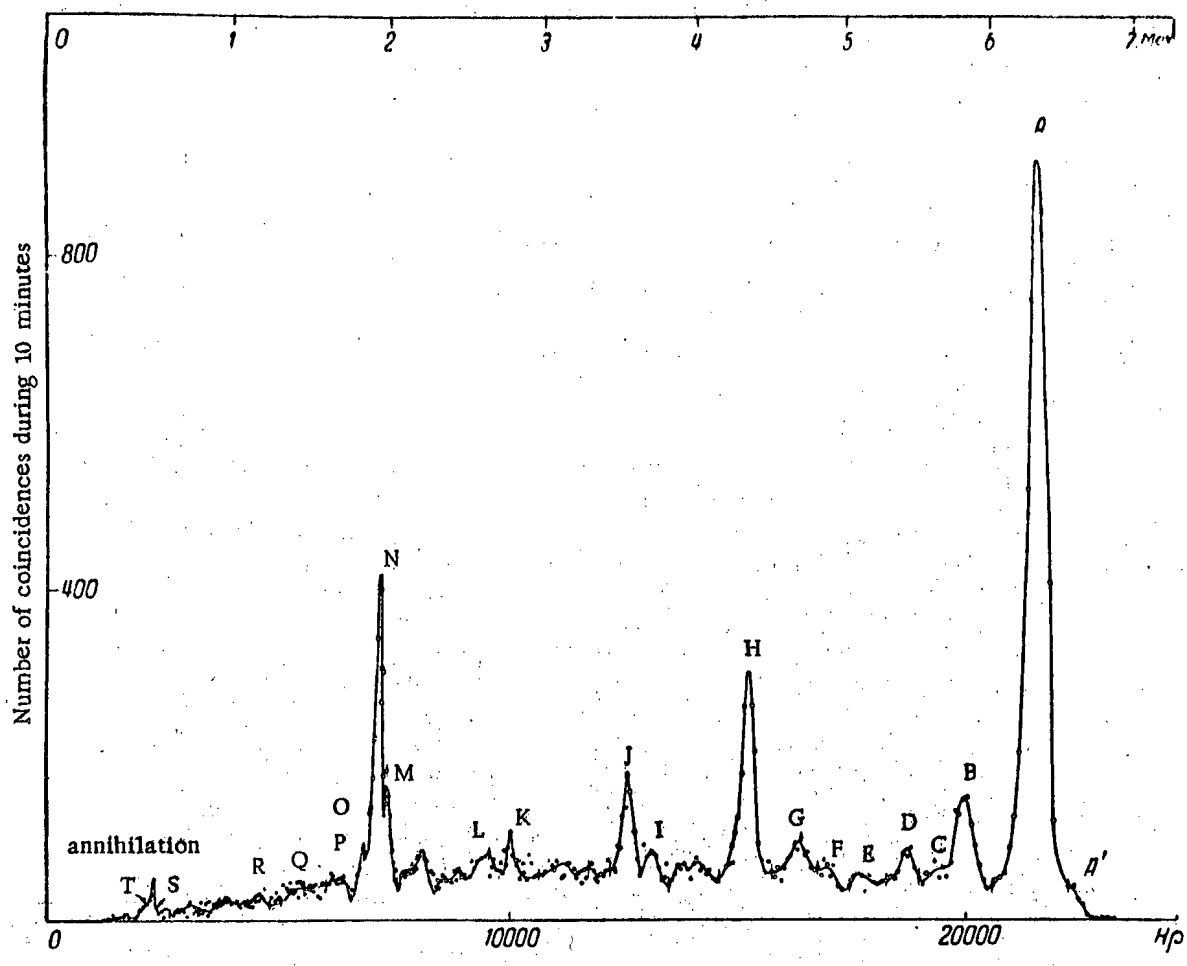

Fig. 1. The directly observed spectrum of γ-rays from CaF_2.

the absence of the sample, and by introducing a correction for the number of electrons from pairs formed by the γ-rays in the radiation along with the Compton electrons.

Fig. 3 shows the corrected γ-ray spectrum for CaF_2. The energy of the γ-rays in Mev is plotted horizontally, and the values of $\nu(E) \cdot H\rho$ are plotted vertically (differing from reference [1] where $\nu(E)$ was plotted vertically). The quantity $\nu(E)$ gives the number of quanta per single neutron capture and per unit energy interval for the γ-rays (1 Mev). The use of the quantity $\nu(E) \cdot H\rho$ is convenient because in this case over a wide energy interval (1.8-10 Mev) the height of the peak is approximately proportional to the intensity of the γ-line as long as the quantity $\frac{\delta}{H\rho}$, where δ is the half-width of the peak, remains constant.

Table 2 gives values of the energy and the intensity of the γ-rays for the CaF_2 and the $Ca^{40}CO_3$ samples obtained in the present work, and also data of other investigators. The intensities of calcium γ-rays are expressed in terms of the numbers of γ-quanta per 100 captured neutrons. The γ-lines given in Table 2 account for approximately 5% of the total energy radiated by calcium nuclei after capturing thermal neutrons.

The determination of the number of quanta per neutron capture was carried out both by normalizing the radiated energy to the neutron binding energy, and also by a comparison in the spectrum of a mixture of nickel and of calcium fluoride of the intensities of γ-lines of 6.4 Mev for the natural mixture of the calcium isotopes and of 8.99 Mev for nickel [1]. In the second method the intensity of nickel γ-rays of energy 8.99 Mev was taken to be equal to 28 γ-quanta per 100 captures (see below), $\sigma_{Ca} = 0{,}43$ barn, $\sigma_{Ni} = 4.5$ barns. The following values of the intensity (number of quanta per 100 captures) of the calcium γ-rays of energy 6.4 Mev were obtained by the methods enumerated above:

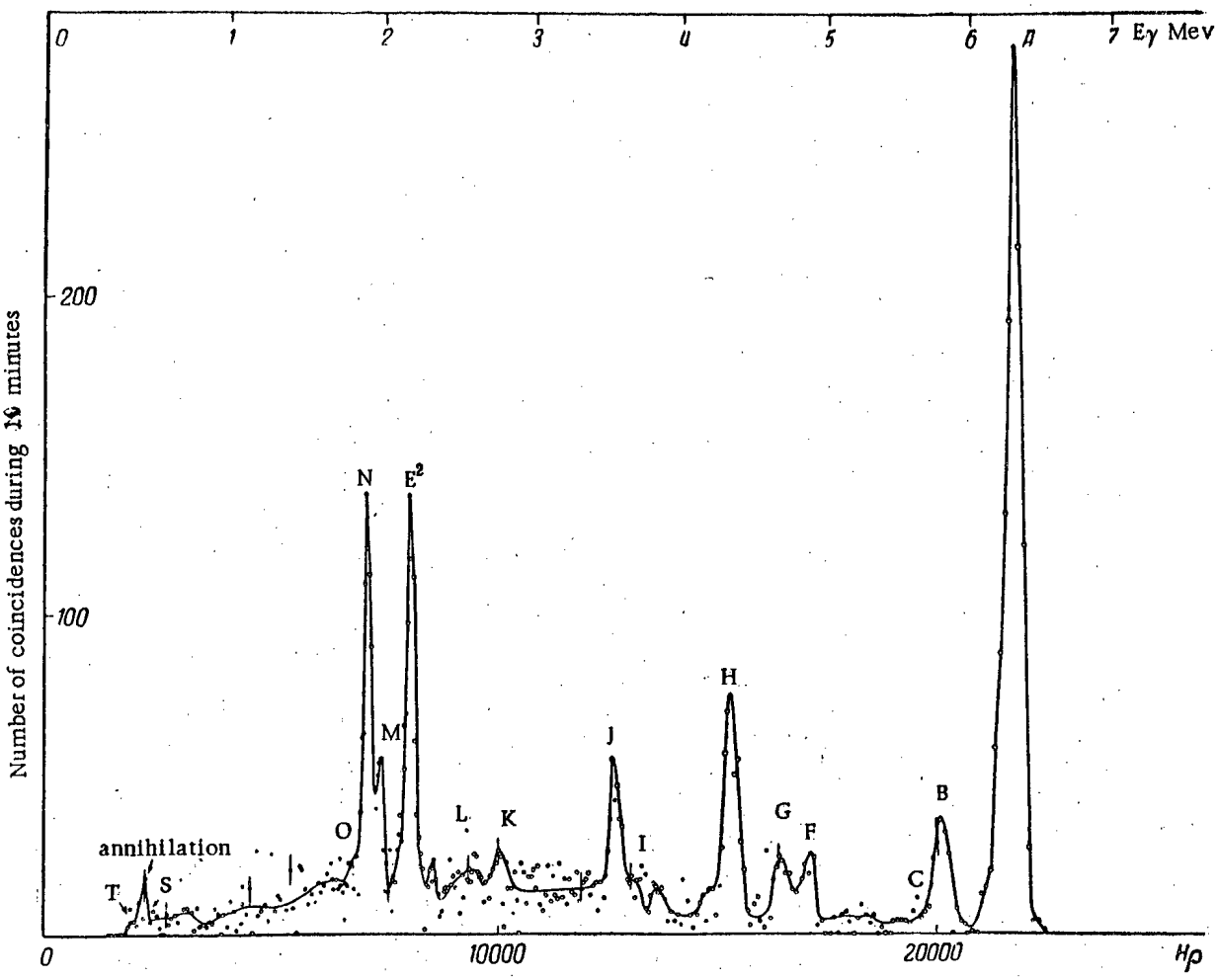

Fig. 2. The directly observed spectrum of γ-rays from $Ca^{40}CO_3$.

1) CaF_2 spectrum —22;

2) $Ca^{40}CO_3$ spectrum —25;

3) comparison of Ni and Ca γ-rays —25.

These values agree among themselves within experimental error which is equal to 10-15%.

Already a simple comparison of the spectra of Figs. 1 and 2 shows that all the lines prominent in the CaF_2 spectrum are also present in the $Ca^{40}CO_3$ spectrum, and vice versa (the 2.23 Mev line in Fig. 2 corresponds to the capture of neutrons by hydrogen present in the container for the enriched sample). The only exceptions are two low intensity lines in the spectrum of CaF_2 of energy 5.5 and 5.15 Mev which apparently are emitted by other calcium isotopes. Their occurence can not be explained by the presence of fluorine since they also occur in the spectrum of CaO which had been measured earlier both by us, and by Kinsey et al. [3]. A comparison of the spectra of the natural mixture of the calcium isotopes and the sample enriched in Ca^{40} shows that the most intense lines with energies 6.4; 5.90; 4.42; 3.60; 2.00 and 1.95 Mev should be ascribed to the Ca^{41} isotope. From the corrected spectra one may estimate what part of the integral $\int \nu(E)\, E\, dE$ taken over the whole spectrum corresponds to the γ-lines listed above. A comparison of the quantities obtained in this way for the two samples of calcium allows one to determine that fraction of the energy which in the spectrum of the natural isotope mixture does not belong to Ca^{41}; this in turn permits one to estimate the upper limit on the magnitude of the radiative capture cross section of Ca^{42} for thermal neutrons. The isotopic cross-section for radiative capture computed in this manner turns out to be not greater than $6.6\ ^{+3}_{-6}$ barns, which is clearly contradictory to the data of Pomerance [4] quoted in Table 1. The reason for this disagreement remains unclear to us.

TABLE 2

Results of the present work				Radiating nucleus	Results of Kinsey et al. [3]		Luminescent spectrometers
Line designation	γ-ray energy in Mev	intensity per 100 captures in quanta			γ-ray energy in Mev	intensity in quanta per 100 captures	
		in Ca	in Ca^{40}				
					7.83±0.05	1	8.2 [8]
					7.43±0.05	1.4	
A'	6,6±0,015	0.7	—	F^{20}			
A	6.406±0,015	22	25	Ca^{41}	6.42±0.03	83	6.8 [8]
B	5.904±0,030	3.8	4.4	Ca^{41}	5.89±0.03	11	
C	5.696±0,030	1.2	1.4	Ca^{41}	5.66±0.06	3	
D	5.50±0,035	1.2	—	(Ca^{43})	5.49±0.05	4	
E	5.15±0,035	0.9	—	(Ca^{43})			
F	4.944±0,030	2.3	3.0	Ca^{41}	4.95±0.03	8	
G	4.764±0,030	2.5	2.9	Ca^{41}	4.76±0.03	6	
H	4.418±0,015	12.3	14.2	Ca^{41}	4.45±0.05	30	
I	3.762±0,020	1.8	2	Ca^{41}			
J	3.60±0,010	6.4	7.4	Ca^{41}	3.62±0.05	16	
K	2.810±0,035	⩾3.6	⩾4.2	Ca^{41}			
L	2.660±0,050	⩾2.0	⩾2.3	Ca^{41}			
	2.230±0,010			D^2			
M	2.004±0,010	12.7	14.7	Ca^{41}			
N	1.944±0,008	39	45	Ca^{41}			1,93 [9]
O	1.844±0,015	6.4	7.4	Ca^{41}			
P	1.790±0,015	⩾3.6	⩾4.2				
Q	~1,48	⩾3.2	⩾3.7				
R	~1,2	⩾4.8	⩾5.5				
S	0.532±0,010	⩾5	⩾6	Ca^{41}			
	0.511±0,005			annihil.			
T	0.463±0,010	⩾9	⩾10	Ca^{41}			

The intensities of the γ-lines quoted in Table 2 which were obtained by Kinsey et al. [3] differ considerably from those obtained by us. In this connection it should be noted that the data of Kinsey et al. were obtained with the old sensitivity curve for their apparatus which was later recalculated by them. In a later paper [5] by these authors a value is quoted for the intensity of the 6.4 Mev γ-line which is much closer to our results: 40 γ-quanta per 100 neutrons captured in the natural mixture of the calcium isotopes.

The energy levels for the Ca^{41} nucleus have been repeatedly studied by the (d, p) reaction. They had been studied by Braams [6] using magnetic analysis of the protons up to an energy of 4 Mev. In the work of Holt and Marsham [7] two more levels were found at higher energies. All these levels are shown in Fig. 4. There we also show a γ-transition scheme according to our data for the Ca^{41} nucleus decaying from the initial state formed by the capute of a thermal neutron. The numbers alongside the arrows representing the γ-transitions denote their intensities expressed as the number of γ-quanta per 100 neutrons captured in Ca^{40}. Underneath the transition scheme the letter designations of the lines are given. At the right side of the transition scheme are given values of orbital angular momentum of the neutron l_n with which it is captured into the given level in the (d,p) reaction, the value of the angular momentum and of the parity I^{π} of the given state, and also its nomenclature according to the shell model. All this information is taken from the work of Holt and Marsham [7].

The following should be noted in regard to the proposed γ-transition scheme for the Ca^{41} nucleus:

1. The presence in the unresolved part of the spectrum of a large number of γ-lines with an energy less than 4 Mev indicates that in the Ca^{41} nucleus apparently there is a large number of transitions to levels of energy higher than 4 Mev.

2. The relatively high intensities of γ-transitions to levels with excitation energies of 3.95; 4.76 and 5.72 Mev do not agree with the value of the orbital angular momentum $l_n = 2$ obtained by Holt and Marsham from an analysis of the proton angular distribution in the (d,p) reaction. Very likely this is connected either with an incorrect assignment of l_n, or with a lack of uniqueness of the γ-transition scheme constructed by us.

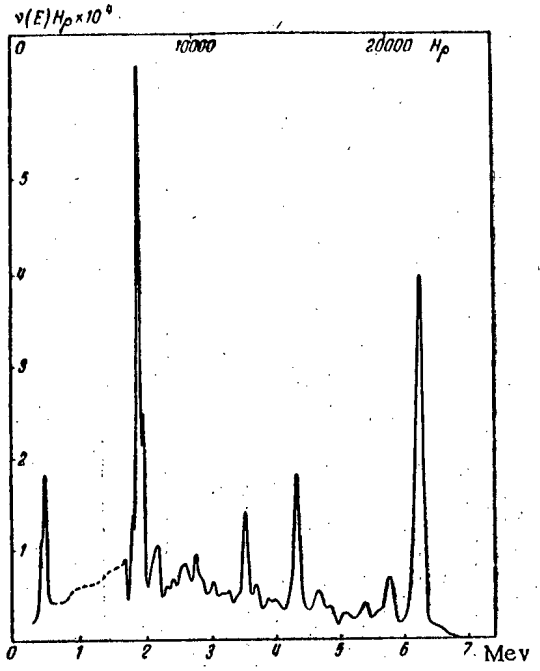

Fig. 3. The corrected spectrum of the γ-rays from CaF_2.

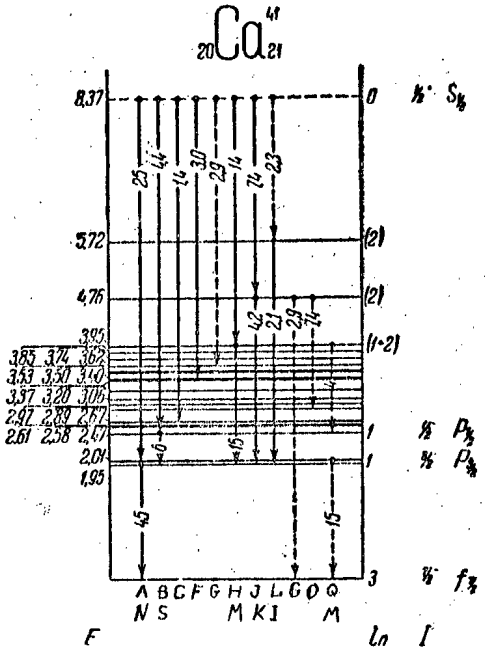

Fig. 4. γ-transition scheme for the Ca^{41} nucleus.

3. For levels of energy 1.95; 2.47 Mev the value $l_n = 1$ was obtained in reference [7]. Comparing the intensities of transitions from the 2.47 Mev level one may determine for it the value of the total angular momentum. In spite of the fact that the transition to the ground level may not be picked out from the unresolved part of the spectrum one may nevertheless assert that its intensity is less by at least a factor six than that of the transition to the 1.95 Mev level. From this it follows that the 2.47 Mev level has the label 1/2 and not 3/2, since in the latter case in accordance with an estimate made with the aid of Weisskopf's formula [10] the ratio of the intensities of the transitions would be equal to 13 instead of the upper limit 1/6 which follows from our data.

4. The intensity of the transition from the initial to the ground state does not exceed 0.02 quanta per 100 neutron captures which is explained by the large difference in the angular momenta of these two states.

Nickel

The measurements were made on a sample of metallic nickel of 2 kg weight.

In Table 3 are given some data on the nickel isotopes.

The total capture cross section of nickel for thermal neutrons was taken to be 4-5 barns. The spectrum of the γ-rays from nickel was investigated in the energy range 0.25-10 Mev. Fig. 5 shows the directly observed and Fig. 6 the corrected spectrum of the nickel γ-rays. At the left of Fig. 5 is given a part of the spectrum in the energy range below 0.5 Mev which was observed in a separate experiment with a thinner radiator – of 25μ thickness instead of 100μ.

Table 4 gives the energies and the intensities of the nickel γ-rays obtained in the present work and also in the work of Kinsey et al. [11]. The determination of the number of γ-quanta per neutron capture was carried out by normalizing the radiated energy to the binding energies of the last neutron in the various nickel isotopes taking into account the percentage contribution of the individual isotopes to the capture cross section of the natural mixture.

From Table 4 it may be seen that the values of the energies and the line intensities obtained by us agree within experimental error with the data of Kinsey et al.; the γ-rays listed in Table 4 carry away 65% of the energy radiated by the nickel isotopes in the reaction (nγ) with thermal neutrons.

TABLE 3

Isotope	Composition of the natural mixture in %	Contribution to the capture cross-section for thermal neutrons (%)	Neutron binding energy in the product nucleus in Mev
Ni^{59}	67.9	69	8.997±0.005 [11] 8.996±0.02 [12]
Ni^{60}	26.2	16	8.31±0.34 *); 8.466±0.03 [14]
Ni^{61}	1.2	0.5	
Ni^{62}	3.7	13	6.66±0.1 **); 6.02±0.14 ***)
Ni^{64}	1.0	0.4	

* Deduced from the data of [15].

** Calculated from Cu^{63} (γn) Cu^{62} with Q = 10.65 ± ± 0.05 Mev [16];
calculated from $Ni^{63} \xrightarrow{\beta^-} Cu^{62}$ with Q = 0.063 Mev [17];
calculated from $Cu^{62} \xrightarrow{\beta+} Ni^{62}$ with Q = 3.93 Mev [17].

*** Calculated from the mass of Ni^{62} and Cu^{63} [15] and from the decay of $Ni^{63} \xrightarrow{\beta^-} Cu^{63}$.

When nickel is irradiated with neutrons the radioactive isotopes Ni^{59} and Ni^{65} are formed. The γ-rays accompanying their decay should not appear in the spectrum since the first isotope has a very long half-life ($T_{1/2} = 5 \times 10^4$ years), and the second gives only a small percentage contribution to the total capture cross section of nickel for thermal neutrons.

The presence of three nickel isotopes (Ni^{58}, Ni^{60} and Ni^{62}) which capture neutrons strongly, and also the complexity of their γ-spectra considerably increases the difficulty of identifying the spectral lines. We have succeeded in identifying only some of the more intense lines.

In order to construct the γ-transition scheme in the Ni^{59} isotope (Fig. 7) we used the energy level schemes found in (d, p) reaction on Ni^{58} [12, 18], and (p, n) reaction on Co^{59} [19], and also in the study of the β^+-decay of Cu^{59} [20] which are given in the same figure. The intensities of the γ-rays are expressed per 100 captures in the given isotope. We also give these the characteristics of certain of these levels which have been established by Pratt [18] through a study of the angular distribution of the protons in the (d, p) reaction. The values of the level energies given at the right have been obtained from the energies of the corresponding γ-rays.

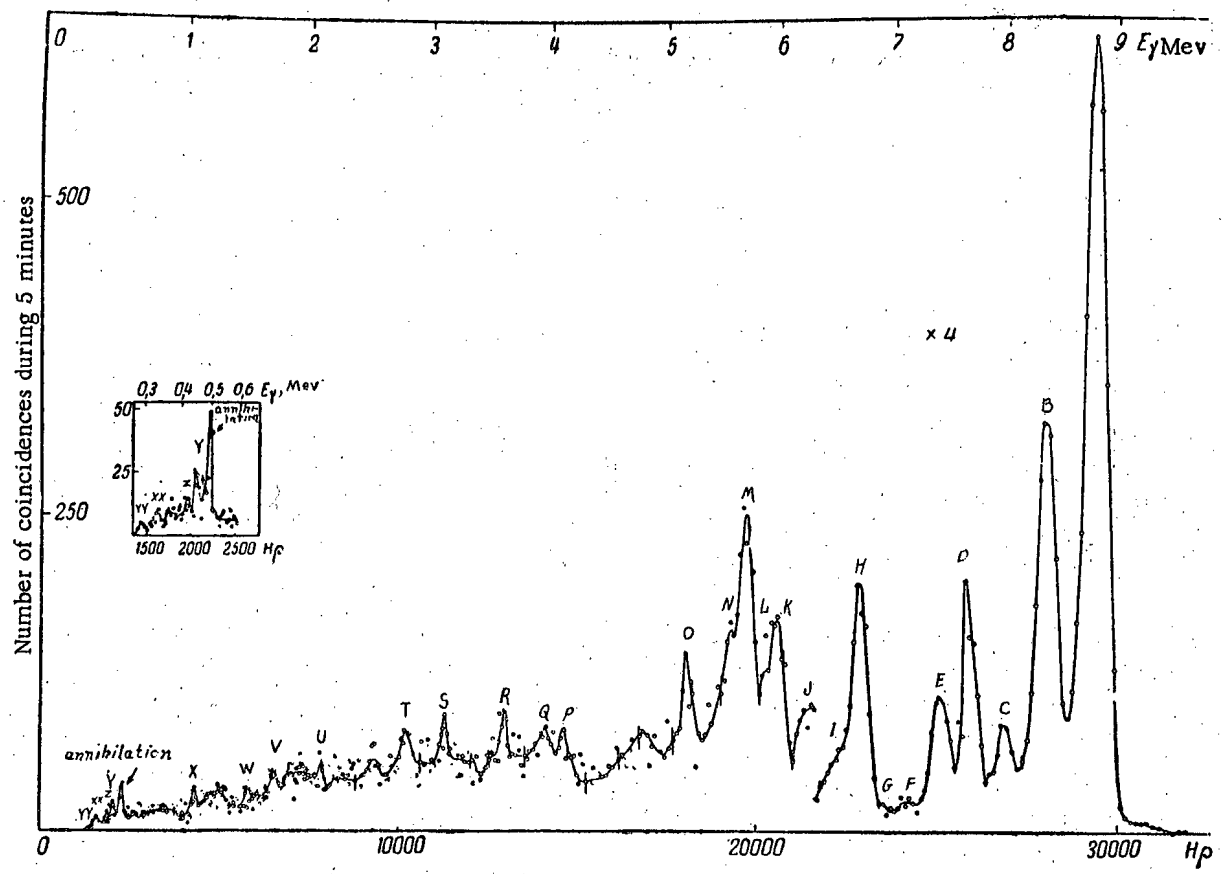

Fig. 5. The directly observed spectrum of γ-rays from nickel.

TABLE 4

Results of the present work			Radiating nucleus	Results of Kinsey's work [11]	
Line designation	γ-ray energy in Mev	I*		γ-ray energy in Mev	I*
A	8,996±0.010	28	Ni^{59}	8,997±0,005	35
B	8.505±0.025	12.3	Ni^{59}	8.532±0,008	14
C	8.095±0.030	2.5	Ni^{59}	8.119±0,010	2.8
D	7.825±0.020	6	Ni^{61}	7.817±0,008	6.5
E	7.575±0.030	5.1		7.528±0,011	4
F	7.19 ±0.050	0.7		7.22 ±0,020	0.5
G	7.015±0.050	0.6		7.05 ±0,020	0,5
H	6.842±0.020	10.8	Ni^{59}	6,839±0,010	9
I	6.639±0.030	2.8		6,58 ±0,020	2
J	6.315±0.030	1.0		6.34 ±0,020	0.6
K	6.135±0.025	1.6		6,10 ±0,020	1,0
L	6.030±0.030	1.3		5,99 ±0,020	0.3
M	5.842±0.025	2.6		5,82 ±0,020	3
N	5.725±0.030	⩾1.3		5,70 ±0,020	0,4
O	5.312±0.030	⩾1.6		5,31 ±0,020	1
P	(4.20±0.04) **	⩾0.7			
Q	(4.05±0.04)	⩾1			
R	(3.67±0.03)	⩾1			
S	(3.17±0.06)	⩾1			
T	(3.03±0.04)	⩾1			
U	(2.15±0.03)	⩾2			
V	(1.74±0.03)	⩾1			
W	(1.53±0.03)	⩾1			
X	(1.10±0.03)	⩾2			
Y	0.467±0.008	⩾6	Ni^{59}		
Z	0.436±0.015	⩾3			
XX	0.330±0.015	⩾7	Ni^{59}		
YY	0.280±0.015	⩾3.5			

* Intensity in quanta per 100 neutrons captured in the natural isotopic mixture.

** The energies are shown bracketed for those γ-lines whose existence has not been established with sufficient certainty.

There is very little information available on the energy levels of the Ni^{61} nucleus. In the study of the (d,p) reaction excited levels were found at 0.61 ± 0.04 Mev [21] and 0.75 ± 0.1 Mev [18]. In the papers of Owen et al. [22] and Smith et al. [23] the β^+ decay of Cu^{61} and the β^--decay of Co^{61} were studied. Fig. 8 gives the disintegration schemes obtained in those investigations. Since all the β-transitions shown in Fig. 8 by solid lines are allowed it follows from these schemes that the ground level of Ni^{61} is described by $5/2^-$, while the excited state with the energy 0.655 Mev is described by either $1/2^-$ or $3/2^-$. Let us also note that the value $5/2^-$ for the angular momentum and for the parity of the ground state of Ni^{61} follows from the shell model.

In the work of Kinsey et al. [11] and of Pratt [18] the intense line B was interpreted as the transition from the initial state to the ground state of the Ni^{61} nucleus whose angular momentum was assumed to be $3/2^-$. Since the value $5/2^-$ is more probable the indicated transition corresponds to a change in the angular momentum of two units and must therefore be very weak. In our case we have the γ-transition Y with the energy 0.467 Mev. The cascade from the transitions B + Y has the energy of 8.972 ± 0.033 Mev which is close to the binding energy of the last neutron in Ni^{59}. This gives us some basis for ascribing the γ-transition B to the Ni^{59} nucleus. The line D may correspond to the transition from the initial state of Ni^{61} to the level of energy 0.655 Mev. The comparatively high intensity of the D line (~38 quanta per 100 captures in Ni^{60}) agrees well with the value $1/2^-$ or $3/2^-$ for the angular momentum and the parity of the 0.655 Mev level. There is no information available on the excited states of the Ni^{63} nucleus.

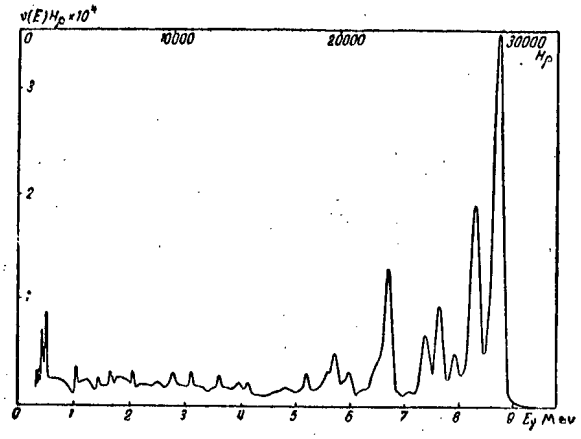

Fig. 6. The corrected spectrum of γ -rays from nickel.

Potassium

The sample weighing 1.5 kg consisted of the salt K_2CO_3. The spectrum of the γ -rays was investigated in the energy range 0.25-8 Mev. The directly observed and the corrected spectra of K_2CO_3 are given in Fig. 9 and 10.

Table 5 gives some data on the stable isotopes of potassium [2]. The total capture cross section for thermal neutrons of the natural mixture of potassium isotopes was taken to be equal to 2.05 ± 0.1 barn.

The values of the energies and of the intensities of the γ -rays obtained by us are given in Table 6 together with the results of other investigations. The reduction of the intensities to the number of γ -quanta per neutron capture was accomplished by means of

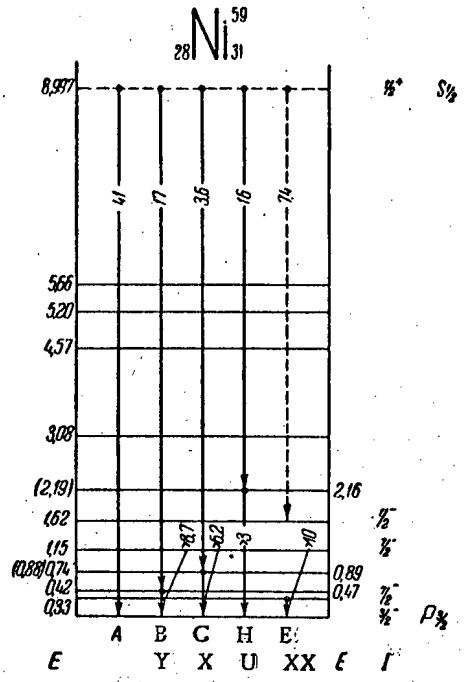

Fig. 7. γ -Transition scheme for the Ni^{59} nucleus.

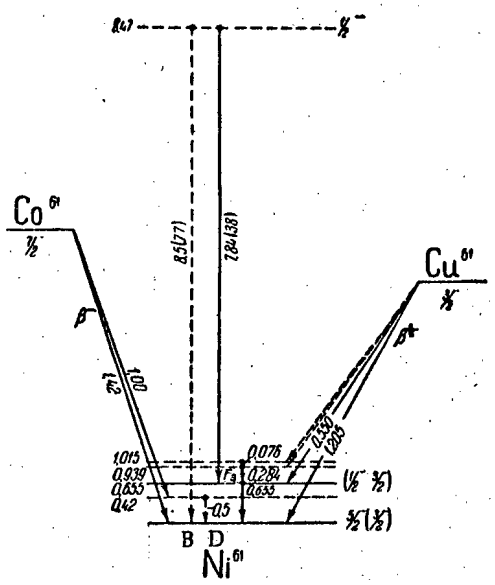

Fig. 8. γ -Transition scheme for the Ni^{61} nucleus.

normalizing the radiated energy to the neutron binding energy. The γ -rays given in Table 6 carry away 60% of the energy radiated by the potassium isotopes on capturing thermal neutrons. From Table 6 it may be seen that within experimental error the results of the present work agree with the results of other workers.

In the spectrum in addition to the γ -rays from neutron capture one should also observe one γ-line of energy 1.51 Mev and of intensity of 1 γ -quantum per 100 neutron captures which is emitted by the Ca^{42} nucleus after the K^{42} nucleus has decayed into it. Apparently it concides with the γ -line of energy 1.51 Mev emitted in the (n, γ) reaction.

In Figs. 9 and 10 dotted lines indicate the region of the spectrum where the γ -line (of energy 7.38 Mev) belonging to Pb^{208} has beensubtracted. The existence of the line B has been established by a repetition of the measurements in which the lead block which shields the sample from the γ -rays coming from the reactor, has been replaced by a bismuth block.

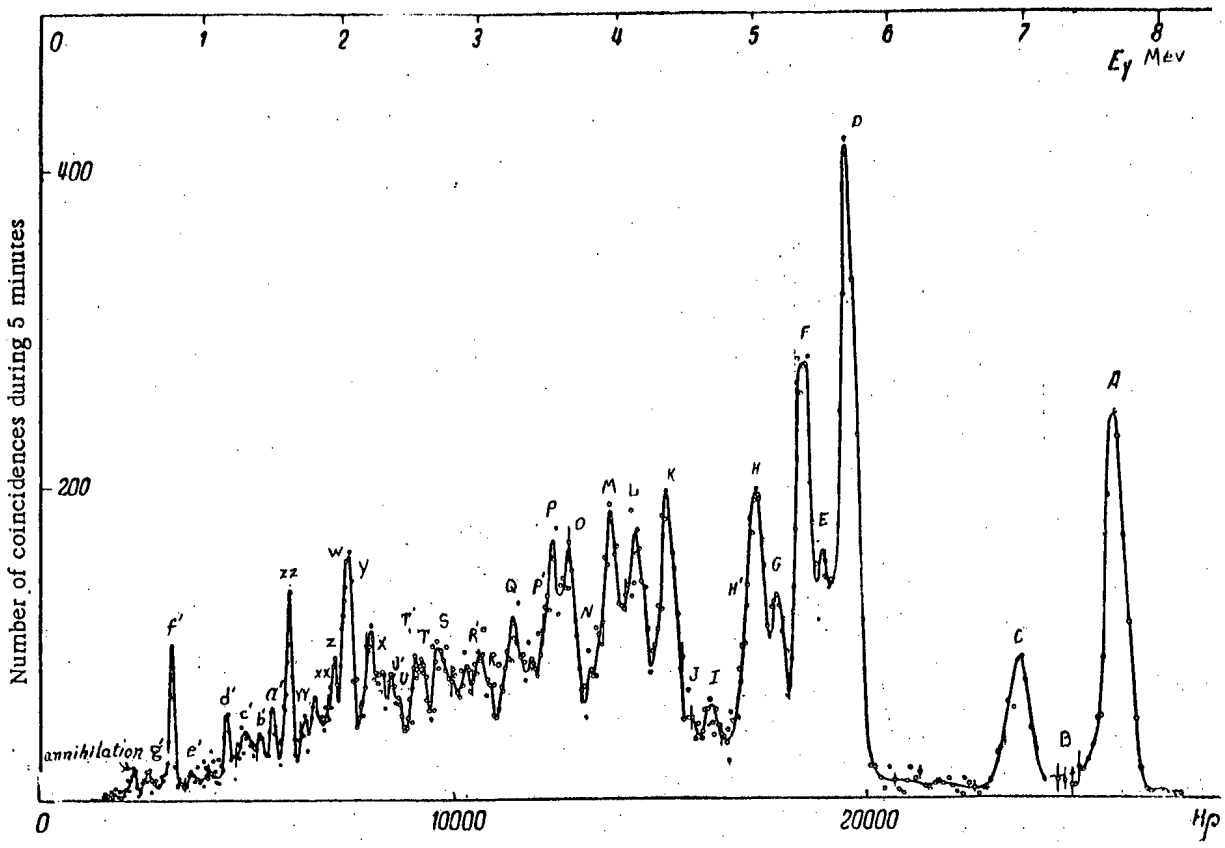

Fig. 9. The directly observed spectrum of the γ-rays from K_2CO_3.

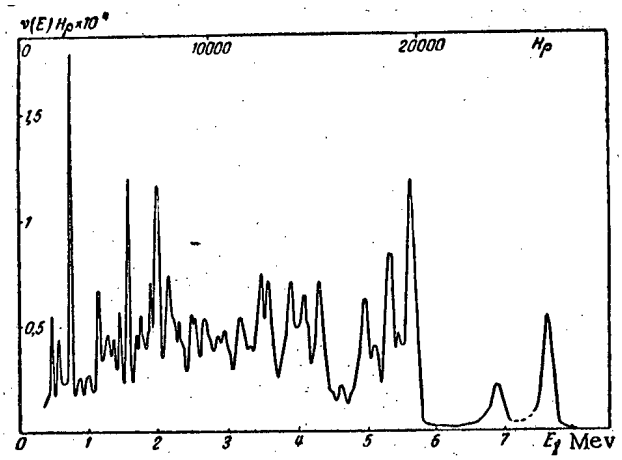

Fig. 10. The corrected spectrum of the γ-rays from K_2CO_3.

TABLE 5

Isotope	Composition of neutral mixture, (%)	σ isot.	Contribution to the thermal neutron capture cross section, %	Neutron binding energy in the product nucleus, in Mev
K^{39}	93.3	1.87	92.25	7.80 ±0.01
K^{40}	0.011	66	0.4	~10
K^{41}	6.68	1.19	4.35	7.35 ± 0.1

The data on the energies of the levels of the K^{40} isotope have been taken from the review article by Endt and Kluyver [2]. In Fig. 11 these lines are represented by solid horizontal lines. In the same figure is given a possible γ-transition scheme for the K^{40} nucleus. To explain the existence of many observed γ-transitions it was necessary to postulate the existence of several as yet undiscovered levels having an excitation energy lying in the region of 2-4Mev. They are represented in Fig. 11 by dotted horizontal lines. At the right side of the diagram are given the characteristics of some of the levels.

TABLE 6

Results of the present work			Radiating isotopes	Results of the work of Kinsey et al. [3], [27]		Result of the work of Braid [9] (γ-ray energy in Mev)
Designation of lines	γ-ray energy in Mev	I*)		γ-ray energy in Mev	I*)	
			K^{41}	9.39 ±0.06	0.02	
			K^{41}	8.45 ±0.02	0.1	
A	7.763±0.01	4.4		7.757±0.008	3.5	
B	7.32 ±0.025	0.2	K^{42}	7.34 ±0.02	0.1	
C	7.000±0.015	1.6		6.994±0.007	1.3	
				6.31 ±0.06	0.3	
D	5.725±0.015	·11		5.740±0.012	6	
	(5.65 ±0.04)	~3		5.66 ±0.02	4	
E	5.515±0.03	~2		5.50 ±0.02	2.5	
F	5.40 ±0.02	6.4		5.38 ±0.03	6	
G	5.25 ±0.05	2.5		5.18 ±0.02	2	
H	5.02 ±0.03	4.5		5.06 ±0.02	3	
H'	4.81 ±0.035	1.5				
I	4.70 ±0.03	~1				
J	4.50 —0.04	~1				
K	4.39 ±0.02	5		4.39 ±0.03		
L	4.11 ±0.03	4		4.18 ±0.05		
M	3.97 ±0.03	5		3.92 ±0.05		
N	3.81 ±0.05	2				
O	3.70 ±0.03	4		3.67 ±0.05		
P	3.60 ±0.03	4				
P'	3.55 ±0.05	~2				
Q	3.40 ±0.05	~4				
R	(3.15 ±0.05)	~1.5				
R'	3.05 ±0.03	~3				
S	2.75 ±0.04	~4				2.80
T	(2.60 ±0.04)	~4				
T'	(2.55 ±0.04)	~4				
U	(2.42 ±0.03)	~2				
U'	(2.37 ±0.03)	~3				
	(2.30 ±0.03)	~3				
Y	2.06 ±0.01	9				
W	2.02 ±0.015	7				2.03
Z	1.95 ±0.02	4				
XX	1.85 ±0.02	~3				
YY	1.75 ±0.02	~3				
ZZ	1.61 ±0.008	13				1.61
a'	1.51 ±0.01	5				
b'	1.40 ±0.02	~2				
c'	1.27 ±0.02	~2				
d'	1.18 ±0.015	7				1.19
e'	0.90 ±0.015	2				
f'	0.77 ±0.007	26				0.77
g'	0.625±0.01	3				

Intensity in quanta

*) Intensity in quanta per 100 neutron captures in the natural mixture of isotopes.

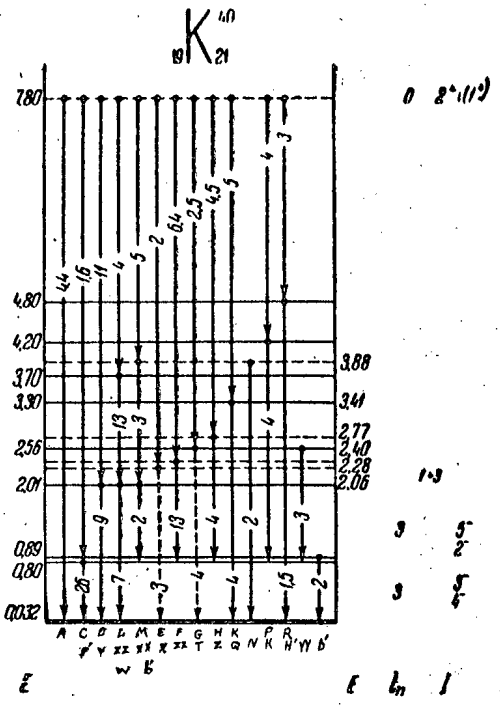

Fig. 11. γ-Transition scheme for the K^{40} nucleus.

The four lower levels of the K^{40} nucleus are of definite interest. In the work of Teplov [24] the values $l_n = 3$ have been obtained for these levels. According to the data of Davis et al. [25] the ground state of the K^{40} nucleus is characterized by 4^-. From the relative intensities of the proton groups in the (d,p) reaction it is possible to establish the character of all four levels, viz. 4^-, 3^-, 2^- and 5^- in order of increasing energy [26]. The values of the total angular momenta so obtained are confirmed by our measurements of the intensities of the γ-rays of K^{40} if one assumes that the initial state is characterized by 2^+.

The characteristics of the four lowest levels of the K^{40} nucleus given above and also the value $l_n = 3$ common to them all give us some basis for supposing that these states form a nuclear quadruplet due to different mutual orientations of the proton in the $(d_{3/2})^{-1}$ state and of the $f_{7/2}$-neutron.

LITERATURE CITED

[1] L. V. Groshev, B. P. Adyasevich, A. M. Demidov, Physical Investigations (Reports of the Soviet delegation at the International Conference on the Peaceful Uses of Atomic Energy) Acad. Sci. USSR Press, 1955, p. 252, and also Report at the session of the Acad. Sci. USSR, July, 1955.

[2] P. M. Endt, J. C. Kluyver, Revs. Modern Phys. 26, 95 (1954).

[3] B. B. Kinsey, G.A.Bartholomew, W. H. Walker, Phys. Rev. 85, 1012 (1952).

[4] H. Pomerance, Phys. Rev. 88, 412 (1952).

[5] B. B. Kinsey, G.A.Bartholomew, Phys. Rev. 93, 1260 (1954).

[6] C. M. Braams, Bull. Am. Phys. Soc. 29, No. 1, 26 (1954).

[7] J. R. Holt, T. N. Marsham, Proc. Phys. Soc. (London) A 66, 565 (1953).

[8] B. Hamermesh, V. Hummel, Phys. Rev. 88, 916 (1952).

[9] T. H. Braid, Phys. Rev. 91, 442A (1953).

[10] V. F. Weisskopf, Phys. Rev. 83, 1073 (1951).

[11] B. B. Kinsey, G.A. Bartholomew, Phys. Rev. 89, 375 (1953).

[12] C. E. McFarland, M. M. Bretsher, F. B. Shull, Phys. Rev. 89, 892 (1953).

[13] A. H. Wapstra, Physica 21, 385 (1955).

[14] D. C. Hoesterey, Note in [13].

[15] T. L. Collins, A. O. Nier, W. H. Johnson, Phys. Rev. 86, 408 (1952).

[16] D. M. vanPatter, W. Whaling, Revs. Modern Phys. 26, 402 (1954).

[17] R. W. King, Revs. Modern Phys. 26, 327 (1954).

[18] W. W. Pratt, Phys. Rev. 95, 1517 (1954).

[19] P. H. Stelson, W. M. Preston, Phys. Rev. 86, 807 (1952).

[20] L. Lindner, G. A. Brinker, A. C. Pieterse, Physica 21, 745 (1955).

[21] D. C. Hoesterey, Phys. Rev. 87, 216 (1952).

[22] G. E. Owen, C. S. Cook, P. H. Owen, Phys. Rev. 78, 686 (1950).

[23] L. A. Smith, R. Haslam, J. Taylor, Phys. Rev. 84, 842 (1951).

[24] I. Teplov, Dissertation, 1954.

[25] L. Davis, Jr.,Darragh E. Nagle, J. R. Zacharias, Phys. Rev. 76, 1068 (1949).

[26] H. A. Enge, Phys. Rev. 94, 730 (1954).

[27] G.A.Bartholomew, B. B. Kinsey, Can. J. Phys. 31, 327 (1953).

INVESTIGATION OF GAMMA-RAYS EMITTED BY NUCLEI OF TITANIUM IRON AND SILICON ON CAPTURING THERMAL NEUTRONS

B. P. Adyasevich, L. V. Groshev, A. M. Demidov

The energies and intensities of γ-rays arising when thermal neutrons are captured in titanium, iron and silicon were measured by a magnetic sprectrometer which analyzes the Compton-electrons. The γ-ray spectra were studied in the energy interval 0.25-12 Mev. The intensities of the γ-rays are expressed in terms of the number of γ-quanta per 100 neutron captures. Possible γ-transition schemes have been constructed for Ti^{49}, Fe^{57} and Si^{29} nuclei.

The present work is a continuation of the study of γ-spectra, emitted by nuclei after capturing thermal neutrons, carried out with the aid of a magnetic γ-spectrometer [1]. In the present paper are given the results of the measurement of the energies and of the intensities of γ-rays emitted by the nuclei of titanium, iron and silicon.

The measurement of the intensity (number of γ-quanta per capture) was carried out by means of normalizing the radiated energy to the binding energy of the neutron in the nucleus under investigation.

Titanium

A cylinder of titanium of 80 mm diameter, 180 mm long and weighing 500 g was used for the measurements. In Table 1 are given data on the percentage content of the isotopes in the natural mixture, and also the binding energy of the last neutron and the contribution of the individual isotopes to the total neutron capture cross section. The total thermal neutron capture cross section was taken equal to 5.8 barns.

The spectrum of the γ-rays of titanium was studied in the energy region 0.25-12 Mev. The directly observed and the corrected spectra of the γ-rays from titanium are shown in Figs. 1 and 2. The energies and the intensities of the γ-lines are given in Table 2. The gamma rays given in Table 2 carry away 90% of the energy radiated by the titanium isotopes. The data on the energies and the intensities of the γ-rays obtained by other investigators agree well with our results (Table 2).

From Table 1 it follows that the spectrum consists essentially of the γ-rays of Ti^{49}. Only γ-rays with energies greater than 7 Mev may be directly attributed to the other isotopes of titanium.

In Fig. 3 is given a possible γ-transition scheme for Ti^{49}. On the left are given energies of the levels found by Pieper [4,11] in studying the reactions Ti^{48} (d, p) Ti^{49}, and on the right are given values of the energies of those levels whose existence is assumed in order to account for certain intense γ-transitions. Dotted lines show those levels whose existence has been assumed by us. On the right side of the diagram are given level characteristics obtained by Bretscher et al. [12]. The following remarks can be made with respect to the γ-transition scheme of Ti^{49}:

1. γ-ray cascades in general end on the level of energy 1.4 Mev from which a transition occurs to the ground level. This is indicated by the high intensity of this last transition (90 γ-quanta per 100 neutron captures).

2. The orbital angular momentum of the neutron for levels with energies of 1.4 and 1.74 Mev is equal to unity [12]. The absence of an intense γ-transition from the 1.74 Mev level to the ground state (its intensity is less than 0.7 γ-quantum per 100 captures) allows one to attribute to it the characteristic $1/2^-$.

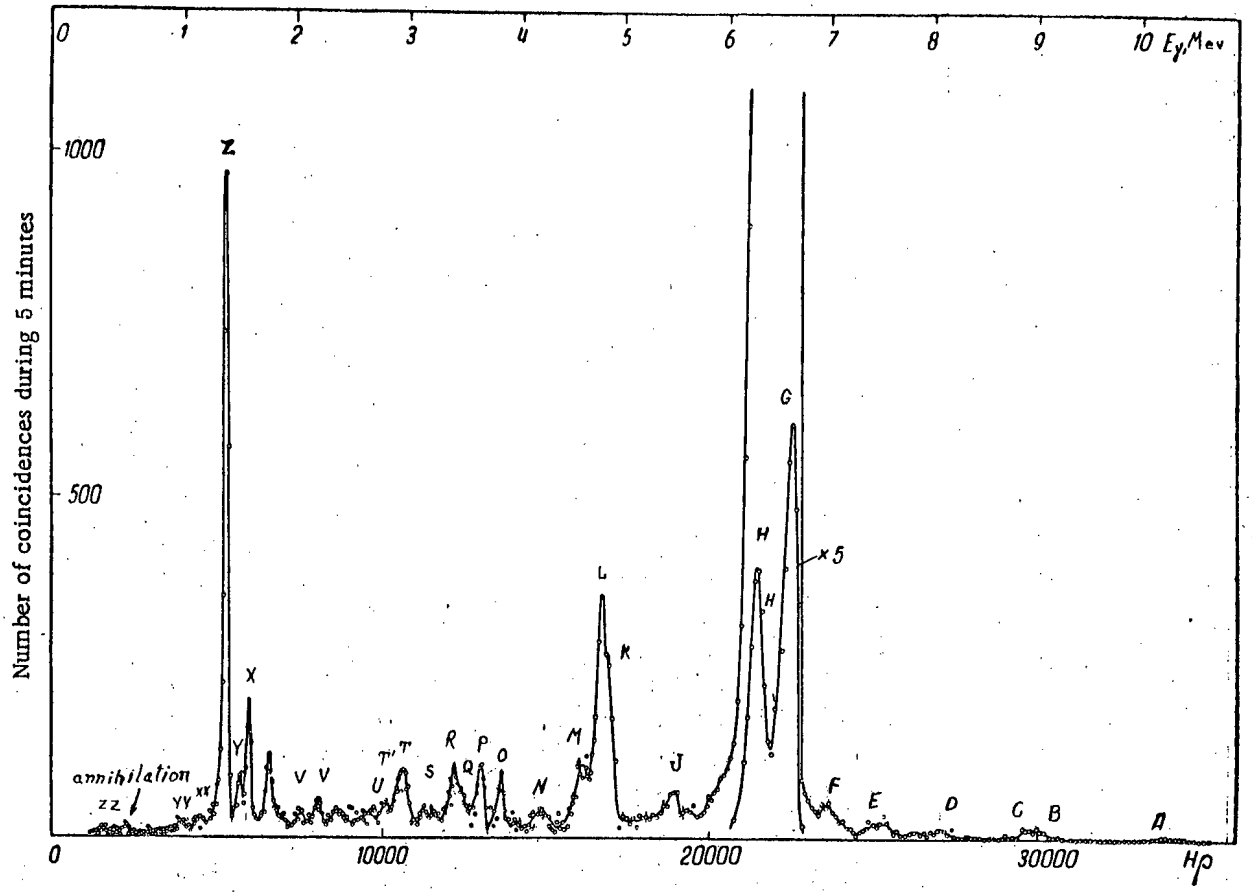

Fig. 1. The directly observed spectrum of γ-rays from titanium.

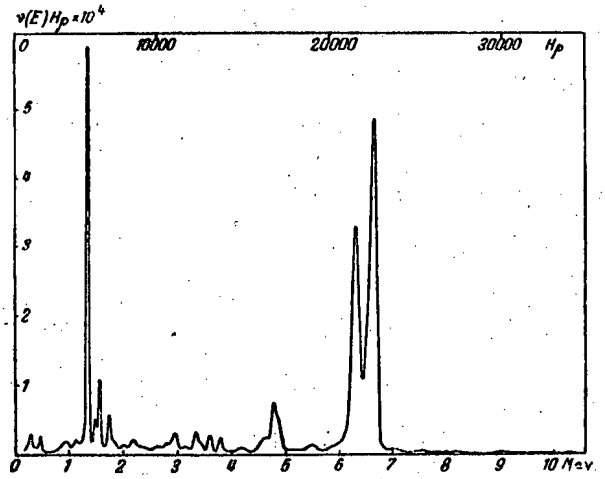

Fig. 2. The corrected spectrum of the γ-rays from titanium.

3. Adding up the energies of the individual γ-transitions we obtain the binding energy of the last neutron in the Ti^{49} nucleus. The value of the binding energy obtained by us (8.153 $\pm$ 0.010 Mev) is very accurate in comparision with those known up till now.

γ-Rays of energies 10.49, 9.39, 9.17 and 8.31 Mev may be emitted by the Ti^{48} nucleus. These transitions correspond to the levels of that isotope found in the study of the β^--decay of Sc^{48} [13] and of the β^+-decay of V^{48} [14], and also of the reaction Ti^{47} (d,p) Ti^{48} [11]. Fig. 4 shows a possible γ-transition scheme

TABLE 1

Isotope	Composition of the natural mixture in %	Binding energy of the neutron in the product nucleus in Mev	Contribution to the thermal neutron capture cross section in %
Ti^{46}	8.0	8.74±0.1 [2]; 8.64±0.11 [3]; 8.67±0.05 [11]	0.8
Ti^{47}	7.8	11.05±0.4 [2]; 11.63±0.11 [3]; 10.36±0.05 [11]	2.1
Ti^{48}	73.4	8.15±0.05 [2]; 7.99±0.08 [3]; 8.04±0.05 [11]	95
Ti^{49}	5.5	10.84±0.05 [11]; 10.99±0.06 [3]	1.6
Ti^{50}	5.3	6.33±0.07 [11]; 7.03±0.2 [5]	0.2

TABLE 2

Results of our work			Data of ref. [6]		Data of ref. [7]—[10] E_γ in Mev					
					[9]	[7]		[8]	[10]	
Designation of the lines	γ-ray energy in Mev	I*	γ-ray energy in Mev	I*	E_γ	E_γ	I*	E_γ	E_γ	I*
A	10.47 ±0.15	0.01								
B	9.39 ±0.05	0.09	9.39 ±0.03	0.1						
C	9.17 ±0.07	0.13	9.19 ±0.03	0.2						
D	8.31 ±0.05	0.2	8.28 ±0.02	0.4						
E	7.66 ±0.04	0.3	7.8 ±0.04	0.4						
F	7.16 ±0.05	0.6	7.38 ±0.01	1.5						
G	6.756±0.01	38	6.756±0.006	53	7					
H	6.56 ±0.03	4	6.53 ±0.02	4						
I	6.42 ±0.02	27.5	6.412±0.006	32						
J	5.67 ±0.06	0.8	5.65 ±0.03	0.4						
K	4.96 ±0.02	2.7	4.96 ±0.01	3.5						
L	4.875±0.02	5.2	4.88 ±0.01	5.0	5					
M	4.68 ±0.03	2	4.67 ±0.03	1.4						
N	(4.3 ±0.06)	0.6								
O	3.86 ±0.02	2.1								
P	3.65 ±0.02	2.4								
Q	3.5 ±0.03	1.2								
R	3.39 ±0.03	2.6								
S	3.20 ±0.04	1.3								
T	3.02 ±0.04	2.8								
T'	2.95 ±0.04	1.5								
U	2.83 ±0.04	1.5								
V	2.22 ±0.03	2.85								
V'	2.08 ±0.03	2.4								
W	1.78 ±0.02	7.5				1.78	7	1.75		
X	1.60 ±0.01	13.0				1.59	13	1.58—1.53		
Y	1.51 ±0.01	5.2				1.50	5			
Z	1.39 ±0.005	85			1.38	1.385	90	1.39	1.4	100
XX	1.18 ±0.02	2.8						1.10—1.06		
YY	1.03 ±0.02	5.7			1.0					
ZZ	0.35 ±0.005	24				0.346		0.334	0.33	37

* Intensity in quanta per 100 neutron captures in the natural mixture of isotopes.

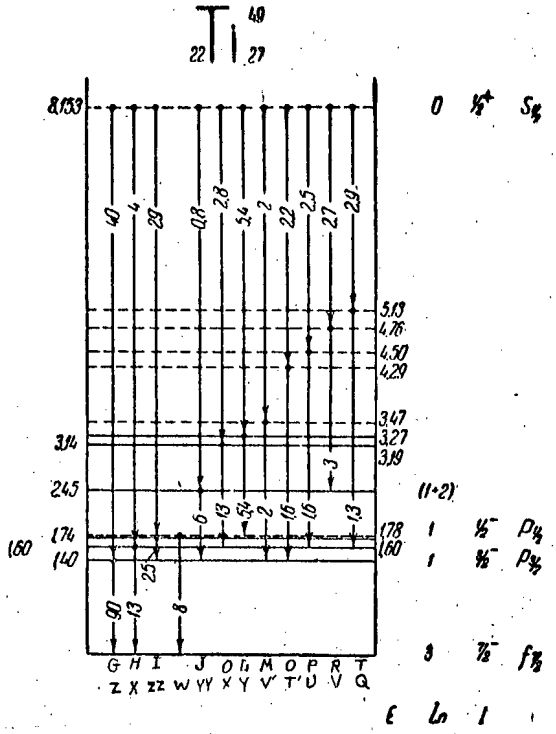

Fig. 3. γ-Transition scheme for the Ti^{49} nucleus.

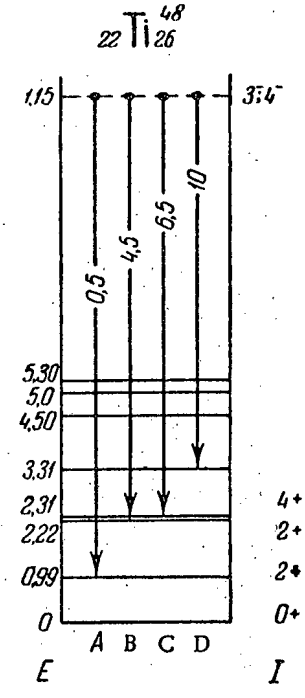

Fig. 4. γ-Transition scheme for the Ti^{48} nucleus.

for the Ti^{48} nucleus. The intensities of the γ-transitions are expressed in terms of the number of γ-quanta per 100 neutron captures in the given isotope. γ-rays of energy 9.39 Mev may also refer to Ti^{50}.

Iron

The sample was in the form of a metallic cylinder of 65 mm diameter, 60 mm long and weighing 1.7 kg.

In Table 3 are collected some data on the isotopes of iron. The total thermal neutron capture cross section of iron is taken equal to 2.43 barns.

The spectrum of the γ-rays of iron was studied in the energy interval 0.25-11 Mev. Figures 5 and 6 give the directly observed and the corrected spectra of the γ-rays from iron. In Fig. 5 there is also shown a portion of the spectrum in the neighborhood of ~1.6 Mev obtained with a radiator of 25 μ thickness. Table 4 gives the energies and the intensities of the γ-rays of iron. For comparison results of other workers are also given there. The energies of the γ-rays obtained in our work agree with in experimental error with the data of other investigators. The disagreement in the intensities of γ-rays of energies 7.25; 6.02 and 5.92 Mev between our data and the results of Kinsey and Bartholomew lies just at the limit of experimental error of both investigations. The γ-rays given in Table 4 carry away 80% of the energy radiated by the isotopes of iron after capturing thermal neutrons.

Data on the neutron absorption cross sections of the individual isotopes of iron allow us to conclude that the iron spectrum consists essentially of the γ-rays from Fe^{57}. γ-Rays from the radioactive isotopes of iron have an intensity of less than 0.5 γ-quantum per 100 neutron captures. Gamma-rays whose energy is greater than the binding energy of the last neutron in the Fe^{57} nucleus refer to the Fe^{55} and Fe^{58} isotopes.

Utilizing the data of references [15,16] on the excited levels of Fe^{55} and the data of [17-19]on the levels of Fe^{58} one may identify some of the γ-transitions (Fig. 7).

A possible γ-transition scheme for Fe^{57} is shown in Fig. 8. In constructing the γ-transition scheme we used the level system of Fe^{57} obtained in the study of the (d, p) reaction [17,20], of the β^+-decay of Co^{57}, and also information on the Coulomb excitation of the Fe^{57} nucleus by α-particles [21]. The energies of the levels given by the authors of these references are given on the left of this diagram. On the right are given values of the level energies obtained in our work. Instead of one level of energy 1.65 Mev found in the (d, p) reaction we postulate the existence of two levels of energies of 1.62 and 1.72 Mev through which there occur two intense γ-ray cascades from the initial state of the nucleus to the ground state. To explain these two intense cascades (J and T) and (L and Q) the existence of levels of energies 3.43 and 2.84 Mev is postulated in addition. The sum of the energies of the γ-quanta of these cascades is equal to the binding energy of the last

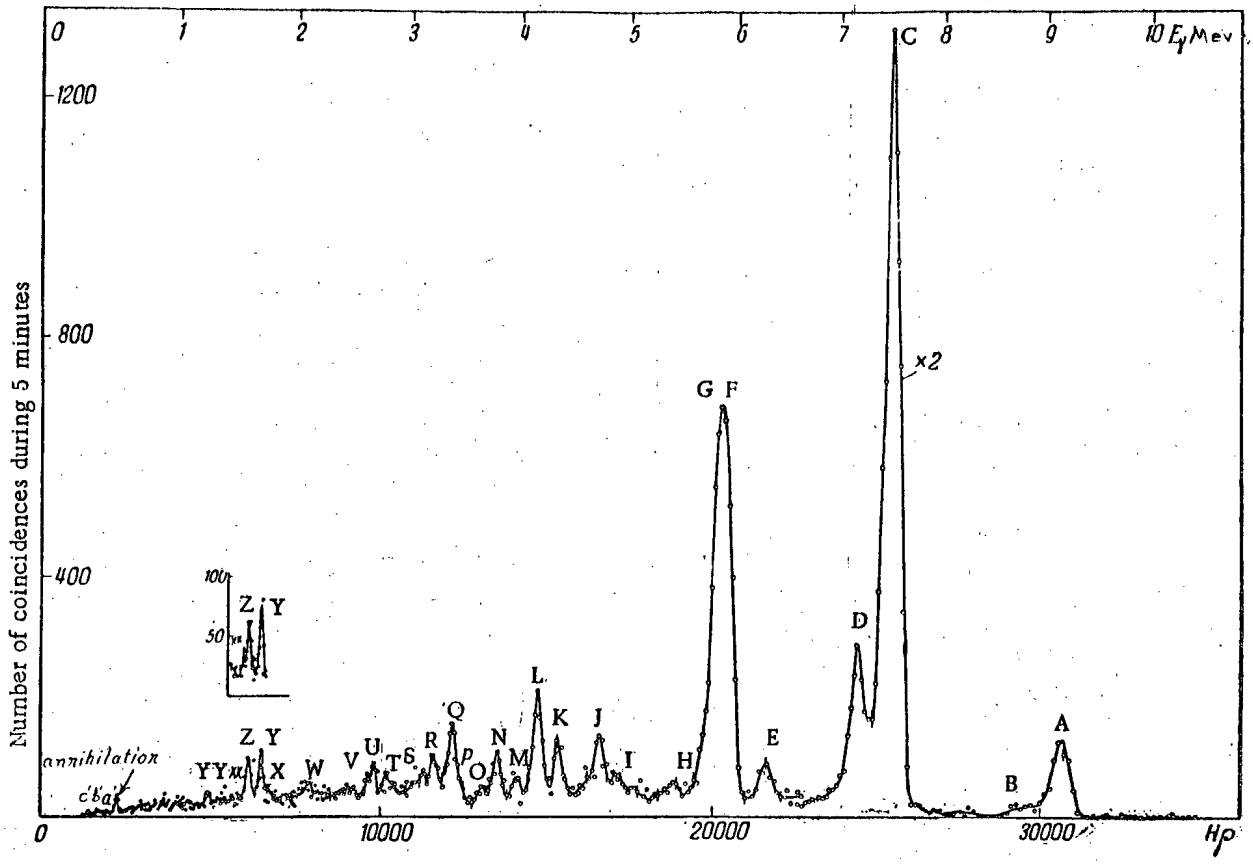

Fig. 5. Directly observed spectrum of γ-rays in iron.

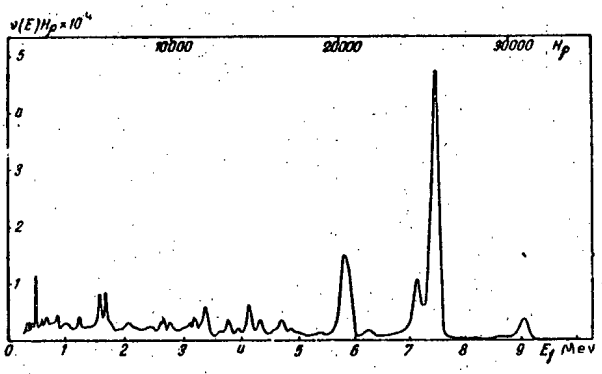

Fig. 6. Corrected spectrum of γ-rays in iron.

TABLE 3

Isotope	Composition of the natural mixture (%)	Neutron binding energy in the product nucleus, in Mev	Contribution to the thermal neutron capture cross section (%)
Fe^{54}	5.81	9.34±0.05[2]	5.1
Fe^{56}	91.64	7.65±0.10[2]	92
Fe^{57}	2.21	10.16±0.04[6]	2.0
Fe^{58}	0.34	6.37±0.42[5]	0.5

neutron in the Fe^{57} nucleus. In Fig. 8 dotted lines show those levels whose existence has not yet been quite definitely established. The fact should be noted that in Fe^{57} the intensity of the F1 transitions to levels of energies 2.5, 1.38 and 1.24 Mev, for which the values of ln = 1 have been formed by Black and by McFarland et al. from the angular distribution of the protons in the (d, p) reaction is less than one γ-quantum per 100 neutron captures.

Silicon

The sample consisted of a cylinder of metallic silicon 130 mm in length, and weighing 1.5 kg. The spectrum of the γ-rays was investigated in the energy range 0.25-11 Mev. Fig. 9 shows the directly observed spectrum and Fig. 10 the corrected spectrum of the γ-rays of silicon.

In Table 5 is given some information on the isotopes of silicon [22].

For the total thermal neutron capture cross-section of silicon the following values are known: σ = 160 ± ± 10, 160 ± 8 and 100 ± 20 millibarns.

TABLE 4

Result of our work			Data of reference [6]		Data of ref. [8] and [9]
Designation of lines	γ-ray energy in Mev	I*	γ-ray energy in Mev	I*	(γ-ray energy, in Mev)
			10.16 ±0.04	0.1	
A	9.295±0.015	2.7	9.298±0.007	2.7	8.5 [9]
B	8.86 ±0.06	0.3	8.872±0.01	0.5	
B'	8.342±0.06	0.2	8.345±0.011	0.8	
C	7.636±0.01	31.5	7.639±0.004	36	7.4 [9]
D	7.275±0.015	5.3	7.285±0.009	3.5	
E	6.43 ±0.025	0.7	6.369±0.009	0.4	
F	6.026±0.015	7.9	6.015±0.007	5.6	6.0 [9]
G	5.925±0.025	8.7	5.914±0.010	5.2	
H	5.51 ±0.025	0.6			
I	4.94 ±0.02	0.9	4.968±0.011	0.5	
J	4.805±0.015	2.1	4.81 ±0.02	1	
K	4.405±0.015	2.2	4.44 ±0.03	1	
L	4.22 ±0.015	4.3	4.21 ±0.03	2	
M	4.034±0.020	1.4			
N	3.844±0.015	2.3	3.86 ±0.05	0.5	
O	3.725±0.025	1.1			
P	3.552±0.02	1.4			
Q	3.43 ±0.015	3.9	3.43 ±0.03	2	
R	3.24 ±0.015	2.9			
S	3.146±0.025	2.1			
T	2.837±0.015	2.1			
U	2.730±0.015	2.9			
V	2.672±0.020	1			
W	2.143±0.010	1.4			
X	1.802±0.015	2.3			1.68—1.55 [8]
Y	1.72 ±0.010	6.4			
Z	1.626±0.012	6.1			
XX	1.53 ±0.015	1.9			
YY	1.236±0.012	1.5			
a'	0.454±0.010	4.1			0.425 [9]
b'	0.364±0.008	6.7			
c'	0.313±0.006	3.2			0.355 [8]

* Intensity in quanta per 100 neutron captures in the natural mixture of isotopes.

TABLE 5

Isotope	Composition of the natural mixture in %	σ_{isot} (millibarns)	σ_{atom} (barns)	Neutron binding energy in the product nucleus in Mev
Si^{28}	92.16	81±24	~0.074	8.473±0.010
Si^{29}	4.71	270±90	~0.013	10.611±0.010
Si^{30}	3.13	410±400 *); 116±23 **); 94±10 **)	~0.004	6.592±0.010

* Oscillator method.
** Activation cross section.

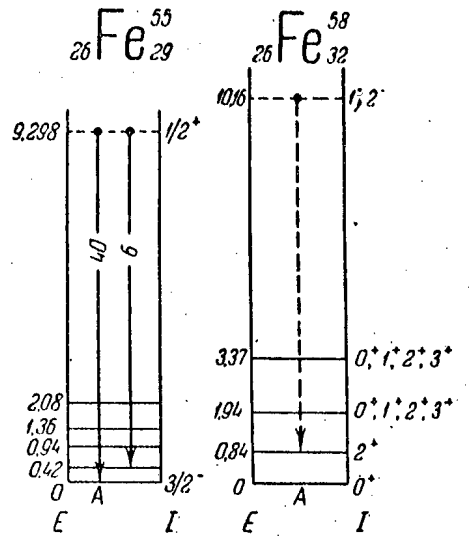

Fig. 7. γ-Transition schemes for the nuclei Fe^{55} and Fe^{58}.

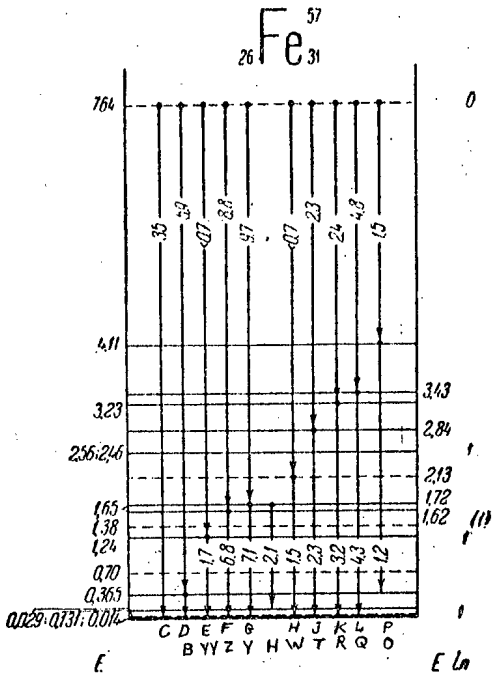

Fig. 8. γ-Transition scheme for the Fe^{57} nucleus.

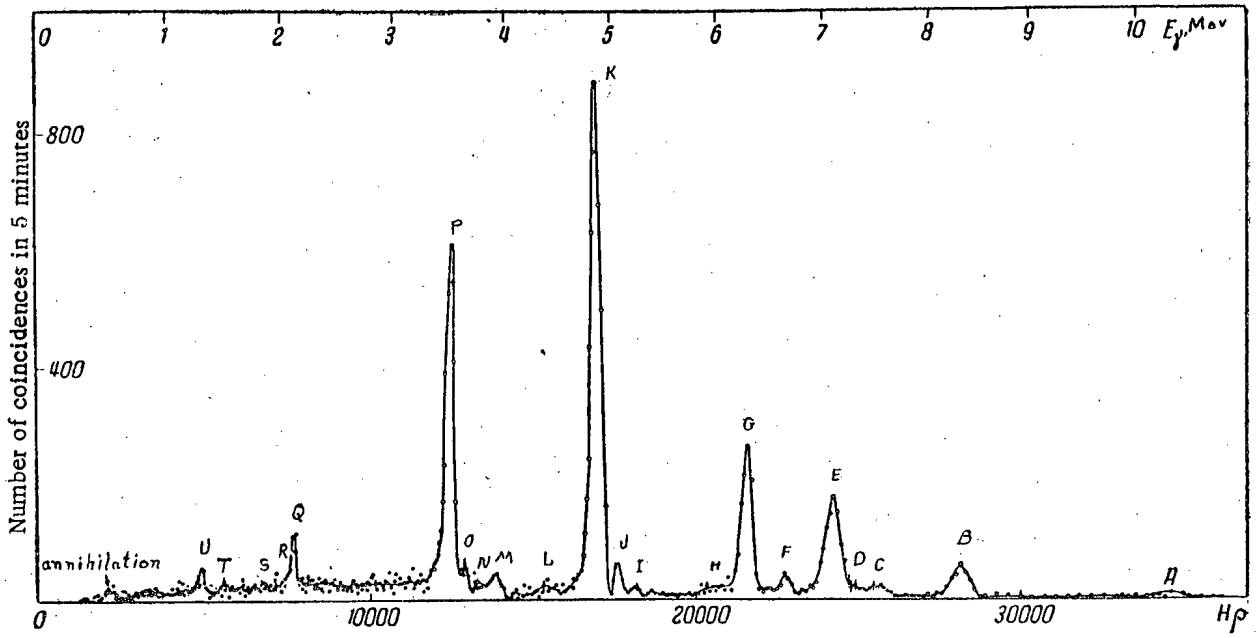

Fig. 9. The directly observed spectrum of γ-rays in silicon.

Table 6 gives the energies and the intensities of the γ-rays measured by us. There we have also given results of measurements carried out by Kinsey et al. with a pair spectrometer [23]and by Braid with a luminescent spectrometer [10]. The values of γ-ray energies found by us agree well with the data of these authors. However, the γ-line of energy 2.69 Mev found in the work of Kinsey et al. and of Braid was not found by us in spite of the fact that special measurements were carried out to observe it. Gamma-rays listed in Table 6 carry away 70 % of the energy radiated by the sample on capturing thermal neutrons. In the next to the last column of Table 6 are given the values of the intensities reported by Kinsey et al. before they had recalculated the sensitivity curve for their apparatus. In reference [24]they give corrected values for the intensities of some of the

TABLE 6

Results of our work			Radiating nucleus	Results of other investigators			
				γ-ray energy in Mev		I*	
Designation of lines	γ-ray energy in Mev	I* in the natural mixture		Kinsey et al. [23]	Braid [10]	in the natural mixture [23]	for Si^{29} [24]
A	10.59 ±0.030	0.2	Si^{30}	10.599±0.011		0.4	
B	8.482±0.015	1.6	Si^{29}	8.467±0.008		4	2
C	7.66 ±0.020	0.8	Fe^{57}	7.79 ±0.05		1	
D	(7.38 ±0.030)	0.5	Si^{30}	7.36 ±0.08		2	
E	7.224±0.030	6.1	Si^{29}	7.18 ±0.03		9	8
F	6.758±0.020	1.4	Si^{30}	6.76 ±0.04		4	
G	6.354±0.015	9.2	Si^{29}	6.40 ±0.03		19	11
H	6.041±0.050	1	Si^{29}	6.11 ±0.05		4	
I	5.242±0.030	0.8					
J	5.118±0.015	2.3	Si^{29}	5.11 ±0.04		9	8
K	4.930±0.010	37.4	Si^{29}	4.933±0.005		112	75
L	(4.30 ±0.05)	2					
M	3.976±0.020	4.2	Si^{29}				
N	~3.8	~3	Si^{30}				
O	3.667±0.020	3.2	Si^{29}				
P	3.547±0.010	36.5	Si^{29}	3.54 ±0.006		94	60
	—	—		2.69 ±0.05	2.65	65	
Q	2.10 ±0.010	12.8	Si^{29}		2.13		
R	1.95 ±0.020	3.4					
S	~1.7	~3	Si^{29}				
T	~1.5	~3	Si^{29}				
U	1.28 ±0.010	16	Si^{29}				

* Intensity in quanta per 100 neutron captures.

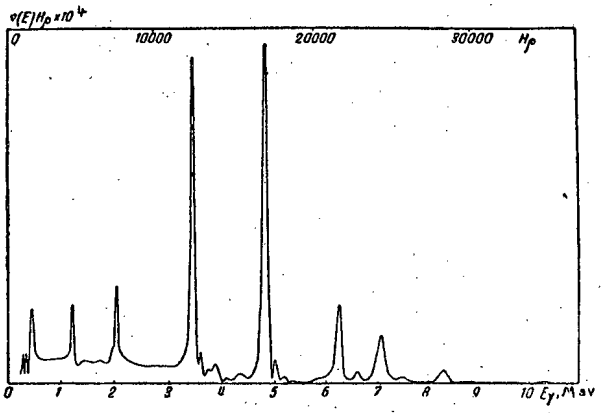

Fig. 10. Corrected spectrum of the γ-rays of silicon.

γ-rays of Si^{29} calculated per 100 neutron captures in the Si^{28} isotope. These data are given in the last column of Table 6.

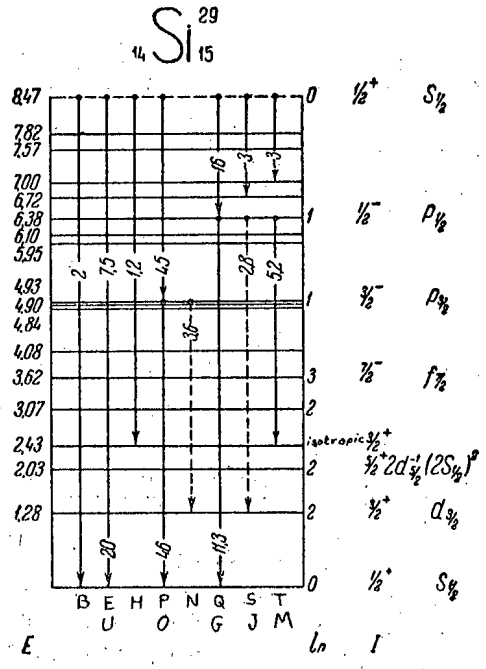

Fig. 11. γ-transition scheme for the Si^{29} nucleus.

In Fig. 11 is given the γ-transition scheme for the Si^{29} nucleus. In construcing the level scheme shown in Fig. 11 we used in addition to the review article [22] the data of Khromchenko [25] who found levels in Si^{29} of energy higher than 6.4 Mev. On the right of this diagram are shown characteristics of levels determined by Holt and Marsham [26]. On the γ-transition scheme numbers of γ-quanta are given per 100 neutron captures by the Si^{28} nuclei. They have been calculated

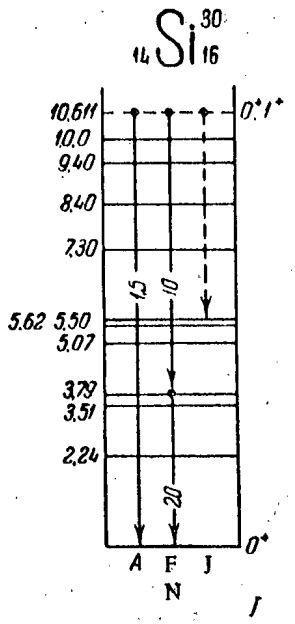

Fig. 12. γ-Transition scheme for the Si^{30} nucleus.

TABLE 7

Transition energy (Mev)	Type of radiation	Angular momentum and parity of the initial state	Angular momentum and parity of the final state	$S \cdot \frac{M^2}{2D}$
3.55	E1	$^1/_2+$	$^3/_2-$	0.3
2.10	E1	$^1/_2+$	$^1/_2-$	1
8.47	M1	$^1/_2+$	$^1/_2+$	0.03
7.22	M1	$^1/_2+$	$^3/_2+$	0.2
6.04	M1	$^1/_2+$	$^3/_2+$	0.05

on the assumption that γ-rays emitted by the Si^{29} nucleus amount to 80% of the spectrum emitted by the sample. The unresolved part of the spectrum which comprises ~30% of all the energy radiated by the sample lies in the energy region below 3.5 Mev. Possibly not all the γ-rays which constitute this part of the spectrum belong to Si since we did not know the percentage content of all the impurities which might be contained in the sample.

Fig. 12 shows the energy level scheme for the Si^{30} nucleus. In addition to the principal transition one may identify in this isotope the cascade of the two γ-transitions F and N.

The total radiative width D_γ is known for the Si^{29} nucleus [24]. From the known characteristics of this nucleus one may determine the multipolarity of a number of transitions starting in the initial state. Similarly to the way in which it is done in references [24] and [1] one may find partial radiative widths and compare them with the theoretical values obtained from Weisskopf's formulas. The results of such a comparison are given in Table 7. In the last column of this table are given the ratios of the experimental values of the partial radiative widths to the theoretical ones.

The values of these ratios obtained by us for transitions with different energies are in agreement with the data obtained earlier for nuclei in this region of atomic weights [24,1].

LITERATURE CITED

[1] L. V. Groshev, B. P. Adyasevich, A. M. Demidov. Physical investigations (Reports of the Soviet Delegation to the International Conference on the Peaceful Uses of Atomic Energy), Acad. Sci. USSR Press, 1955, p. 252 and also Report at the Session of the Acad. Sci. USSR, July, 1955.

[2] J. A. Harvey, Phys. R v. 81, 353 (1951).

[3] T. L. Collins, A. O. Nier, W. H. Johnson, Phys. Rev. 86, 408 (1952).

[4] G. F. Pieper, Phys. Rev. 87, 215 (1952).

[5] A. H. Wapstra, Physica 21, 385 (1955).

[6] B. B. Kinsey, G. A. Bartholomew, Phys. Rev 89, 375 (1953).

[7] H. T. Motz, Phys. Rev. 93, 925 A (1954).

[8] M. Reier, M. H. Shamos, Phys. Rev. 100, 1302 (1955).

[9] B. Hamermesh, V. Hummel, Phys. Rev. 88, 916 (1952).

[10] T. H. Braid, Phys. Rev. 90, 355 A (1953).

[11] G. F. Pieper, Phys. Rev. 88, 1299 (1952).

[12] M. M. Bretsher, G. R. Alderman, A. Elwin, Phys. Rev. 96, 103, 826A (1954).

[13] B. Hammermesh, V. Hummel, L. Goodman, D. Engelkemeir, Phys. Rev. 87, 528 (1952).

[14] R. L. Roggenkamp, C. H. Pruett, R. G. Wilkinson, Phys. Rev. 88, 1262 (1952).

[15] P. H. Stelson, W. M. Preston, Phys. Rev. 82, 655 (1951).

[16] M. Deutsch, A. Hedgran, Phys. Rev. 75, 1443 (1949).

[17] McFarland, Shull, Elwin, Zeidman, Phys. Rev. 99, 655 (1955).

[18] G. E. Mak, Revs. Modern Phys. 22, 64 (1950).

[19] L. S. Cheng, J. L. Dick, J. D. Kurbatov, Phys. Rev. 88, 887 (1952).

[20] C. Black, Phys. Rev. 90, 381 (1953).

[21] G. M. Temmer, N. P. Heydenburg, Phys. Rev. 93, 351A (1954).

[22] P. M. Endt, J. C. Kleuver, Revs Modern Phys. 26, 95 (1954).

[23] B. B. Kinsey, G.A.Bartholomew, Phys. Rev. 85, 1012 (1952).

[24] B. B. Kinsey, G.A.Bartholomew, Phys. Rev. 93, 1260 (1954).

[25] L. M. Khromchenko, Bull. Acad. Sci. USSR, Phys. Ser. 19, 277 (1955).

[26] J. A. Holt, T. N. Marsham, Proc. Phys. Soc. (London) A 66, 565 (1953).

[27] B. B. Kinsey, G.A.Bartholomew, Can. J. Phys. 31, 927 (1953).

EXPERIMENTS ON THE CREATION OF EINSTEINIUM AND FERMIUM IN A CYCLOTRON

L. I. Guseva, K. V. Filippova, Yu. B. Gerlit, V. A. Druin, B. F. Myasoedov, and N. I. Tarantin

In this article we present the results of some experiments on the creation of einsteinium and fermium by cyclotron irradiation of a uranium target with quintuply charged nitrogen ions (N V) and sextuply charged oxygen ions (O VI).

The half-lives and α-particle energies were measured with the aid of photographic plates, an ionization chamber with a spherical electrode, and a twenty-channel pulse-amplitude analyzer. The separation of the transplutonic elements was performed by a chromatographic method.

The first communication on the creation of einsteinium in a cyclotron appeared in 1954 in an article by A. Ghiorso and others [1]. Einsteinium isotopes of mass numbers 246 and 247 were separated from a uranium target that had been irradiated by nitrogen ions. The einsteinium isotope E^{246} decays by means of K-capture into Cf^{246} with a half-life of a few minutes, and E^{247} in addition to K-capture suffers α-decay with a half-life close to 7 minutes and an α-energy of 7.35 Mev.

Somewhat later, Swedish investigators [2] isolated from uranium irradiated with oxygen ions the isotope fermium with an assumed mass number of 250, a half-life for α decay approximately 30 minutes and an α-particle energy of 7.7 Mev.

In the present paper we present some results of a few experiments (performed in 1955) on the creation of einsteinium and fermium isotopes by bombardment of uranium targets by nitrogen and oxygen nuclei. The Academy of Sciences of the USSR cyclotron with magnetic pole-pieces of diameter 150 cm, was used to accelerate quintuply charged nitrogen ions and sextuply charged oxygen ions.

The nitrogen ions were obtained from a slit source [3], made especially for the present investigation. The nitrogen ion energy at the final radius was 105 Mev, and the ion current was $5 \cdot 10^{7}$ amps.

The sextuply charged ions of oxygen were obtained as a result of "stripping" doubly charged ions of oxygen on the molecules of the remaining gas in the cyclotron chamber. The maximum energy of the accelerated sextuply charged oxygen ions at the final radius was 120 Mev, and the current of ions with energies greater than 100 Mev was $3 \cdot 10^{-9}$ amps.

In the experiment α-radioactive transplutonic elements were studied. The half-lives and energies of the α-particles were determined with the aid of an ionization chamber with a spherical electrode and a twenty-channel pulse-amplitude analyzer.

In those cases when the number of disintegrations was insufficient for recording with the cloud chamber, the measurement of the α-energies and half-lives was performed by the method of thick photographic plates. In this work photographic plates of type "T" were used without a protecting gelatin layer, and with a resolving power of 0.4 Mev for α-energies of 5 to 8 Mev.*

Obtaining Einsteinium

When a uranium target is bombarded by ~100Mev nitrogen ions, in addition to the reaction of complete

*The type "T" photographic plates were especially constructed and prepared in the laboratory of K. S. Bogomolov at the Scientific Institute of Motion Picture Photography.

capture of the nitrogen nucleus with subsequent emission of 4-7 neutrons, reactions of partial penetration of the nitrogen nucleus are also possible; these come about as the result of splitting off an α-particle or a proton from the bombarding nucleus. Therefore, in the interaction of nitrogen ions with uranium nuclei, simultaneously with the creation of einsteinium isotopes, the creation of californium and berkelium isotopes also takes place. The result of these reactions is the possible creation of the isotopes $E^{245-248}$, $Cf^{244-248}$, $Bk^{243-245}$.

To obtain einsteinium, a plate of uranium metal of thickness 0.1 mm and dimensions 5 x 15 mm was subjected to irradiation by accelerated nitrogen ions for 15-30 minutes. In 10-15 minutes after the irradiation, the uranium target was placed in the ionization chamber. The relatively great thickness of the active layer of the target and the intense β-radiation caused by the decay of the fission fragments that had been created to a large degree impaired the resolving power of the ionization chamber. Nevertheless, with the help of a collimator, groups with energies of 7.0-7.5 Mev were separated from the α-spectra of the products. The results of the measurements on the half-life of the elements emitting this group of α-particles are presented in Figure 1.

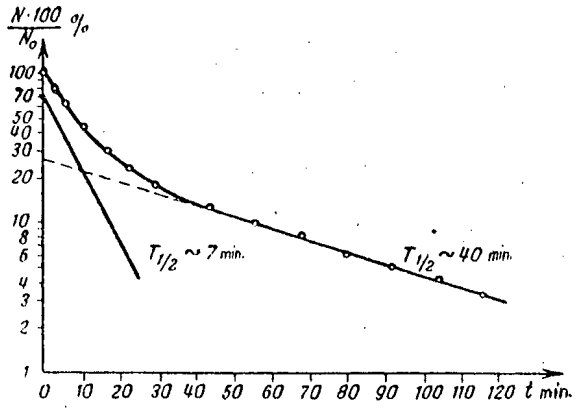

Figure 1. The decay of isotopes with α-energies of 7.0-7.5 Mev.

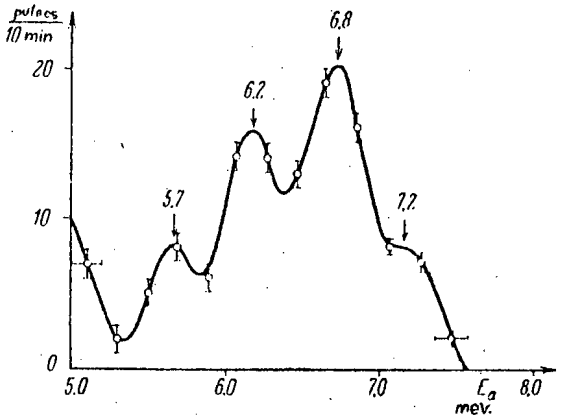

Figure 2. The α-spectrum of the transplutonic elements.

Analysis of the curve indicates the presence of two half-lives equal to about 7 and 40 minutes. The 7-minute half-life would seem to be due to the isotope E^{247}, and the 40-minute one, to the isotope Cf^{244}, whose half-life, according to the data in the literature, is 45 minutes, and whose α-particle energy is 7.15 Mev.

In order to further identify the products of the reaction, the separation of the transplutonic elements from the uranium base and the fission fragments was undertaken. The separation was carried out by the precipitation of fluorides with 200 micrograms of lanthanum used as the carrier. The decomposition of lanthanum fluoride was accomplished by nitrous acid in the presence of boric acid, after which lanthanum hydroxide was precipitated and dissolved in hydrochloric acid. The salt solution was applied to a platinum disc, and then the target was dried and baked. The thickness of the target layer prepared in this way was about 10 micrograms per square centimeter.

The α-particle spectrum of the transplutonic elements after their separation from the uranium and the fission fragments, obtained with the aid of an ionization chamber, is presented on Figure 2.

On the above spectrum three groups of α-particles can be seen, with energies of 5.7 ± 0.2; 6.2 ± 0.2; 6.8 ± 0.2 and 7.2 ± 0.2 Mev. The α-particle group with energy 7.2 Mev evidently belongs to the isotope Cf^{244}, a large fraction of which has disintegrated by the time of measurement. The α-particle group with energy 7.35 Mev, observable immediately after the end of irradiation and belonging to the short-lived isotope E^{247}, is not visible here since the time from the end of irradiation to the beginning of the measurement is significant.

Further analysis of the products of the reaction was carried out by the chromatographic method. The separation of the transplutonic elements was carried out in a column, diameter 2 mm, height 17 cm at 85°C on a cationite (type Douex-50) with a 0.4 M solution of ammonium lactate at pH = 4.3. The time spent in separating the transplutonic elements did not exceed one hour in any of the experiments. The transplutonic elements were not separated from the carrier, since preliminary experiments on the disintegration of americium and curium for identical conditions showed that the presence of 200 micrograms of lanthanum do not interfere with the disintegration and has no influence on the positions of the chromatographic maxima.

The measurement of the total α-activity in the drops after the chromatographic separation, and the determination of the α-particle energies of the eluted elements was carried out with the aid of photographic plates, for which the targets with the drops on them were brought into contact with the photographic plates. The half-life of the elements being studied was determined from the photographic plates by counting the number of α-disintegrations in a given time interval.

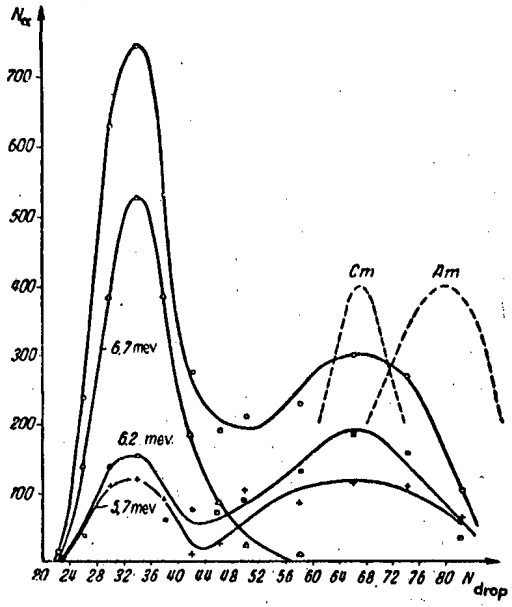

Figure 3. Elution curve of the transplutonic elements. Time from the end of irradiation to the start of chromatographic separation — 4 hours; duration of exposure of the photographic plates — 36 hours.

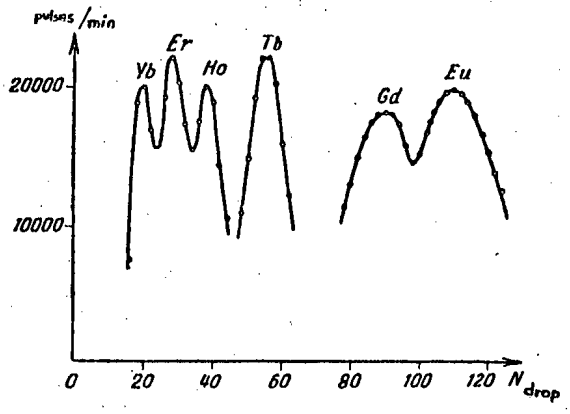

Figure 4. Elution curves of rare-earth elements.

Figure 3 shows the curves of washing out, drawn for the number of α-particles with energies of 5.7 ± 0.2; 6.2 ± 0.2 and 6.7 ± 0.2 Mev, as well as the total curve drawn for all the α-particles of these energies. On the same graph, dotted lines are used to indicate the positions of the chromatographic maxima of americium and curium gotten under the same conditions.

The identification of the elements with periodic number greater than 96 in the chromatographic separation was carried out on the basis of their rare-earth analogs. With this in mind, a preliminary diagram was made for a few of the rare-earth elements (Figure 4).

On the basis of the position of americium and curium and of their rare earth analogs, the displacement coefficient for the chromatographic maxima of the transplutonic elements with respect to that of the rare-earth elements was calculated. It turned out to be 0.73. This value of the coefficient was used for the determination of the positions of the chromatographic maxima of berkelium (40th drop), einsteinium (26th drop), and fermium (21st drop). The position of californium (30th drop) is determined by comparing our results with those of the literature [4].

The presence of a maximum at the 68th drop (Figure 3) indicates the presence of curium isotopes. The maximum at the 34th drop, between the positions of berkelium and californium, is clearly caused by the overlap of the curves for these elements. The close values for the α-energies of the isotopes of berkelium and californium that were obtained, and the insufficient resolution of the photographic plates does not allow us to separate the curves for each of the elements.

The analysis of the results of chromatographic separation, the measurement of the α-particle energies and half-lives, as well as consideration of the possible nuclear reactions [1], allows us to make some hypotheses regarding the products that were obtained in the reaction.

The elution maxima that occur for the elements at the 34th drop are probably caused by the isotopes Cf^{246}, Cf^{248}, Bk^{243} and Bk^{245}. The 5.7 ± 0.2 Mev α-particles that are observed in about the same numbers immediately after irradiation and after a period of 100 days, come from the basic isotope Cm^{244}, which could have been formed as a result of the capture of an orbital electron of Bk^{244} after chromatographic separation.

The maxima that lie on the 68th drop are clearly connected with the Cm^{240} and Cm^{244} isotopes, which could be formed as a result of decay of Cf^{244} and Bk^{244}.

Comparison of the data on the numbers of the various elements created makes possible some conclusions concerning the cross sections for the reactions between the nuclei of nitrogen and uranium. Indeed, it is possible to carry out an evaluation of the relative probabilities for the reactions of complete and partial capture of the nitrogen nucleus by the target nucleus on the basis of the reactions (N, 6n) and (N, α4n).

The rapid accumulation of Cm^{244} can occur only as a result of the decay of Bk^{244} that is created in the reaction U^{238}(N, α4n) Bk^{244}.

Cf^{246} can be created as a result of the decay of E^{246} which is obtained from the reaction of complete capture of the nitrogen nucleus U^{238}(N, 6n) E^{246}, and is also a result of the partial penetration reaction U^{238}(N, p5n)Cf^{246}. Therefore, the ratio of the number of Cf^{246} atoms to the number of Cm^{244} atoms makes possible an evaluation of the upper bound of the ratio of the cross sections for the reactions U(N, 6n) and U(N, α4n). In our case of a thick target and nitrogen ion energies of 95 Mev, this ratio turned out to be about 0.001.

Obtaining Fermium

The technique of irradiating the uranium target with oxygen ions was the same as that for irradiation with nitrogen ions. The irradiated uranium target was placed into the ionization chamber. With the aid of a collimator, a group of α-particles with energies of 7.4-7.9 Mev was separated.

The half-life of the element emitting the α-particles of the above energies was 30 minutes (Figure 5).

In order to obtain a more accurate measurement of the α-energies, the transplutonic elements were separated from the uranium and fission fragments by the fluoride method. The energy spectrum of the α-particles from the transplutonic elements, which was obtained with the aid of the ionization chamber and with photographic plates, is shown in Figure 6.

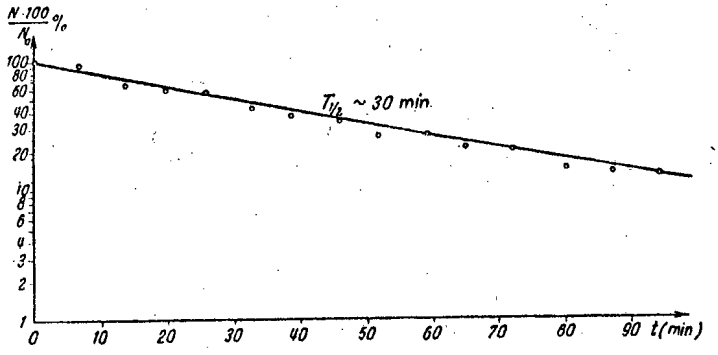

Figure 5. The decay of isotopes with α-energies of 7.4-7.9 mev.

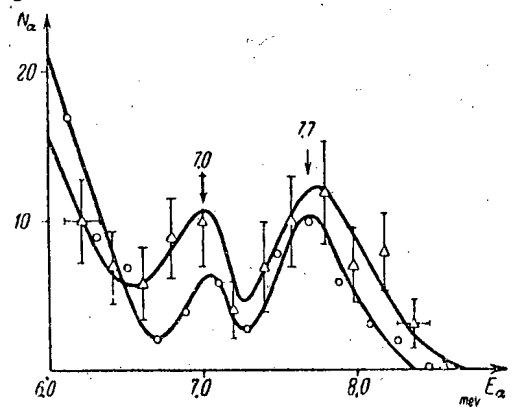

Figure 6. The α-particle spectrum of the transplutonic elements.
Δ—Δ) measurements with the aid of the ionization chamber; o—o) measurements with the aid of photographic plates.

As can be seen on the graph, in both cases α-particles with 7.0 $\pm$ 0.2 and 7.7 $\pm$ 0.2 Mev energies were observed. The half-life of the element that emits α-particles with 7.7 Mev energy is determined with photographic plates, and turns out to be about 30 minutes.

The sum total of the data obtained (the half-life of the element, the α-particle energy, and precipitation with lanthanum fluoride) allows us to make the hypothesis that as a result of irradiation of uranium by oxygen ions, an isotope of fermium is created that has been previously identified [2].

The 7.0 $\pm$ 0.2 Mev α-particle groups probably belong to the isotope Cf^{244}, which could have been created as a result of α-decay of the short-lived isotope Fm^{248}.

CONCLUSIONS

1. Irradiation of uranium by nitrogen ions accelerated to 105 Mev produces an isotope of einsteinium with mass number 247, identified by its half-life and α-particle energies.

2. From a uranium target irradiated by oxygen ions accelerated to 120 Mev, an isotope of

fermium has been separated, identified by its half-life and α-particle energies.

3. Isotopes of californium, berkelium, and curium have been separated, by the chromatographic method, in the amounts of several hundreds of atoms.

In conclusion the authors express their gratitude to associate member G. N. Flerov of the Academy of Sciences of the USSR for directing the work, to Academician A. P. Vinogradov and Professor D. I. Ryabchikov for directing the chemical part of the work, to our co-workers in the cyclotron laboratory, and especially to the group of co-workers under the guidance of Yu. M. Pustovoi, who maintained the operation of the cyclotron during the course of the present work.

LITERATURE CITED

[1] A. Ghiorso, G. B. Rossi, B. G. Harvey, and S. G. Thompson, Phys. Rev. 93, 257 (1954).

[2] H. Atterling, W. Forsling, Z. W. Holm, Z. Melander and B. Astrom, Phys. Rev. 95, 585 (1954).

[3] B. N. Makov, Instruments and Experimental Technique (in press).

[4] D. C. Stewart, "Rare-earth and transplutonium separations by ion exchange resin methods", Paper No. 729, presented by the USA at the International Conference on the Peaceful Uses of Atomic Energy at Geneva, 1955.

THE STANDARDIZATION OF RADIOACTIVE PREPARATIONS

K. K. Aglintsev, F. M. Karavaev, A. A. Konstantinov, G. P. Ostromukhova, E. A. Kholnova

The article describes methods and apparatus used in the D. I. Mendeleev All-Union Scientific Research Institute of Metrology for the accurate measurement of a number of dosimetric characteristics of radioactive preparations: activity (calorimetric and ionization methods and the method of absolute β-counting), γ-equivalent (ionization chamber with 4π solid angle), and the magnitude of the dose of γ-radiation (normal ionization chamber).

The limits within which measurements can be made and the accuracy of the results are indicated.

For practical applications of radioactive substances it is necessary to know the fundamental physical characteristics of the isotopes being used and the fundamental parameters of the preparations made from these isotopes.

Among the more important physical characteristics of the isotopes are: the maximum energy and the nature of the energy distribution in the β-spectrum of the isotope, the wavelengths and the number of quanta per decay process for the lines of the γ-spectra, and also the number and the values of the energies of the conversion electrons. In the case of complex β-spectra the information indicated above must be approximately known for each of the components of the β-spectrum, as well as their relative intensity. In addition to the data relating to the β- and γ-spectra one must also know the half-life for the decay of the radioactive isotope.

Among the fundamental parameters of radioactive preparations are: activity of the preparation dimensions, weight, nature of the container. For preparations having a relatively large volume one also needs data on the distribution of the activity throughout the volume in those cases when it is not distributed uniformly.

A knowledge of the activity of an isotope preparation with known β- and γ-spectra enables one to find easily its total radiation; however, in using the preparation it is more important to know its external radiation which differs from the total radiation as a result of the self-absorption of the radiation in the preparation, and of the absorption in the container.

The activity of preparations may be measured in curies or in disintegrations per second. The effect of the γ-radiation of the preparation determines the dose to which it gives rise in roentgens; moreover, one can draw conclusions on the effect of γ-radiation if one knows the γ-equivalent of the preparation in gram-equivalents of radium. The effect of β-radiation may be expressed in physical roentgen equivalents.

In order to ensure a uniformity of measurement in any field of measurement there exist standards and standard equipment which set up the units of the corresponding physical quantity, and also there exists a system of calibration and of checking standard and operating measuring instruments.

The setting up of the two units – curie and roentgen – is accomplished by means of standard equipment, the setting up of the unit gram-equivalent of radium is accomplished by means of the state radium standard which consists of two radium preparations contained in thin-walled glass ampoules [1] and [2].

The most precise are the measurements of γ-equivalents of the preparations in gram-equivalents of radium.

The measurement of the γ-equivalent of preparations are carried out on two standard sets of equipment be means of comparing the γ-intensity of the preparation being measured with a standard or master preparation of radium.

Each of the standard sets of apparatus consists of an ionization chamber with a 4π solid angle connected to an electrometer device for the measurement of small currents. For the measurement of preparations in the range from 1 to 1000 mg-equivalents of radium an ionization chamber is used which consists of two concentrically placed aluminum spheres of walls 5 mm in thickness. The space between the spheres is the ionization volume of the chamber. The magnitudes of the ionization currents produced in the chamber by preparations having γ-equivalents within the range indicated above lie within the limits from $1.5 \cdot 10^{-11}$ to $1.5 \cdot 10^{-8}$ amp. To measure such currents we measure a compensating circuit due to Townsend [3] with a quadrant electrometer of sensitivity up to 800 divisions/volt and with a set of condensers of constant capacity. The circuit diagram of the apparatus is given in Fig. 1. The preparation being calibrated and the standard preparation of radium are in turn placed inside the chamber.

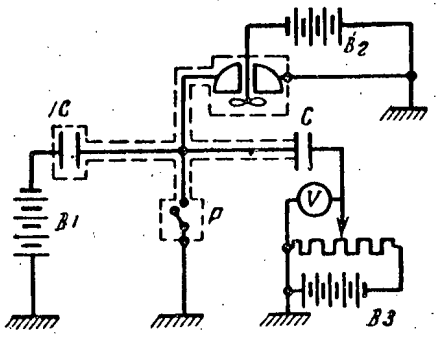

Figure 1. Circuit diagram for the standard apparatus for the measurement of γ-equivalents of preparations in the range from 1 to 1000 mg-equivalents of radium. IC – ionization chamber; B_1, B_2, B_3 – potential batteries; R – relay; C – standard condenser; V – voltmeter.

The values of the γ-equivalents are measured by this apparatus with an error of from 0.5 to 2% [4].

The measurement of less active preparations which produce in the chamber an ionization current comparable to the normal leakage current (background) are carried out on another apparatus in which the so-called compensated chamber is used [5]. The latter consists of two identical cylindrical brass chambers separated by a lead block and connected in opposition; in the absence of the preparations from the chambers the difference current is equal to zero. The measured and the standard preparations are placed in turn into one of the chambers. The values of the currents produced in the chamber by preparations with a radium content of from 1 to 0.001 mg-equivalents lie within the limits of from $5 \cdot 10^{-11}$ to $5 \cdot 10^{-14}$ amps. To measure such currents we use a dc. amplifier using a bridge circuit with an electrometer tube [5]. The circuit diagram of the apparatus is given in Fig. 2. It used the compensating method for measuring the ionization current. The

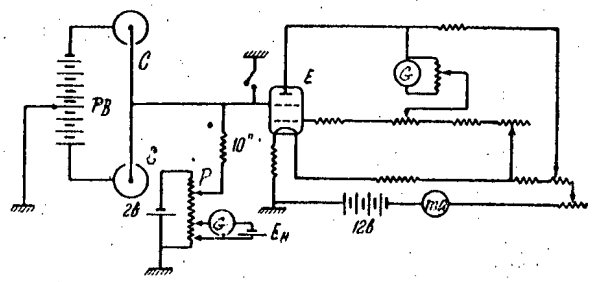

Figure 2. Diagram of the standard apparatus for the measurement of γ-equivalents of preparations from 1 to 0.001 mg-equivalents of radium. C – compensating chamber; P – potentiometer; E_n – normal element; E – electrometer tube; G – galvanometer; MA – milliammeter; PB – potential battery.

drop of voltage produced by the ionization current across the input resistor is compensated by a potential whose magnitude is determined by means of the potentiometer. In this case the amplifier is used only as a null indicator. The errors of measurement of γ-equivalents in the range 1 to 0.001 mg-equivalents of radium lie within the limits of 1 to 5-8%.

Corrections are made to the values of γ-equivalents determined by means of the apparatus described above for the geometrical dimensions of the preparations and for the absorption of γ-rays in the preparations ("self-absorption").

The magnitude of the γ-equivalent of a radioactive preparation depends on the conditions of measurement, principally on the filtering of γ-radiation, and also on the geometry, type and material of the walls of the ionization chamber. Figures 3 and 4 show the dependence of the γ-equivalents of Co^{60}, $(Zr + Nb)^{95}$, Ag^{110} and Sb^{124} on the filtering of the γ-radiation by different thicknesses of lead for broad (solid curves) and for narrow (dotted curves) beams of γ-rays.

The measured value of the γ-equivalent of the preparation in g-equivalent of radium enables one to determine the ionizing effect of this preparation in roentgens per hour at a distance of 1 m. Indeed, since 1 g of radium in a platinum container of 0.5 mm thickness gives at a distance of 1 m a dose of 0.84 r/hr, then a preparation of M g-equivalent of radium will give under identical conditions a dose of 0.84 M r/hr. Thus the γ-equivalent of a preparation characterizes the external γ-radiation of the preparation under given conditions.

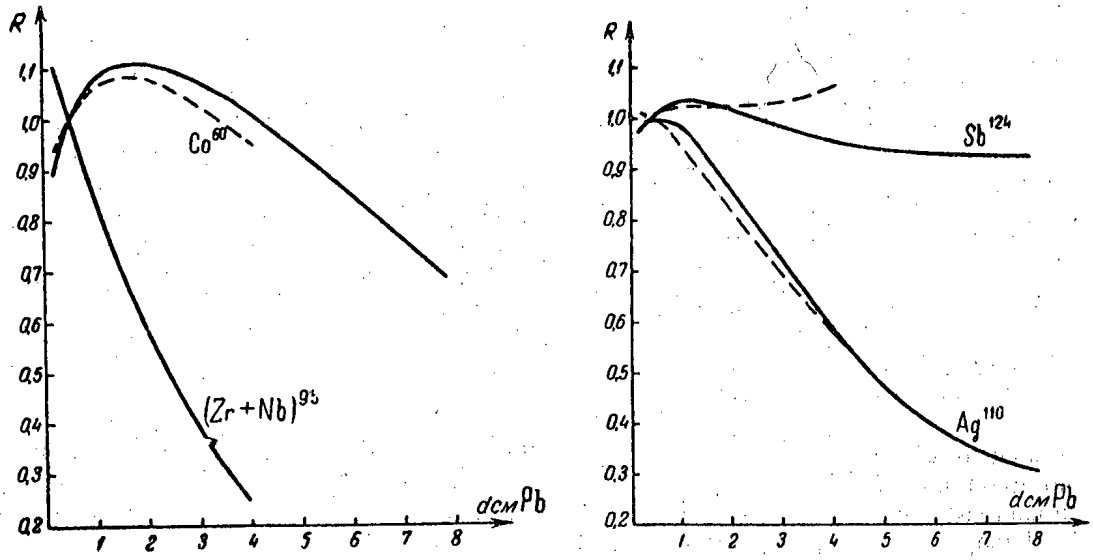

Figures 3 and 4. The dependence of the γ-equivalents of Co^{60}, $(Zr + Nb)^{95}$, Ag^{110} and Sb^{124} on filtering. The thickness of the lead filter is plotted along the horizontal axis, while along the vertical axis is plotted the ratio of the value of the γ-equivalent for various filter thicknesses to its value with a filter 0.5 cm thick.

The transition from the magnitude of the γ-equivalent of the given preparation to the value of its activity in curies is possible only if the γ-quanta energies are known, as well as their number per single disintegration of the radioactive substance, the efficiency of the ionization chamber for γ-quanta of different energies, and the effect of self-absorption of γ-rays in the given preparation.

For absolute measurements of the activity in curies we use the method of absolute counting of β-particles, and also the calorimetric method. The problem of the absolute counting of β-particles by means of a counter, in spite of being simple in principle, becomes very difficult if one must achieve an accuracy of the order of 3%. Fundamental difficulties arise because in the continuous β-spectra there are always some β-particles with low energies which are easily absorbed.

The method of absolute counting of β-particles with the aid of a "4π counter" consists of counting all the β-particles from a given radioactive source in the total solid angle 4π. The "4π counter" is made up of two counters between which the radioactive source is placed. For absolute measurements by means of the "4π counter" the following corrections have to be introduced:

1) for absorption of β-particles in the film on which the radioactive source has been deposited; this correction may be easily determined with the "4π counter" itself;

2) the self-absorption of β-particles in the source itself;

3) the missing of β-particles because of the "dead-time" of the counter, and of the finite resolving power of the recording electronic circuit.

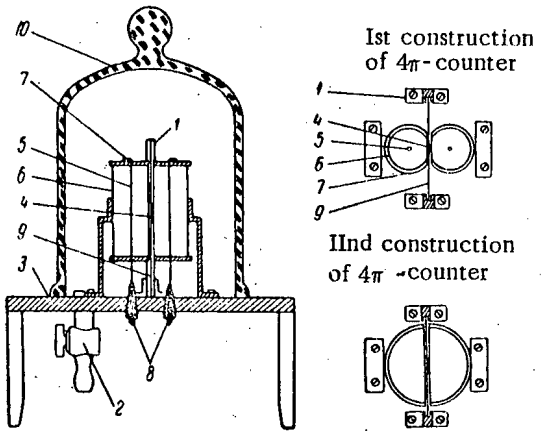

Figure 5. Diagram of "4π counter".
1) Stand; 2) stopcock; 3) brass table; 4) preparation; 5) counter wire; 6) body of counter; 7) polystyrol top; 8) polystyrol insulators; 9) aluminum foil; 10) glass bell-jar.

Figure 5 gives a schematic diagram of an apparatus with a "4π counter". In our apparatus two different types of construction of "4π counters" were used [6,7]. The first of these consists of two cylindrical counters sliced off along the generator between which the source is placed. This "4π counter" was filled with a mixture of argon and ethyl alcohol and served for counting the β-particles in the Geiger regime. With its aid one could measure preparations with activities from $5 \cdot 10^{-8}$ to 10^{-10} curies with an accuracy of 2-4% for thin preparations.

The second construction of the "4π counter" is in the form of two half-cylinders with the source between the half-cylinders; it was used to count the β-particles in the proportional counter regime. For this the apparatus was filled with methane to a pressure of 30-50 cm of mercury.

With the aid of the "4π counter" working in the proportional counter regime one may measure preparations with activities from $5 \cdot 10^{-7}$ to $5 \cdot 10^{-11}$ curie with an accuracy of 1-3% for thin preparations.

Although the method of absolute counting of β-particles which utilizes the principle of a definite solid angle is not very accurate, nevertheless it is widely used because of its simple and universal nature. The principle of the method is very simple. The radioactive preparation on thin backing is placed underneath the counter. β-Particles emitted within the limits of a given solid angle bounded by a calibrated diaphragm reach the counter and are recorded. The total number of β-particles emitted into the angle 4π will be equal to $N = \frac{4\pi}{\Omega} N_\Omega$, where N_Ω is the number of β-particles counted within the given solid angle and Ω is the magnitude of the solid angle.

However, in order to be able to determine the absolute number of β-particles by means of this method a number of corrections must be introduced [8].

The introduction of these corrections considerably lowers the accuracy of the method, which at best approaches 4-6 %. The greatest contribution to the error comes from determining the solid angle. By this method our apparatus can measure β-activities of the order from 10^{-5} to 10^{-8} curie.

A comparison of the two methods of absolute counting of β-particles shows that the method of the "4π counter" is the more accurate one, and at the same time it is simpler in principle. The method of the "4π counter" is also the most sensitive of all the known methods for measuring β-activity. With a long series of

measurements of β-active substances one may easily use the "4π counter" method to calibrate a serial end counter for each individual radioactive isotope.

In order to compare the two methods described above with other methods of absolute counting of β-particles, for example the calorimetric or the ionization method one must know accurately the quantity of the radioactive substance. In order that the correction for self-absorption of the β-particles in the preparation itself should be small it is necessary to take tenths or hundredths parts of a milligram of the radioactive substance. It is very difficult to weigh such small quantities on a microbalance. Therefore, for the determination of the quantity of a radioactive substance which emits γ-rays in addition to β-rays one employs the comparison of the γ-equivalent of the source with the γ-equivalent of another larger quantity of radioactive substance, the so-called reference quantity. The reference quantity of the substance was taken of about 10 mg weight, and such quantities may be weighed with sufficient accuracy. Usually several (five-six) reference quantities were prepared; they were compared with each other and from them that one was selected which agreed best with the others.

The comparison of the γ-equivalent of the reference quantity of radioactive substance with the γ-equivalent of the source was made by means of a scintillation γ-spectrometer. The method of γ-weighing is very reliable, and always gave good results.

In the case that the radioactive substance emits only β-particles, as is the case for example with P^{32}, first a relatively large volume of the substance is weighed, and then a certain small portion of this quantity is taken whose weight does not exceed a fraction of a milligram.

The method of measuring activity by means of standard apparatus using counters becomes inaccurate for thick preparations. For such preparations the calorimetric method was used successfully for which the thickness of the preparation presents no obstacle.

Calorimetric determinations of the activity of radioactive preparations are based upon the fact that the amount of heat liberated when the radiations from a radioactive preparation are absorbed is proportional to the number of nuclei which have disintegrated.

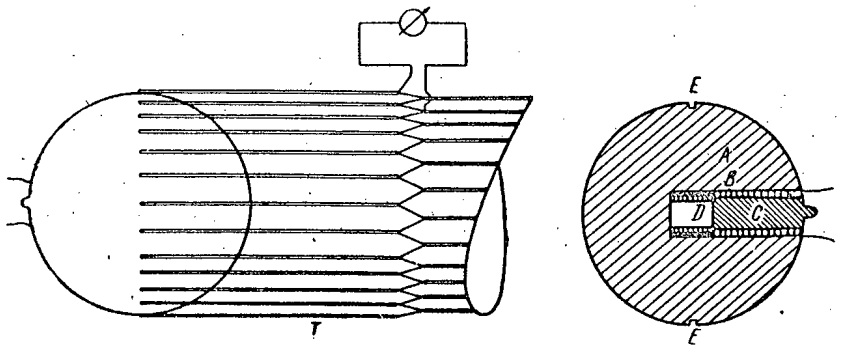

Figure 6. Schematic diagram of a γ-calorimeter. A) Body of the calorimeter; B) heating coil; C) plug; D) space for preparation; E) place where thermocouples are affixed; T) thermocouple.

In order to measure the absolute activity of radioactive preparations we have built colorimetric apparatus of two types: a) a differential double calorimeter for the measurement of the activity of preparations by means of their γ-radiation; b) an isothermal calorimeter based on the principle of evaporation of liquid nitrogen which was designed to measure the activity of preparations by their β-radiation [9-11].

The γ-calorimeter consists of two identical lead spheres (Fig. 6) mounted on a hard rubber stand inside a

TABLE 1

Characteristics	Calorimeter			
	No. 1	No. 2	No. 3	No. 4
External diameter of the spheres in cm.	10	7	5.5	3.5
Thickness of the absorbing layer in cm.	4.3	2.8	2.1	1.6
Weight of the sphere in g	5944	2030	969	2.2
Number of thermocouples	24	24	20	18
Length of time for equilibrium to be established in hours	8	4	3	1.5
Sensitivity in 10^3 mm/watt	6.44	7.58	13.3	19.6

thermostat. The preparation to be measured is placed into a special space inside one of the spheres of the calorimeter, and the temperature difference between the surfaces of the spheres is observed by means of a copper-constantan thermopile.

The fundamental characteristics of four available γ-calorimeters are given in Table 1.

The sensitivity of the colorimeters was determined by means of calibrating them with heating coils placed inside each sphere.

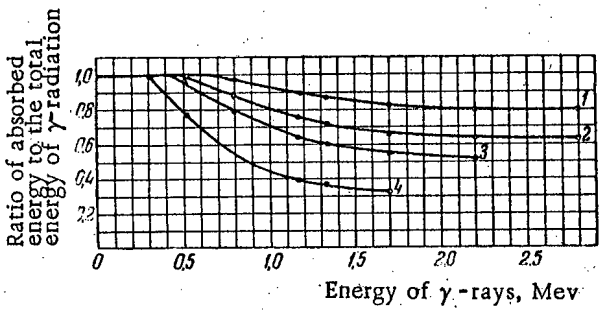

Figure 7. Absorption of γ-rays in γ-calorimeters. 1, 2, 3, 4 – numbers of calorimeters.

In order to calculate the activity of the preparation from the calorimetrically measured quantity of heat one must know the following spectroscopic characteristics of the preparation: a) The energies $h\nu_i$ of all the γ-lines; b) the number α_i of γ-quanta of each energy per individual disintegration, c) the average energy of the β-spectrum E_β. Since the dimensions of the γ-calorimeters do not ensure the complete absorption of all the γ-rays it is in addition necessary to know with a sufficient degree of accuracy what fraction of the radiated γ-energy is absorbed by the calorimeter. This quantity – the coefficient p_i – was calculated for each calorimeter and for γ-quanta of different energies. The results of such calculations are given in Fig. 7.

The expression which relates the number of disintegrations N_0 in the preparation to the quantity of heat W emitted by the preparation inside the calorimeter per second has the form

$$N_0 = \frac{W}{\sum h\nu_i \alpha_i p_i + E_\beta} = \frac{n}{j\left(\sum h\nu_i \alpha_i p_i + E_\beta\right)},$$

where n is the deflection of the galvanometer in millimeters of scale; j is the sensitivity of the calorimeter in mm/watt; E_β is the average energy of the β-spectrum.

The sensitivity of the γ-calorimeters constructed by us permits us to measure preparations with activities from several tens of millicuries and up.

The accuracy with which the γ-calorimeters enable us to determine the absolute activity of the preparations is 3-5%; of them 2-3% are due to the errors of computing the absorption of γ-rays by the calorimeters.

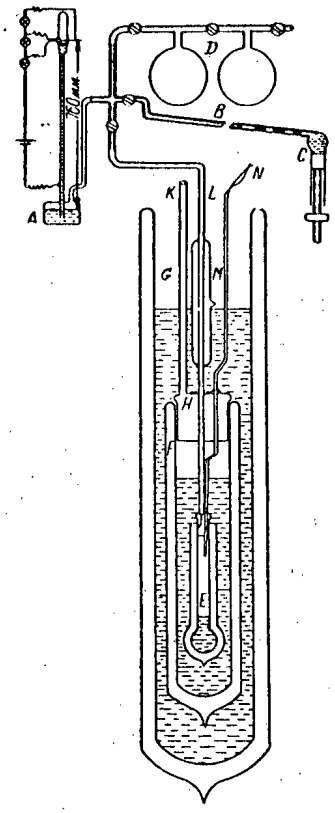

Figure 8. Schematic diagram of the isothermal β-calorimeter.
A) Manometer; B) capillary; C) mercury pump; D) ballast flasks; E, F, G) Dewar flasks; J, H) polished sections; K, L) tubes for removal of nitrogen; M) vacuum jacket; N) electric heater.

The calorimetric apparatus for the measurement of the activity of preparations by their β-radiation consists of three coaxial Dewar flasks filled with liquid nitrogen (Fig. 8). The heat liberated when β-particles emitted by the preparation are absorbed is used to evaporate the liquid nitrogen. The volume of gaseous nitrogen measured by means of a capillary at 760 mm of mercury and 20° C is a measure of the quantity of heat emitted by the source during the time of measurement. The sensitivity of the calorimeter found as a result of calibration turned out to be sufficient to measure sources of power of the order $10^{-4} - 10^{-5}$ watts (i.e. activities of the order of 10 millicuries with an average energy of β-radiation of the order of 1 Mev).

The formula which relates the energy of the preparation measured by the β-calorimeter to the number of disintegrations in the case of pure β-emitters has the simple form:

$$N_0 = \frac{W}{E_\beta} .$$

If the preparation also emits γ-rays then a correction is introduced for their absorption both in the preparation and in the calorimeter itself.

The error with which the β-calorimeter enables us to determine the activity of β-radiators is 3-5%. It is made up of the error in the quantity of heat measured by the calorimeter (1-1.5%), and also of the error of measuring the mean energy of the β-particles. For preparations having a simple β-spectrum the latter amounts to 2-3%; for preparations having a complex β-spectrum E_β is known with less accuracy.

In addition to individual measurements in β- and γ-calorimeters we also made combined measurements with both sets of apparatus. It was shown that combining the results of measuring a preparation in β- and in γ-calorimeters enables one to determine the activity of the sample from the known relative intensities of the γ-lines. The number of γ-quanta per disintegration is in such a case determined simultaneously with the activity of the preparation.

In order to set up the roentgen unit in the region of radiation of energies from 250 kv to 1.5 Mev the standard apparatus [12] (Fig. 9) was constructed which consists of an ionization chamber placed inside a tank of compressed air, of a means for controlling the diaphragm, of an electrical measuring device, and of a high voltage battery for supplying the chamber. The air pressure in the tank may be raised to 15 atmos, which permits one to utilize the ionization produced by electrons with energy up to 1.5 Mev. A schematic diagram of the apparatus is given in Fig. 10.

The ionization chamber of plane type consists of a measuring electrode, two guard electrodes, a potential electrode and a potential divider for smoothing out the electric field inside the measuring volume of the chamber. The distance between the electrodes is 40 cm, the applied potential difference is up to 15 kv.

The γ-preparations to be measured are placed inside the lead block of the diaphragm device; the beam of γ-rays is obtained by means of a system of calibrated diaphragms whose diameter is held to an accuracy of 0.01%. The ionization current is measured by means of a bridge circuit with an electrometer tube.

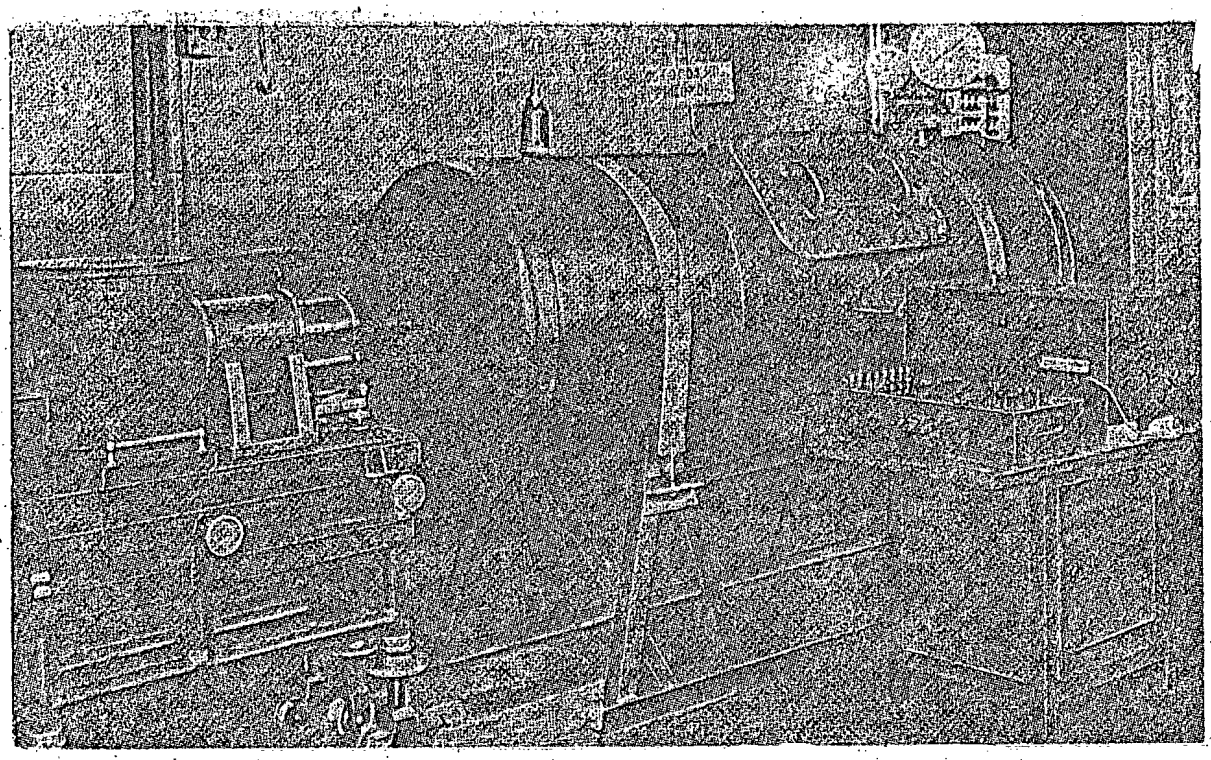

Figure 9. Standard apparatus for measuring γ-radiation in roentgens (general view).

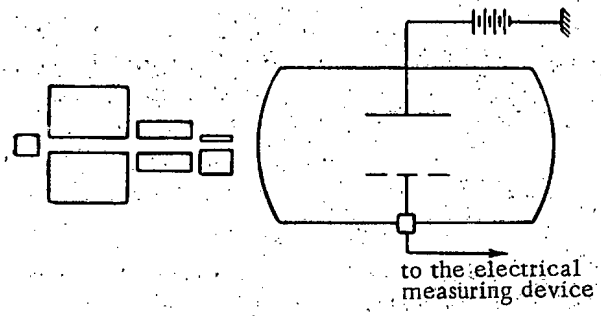

Figure 10. The standard apparatus for the measurement of γ-radiation in roentgens (schematic diagram).

The standard apparatus for measuring γ-rays in roentgens was compared using γ-radiation from Cr^{51} with the State Standard for the roentgen; the results of measurements agreed with limits of 1,5 %.

The use of the standard equipment described here enables us to determine the external γ-radiation of preparations with an accuracy of approximately 3%, and thus to provide a reliable value of the dose in r/hr at a definite distance from the preparation.

An important requirement for the standardization of radioactive preparations is the absence in them of radioactive impurities. We use a scintillation γ-spectrometer for the control of radiochemical purity, and we also measure the decay half-lives of the preparations. The latter measurements are made by the method of consecutive measurements of γ-equivalents and by the method of the differential chamber.

TABLE 2

Name of apparatus	Quantity measured	Limits of measurement	Error of measurement, (%)
Apparatus for measuring γ-equivalents	γ-equivalent	1-1000 mg-equiv. Ra	0.5-2
		0.001 mg-equiv. Ra	1-8
Counter with 4π solid angle	Activity	$5 \cdot 10^{-7}$–$5 \cdot 10^{-11}$ curie	1-3
Counter with a definite solid angle	"	10^{-5}–10^{-8} curie	2-4
γ-calorimeter	"	0.05-10 curies	3-5
β-calorimeter	"	0.01-10 curies	3-5
Standard apparatus for measuring γ-rays in roentgens	Dose	10-1000 μr/sec	3

Thus the apparatus described above allows us to determine the activity, the total and the external radiation of preparations. In Table 2 is given a summary of the data on the various apparatus.

Consecutive measurements of radioactive preparations on all the types of apparatus described above enable us to obtain dosimetric characteristics of the preparations (activity, total and external radiation) and to carry out a check on the results of measurements by different methods.

LITERATURE CITED

[1] L. N. Bogoyavlensky, Herald of the All-Union Scientific Research Institute of Metrology, 26 (42), 3 (1939).

[2] K. K. Aglintsev, Herald of the All-Union Scientific Research Institute of Metrology. 7 (52), 33 (1941).

[3] K. K. Aglintsev, Dosimetry of Ionizing Radiations. State Tech. Press, (1950).

[4] K. K. Aglintsev, F. M. Karavaev, Herald of the All-Union Scientific Research Institute of Metrology, (in press).

[5] F. M. Karavaev, Herald of the All-Union Scientific Research Institute of Metrology, (in press).

[6] B. Rossi, H. Staub, Ionization Chambers and Counters, For. Lit. Press, Moscow, 1951, (translation).

[7] R. Cohen, Ann. phys., 7, 185 (1952).

[8] A. A. Konstantinov, Herald of the All-Union Scientific Research Institute of Metrology. (in press).

[9] K. K. Aglintsev, E. A. Kholnova, Doklady Akad. Nauk. 98, 3, 357 (1954).

[10] K. K. Aglintsev, E. A. Kholnova, Herald of the All-Union Scientific Research Institute of Metrology, (in press).

[11] E. A. Kholnova, Herald of the All-Union Scientific Research Institute of Metrology, (in press).

[12] K. K. Aglintsev, G. P. Ostromukhova, M. F. Yudin, Herald of the All-Union Scientific Research Institute of Metrology. (in press).

ON THE QUESTION OF THE NATURE OF RADIATION DAMAGE IN FISSIONABLE MATERIALS

S. T. Konobeevsky

This article gives a survey of the theory of radiation damage in materials irradiated by fast particles. An attempt is made to describe the processes of phase transformations under neutron irradiation of fissionable materials with the aid of diffusion equations. In this way an expression for the coefficient of diffusion D is obtained. The possible result of the effect of thermal spikes on the structure of the eutectoid a + γ' is investigated for an annealed uranium-molybdenum alloy.

Under irradiation of solid bodies by a neutron flux, their properties change significantly. The hardness and the yield point (in metals) increase, the capacity for plastic deformation, heat conductivity, and electric conductivity decrease. In some cases the density, both macroscopic and as measured by x-rays, decreases.

Many of these changes are reminiscent of those that arise on plastic deformation of solid bodies, and therefore we may suppose that the reasons for the one and the other are due to the same changes in the lattice structure. A more careful study of the properties of matter, however, especially the character of the reverse change of the properties under annealment, leads to the conclusion that the structural effects due to irradiation of matter, although often identical with the changes caused by cold working, are nevertheless different from them; this is related to the particular way in which they arise.

The theory of radiation damage caused by fast particle irradiation has recently been intensively developed by several authors. The first ideas on the question were formulated by Bohr [1] and were later developed by Seitz [2]. Seitz considered basically two types of damage caused by the bombarding particles: ionization and "displacement" collisions. Ionization takes place for charged particles, and only for energies of these particles that are greater than a certain critical value E, given by

$$E = \frac{M}{m} E_{ion} \qquad (1)$$

where E_{ion} is the ionization potential of the target particle (atom), M is its mass, and m is the electron mass.

After the loss of part of the energy to ionization, which is the most probable process for the high-energy particles, the probability of elastic collisions with the target atoms begins to be significant, in which case, the energy is transferred to the atom as a whole. In this process a large fraction of the elastic collisions should lead to displacement of target atoms from their normal positions in the lattice, since the average energy transferred in the elastic collisions is usually large, and the energy necessary to create a pair of defects consisting of an interstitial atom and a vacancy is no greater than 25 ev. The atoms are displaced into a neighboring more distant cell, leaving an empty "hole" or vacancy in their original place. Thus, as a result there arises a pair of defects, which is usually called a Frenkel pair. The original atoms can, in their turn, cause secondary pairs, tertiary pairs, and so on. In creating a pair, the work expended by the bombarding particle is transformed in part into the potential energy of the displaced atoms, which uses up about 10 ev, and partly into the excitation elastic crystal vibrations. It is clear that these same vibrations can be excited by weak collisions that do not cause any pair defects.

As an example, we shall calculate the energy "balance" for a pair of fragments caused by the fission of

uranium [3]. For that part of the flight in which the excitation of electrons is basic, about 2.7% of the energy is used up by the elastic collisions. In addition, another 0.3% is expended after the fission fragments lose the ability to ionize uranium atoms. Almost half of all of this energy goes to the creation of fast displaced atoms. Each of these has an average energy of about 375 ev, and creates up to three atoms in the next generation. Thus according to Seitz one fission in metallic uranium leads to about 25,000 displaced atoms.

As is seen from the above data, a significant amount of energy of the original particle goes to the excitation of atomic lattice vibrations. In addition to this, we should take account of the "delayed" liberation of thermal energy that is connected with the recombination of pair defects that are close together. This whole region where the kinetic energy of the original particle is transformed into the energy of elastic lattice vibrations is the region of the "thermal spike" distributed along the path of the particle.

The question of the deceleration of the fast atoms in solid matter has recently been considered in more detail by Brinkman.

Brinkman [4] differentiates between two regions of influence for the original fast particle. For large kinetic energy of the original particle (atom) the elastic collision density is small. As a result of this, only a relatively small amount of heat is given off, which leaves the region of the thermal spike more rapidly than is possible for the recombination to take place between the Frenkel pairs that were created by the first impulse given to the atomic lattice by the original particle. In this region the first (as well as the secondary and tertiary) defects may be preserved, and the Seitz theory can be used in it to calculate the number of elementary lattice defects caused by irradiation. After the original particle slows down and its free path becomes comparable to the interatomic spacing, the energy lost to collisions increases so much that all the remaining energy of the particle is used up at once, being distributed by means of collisions between a large number of atoms and causing a local temperature increase. This region is called a "displacement spike" by Brinkman.

As a result of the liberation of a very large amount of energy in a short time, the temperature in the region of the displacement spike increases sharply. The matter is then in a state reminiscent of the critical state. The atoms in this region intermix, and in the crystallization that follows, they are displaced, and occupy new positions. It is clear that in this region the original defects consisting of vacancies and interstitial atoms cannot remain preserved. The cooling off and hardening proceeds extremely rapidly. Brinkman assumes that the crystallization re-establishes the original lattice, since the surrounding unmelted crystal is the controlling center for crystallization. After hardening, however, secondary defects in the form of dislocations and partly disoriented subgrains may occur in the region of the displacement spike.

In order to evaluate the size of the displacement spike region and the energy going into heating it, Brinkman establishes the relation between the energy of the particle and its free path, equating the energy of the displacement spike to the energy for which the free path becomes equal to the interatomic spacing. The interaction potential between identical atoms at close distances is determined by the screened nuclear charge:

$$v(r) = \frac{Z^2e^2}{r} e^{-r/a} (1 - r/2a), \tag{2}$$

where a is the effective radius of the atom's electron cloud

$$a = 2.09\, a_0 Z^{1/3},$$

a_0 is the Bohr orbit radius $0.528 \cdot 10^{-8}$ cm, and Z is the atomic number.

At large distances, the potential can be expressed by the Born-Mayer repulsion term

$$v(r) = Ae^{-Br}, \tag{3}$$

where the constants A and B are derived from experiments on compressibility. From this we may obtain an expression for the universal dependence of the free path of an atom in the lattice on its energy, which is presented graphically in Figure 1 by showing the relation of the two parameters

$$P \equiv \frac{la_0^2}{r_0^3 Z^{2/3}} \quad \text{and} \quad Q \equiv \frac{E\varepsilon_0}{Z^{14/3}}, \tag{4}$$

one of which is proportional to the free path $\underline{l}$, and the other to the energy E. Here r_0 is the interatomic spacing, and ϵ_0 is the energy necessary to free an atom from the lattice, equal to 25 ev; for the rest of the notation, see above.

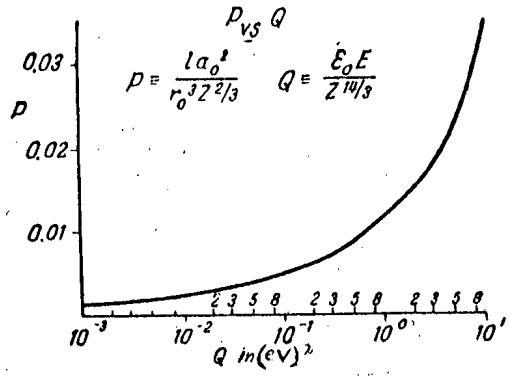

Figure 1. The dependence of the mean free path of an atom on its energy (according to Brinkman).

From the graph of Figure 1 it is possible to find the free path for an energy E. In order to do this it is first necessary to determine Q from the values of Z and ϵ_0, and then to find on the graph the value of P for the given Q, and thus to find $\underline{l}$ if the interatomic distance r_0 is known. The reverse problem can also be solved; i.e., it is possible, for a given free path, to determine the energy corresponding to it. For instance, for uranium the free path equal to the distance between closest atoms, that is 2.8 A, is attained at an energy close to 350,000 ev. This means that the first atom of uranium dislodged from the lattice by a fission fragment will slow down to 350,000 ev while creating mainly pair defects (secondary, tertiary, etc.). When its energy has been reduced to the above value, it is sharply decelerated, giving up its remaining kinetic energy to heating up the displacement spike region.

It would hardly be correct to attach too much meaning to the qualitative results obtained by Brinkman. Not to mention the somewhat arbitrary choice for the interaction potential (2), it is also impossible to consider the choice of the criterion for the occurrence of a thermal spike very well grounded, namely the requirement that the free path $\underline{l}$ be comparable to the closest atomic spacing in the lattice. As can be seen from the graph of Figure 1, the energy changes sharply with the critical free path that is chosen, and therefore the magnitude of the energy liberated in the displacement spike and the size of the displacement spike region both depend strongly on the choice of the free path. Thus it can be shown that doubling the critical free path in uranium corresponds to an increase of the displacement spike energy by a factor of 7 or 8.

All the above refers to the fate of the original atom that gets its momentum from the fast particle. The latter may be any heavy charged or neutral particle. Let us consider the effect of a fast neutron. As is well known, a neutron colliding with an atom transfers to it a fraction of its energy equal to [5]

$$\frac{2}{A + 2/3} \cdot \qquad (5)$$

For most elements with atomic weight A~100, a fission neutron with average energy of 2 Mev imparts an energy close to the value for creating a displacement spike. For heavier atoms, the energy transferred by a neutron in most of the collisions may be too little for the development of any significant thermal spike region. For light atoms, the energy liberated at the end of the flight is generally insufficient for creation of a displacement spike. Therefore the role of thermal spikes would seem to be small for matter irradiated by fast neutrons. The change in the properties of these materials must be related to the accumulation of Frenkel defects. This is partly verified by the existence in such materials of a definite, though not always well defined, activation energy for the removal of changes due to radiation. The role of thermal spikes in these materials would seem to reduce to the radiative annealing of point defects (vacancies and interstitial atoms) and perhaps to the accumulation of secondary coagulated defects.

The effect of fission fragments is much more significant in fissionable materials (in uranium).

At the start of its path a multiply ionized fragment (having lost from 20 to 25 of its electrons) is slowed down principally by the ionization of uranium atoms. The path of the fragment remains straight, since the momentum transferred to the atoms in this way is not great. In this region, however, a finite probability of elastic collisions begins to develop. Along its path the fission fragment gives rise to a large number of moving uranium atoms, since the fraction of its energy transferred to a uranium atom by the fragment in elastic collisions is sufficiently great. The atoms, whose energy is no larger than $3\text{-}5 \cdot 10^5$ ev must distribute their energy in the form of displacement spikes (according to Brinkman). The more energetic ones can give rise to secondary displaced atoms, which also almost immediately give up their energy in the form of elastic waves. If we include

in this the elastic vibrations, brought about both by the fission fragments and by the original moving atoms through collisions that do not cause displacement, and include also the heat liberated in the displacement spike regions as a result of the recombination of previously existing defect pairs in the lattice, then the whole process that goes on along the paths of the pair of fast fission fragments can be represented as the rapid liberation of heat, giving rise to a high temperature "peak" whose duration is about 10^{-10}-10^{-11} seconds.

Because of the complexity of the process described, it is hardly possible at the present time to perform an accurate calculation taking into account all the elementary phenomena that occur in the lattice of a solid fissionable material. Taking account of the general calculations made earlier by Seitz, and not forgetting that the mechanism for creation of displacement spikes does not allow for the accumulation of a significant number of defects with a high potential energy, we may estimate that about 3-5% of the total fission energy is liberated in the form of a thermal pulse. This is about $5\text{-}10 \cdot 10^6$ ev per fission, which is equivalent to the heat energy sufficient to heat about $3\text{-}5 \cdot 10^7$ atoms, or a region of $0.6\text{-}1.0 \cdot 10^{-15}$ cm^3, to a temperature of 2000°.

A more accurate value for these numbers, as well as the proof of the actual existence of thermal spikes themselves, should be expected from experiment.

In the published literature there is only one experiment that can be considered a more or less convincing proof of the existence of thermal spikes in fissionable materials, and supplies the basis for an attempt at the application of a qualitative calculation to the phenomenon.

In reference [6] an experiment on the irradiation of an alloy of uranium with 9% Mo is described. As is well known, at a temperature higher than 600°C, molybdenum is relatively easily dissolved in the γ-phase of uranium. The solid solution of molybdenum in γ-uranium that is thus created, is quite metastable at low temperatures and does not dissociate on cooling. It can, however, be brought into an equilibrium state by slow annealing in the region of 400-500°C. The alloy with 9% molybdenum then dissociates into two phases: α-uranium and the γ'-phase, which is an intermetallic compound which seems to have the composition U_3Mo and is structurally very similar to γ-uranium. These two phases occur in γ-uranium on annealing in the form of a thin laminar eutectoid composed of alternating lamina of the α- and the γ'-phases. The thickness of the lamina depends on the annealing temperature; in the usual cases, it is about 1 μ.

Specimens in the form of wires and foils were made out of the alloy of uranium with 9% Mo. Some of the specimens were studied in the tempered (homogenized) state, and the rest in the annealed state. In the latter, the initial structure was a highly dispersed mixture $\alpha + \gamma'$ in the form of eutectoids of the laminar type. The specimens were subjected to irradiation by a neutron flux ($10^{19} - 10^{20}$ neutrons/sec), and steps were taken to insure that the temperature did not go higher than 50-80°C. It was established by means of measuring the properties, microanalysis, and x-ray studies, that under this irradiation heterogeneous samples were transformed into the homogeneous state. The transition depends on the dose of radiation that was received, and is thus a direct result of the neutron radiation.

In the present article an attempt is made to interpret the above phenomena as the result of a sort of diffusion that takes place in fissionable material under the influence of radiation that creates microscopic regions of intense intermixture. If a fission event takes place at the boundary between the phases of the heterogeneous structure, then a result of this must be that an average concentration is established throughout the region of the thermal spike (Figure 2).

The heat is carried away from the region of such a thermal spike, as will be shown by the calculations below, in a very short time. As a result of this, the occurrence of a spontaneous center of crystallization in the thermal spike region is very unlikely, and the crystallized region takes on the structure of one of the neighboring lattices. It can thus crystallize in the form either of a supersaturated α-tempered alloy, or in the form of the γ'-phase. As further diffusion goes on and the average composition is smoothed out, the molybdenum will be transformed primarily into the γ-phase, which will lead finally to homogenization under the influence of the radiation.

Let us now attempt some quantitative calculations.

The liberation of the large amount of fission energy in a small volume leads to a very high temperature and intense mixing of the atoms in this volume.

The temperature in the region of the spike can be calculated if we have some idea as to the form of its distribution. Assuming that this form is not very different from a spherical distribution, we may solve the problem of heat transfer from a point source in which the energy q appears suddenly.

From the theory of heat conduction it is well known that the distribution of the excess temperature T as a function of the coordinate r and the time t can be expressed in the following form:

$$T = \frac{q}{\rho c} \cdot \frac{1}{(4\pi k t)^{3/2}} e^{-r^2/4kt}, \tag{6}$$

where ρ is the density, c is the thermal capacity, and k is the coefficient of heat conduction of the medium.

At each point r, as the heat pulse reaches it, the temperature increases to a maximum $T_{max}(r, t)$ and then drops. The time t_{max} is found from the condition

$$\left(\frac{\partial T}{\partial t}\right)_{t=t_{max}} = 0; \quad t_{max} = \frac{r^2}{6k}$$

whence

$$\left.\begin{aligned} T_{max} &= \left(\frac{3}{2\pi e}\right)^{3/2} \frac{q}{\rho c} \frac{1}{r^3}; \\ r &= \left(\frac{q}{T_{max}\,\rho c}\right)^{1/3} \left(\frac{3}{2\pi e}\right)^{1/2}. \end{aligned}\right\} \tag{7}$$

If we take the temperature T_{max} as, for example, equal to 2000 °C, then it is easy to find the radius of the sphere which, as the temperature pulse passes, is heated to at least this temperature. Thus for uranium, putting $q = 1.6 \cdot 10^{-12}$ cal (10^7 ev), we find that $r_{2000} = 0.52 \cdot 10^{-5}$ cm; $t_{max} = 0.74 \cdot 10^{-10}$ sec.

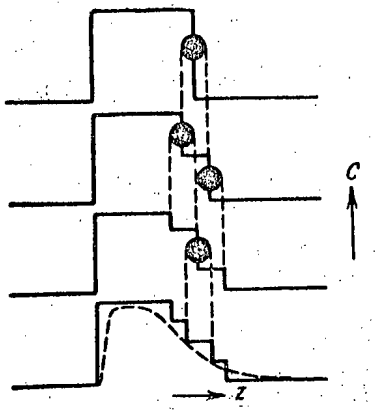

Figure 2. Schematic diagram of the diffusion that takes place under the influence of "thermal spikes" (circles) caused by a fission event.

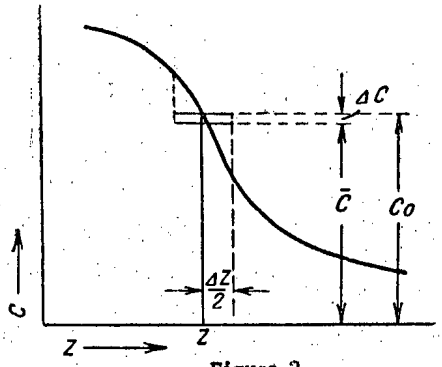

Figure 3. The change (decrease) in concentration in the region of the thermal spike for the initial sinusoidal distribution.

If we wish to determine the conventional average pulse velocity, meaning by this the expression r/t, then we get $r/t = 0.7 \cdot 10^5$ cm/sec, i.e., less than the velocity of sound in the metal ($2\text{-}3 \cdot 10^5$ cm/sec). This to some extent justifies the application of the calculation based on the macroscopic theory of heat conduction. It would seem less meaningful to extend such calculations to the higher temperatures that occur in the central zone of the thermal spike. An attempt to maintain the principle of the calculation can be justified, however, since the only constant connected with the medium that enters into Formula (7) is the volumetric heat capacity (ρc), which could hardly be very different.

Analogously, it is possible to perform the calculation if it is assumed that the length of the path along which the energy of the fission fragments is transferred to the uranium atoms is significantly greater than the region through which the heat is distributed around the particle trajectory. The shape of the spike region will then be different, of course, but the total volume of the region and the number of atoms in the heated zone changes only slightly. Therefore, to avoid unnecessary complications in the calculation, it will be assumed in what follows that the thermal spike is spherical in shape.

We shall now show that the smoothing out of the concentration in the separate parts, which is caused by the thermal spikes, is analogous to diffusion. Let us consider a laminar distribution of the concentration which, for simplicity, we shall assume to be a cosine law:

$$C = C_0(1 + \alpha \cos 2\pi Z/\lambda), \tag{8}$$

where C does not depend on either x or y.

Let us assume also that after the heat pulse arrives at the point whose coordinate is Z, the concentration will be smoothed out on the section ΔZ (Figure 3).

If ΔZ is small compared to λ, then the ordinate of the section may be considered the concentration at the point Z after it is heated.

The new value of C should then be taken as

$$\overline{C} = \frac{1}{\Delta Z} \int_{Z-\Delta Z/2}^{Z+\Delta Z/2} C(Z)\, dZ. \tag{9}$$

After a simple transformation, we get

$$\overline{C} = C_0 \left(1 + \frac{\alpha\lambda}{\pi \Delta Z} \cos \frac{2\pi}{\lambda} Z \sin \frac{2\pi}{\lambda} \frac{\Delta Z}{2}\right). \tag{10}$$

or, expanding the sine into a power series, and taking only the first two terms,

$$\overline{C} = C_0 \left(1 + \alpha \cos \frac{2\pi}{\lambda} Z - \alpha \cos \frac{2\pi}{\lambda} Z \cdot \frac{\pi^2}{6} \frac{(\Delta Z)^2}{\lambda^2}\right). \tag{11}$$

Comparing this with (8), we see that as a result of one thermal spike the local concentration changes (decreases) by an amount

$$\Delta C = C_0 \alpha \cos \frac{2\pi}{\lambda} Z \cdot \frac{\pi^2}{6\lambda^2} (\Delta Z)^2 \tag{12}$$

Neglecting superposition (coincidence) of spikes, it is easy to reason that the whole volume of the metal goes through the state of a thermal spike in the time $\Delta \tau$, which can be written

$$\Delta \tau = \frac{1}{Nv}, \tag{13}$$

where N is the number of thermal spikes per cubic centimeter per second, and v is the volume of a thermal spike.

Let us consider the expression

$$\frac{\Delta C}{\Delta \tau} = N C_0 \alpha \cos \frac{2\pi}{\lambda} Z \cdot \frac{\pi^2}{6\lambda^2} v (\Delta Z)^2. \tag{14}$$

This expression can clearly be identified with the diffusion equation

$$\frac{\partial C}{\partial t} = D \frac{\partial^2 C}{\partial Z^2} = D C_0 \alpha \cos \frac{2\pi}{\lambda} Z \cdot \frac{4\pi^2}{\lambda^2}, \tag{15}$$

if we put

$$D = N \frac{v (\Delta Z)^2}{24}. \tag{16}$$

The above result can be generalized if we assume that it is valid for an arbitrary initial distribution. Thus the action of the thermal pulses due to fission should cause diffusion with the coefficient given by (16), and this is valid for arbitrary average (macroscopic) temperature.

From the quantities entering into the expression for D, the value of N is easy to determine if the heat liberated is known in watts per gram

$$N = W \cdot 3 \cdot 10^{10} \cdot \rho, \tag{17}$$

$(\Delta Z)^2$ is the mean square linear dimension directed along the concentration gradient, of the region in which the heat is liberated; for instance, for a spherical region, it is equal to $^2/_3 r^2$.

Inserting all these quantities in (16) and making use of Formula (7), we obtain the following expression for the diffusion coefficient D:

$$D = 0.452 \cdot 10^8 \frac{\rho}{(\rho c)^{5/3}} \left(\frac{q}{T}\right)^{5/3} \cdot W \ \text{cm}^2/\text{sec}.$$

If we take $\rho c = 0.514$ ($\rho = 18.7$ [7] for uranium) and express the energy E liberated in a thermal spike in kev instead of in calories, then we get the following expression for D

$$D = 1.16 \cdot 10^{-18} \left(\frac{E}{T}\right)^{5/3} W. \tag{18}$$

Now let us investigate the possible result of the effect of thermal spikes on the structure of the eutectoid $\alpha + \gamma'$ in the annealed uranium-molybdenum alloy. This eutectoid, as was mentioned above, is of a laminar structure with a period of the order of 1 μ, depending on the annealing temperature of the preliminary tempered alloy. The exact structure of the γ'-phase is not established. It is assumed to be U_3Mo. The α-phase is pure uranium. The ratio of the thickness of the layers of the α-phase to those of the γ'-phase is about 3 to 1 (more exactly, 77 to 23).

As is clear from the above, the concentration of the Mo in the uranium will gradually be smoothed out under the influence of the thermal spikes. If the concentration at the minimum (in the region of the α-phase) attains a value close to 8 or 9 percent, then this region will be unable to crystallize in the α-phase, and the γ-phase must result. As time goes on, smoothing out of the concentration will gradually take place, until a completely homogeneous solid solution will have developed. In the γ'-phase regions, the reduced molybdenum concentration also causes an unstable γ'-phase, and makes it transform into an equilibrium form, the γ-solid solution.

The following simple calculation can give us some idea as to the rate at which the above process proceeds.

For any periodic linear concentration distribution, with a center of symmetry, of an element B in A, the solution of the diffusion equation gives an expression

$$C(Z, t) = C_0 + \sum C_n \cos\frac{2\pi n}{\lambda} Z \cdot e^{-\frac{4\pi^2 n^2}{\lambda^2} \cdot Dt}. \tag{19}$$

Here C_n are the Fourier coefficients of the initial distribution C(Z, 0). It is well known that, due to the damping of the higher harmonics, some time after the beginning of the process only the first harmonic is significant, and the distribution can be expressed by a simple cosine. Thus in order to investigate the rate of the smoothing out process, only the expression

$$e^{-\frac{4\pi^2}{\lambda^2} \cdot Dt}, \tag{20}$$

which is the factor determining the damping of the first harmonic, need be analyzed. The time for homogenization can be found if we equate the value of this factor to some conventional minimal value, say 0.1, which in our case is entirely sufficient.

Putting

$$\frac{4\pi^2}{\lambda^2} Dt_{hom} = \ln 10$$

we obtain for the total energy Wt liberated per gram, the expression

$$Wt = \frac{\ln 10 \cdot 10^{18} \lambda^2}{4\pi^2 1.16} \left(\frac{T}{E}\right)^{5/3}.$$

Agreement with experimental data is achieved (see reference [6]) if we put

$$\frac{T}{E} = 0.11.$$

In order to determine the energy of the thermal pulse, we must know the temperature necessary for complete intermixing of the atoms in the thermal spike region. If it is entirely reasonable to set it equal to 2000°, which is twice as high as the melting point, then E ≈ 18 Mev.

This is somewhat higher than the evaluation made above, and may make it necessary to introduce some corrections into the theory. Remembering the approximate character of the theory sketched out in this article, it is hardly possible to pretend that it is very accurate. It would seem, however, that it gives sufficient basis for the statement that the diffusion processes that are observed to occur on the irradiation of fissionable materials by neutrons are caused by the action of fast fragments that lead to thermal spikes.

LITERATURE CITED

[1] H. Bethe and Yu. Ashkin, The Penetration of Radiation Through Matter, Experimental Nuclear Physics, Edited by Segre, Foreign Lit. Press, 1955; also A. I. Zakharov, Prog. Phys. Sci. 57, 4 (1955).

[2] F. Seitz, Discuss. Faraday Soc. 5, 271 (1949); also Seitz and Keller, Metallurgy of Nuclear Energy and the Effect of Radiation (Reports of Foreign Scientists at the International Conference on the Peaceful Uses of Atomic Energy), Metallurgy Press, 1956, Vol. II, p. 417.

[3] F. Seitz, Coll., The Effect of Radiation on Semiconductors and Insulators, Edited by Ryvkin, Foreign Lit. Press, 1954.

[4] J. A. Brinkman, J. Appl. Phys. 25, 961 (1954).

[5] S. Glasstone and M. Edlund, The Foundations of Nuclear Reactor Theory, Foreign Lit. Press, 1954.

[6] S. T. Konobeevsky, N. F. Pravdyuk, and V. I. Kutaitsev, Investigations in the Field of Geology, Chemistry and Metallurgy (Reports of the Soviet Delegation at the International Conference on the Peaceful Uses of Atomic Energy), Acad. Sci. USSR Press, 1955, p. 263.

[7] D. Murray, Introduction to Nuclear Technology, Edited by P. E. Stepanov, Foreign Lit. Press, 1955.

THE PENETRATION OF GAMMA-RAYS THROUGH WATER, IRON, LEAD, AND COMBINATIONS OF IRON AND LEAD

S. G. Tsypin, V. I. Kukhtevich and Yu. A. Kazansky

The dose rate attenuation of γ-rays is measured in iron, water, and lead for "infinite" geometry. The dose rate attenuation of γ-rays is measured in mixtures of iron and lead for "barrier" geometry. The experimental data obtained is compared with the results of calculations as presented in reference [1].

I. The penetration of γ-rays through iron, water, and lead for "infinite" geometry

The experimental verification of the theoretical calculations for γ-ray dose rate attenuation in various substances as presented in reference [1] is the subject of several articles [2-5], which refer to work carried out under conditions of so-called "infinite" geometry.

In these experiments the penetration of γ-rays through water, iron, and lead was investigated. The experimental results agree well with the calculations [1]. In the published experiments, however, there is no reference to low-energy γ-rays (about 0.5 Mev) or those of about 3 Mev passing through matter.

In this section we present the results of measurements on the attenuation of γ-ray spectra from isotropic point sources of Au^{198} by iron, and Na^{24} by lead and water for the conditions of "infinite" geometry.

Experimental set-up. The Na^{24} γ-ray source was a nickel sphere whose radius was 14 mm and whose wall thickness was 0.1 mm, filled with NaF. Its activity at the start of the experiment was about 1 curie. The Au^{198} γ-ray source was a gold plate of thickness 0.5 mm, whose area was 10×10 mm^2. Its activity at the start of the experiment was of the order of 15 curies.

Small ionization chambers which satisfied Gray's [6] conditions were used to measure the γ-ray dose rate. The volume of the ionization chamber was 1 cm^3, the thickness of the bakelite-graphite wall was 2 mm. In order to ensure secondary electron equilibrium for the measurements with the Na^{24} γ-ray source, graphite caps of 5.5 mm thickness were added to the ionization chambers. The variation in the charge of the chambers was determined by a standard electrometer.

The measurement of the γ-ray dose rate attenuation in water was carried out in a tank whose diameter was 6 meters and whose depth was 4 meters. The source and the detector were no less than 1.5 meters from the walls of the tank, and 2 meters from the bottom.

In order to measure the γ-ray attenuation by iron, the source was placed into an opening in an iron block in such a way that the thickness on the sides and in the rear was 20 cm. Iron plates whose area was 60×60 cm^2 and whose thickness was 1 cm were placed between the γ-ray source and the ionization chamber. The ionization chambers were inserted into a groove in an iron block of dimensions $24 \times 24 \times 20$ cm^3.

The measurement of γ-ray attenuation by lead was carried out on a similar set-up of the following dimensions: around the source, 20 cm; lead plates, $40 \times 40 \times 1$ cm^3; lead block for the ionization chambers, $24 \times 24 \times$ $\times$ 15 cm^3.

Results of the measurements. The experimental points of γ-ray dose-rate attenuations for the Na^{24} source in water and lead and the Au^{198} source in iron are presented in Figures 1, 2, and 3. On the ordinate axis are plotted the magnitudes of the γ-ray attenuation.

$$T_{exp}(x) = \frac{D(x)}{D_0(x)}, \qquad (1)$$

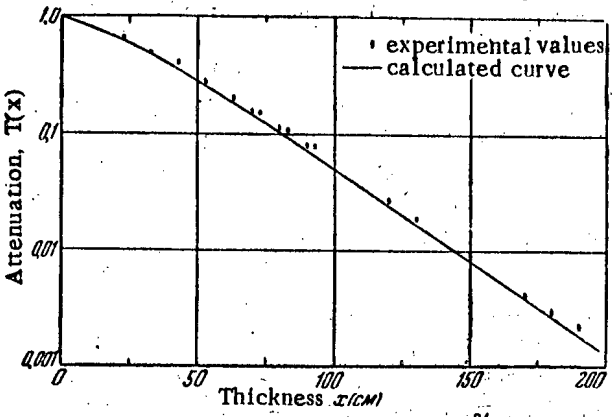

Figure 1. Attenuation of γ-rays from Na^{24} by water ("infinite" geometry).

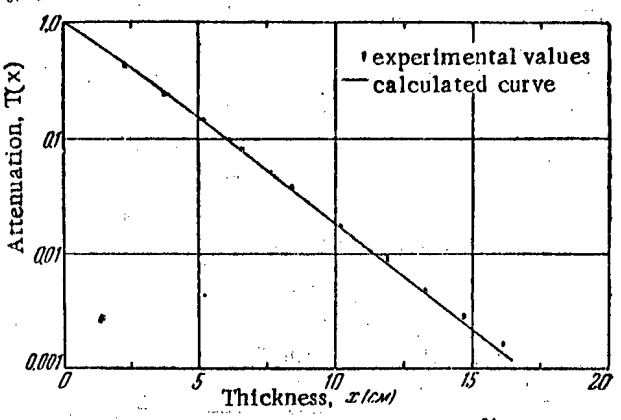

Figure 2. Attenuation of γ-rays from Na^{24} by lead ("infinite" geometry).

where D(x) is the ionization measured by the ionization chamber in the matter, and $D_0(x)$ is the ionization measured by the ionization chamber at the same point in the absence of the substance being investigated.

The thickness x of the substance being investigated is plotted on the abscissa in centimeters.

Since the γ-ray sources were of finite dimensions, the quantities $D_0(x)$ and D(x) include corrections that take into account the scattering of the γ-radiation by the sources. These corrections always increase the value of the attenuation $T_{exp}(x)$ and increase as the thickness of matter x increases. They are as large as 2% for the Au^{198} γ-ray source in iron, and 3% for the Na^{24} γ-ray source in lead; for water and the Na^{24} source these corrections are no larger than 2%.

For the γ-ray spectra [7] emitted by Na^{24} and Au^{198} the curves (see Figures 1, 2, and 3) of γ-ray attenuation in water, lead, and iron are calculated by the formula

$$T_{calc}(x) = \sum_{i=1}^{n} p(E_i)\, B(E_i;\ x)\, e^{-\mu(E_i)x}, \qquad (2)$$

where $B(E_i; x)$ is the dose rate buildup factor for γ-rays of energy E_i in a thickness x of the given material. The values of $B(E_i; x)$ are obtained by interpolation and extrapolation of the data presented in reference [1]; $\mu(E_i)$ is the absorption coefficient for γ-rays of energy E_i in the given material. The values of the coefficients $\mu(E_i)$ are taken from reference [8]; $p(E_i) = \frac{E_i \sigma(E_i) K_i}{\sum_{i=1}^{n} E_i \sigma(E_i) K_i}$ is the fraction of the ionization caused by γ-quanta of energy E_i for x equal to zero; $\sigma(E_i)$ is the absorption coefficient of γ-rays with energy E_i in air; K_i is the fraction of γ-rays with energy E_i in the total spectrum of the source.

The experimental values obtained for the γ-ray dose rate attenuation with the Na^{24} source in water (Fig. 1) have a maximum experimental error of 5% and differ from the calculated curve on the average by 10%. Agreement of the experimental and calculated data may be considered satisfactory, since the error in the determination of the dose rate buildup factor $B(E_i; x)$ in this case is 10-15%.

The experimental values of the dose rate attenuation of Na^{24} γ-rays in lead (Figure 2) agree with the calculated curve within the limits of experimental error (3%) and the errors of calculation (5% due to the error in determining the value of $B[E_i; x]$).

There is a significant difference between the experimental and calculated data for the γ-ray dose rate attenuation for the Au^{198} source in iron (Figure 3). This difference is about 20% for a maximum experimental error of 3%. The value for B(0.411; x) in this case was obtained by extrapolation of the data of reference [1]; it would seem that in so doing the error involved in the extrapolation is no larger than 3-5%.

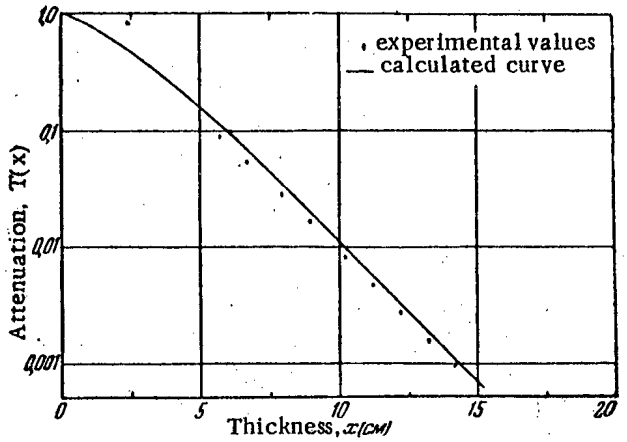

Figure 3. Attenuation of γ-rays from Au^{198} by iron; ("infinite" geometry).

The experimental values for the buildup factor for 0.66 Mev γ-rays in water that were obtained in reference [9] differ by approximately 20% from the calculated values derived by the method developed in reference [1]. This fact also indicates an inaccuracy (of about 20%) in the calculations in the region of low-energy γ-rays.

II. The penetration of γ-rays through combinations of iron and lead for "barrier" geometry

The dose rate attenuation of γ-rays from a point isotropic source of Co^{60} successively by iron and lead for the conditions of "barrier" geometry was measured.

The source, a 1 cm diameter cylinder of height 1 cm and activity 0.71 curies, was placed into a lead container with a 62 degree angle conical opening. The ionization chamber, with an additional graphite cap with a wall thickness of 2.1 mm, was 62.5 cm away from the source. The iron and lead plates were 40 x 40 cm^2.

A packet of iron plates of total thickness $d_1 = 11.8$ cm was placed at a distance of 45.9 cm from the source; close to it was placed a packet of lead plates of total thickness $d_2 = 2.8$ cm. The ionization chamber was at a distance of 2 cm from the lead plates.

The chosen distances, dimensions of the cone, and the area of the iron and lead plates made possible measurements under wide beam conditions [10-11].

The measured value of the dose rate attenuation of γ-rays from the Co^{60} source by successive penetration of iron and lead was

$$T_{exp}(d_1+d_2)=(5.36\pm 0.15)\cdot 10^{-3}.$$

There is a correction included in this value to take account of the radiation scattered by the source and the walls of the cone. The correction turned out to be 16.5%.

The calculation of the dose rate attenuation was carried out by the formula

$$\begin{aligned} T_{calc}(d_1+d_2) = \\ = \int_0^{1.2\,Mev} N(E)\,E\sigma(E)\,B_{Pb}(E;d_2)\,e^{-\mu_{Pb}(E)d_2}dE + \\ + p(E_1)\,e^{-\mu_{Fe}(E_1)d_1}\cdot e^{-\mu_{Pb}(E_1)d_2}\cdot B_{Pb}(E_1;\ d_2) + \\ + p(E_2)\,e^{-\mu_{Fe}(E_2)d_1}\cdot e^{-\mu_{Pb}(E_2)d_2}\cdot B_{Pb}(E_2;d_2), \end{aligned} \qquad (3)$$

where

$$\begin{aligned} \int_0^{1.2\,Mev} N(E)\,E\sigma(E)\,dE = \\ = T_{exp}(d_1) - p(E_1)\,e^{-\mu_{Fe}(E_1)d_1} - p(E_2)\,e^{-\mu_{Fe}(E_2)d_1}, \end{aligned}$$

where $E_1 = 1.17$ Mev; $E_2 = 1.33$ Mev; N(E) is the γ-ray spectrum of the Co^{60} source in iron at a thickness d_1 for the condition of "infinite" geometry (according to the data of reference [12]), and $T_{exp}(d_1)$ is the experimental value of the attenuation of the Co^{60} γ-rays by iron in the "barrier" geometry.

A calculation was carried out by Formula (3), on the assumption of identical γ-ray spectra in iron for the conditions of "barrier" and "infinite" geometry. In the calculation by Formula (3), the back radiation of the γ-rays from the lead was not taken into account, since additional measurements showed that it is less than 2%. The calculated value was

$$T_{calc}(d_1 + d_2) = 5.7 \cdot 10^{-3},$$

which differs from the experimental one by 6%.

It should be noted that when the positions of the iron and lead plates were interchanged (the lead plates were placed closer to the source), the magnitude of the dose rate attenuation of the γ-rays changed significantly. It was found that the ratio of the γ-ray attenuations for the two cases mentioned is

$$\frac{T_{exp}(d_2 + d_1)}{T_{exp}(d_1 + d_2)} = 1.5.$$

The change in the magnitude of the γ-ray dose rate attenuation in the "barrier" geometry, which occurs on interchanging the positions of the iron and lead plates, can be explained by the difference in the spectra of the scattered γ-quanta from iron [12] and lead [3], and by the dependence of the γ-ray absorption coefficient on the energy [8].

In conclusion, the authors express their deep gratitude to Doctor of Physico-Mathematical Sciences A. K. Krasin for much valuable advice and for his constant interest in the work.

LITERATURE CITED

[1] U. Fano, Nucleonics 11, 9 (1953).

[2] G. R. White, Phys. Rev. 80, 154 (1950).

[3] J. O. Elliot, R. T. Farrar, R. D. Myers and C. F. Ravilious, Phys. Rev. 85, 1048 (1952).

[4] C. Garrett and G. N. Whyte, Phys. Rev. 95, 889 (1954).

[5] P. A. Roys, K. Shure and J. J. Taylor, Phys. Rev. 95, 911 (1954).

[6] L. H. Gray, Proc. Roy. Soc. (London) A122, 647 (1928).

[7] J. M. Hollander, I. Perlman and G. T. Seaborg, Revs. Mod. Phys. 25, 469 (1953).

[8] U. Fano, Nucleonics 11, No. 8, 8 (1953).

[9] R. B. Theus, L. A. Beach and W. R. Faust, J. Appl. Phys. 26, 294 (1955).

[10] H. O. Wyckoff, R. J. Kennedy and W. R. Bradford, J. Research Natl. Bur. Standards 41, 223 (1948).

[11] R. J. Kennedy and H. O. Wyckoff, J. Research Natl. Bur. Standards 44, 157 (1950).

[12] G. N. Whyte, Can. J. Phys. 33, 96 (1955).

GENETIC TYPES OF MINABLE URANIUM DEPOSITS

D. Ya. Surazhsky

Natural uranium concentrations are formed under the most diversified conditions, which embrace the last stages of the magnetic process, metamorphism, the sedimentation cycle and weathering processes.

Uranium deposits are divided into four classes: 1) magmatic deposits; 2) sedimentary syngenetic deposits; 3) sedimentary-metamorphic deposits; 4) weathering deposits.

Deposits of the first class include pegmatites, pegmatoid veins, hydrothermal veins, which are formed by the filling of open cavities, and bedding planes of hydrothermal-metasomatic origin.

Deposits of the second class are represented by uraniferous marine shales and phosphorites.

Deposits of the third class include minable bodies of uranium in limestone and carbonaceous silicic shales.

The fourth class includes blacket deposits in sandstones, conglomerates, subbituminous coals and lignites.

This article provides a general description of uranium deposits and touches on problems concerning the sources of the ores, the nature of the ore-controlling and ore-localizing structures, the composition and physical properties of ore-bearing solutions and the conditions for deposition of the metal.

The minable uranium deposits that are known at the present time can be divided into six large groups according to the form of the ore bodies and the character of the mineralized and ore-containing quartz rocks. The first group contains uraniferous pegmatites and pegmatoid veins; the second group contains quartz quartz-carbonate and fluorite-barytic veins in igneous and strongly metamorphized sedimentary rocks; to the third group belong bedding planes in strongly metamorphised sedimentary rocks; the fourth group contains uraniferous beds of sedimentary rocks of marine origin; in the fifth group are bedding planes in weakly metamorphized sedimentary rocks; and in the sixth group are bedding planes and lens deposits in normal sedimentary rocks of continental facies.

This grouping has been made here principally for convenience in the later description. In addition to the general description of deposits in the separate groups on the basis of information in the literature the main aspects of their genesis will be considered, primarily questions concerning the sources of the ores, the nature of ore-controlling and ore-localizing structures, the composition and physical properties of ore-bearing solutions and the conditions for the deposition of the metal. In conclusion a genetic classificatory scheme will be derived from the factual material that has been discussed.

Uraniferous Pegmatites and Pegmatoid Veins

These ore formations of the most varied shapes are genetically closer to granitic intrusions. The predominating shape is that of slab-like vein bodies; often beaded and lenticular veins are found.

The uranium in pegmatites is separated either in the form of independent minerals (uraninite and its oxidation products) or in the form of an isomorphic addition to niobium tantalates and titanium niobates of various composition. Sometimes carbouranium is also found. Uraninite and complex oxides of uranium, niobium, tantalum and titanium are usually adapted to the most diversified portions of the pegmatic bodies. They are found most frequently in zones which are rich in perthite, when the uraninite is closely associated mainly with finely flaked muscovite and albite-oligoclase. Euxenite-polycrase minerals are usually found together with beryllium; microlite and pyrochlore with lipidolite and spodumene; samarskite with muscovite; ortite and betafite, with biotite [1].

All of these minerals are evidently products of the fractional crystallization of a pergmatitic melt. The magmatic origin of uraniferous pegmatites (and of the uranium contained in them) can be considered indisputably established in the majority of cases.

The pegmatites are not of great practical importance as the source of uranium minerals. Out of many hundreds of pegmatitic veins comprising separate pegmatite fields only a handful, and at best only a few tens, have sufficient uranium to be of interest. And in these the body of uranium minerals is of a narrowly localized character, forming spearate nodes which are usually of very small size. Until very recently the annual yield of uranium minerals from these deposits was a few tens of kilograms obtained as byproducts of the processing of pegmatites for their mica and feldspar. Comparatively recently in Canada, in the vicinity of Lake Charlebois and at other points in the Province of Saskatchewan, regions of migmatitic rocks have been discovered which contain uraninite as a component of quartz-feldspar veinlets [2]. These deposits can be considered as possible large sources of ores which are poor, but comparatively rich in uranium.

According to the latest information a minable deposit of uraniferous pegmatites has also been discovered in the Colorado Front Range [3].

Close to the pegmatites are special uranium-titanium veins composed principally of quartz and uranium titanates, mainly davidite [(Fe, Ce, U) (Ti, Fe, V, Cr) (OOH)], ilmenite and rutile. To this type belong the vein deposits of Radium Hill in South Australia, which are of great industrial importance [4], [5].

Quartz, Quartz-Carbonate and Fluorite-Barytic Veins

These veins occur both in igneous rocks (predominantly in acid granitoids, acid effusives and in rocks of subeffusive facies) and in strongly metamorphized sediments.

The position of the ore fields is determined in the majority of cases by large discontinuities of varying character and origin: normal faults, upthrusts, wide shear zones etc. which can usually be traced for hundreds of kilometers. All of these dislocations do not, as a rule, contain uranium ores, being ore-controlling but not ore-enclosing structures.

Uranium ores are ordinarily localized in the smaller fractures or shear structure adjacent to large faults or are distributed in the related granulation zones.

The most productive ore veins are usually found in rocks that are rich in divalent iron or organic matter, i.e., in amphibolites and carbonaceous, chloritic and hornblende shales. When the enclosing rocks are igneous the uranium mineralization is connected with zones of chloritization and talc formation which were formed in the pre-uranium stage of the ore process.

Deposits of this type are extremely varied with regard to the character of their mineral paragenesis. The most important ore formations are those of uranium proper, uranium-nickel-cobalt-bismuth-silver ("five elements") uranium-multimetallic, and uranium-molybdenum.

The veins of uranium proper are of very simple composition. Besides pitchblende they contain only hematite and small quantities of the usual sulfides: chalcopyrite, galenite, pyrite and sometimes fahlerz. Vein minerals are represented mainly by quartz and carbonates. Frequently dark violet, almost black, fluorite is associated with these. The veins seldom contain zeolites and mellitic barite. The minerals usually are deposited in the following order: quartz (frequently encrusting the walls of the vein), pitchblende, pink dolomite.

Uranium-nickel-cobalt-bismuth-silver veins differ sharply from the veins of uranium by their much more complicated mineral complex, and by the predominance of arsenides and sulfo-arsenides of nickel, cobalt, iron (niccolite, smaltite-chloanthite, rammelsbergite-safflorite, gersdorffite, glaucodot, lollingite, arseno-pyrite) and by the appreciable development of native elements (silver, arsenic, bismuth) as well as arsenites and sulfo-antinomites (proustite, stephanite, tetrahedrite, tennantite, pyrargyrite etc.) and, finally, by multistage ore-forming processes. Typical representatives of this formation are the Great Bear Lake veins in Canada in which four successive stages of mineralization are distinguished [6]: 1) pitchblende-quartz (quartz, pitchblende with a small amount of nickel and cobalt diarsenides), 2) arsenide-quartz (quartz, diarsenides, cobaltine, hematite, native bismuth), 3) sulfide-carbonate (dolomite, sphalerite, galenite, tetrahedrite, freibergite, chalcopyrite, bornite), 4) carbonate-silver (rhodochrosite, strömerite, jalpaite, argentite, hessite, native silver). In some deposits represented by veins of this formation two mineral zones are distinguished: an upper silver zone and a lower nickel-cobalt-bismuth zone. In this case the uranium ores are found at a different depth. On the upper levels of the deposits they are accompanied by silver ores, and on the lower levels by nickel and cobalt arsenides, native bismuth etc.; still lower they appear in the form of monometallic pitchblende veins. Similar

relationships enable us to regard silver and nickel-cobalt ores as products of deposition from the same solution whose composition was changed by fractional distillation. Pitchblende evidently resulted from an independent stage of ore formation which preceded silver-cobalt mineralization and which was localized in the same cracks but at an earlier time.

Polymetallic uranium veins are characterized by an abundance of simple sulfides: pyrite, galenite, sphalerite, chalcopyrite, sometimes with arsenopyrite, bismuthine and complex lead-bismuth-silver sulfur salts. Vein minerals are represented mainly by quartz of several generations as well as by carbonates, barite and fluorite. The latter sometimes comprises the main body of the ore.

Several stages can usually be distinguished in the process of mineralization. In one of the polymetallic uranium deposits the earlier stages are represented by quartz and sulfides, the intermediate stages by quartz, barite and carbonates, and the later stages by carbonates and pitchblende. In other deposits, such as those in Gilpin (Colorado) the uranium-quartz stage precedes the quartz-carbonate-sulfide stage [7].

Uranium-molybdenum veins contain, in addition to pitchblende and its oxidation products, some significant amounts of molybdenite. The accessory minerals which are found are hematite and the usual sulfides: chalcopyrite, galenite, pyrite and sometimes tennantite. The lode consists of quartz, carbonate and a small amount of dark fluorite. In these deposits the pitchblende stage of mineralization is one of the earliest.

In all uranium lodes the pitchblende stage proper is characterized by colloform structures not only of the pitchblende but also of such minerals as carbonates, sulfides, chlorite etc. A metacolloidal ore structure is typical evidence of strong supersaturation of solutions and of the formation of gels which were not able to react chemically with the wall rocks. Therefore the formation of the ore bodies takes place exclusively through the filling of open cavities. Metasomatosis plays an insignificant part.

The most characteristic alteration of adjacent wall rocks is the so-called "red alteration" which was noticed particularly in the study of the Great Bear Lake deposits and of a deposit in the Beaver Lodge Lake region [9]. This includes both igneous and metamorphic rocks and is caused by hematization of the principal rock-forming minerals: quartz, albite and carbonates. "Jasperoid" is formed in the surrounding zones, which consist principally of quartz, magnetite, sericite, chlorite and carbonates.

Polymetallic pitchblende veins are often accompanied by quartz, chlorite and sericite zones. Propylitization is also very common, as a result of which there is a great loss of alkali metals, principally sodium, from the wall rocks. In comparatively few cases epidotization is also observed.

The high temperature forms of changes in adjacent wall rocks – greisenization, muscovitization and tourmalinization – are not characteristic of endogenous uranium deposits.

At the present time the great majority of investigators believe that the uranium in vein deposits was most likely removed from the magma in the form of a uranyl ion in sulfate or carbonate solutions [10].

Modern study of vein filling and of adjacent wall rock alterations suggest highly concentrated solutions of complex composition with a high content of volatile components: arsenic, fluorine, boron, carbon dioxide etc., and bearing also a considerable amount of silica as well as calcium, magnesium barium and trivalent iron. Quite frequently (but not always) these elements are associated with bismuth, silver, cobalt, nickel, zinc, lead and molybdenum.

According to their mineral associations the great majority of lodes belong to mesothermal deposits which form at temperatures from 175° to 300° C and at depths from 1200 to 3600 m [11].

In the precipitation of the primary uranium minerals from the solutions the principal role is apparently played by oxidation-reduction reactions such as

$$3H_2O + 2Fe^{+2} + (UO_2)^{+2} \rightarrow Fe_2O_3 + UO_2^{+4} + 6H,$$

which result in the simultaneous formation of pitchblende and hematite. It is also possible that pitchblende is precipitated from uranyl sulfate solutions by hydrogen sulfide in the reaction

$$H_2S + (UO_2^{+6})^{+2} + 4H = S + UO_2^{+4} + 2H_2O.$$

Since ore bodies are formed only by deposition in open cavities, the structural control is extremely important. The principal ore-controlling structures are regional faults; the principal ore-localizing structures are the associated fractures and shear structures of the second and higher orders.

Vein deposits of uranium, "five-elements", uranium-polymetallic and uranium-molybdenum strata serve as the principal sources of crude uranium on the earth. In addition, appreciable bodies of uranium minerals are also encountered in many tin-tungsten, copper, gold and other veins, although their industrial value is very small.

Bedding Planes and Strongly Metamorphized Sedimentary Rocks

As a rule these deposits are not clearly dependent on large disjunctions. During their formation the dominant role is played by the selective replacement of the material of sedimentary-metamorphic strata, where the principal factor controlling the distribution of the ore is the composition of the wall rock. Most favorable for ore deposition are iron hornstones and carbonaceous and silicified dolomitized shales.

Three types of ore strata are distinguished:

a) uranium strata, in which pitchblende is the only pay ore;

b) iron-uranium strata, characterized by a strong predominance of magnetite and hematite;

c) copper-uranium strata, in which the dominant role is played by copper sulfides, sometimes in association with cobalt, nickel and molybdenum sulfides and also with native elements (copper, silver) and thallium minerals.

In all of these deposits the main body of uranium ore is represented by a fine and relatively uniform dissemination of small pellets of the primary uranium minerals; among the latter, besides the amorphous form, an appreciable role is played by the crystalline modifications of pitchblende ore.

Metasomatosis appears in a varied and pronounced form. Usually it manifests itself in successive processes of albitization, carbonatization and quartzification of the ore-enclosing rocks. Uranium mineralization begins in the first (alkali) stage, but it is associated mainly with the second (carbonate) stage of metasomatosis.

It is frequently observed that even in homogeneous seams or sheets the replacement does not embrace the entire rock mass but is localized in separate portions which are sometimes sharply delimited from portions that are comparatively weakly affected by metasomatosis. The reason for this is found in the very mechanism of metasomatic replacement, which can occur only in rocks which are characterized by definite (very small) pore sizes [12]. Evidently the zones of such capillary porosity along which there is especially intensive replacement are also channels controlling the movement of solutions even in a medium which is entirely homogeneous as to chemical and mineralogical composition. Judging from the character of the new formations, the agents of uranium transport and deposition were comparatively slightly concentrated and therefore very mobile alkali hydrothermal solutions which entered into vigorous interaction with the wall rock. These were characterized by a comparatively simple composition and the complete absence of volatile elements except water and carbon dioxide. The source of the uranium in these deposits is debatable. Some believe that the uranium was derived from the crystallized magma at depth; others believe that the role of the hydrothermal solutions amounts merely to the redistribution of uranium that was originally disseminated in the enclosing sedimentary rocks.

Examples of this type of deposit are the uranium and copper-uranium deposits of the Catherine-Darwin region in Southern Australia [13].

Uraniferous Beds in Normal Sedimentary Rock of Marine Origin

These are usually nondislocated or sometimes very slightly dislocated deposits in marine basins covering extensive areas. Here the uranium almost never or never has independent mineral forms, but is associated mainly with organic matter and with calcium phosphates. The principal representatives of this group of deposits are dark bituminous shales and phosphorites of marine origin.

Uranium-bearing shales are characterized by comparatively small thicknesses compared with other strata deposited in the same length of time, by a high organic content (mainly in the form of organic residues), and by an absence or insignificant amount of calcium carbonate.

In the phosphorites the uranium content is increased about in proportion to the increase in phosphates, and is decreased in the varieties which are rich in calcium carbonate. Coarse-grained phosphatic formations contain more uranium than fine-grained formations: sometimes alumophosphates considerably enriched with uranium, which were formed by the weathering of phosphorite-bearing strata [14].

At the present time it is customarily assumed that the direct source of the uranium in marine shales and phosphorites was ocean water and that the uranium was precipitated at about the same time as the deposition

of sediments. The deposition of uranium in shales and phosphorites takes place most likely through adsorption by carbonaceous matter or calcium phosphate.

Many peculiarities of uraniferous shales point to their formation near the edge of the continental shelf. It is known, in particular, that the richest portions of the uraniferous alum shales of Sweden are lagoonal facies of the upper Cambrian Sea and that the uraniferous shales of Wyoming were formed under similar conditions.

Deposits of uraniferous marine shales and phosphorites are characterized by very large accumulations of uranium, but because of the low metal content of the ore (a few hundredths or thousandths of one percent) they have thus far been utilized very little.

Bedding Planes in Slightly Metamorphized Sedimentary Rocks

Beds of this group are associated with deposits in both marine and continental basins and are, as a rule, adapted to intensive folding belts. They differ from sedimentary (syngenetic) deposits proper by considerably smaller dimensions, a higher and markedly nonuniform metal content, and by the separation of the main uranium body in the form of individual uranium minerals – uranium blacks and a small amount of pitchblende. In the upper oxidized portions of these deposits there is infrequent development of uranium vanadates such as carnotite and tyuyamunite.

The most important ore-enclosing rocks are carbonaceous silicic shales and organic limestones. They usually show clear signs of metamorphosis: sericitization of the argillaceous matter, carbonification of the organic matter, and the development of such clear metamorphic formations as porphyroblasts, metacrystals and pseudohydrothermal veinlets containing ankerite, quartz, pyrite and chalcopyrite.

R. V. Getseva (in a private communication) after a careful study of one of these deposits concluded that the ore bodies are formed possible as the result of the redistribution of syngenetic uranium and by the metamorphosis of the enclosing strata, and that the principal factor involved in the extraction of uranium from the metamorphogenic solutions was its sorption by organic matter.

Bedding Planes and Lenses in Normal Sedimentary Rocks of Continental Facies

These deposits are divided into two subgroups. One of these is associated with rocks of fluvial origin, mainly sandstones and conglomerates; the other with caustobiolites.

Deposits of the first group have been most intensively studied on the Colorado Plateau. Here the "primary" ores contain uranium in the form of oxides of lower valence (pitchblende and tetravalent uranium silicates) and vanadium in the form of hydrates [15]; usually they also contain copper and iron sulfides and small quantities of molybdenum, cobalt, nickel, lead, zinc, selenium and arsenic.

The oxidized ores are characterized by the development of high-valence compounds of uranium and vanadium, mainly carnotite and tyuyamunite. The ore bodies are lenticular and oriented in accordance with the stratified rock and are usually adapted to deposits of plant residues. According to the observations of American geologists the localization of the ore also depends on the water permeability of the rock, the "transmission coefficient" (i.e., the product of the permeability of a given layer by its thickness) and on the presence of waterproof barriers [16].

Frequently there is a clear adaptation of the uranium ores to the boundaries between rocks with different water permeabilities, such as sandstones and argillites. The most productive areas are those within which there is a rapid change of facies at short intervals. A favorable factor is the presence in the upper part of the stratigraphic profile of layers with a large "transmission coefficient" and blocks containing vulcanic ash or the detritus of other effusive rocks. In many cases, especially in the Salt Wash strata of the Morrison formation, the ore bodies are enclosed in isolated lenses of arkosis sandstones surrounded by argillites of considerably lower permeability. In the Triassac deposits of the Shinarump formation (Arizona) the high uranium concentrations also bear isolated lenses of conglomerates in oblique sandstone layers.

In a number of the important ore districts of the Colorado Plateau the uranium-bearing ore deposits are bounded by ancient stream channels cut through the basement complex. It has been found that the most important rocks with regard to uranium content are the fluvial rocks which fill winding and irregularly eroded gorges which have a deep and narrow profile and a rough bottom [17]. The ore is concentrated mainly in the upper parts of the channels, in hollows at the bottom, on the side, and at bends of the ancient streams. The lower part of the channels which are overloaded with argillitic material, are not favorable for uranium ores. Reddish

Genetic Classification of Minable Uranium Deposits

Classes and Types of Deposits	Principal genetic features			
	Probable source of uranium	Probable nature of the uranium-bearing solution	Probable methods of uranium deposition	Ore-localizing and ore-regulating structures
I. Magmatic Deposits				
1) Pegmatites and pegmatoid veins: a) granitic pegmatites with uraninite and/or complex oxides of uranium, tantalum, niobium, titanium etc.; b) pegmatoid veins with iron and uranium titanates	Crystallized magma	Residual molten magma	Direct crystallization from molten mass	Not established
2) Hydrothermal deposits: a) uranium, uranium-polymetallic, uranium-nickel-cobalt-bismuth-silver, uranium-molybdenum and other veins formed in open cavities	The same	Hypogene highly concentrated sulfate and carbonate solutions of complex composition with high content of volatile components	Oxidation-reduction reactions in presence of divalent iron	Fractures and shear structures adjacent to regional faults
b) uranium, iron-uranium, copper-uranium and other beds formed by metasomatosis of wall rock	The same or disseminated mineralization of enclosing rocks	Hypogene weakly concentrated alkali and alkali-earth solutions of comparatively simple composition with low content of volatile components	The same	Zones of optimal porosity
II. Sedimentary (syngenetic) deposits				
1) Marine shales 2) Marine phosphorites	Ocean water		1) Sorption by organic matter 2) Coprecipitation with calcium phosphates	
III. Sedimentary-metamorphogenetic deposits				
1) Beds in limestones 2) Beds in carbonaceous-silicic shales	Rocks containing uranium in disseminated form	Metamorphogenic solutions of undetermined composition	Oxidation-reduction reactions in the presence of organic matter	Interplanar cracks, higher order folds
IV. Weathering deposits				
1) Beds in sandstones and conglomerates 2) Beds in subbituminous coals and lignites	The same	Ground waters containing alkali and alkali-earth uranyl carbonates	Dissolution of uranyl-carbonate complexes in low pH zone; sorption by organic matter	Zones of optimal porosity

Declassified and Approved For Release 2013/04/03 : CIA-RDP10-02196R000100090002-3

sandstones and argillites near uranium ore deposits are bleached and acquire a grayish coloration [18-20]. The difference in coloring of ore-bearing and non-ore-bearing rocks is extensively used to guide prospecting for new uranium deposits on the plateau. For this purpose special colorimetric maps are sometimes drawn up.

The same subgroup of deposits can include the gold-bearing conglomerates of the Witwatersrand in South Africa, which in addition to gold contain an appreciable quantity of pyrite, uraninite, thucholite, sericite and chlorite as well as small quantities of sulfides of cobalt, nickel, copper, lead and zinc [21] and the similar ancient conglomerates of the Blind River (Canada) district, which at the present time is attracting greater interest because of the presence of uraninite, thucholite and brannerite in minable quantities [22].

The question of the origin of uranium ores in sandstones and conglomerates has thus far been hotly debated.

It must be emphasized that there are important differences in the conditions for the formation of uranium ores in the conglomerates of the Witwatersrand and Blind River on the one hand, and the Colorado Plateau on the other, as is revealed by the difference in their material composition, morphology etc. Therefore their inclusion in the same genetic group is arbitrary.

However, the majority of investigators believe that these ores in their present form were deposited after the formation of the enclosing rocks, i.e., that these deposits are epigenetic. The earlier syngentic hypothesis [23] can be rejected on the basis of such facts as the presence of uranium deposits in more than 20 stratigraphic horizons of the Colorado Plateau whose age varies from the Permian to the Tertiary period; the small likelihood of placer deposits of uraninite; the usual association of uranium deposited by chemical and biochemical processes with fine-grained shales or phosphorites but not with coarse-grained sandstones [11]. Serious opposition to the hypothesis of syngenetic formation of uranium ores in sandstones was expressed by Stieff, Stern and Milkey (quoted in [24]), who showed that the average age of the plateau ores as determined by the lead method is 71 million years or approximately one half the age of the host rocks.

However, even among the adherents of the syngenetic hypothesis for the plateau there is no unified opinion regarding the sources of the ores.

Some suggest that the ore deposits result from the action of ground water in extracting uranium from volcanic tuffs and other rocks associated with the deposits [25, 26]. Others assume that the uranium transport agents were hypogene solutions, possibly strongly diluted ground waters, and that the source of the metal is the magma crystallized at depth [21]. This hypothesis is, in general, very unlikely if one takes into consideration the fact that the majority of ore deposits of this type do not manifest any relationship to igneous rocks and fractures and that the composition of the rocks (especially the presence of vanadium) and alterations of the enclosing rocks are not characteristic of a hydrothermal process.

Uraniferous coals contain uranium principally in the form of uranium blacks or uranium-organic compounds of unknown composition. As a rule, the largest uranium content is found in semibituminous high-ash coals, and the smallest content in bituminous coals and anthracites. The coals which contain minable uranium ore are usually low grade fuel [27].

The origin of the uranium in coals is apparently the same as that in sandstones of the Colorado Plateau.

The lignite in South Dakota has been found to contain considerable concentrations of uranium only when located directly below the nonconforming White River formation [28]; tower layers of the lignite can bear ores when they lie in coarse-grained sandstones or other water-permeable rocks. Moreover, the maximum uranium content is usually observed in the upper part of each layer. This suggests that the uranium in coals is deposited by ground waters and that the sources of the uranium are the uraniferous volcanic rocks of the White River formation. The comparatively high uranium content of high-ash coals can be explained by the fact that they are more water-permeable than low-ash bituminous coals and anthracites [19].

In the deposition of uranium the adsorption of the metal by organic matter was evidently of the greatest importance. Certain experimental work has shown that subbituminous coal, lignite and peat extract irreversibly more than 98% of the uranium in a solution containing about 0.02% of the metal [29]. It is suggested that uranium-enriched coals are the most likely result of deposition of the metal from solutions of alkali uranyl carbonates or alkali-earth uranyl carbonates which decay in the presence of acids extracted from lignite, with the formation of metal-organic compounds that are comparatively stable in a low pH zone [30].

Thus the epigenetic character of the uranium in coals can be established quite definitely in general. Another hypothesis, that the uranium in coal was originally concentrated in living plants, is improbable since even under the most favorable conditions the uranium content in the ash of living plants seldom reaches 0.01%, whereas the ashes of uranium-bearing coals and lignites are marked by a higher content.

Among deposits in sedimentary rocks of continental facies the most important at present are the uraniferous sandstones and conglomerates which are, in particular, the principal source of uranium ore in the United States.

General Conclusions

This short summary shows that natural uranium concentrations are formed under the most diversified conditions including the last stages of the magmatic process, metamorphism, the sedimentary cycle and weathering processes.

According to the conditions of formation the uranium deposits can be divided conveniently into four genetic classes: 1) magmatic deposits; 2) syngenetic sedimentary deposits; 3) metamorphic sedimentary deposits; 4) weathering deposits.

The first class includes pegmatites and hydrothermal veins (the first and second groups described above). It can also apparently include bedding planes in strongly metamorphized sediments (third group), although the source of the uranium is still in dispute. The second class includes uranium-bearing beds of normal sedimentary rocks (fourth group). The third group includes bedding planes in slightly metamorphized rocks (fifth group). The fourth class of deposits is represented by bedding planes and lenses in normal sedimentary rocks of continental facies (sixth group).

The general scheme of classification of uranium deposits which results from the foregoing discussion is presented in the table.

LITERATURE CITED

[1] L. R. Page, Econ. Geol. 45, 12-34 (1950).

[2] J. B. Mawdsley, Canadian Mining Met. Bull. 482, 366-375 (1952).

[3] V. E. McKelvey, U. S. Geol. Survey Bull. 1030 A (1955).

[4] L. W. Parkin, K. P. Glasson, Econ. Geol. 49, 815-825 (1954).

[5] R. D. Nininger, Minerals for Atomic Energy, N. J. D. van Nostrand Company Inc., New York, 1954.

[6] R. Murphy, Trans. Can. Inst. Mining Met. 49, 426-435 (1946).

[7] Uranium Deposits in the United States. The Geology of Atomic Raw Materials. (Reports of foreign scientists at the International Conference on the Peaceful Uses of Atomic Energy.) (Russian translation) 1956, pp. 220-237.

[8] D. F. Kidd and M. H. Haycock, Bull. Geol. Soc. Am. 46, 879-960 (1935).

[9] A. H. Lang, Econ. Geol, Ser. 16 (1952).

[10] V. E. McKelvey, D. L. Everhart and R. M. Garrels, The Geology of Atomic Raw Materials. (Reports of foreign scientists at the International Conference on the Peaceful Uses of Atomic Energy) 1956, pp. 25-52.

[11] W. Lindgren, Mineral Deposits, United Sci.-Tech. Press, People's Commissariat of Heavy Industry, USSR, 1934, Vol. 1 (translation).

[12] G. W. Bain, Econ. Geol. 31, 5 (1936).

[13] C. J. Sullivan and R. S. Matheson, Econ. Geol. 47, 751-758 (1952).

[14] V. E. McKelvey and J. M. Nelson, Econ. Geol. 45, 35-53 (1950).

[15] A. Rosenzweig, J. W. Gruner and L. Gardner, Econ. Geol 49, 351-361 (1954).

[16] D. A. Jobin, The Geology of Atomic Raw Materials (Reports of foreign scientists at the International Conference on the Peaceful Uses of Atomic Energy) 1956, pp. 432-441.

[17] L. Miller, Econ. Geol. 50, 156-169 (1955).

[18] J. A. Masters, Econ. Geol. 50, 111-126 (1955).

[19] J. W. Isachsen, J. W. Mitcham, H. B. Wood, Econ. Geol. 50, 127-134 (1955).

[20] R. J. Wright, Econ. Geol. 50, 127-134 (1955).

[21] C. F. Davidson, Mining Mag. 88, 73-85 (1953).

[22] R. J. Traill, Can. Mining J. 75, 63-68 (1954).

[23] R. P. Fischer, Econ. Geol. 32, 906-951 (1937).

[24] H. Faul, (ed.), Nuclear Geology, N. Y., 1954.

[25] F. F. Koeberlin, Econ. Geol. 33, 458-461 (1938).

[26] J. W. Gruner, Mines Mag. 44, 53-56 (1954).

[27] J. D. Vine, Uranium-bearing Coal in the U. S. Report No. 55 at the International Conference on the Peaceful Uses of Atomic Energy, 1955.

[28] N. M. Denson and J. R. Gill, Uranium-bearing Lignite and Its Relation to Volcanic Tuffs in Eastern Montana and Dakotas. Report No. 57 at the International Conference on the Peaceful Uses of Atomic Energy, 1955.

[29] G. W. Moore, Econ. Geol. 49, 652-658 (1954).

[30] J. A. Breger, M. Deul and S. Rubinstein, Econ. Geol. 50, 206-226 (1955).

SOME TOPICS IN THE ECONOMICS OF ATOMIC ENERGY

S. M. Feinberg, S. A. Skvortsov

In this article a survey is made of materials published in foreign literature on topics in the economics of atomic energy.

The following topics are considered: the component parts of the cost of electrical energy; the cost of nuclear fuel and auxiliary materials; capital cost of construction of an atomic electric power station and its dependence on the type of the reactor; nuclear fuel cycles and the magnitude of the fuel component of cost of electrical energy; the choice of economical steam parameters; the question of supply of raw material for uranium fuel and the choice of reactor type.

On this basis a general discussion is given of the question of the cost of electrical energy in atomic electrical power stations, and forecasts are made in regard to the possibilities of a wide scale development of atomic energy.

The general outlook for a wide scale utilization of nuclear reactors for the production of electrical energy is determined by a number of economic factors. Therefore it is easy to understand the interest shown by the scientific and technical community in questions of economics of atomic energy.

In the course of the last few years a number of articles on these topics has appeared in the foreign literature. A number of interesting papers on this subject was presented at the International Conference on the Peaceful Uses of Atomic Energy held in Geneva. Although the indices used in a capitalist economy can not be automatically taken over under the conditions of a socialist economy, nevertheless many characteristic data and conclusions are of considerable interest also for us. The aim of this review is to acquaint the Soviet reader with some of the more interesting data.

Before coming to the main question it is appropriate to make a remark on the increase in optimism in the evaluations made of the economics of atomic energy. Only a few years ago the majority of American specialists held the opinion that atomic power stations could compete with coal powered ones only in those countries and regions in which the cost of coal is high. Therefore it was supposed that in the U. S. A. where the cost of coal is considerably lower than the world average cost the possibilities for the development of atomic energy were very limited. About a year ago a well-known expert in the field of economics of atomic energy J. A. Lane asserted that the cost of atomic electric energy will at best come down to the average cost of electrical energy generated in the coal powered electric stations of the U. S. A. . However, in the paper [1] presented by him at the Geneva Conference it was already supposed that during the next 20 years the capital invested in the U. S. A. in atomic energy may reach 25 billion dollars. Without any doubt the reason for this increase in optimism lies in the extremely rapid development in the technology of reactor construction and of the procurement and processing of nuclear fuel and of auxiliary materials (zirconium, heavy water, etc.).

Below we shall attempt to answer certain questions of principle arising in the evaluation of the possibilities of development of atomic energy basing ourselves on data published by foreign authors.

The Structure of the Cost of Electrical Energy

At the present time atomic energy is utilized by means of converting it into heat energy in nuclear reactors and of subsequently transforming this heat energy into mechanical and electrical energy by means of turbogenerators. This makes the general schematic outline of an atomic electrical power station very similar to that of a conventional thermal electric power station. The steam turbine and the electrical parts of an atomic

TABLE 1 [2]

Components of cost	cents/kw-hr	% of total cost
1. Fuel component of cost	0.28	40
2. Capital component of cost	0.32	46
3. Operational expenses (labor cost and expenditure on upkeep)	0.10	14
Total	0.70	100

TABLE 2 [3]

Capital Cost Component

Nature of charges	Magnitude of charges in %	
	for Canada	for USA
1. Profit	4	6
2. Depreciation charges	2.5-3.5	3-5
3. Taxes	2	4.5
4. Insurance premiums	1	0.1
Total	~10	~15

TABLE 3 [6]

Average Cost of 1 kw-hr. of Electrical Energy Generated by Coal Powered Electric Stations in Different Countries in 1947

	Average cost of electrical energy in cents/kw-hr.
Argentine:	
Continent	1.6
Islands	1.7-1.8
Great Britain	0.95
USA	
Power stations at coal mines	0.575-0.675
Near mines or waterways	0.700-0.825
Far from mines, coal delivered by rail	0.850-0.950

electric power station differ but little from those of the conventional electric power station. The essential difference consists of replacing the usual steam boilers together with the fuel preparation and storage facilities by atomic steam generators. Therefore the structure of the economics of atomic and thermal electric power stations will be very similar to each other.

To illustrate the cost structure of electrical energy generated by thermal electric power stations we present data (see Table 1) typical of a modern coal powered electric station in the U. S. A. with high steam parameters and with a coal consumption rate of about 0.4 kg/kw-hr. with the average cost of 1 ton of coal in the U. S. A. being 7 dollars.

The cost of fuel amounts only to 40% of the total cost of 1 kw-hr. Because the average cost of coal in other countries is higher than in the U. S. A. the fuel component of cost in these other countries is relatively higher, reaching 60-70%.

The following items enter into the capital cost component: profit, depreciation, taxes, insurance premiums, etc. In Table 2 average figures are given for Canada and the U. S. A.

The capital expenditures on large modern coal powered electric stations in the U. S. A and in Canada amount to 120 to 180 dollars per kilowatt of installed power. In evaluating the capital cost component the load factor for the station is assumed to be 80%. The capital expenditures attributable to that part of the equipment of a coal powered electric station which is used to generate steam (the boiler room, the system of feeding and processing the fuel, etc.) amount to approximately 30% of the total cost of the power station according to the estimates of the American experts.

The operational costs for coal powered electric stations (wages and upkeep costs) amount to 10-15% of the cost of electrical energy, while the upkeep costs amount to about 30% of the total operational costs.

In Table 3 figures are presented which give some idea of the cost of electric energy generated in coal powered electric stations in different countries.

The average costs of electrical energy given in Table 3 have been calculated for a modern power station of 100,000 kw with a load factor of 50%.

We now proceed to consider the components of the cost of electrical energy generated by atomic electric power stations.

TABLE 4

Cost of Nuclear Fuel, Auxiliary Materials, and Processing Operations [1], [3], [5]

Designation	Cost in dollars per kg
1. Natural uranium hexifluoride	40
2. Natural uranium	44
3. Natural thorium	approximately 40
4. Enriched uranium (1%)	75-95
5. Enriched uranium (2%)	200-300
6. Enriched uranium (3%)	350-600
7. Enriched uranium (5%)	700-1200
8. Enriched uranium (90%)	$(15-30)\cdot 10^3$
9. Zirconium free of hafnium	20
10. Heavy water	60-66
11. Chemical processing of uranium into uranium hexifluoride or the reverse	4
12. Mechanical processing of uranium	9
13. Canning	7
14. Element extraction and deactivation	13
15. Preparation of heat generating elements of the active zone of a fast neutron reactor	22
16. Preparation of the heat generating elements of the reproducing zone of a fast neutron reactor	11
17. Chemical processing and deactivation of thorium in the reproducing zone of a homogeneous reaction with extended reproduction	13
18. Chemical processing and extraction of nuclear fuel	4×10^3

The Cost of Nuclear Fuel and Auxiliary Materials

For the production of atomic energy nuclear fuel is used, the raw material for which is natural uranium and thorium. Industrial reserves of these materials, as well as the cost of mining and processing them have a great bearing on the economics of atomic energy. The cost of auxiliary materials (zirconium, heavy water, etc.) and the processing cost for nuclear fuel (chemical processing of uranium, mechanical processing of uranium, canning of uranium rods, element extraction, deactivation, etc.) are also important. In spite of the fact that the literature contains only fragmentary data on all these questions, nevertheless it is possible to form a general idea which is sufficient for an estimate of the economic possibilities of atomic energy. In Table 4 are given some of the published data.

We note that the cost of U^{235} obtained by the gaseous diffusion method exceeds that of natural uranium by a factor of 400-800. However, with the present level of industrial production of enriched U^{235} the latter has become a relatively inexpensive fuel. In burning 1 kg of U^{235} one obtains approximately 20×10^6 kw-hrs of heat energy whose cost amounts to about 0.075 to 0.15 cents/ kw-hr. At the same time the cost of heat energy obtained from burning coal (calorific value 8000 kw-hr/ton, cost 7 dollars/ ton amounts to about 0.09 cents/ kw-hr.

Thus, enriched uranium obtained from gas diffusion separators is approximately equivalent in cost to coal. The use of economical fuel cycles in atomic installations may reduce the relative expenditures for nuclear fuel by factors of ten compared to the corresponding cost in coal powered electric stations.

Capital Construction Costs of an Atomic Electric Power Station

Tentative plan data with respect to capital expenditures on the construction of atomic electric power stations in the U. S. A. and in England are given in Table 5.

Capital expenditures per kilowatt of installed power of the proposed atomic electric power stations fluctuate from approximately 180 to 650 dollars. These figures are the result of tentative estimates of expenditures required for the construction of atomic electric power stations which are planned to be built in the U. S. A. and

in England. The considerable spread in the figures is explained by the different variants of the design of the reactors and of the other equipment of the power stations and also to a certain extent by the inaccuracy of the estimates. These data refer to the cost of the first "one-of-a-kind" installations. If several stations of the same model were to be constructed the cost of atomic electric power stations must decrease and approach that of coal powered electric stations. Nevertheless, at the present time when one makes estimates of the cost of electrical energy one must take into account the relatively high capital investments needed for the construction of atomic electric power stations.

In the opinion of all the authors the way in which the capital investments are to be prorated in computing the cost of electrical energy is the same for atomic electric power stations as for coal powered ones.

TABLE 5 [1], [4], [6]
Relative Capital Expenditures Depending on the Type of the Nuclear Reactor

Reactor type	Capital expenditures in dollars per kw of installed power
Regenerative reactors:	
with ordinary water moderator	From 183 to 250
with heavy water moderator	about 350
with graphite moderator and water or sodium coolant	From 243 to 323
with graphite moderator and gas coolant	From 560 to 645
Breeder reactors:	
fast neutron reactors	From 269 to 500
slow neutron reactors	From 240 to 260

Nuclear Fuel Cycles and the Magnitude of the Fuel Component of the Cost of Electrical Energy

The most convenient nuclear fuel is lightly enriched uranium (up to 90% U^{235}) since its use considerably decreases the size of the reactor, and also its cost. In the active zone of a reactor with enriched U^{235} one may use such materials as stainless steel, and may use high working temperatures; therefore in its steam parameter such an atomic electric power station will be as good as the best coal powered ones. However, the use of only highly enriched uranium considerably increases the fuel component of the cost of electrical energy and the cost of the initial fuel loaded into the reactor. Therefore economically more promising is the use of more complicated fuel cycles with regeneration or with "breeding" of nuclear fuel.

For such reactors the question of economizing neutrons is of fundamental significance, the criterion for this being the reproduction coefficient for the nuclear fuel. This coefficient which is the ratio of the number of atoms of secondary nuclear fuel formed in the reproduction zone to the number of burned up atoms of the primary nuclear fuel may vary within rather wide limits depending on the construction of the reactor.

The reproduction coefficient for regenerative reactors approaches 1, for a homogeneous water thorium breeder reactor it approaches 1.2, and for a fast neutron breeder reactor it approaches 1.6.

Using the tentative data given in Table 4 on the cost of nuclear fuel, and of the basic technological operations associated with fuel processing, Lane has computed the fuel component of the cost of electrical energy for various nuclear fuel cycles [1]. In these calculations it was assumed that the allowance for the cost of the initial nuclear fuel load is 4%, while the cost of new nuclear fuel accumulated in the reactor and extracted from it after chemical processing (plutonium or U^{235}) is equal to the cost of U^{235} (15-30 dollars/gm). Such an evaluation of the cost of nuclear fuel formed in a nuclear reactor seems wholly justified since from the point of view of utilizing nuclear fuel for generating electrical energy plutonium (even if it contains large amounts of Pu^{240}) and U^{233} are approximately equivalent to highly enriched U^{235}.

Estimates for the fuel component of the cost of 1 kw-hr of electrical energy with a uranium burn-out of 10,000 megaw-days/ton or approximately 10 kg of fission products per ton of uranium for regenerative reactors are given in Table 6.

It should be noted that a burn-out of 10,000 megaw-days/ton for the uranium loaded into the reactor does not represent a limiting case. It is known that with a reproduction coefficient of 0.8 it is already possible to achieve a burn-out of 30 kg/ton if recycling is used, i.e. if several cycles of nuclear fuel processing are utilized. In this connection it is of interest to investigate the magnitude of the fuel component of the cost as a function of the extent of burn-out. From Fig. 1 it may be seen that at low burn-out (10,000 megaw-days/ton) the fuel component depends strongly on the extent of burn-out, while as the burn-out increases

TABLE 6

Fuel Component of the Cost of Electrical Energy for Regenerative Reactors

	Cost of U^{235} 15 dollars/gm, cost in cents/kw-hr with uranium enriched to			Cost of U^{235} 30 dollars/gm, cost in cents/kw-hr with uranium enriched to		
	0,7%	1,0%	2,0%	0,7%	1,0%	2,0%
Raw material (natural uranium)	0,061	0,096	0,216	0,061	0,108	0,268
Enrichment	0	0,018	0,106	0	0,039	0,245
Processing of UF^6 into metal	0	0,007	0,007	0	0,007	0,007
Fabrication of heat generating elements	0,013	0,013	0,013	0,013	0,013	0,013
Canning of heat generating elements	0,010	0,010	0,010	0,010	0,010	0,010
Chemical treatment of burned-out fuel	0,020	0,020	0,020	0,020	0,020	0,020
Charge for initial fuel load	0,104	0,164	0,372	0,104	0,197	0,563
	0,013	0,021	0,053	0,013	0,026	0,081
Profit on amount of Pu^{239} produced	0,117	0,185	0,425	0,117	0,223	0,644
Cost of depleted uranium	—0,095	—0,123	—0,186	—0,187	—0,246	—0,370
	0	0	—0,110	0	0	—0,139
Net fuel cost	0,022	0,062	0,129	0,070	—0,023	—0,135

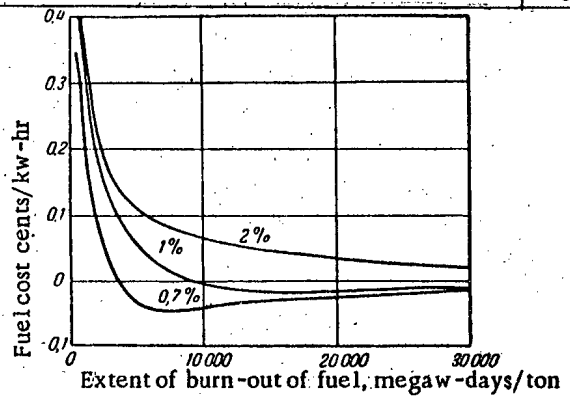

Fig. 1. Cost of fuel in regenerative reactors. Initial data: thermal efficiency-25%; initial reproduction coefficient-1.0; cost of natural uranium-40 dollars/kg; no allowance has been made for the cost of the initial loading of the reactor with fuel.

from 10,000 to 30,000 megaw-days/ton this dependence becomes much less pronounced. This circumstance justifies the choice of 10,000 megaw-days/ton as the basis for computing the fuel component of the cost of electrical energy when a regenerative fuel cycle is used for the reactor.

Thus in regenerative reactors with an initial cost of U^{235} of 15 dollars/gm the fuel component varies between 0.02 and 0.13 cents/kw-hr depending on the degree of initial enrichment, while with an initial cost of U^{235} of 30 dollars/gm and with the fuel enriched to 1% the fuel component of the cost of electrical energy becomes negative, and varies between -0.07 and -0.023 cents/kw-hr. A situation arises which at first glance is paradoxical: the more expensive is U^{235} the cheaper is the electrical energy produced. However, this is explained by the fact that the reactor is a generator of energy which not only burns up nuclear fuel, but also reproduces it. Because in breeder reactors the quantity of nuclear fuel increases in the course of their operation the profit due to the accumulation of secondary fissionable material is considerable. Insofar as the most economical regenerative nuclear reactors operate successfully with an average enrichment of 1% the estimates given above give for the maximum value of the fuel component a figure of 0.06 cents/kw-hr, i.e., it is 5 times lower than that for coal powered electric stations (where the fuel component of the cost is on the average equal to 0.3 cents/kw-hr).

The fissionable nuclear fuel and the isotopes needed for the production of secondary nuclear fuel may either be used in the form of a homogeneous mixture (single-zone reactor), or separately: the primary fissionable material is placed at the center of the reactor (the active zone), while the material for the reproducting of fuel is placed

TABLE 7 [1]

The Fuel Component of the Cost of Electrical Energy for Breeder Reactors (cents/kw-hr)

Reactor type	Fast neutron	Homogeneous
Reproduction coefficient	1.6	1.2
Manufacture of heat-generating elements:		
for the active zone	0.012	–
for the reproducing zone	0.040	–
Preparation of a suspension of thorium in heavy water	–	0.001
Preparation of a solution of uranyl sulphate in heavy water	–	0.001
Chemical processing of fuel:		
in the active zone	0.007-0.021	0.017
in the reproducing zone	0.024-0.067	0.091
	0.083-0.140	0.110
Allowances for fuel loading:		
in the active zone	0.028-0.056	0.005-0.010
in the reproducing zone	0.017-0.035	0.005
Aging of burned-out fuel	–	0.003
Allowance for the initial load of heavy water and for loss replacement	–	0.025
	0.128-0.231	0.148-0.153
Profit on account of plutonium or U^{233} produced	-(0.10-0.20)	-(0.037-0.075)
Net cost of fuel	0.028-0.031	0.111-0.078

NOTES: 1. The cost of the initial load of nuclear fuel is calculated on the assumption that the heat transfer per kgm of uranium is 100 kw of heat in the active zone, and 15 kw of heat in the reproducing zone. 2. The extent of burn-out of plutonium in the active zone in the course of one cycle is assumed to be 20%. 3. The cost of 1 gm of U^{235} is between 15 and 30 dollars.

along the periphery (the reproducing zone). Having the economy of neutrons and the decrease in the size of the initial fuel load into the reactor in mind one usually gives preference to a two-zone reactor; often natural uranium is placed not only into the reproducing zone but also into the active zone.

If one uses in the active zone a mixture of 10% Pu^{239} and 90% U^{238}, and in the reproducing zone 99% of U^{238} and 1% of Pu^{239} the fuel component of the cost of electrical energy will amount to approximately 0.03 cents/ kw-hr (Table 7) according to Lane's [1] calculations.

In the majority of proposals for homogeneous water breeder reactors the two zone principle is employed. A solution of uranyl sulphate in heavy water (3 gm of U^{235} per liter) may be used in the active zone, and a suspension of thorium oxide (ThO_2) in heavy water (1000 gm per liter) may be used in the reproducing zone. The accumulation of U^{233} in the reproducing zone may reach an equilibrium value (3 gm per liter of heavy water).

The chemical processing of fuel in homogeneous reactors consists of the removal of fission products from the solution in the active zone, and of the extraction of U^{233}. If the cost of chemical processing of uranium is the same as that for thorium (13 dollars per kg). The cost of extraction of U^{233} will be approximately 4 dollars per gm. If at the same time the burn-out coefficient per fuel cycle is 75% for U^{233}, then in accordance with Lane's calculations [1], the fuel component is characterized by the data presented in the second column of Table 7.

Economical Steam Parameters

As has been shown above the fuel component of the cost of electrical energy is quite small if breeding of nuclear fuel is taken into account. Because of this, the question of the desirability of, and of the economic returns due to an increase in the thermal efficiency has a different solution in the case of atomic electric power stations than in the case of coal powered ones. The economic effect of increasing the thermal efficiency may in the present case be much less pronounced than in the case of coal powered electric stations. In some cases a decrease in the thermal efficiency may actually lead to an increase in the economic returns of the electric power station.

In coal powered electric stations where the fuel component may amount to as much as 60-70% of the total cost of electrical energy an increase in the thermal efficiency leads first of all to a corresponding decrease in the cost of the electrical energy because of a decrease in the amount of fuel required. An increase in the thermal efficiency of an atomic electric power station for which the fuel component is small may lead to an appreciable decrease in the cost of energy only in the case of its being accompanied by a decrease in the capital investment, since although the consumption of nuclear fuel is decreased by an increase in the thermal efficiency, the reproduction of fuel is decreased at the same time.

Moreover, one must keep in mind that an increase in thermal efficiency is usually connected with an increase in the steam parameters, and consequently with an increase of the temperature and of the pressure in the active zone, and this may lead to a decrease in the operational life-time of the heat generating elements, or to the necessity of utilizing inside the active zone structural materials which absorb neutrons strongly (for example, the replacement of aluminum and of zirconium by stainless steel), which may in turn decrease the reproduction coefficient for the nuclear fuel. All this may lead to a deterioration of the operational characteristics of the power station, and in the final analysis to a deterioration of its economic indices.

Thus an increase in the thermal efficiency of an atomic electric power station will not necessarily always be profitable. Conversely, in a number of cases a lowering of the thermal efficiency accompanied by a decrease of capital investment may lead to a lowering of the cost of electrical energy, and may therefore be economically justified. Because of the strong influence of capital investments and because of the relatively small fuel component an increase in the steam parameters of an atomic electric power station is advantageous only until the point is reached when an increase in the temperature requires specially alloyed steels (for example austenite steel), since this is accompanied by an increase in capital expenditures per unit of installed power.

According to Lane's calculations there exists a dependence shown in Fig. 2 between the steam temperature, the thermal efficiency of the power station, and the cost of the turbogenerating part of the atomic electric power station (per kw of installed power). A change in the steam parameters from medium values (saturated steam ~250°C in water-water reactors) to high values (superheated steam 550°C) leads to a decrease of capital expenditures on the turbogenerator from 115 to 90 dollars/ kw. At the same time, as may be seen from Table 5, the replacement of a reactor with a water moderator by, for example, a graphite-sodium reactor which allows one to obtain superheated steam of high parameters, may lead to an increase in the capital expenditures of 60-80 dollars/kw, which will exceed by several fold the saving made on the turbogenerator part of the power station. An increase in the thermal efficiency of an atomic electric power station at the expense of going over to high values of the steam parameters is justified economically only in that case when it does not lead to an excessive increase in the reactor part of the power station, and in the operational expenses. It is self-evident that an increase in the steam parameters and in the thermal efficiency of atomic electric power stations with the capital expenditures and the reproduction coefficient remaining constant remains an important problem in the field of atomic energy.

The Cost of Electrical Energy Generated by Atomic Electric Power Stations

From Tables 6 and 7 it follows that the fuel component of the cost of electrical energy generated by atomic electric power stations is less than the average cost of the fuel component for the coal powered electric stations in the U. S. A. by a factor of 4-5. Operational expenses which include wages and up-keep costs are only slightly higher for the coal powered electric stations.

Therefore capital expenditures play a decisive role in determining the cost of electrical energy. We have already seen that the most optimistic estimates for the capital investments in the case of water-water reactors at the present time are only beginning to approach the highest estimates of the cost of coal powered electric power stations.

However, estimates of capital expenditures required for the construction of atomic electric power stations have shown during the last few years a steady and rapid fall. This, without any doubt, is evidence for the fact that the rapidly developing technology of atomic reactors is making the capital expenditures for the construction of atomic electric power stations approach those for coal powered ones.

Table 8 gives the total cost of 1 kw-hr of electrical energy computed on the basis of the tentative data taken from Table 5 with respect to the capital investments for the construction of atomic electric power stations.

TABLE 8 [1], [4], [9]

Estimates of the Cost of Electrical Energy Generated by Atomic Electric Power Stations With Reactors of Different Types

Reactor type	Fuel cycle	Cost of electrical energy in cents/kw. hr			
		Fuel component	Operational component	allowance for capital investment	Total
Regenerative reactors					
Moderator and coolant-ordinary water	Uranium enriched to 1%	—0.02—0,06	0,1	0.26—0,54	0.34—0,7
Moderator-heavy water	Natural uranium	—0.07—0,02	0,1	0,50—0,75	0,53—0,77
Moderator-graphite, coolant ordinary water	Slightly enriched uranium	—0.02—0,06	0.1	0.36—0.54	0.44—0,7
Moderator-graphite, coolant--gas	Slightly enriched uranium	—0,02—0,06	0.1	0.80—1;38	0.88—1.54
Moderator graphite, coolant-sodium	Slightly enriched uranium	—0.02—0,06	0.1	0.35—0.69	0,43—0.85
Breeder reactors					
Fast neutron		—0,03	0.1	0,38—1,07	0.51—1,20
Slow neutron		0.08—0.11	0,1	0.34—0,56	0,52—0,77

Note: Maximum allowance for capital investment were assumed to be 15%, while the minimum allowances were assumed to be 10%. The amount of capital investment was taken from Table 5. It has been assumed that the power station is operated at full power (7000 hours per annum).

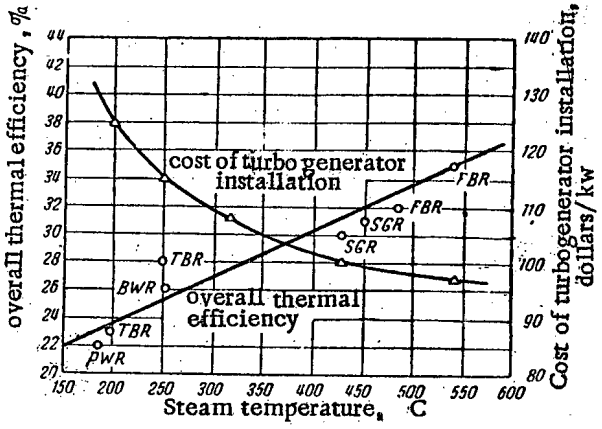

Fig. 2. Characteristics of the turbogenerator installation of an atomic electric power station.

It should be noted that at the present time breeder reactors do not appear to be economically more profitable than reactors with a regenerative cycle. It may be supposed that their main advantage, which consists of the lower requirements for nuclear raw materials, brought about by a greater extent of burn-out, will begin to tell in the course of time.

The principal conclusion consists of the fact that even under the conditions existing in the U. S. A., which are particularly unfavorable for the competition of atomic with coal generated power, one may even now choose such types of atomic electric power stations which will generate electrical energy at a cost which is lower than the average cost of energy generated by coal powered electric stations. In other western countries the outlook for the competition of atomic versus coal generated energy is even more favorable — for large regions of the world atomic energy may be considered to be economically attractive.

Is Mankind Threatened by a Uranium Famine? What Type of Reactors Should be Built?

Let us now throw some light on another question which is not without importance: is not the development of atomic energy limited by the natural supplies of uranium and thorium? In this connection we shall also consider the question, what type of reactor — a regenerative or a breeder one — will find the widest application for atomic electric power stations?

The earth's crust contains approximately 3×10^{-4}% of uranium and 8×10^{-3}% of thorium which amounts to thousands of trillions of tons. However, both uranium and thorium are very widely dispersed, and according

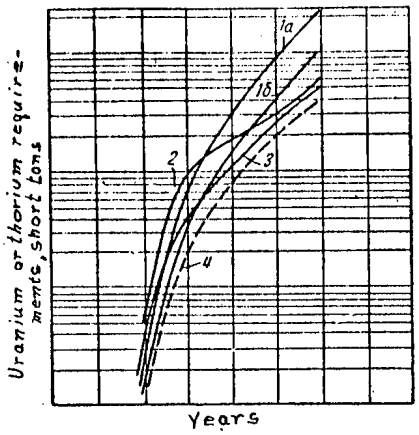

Fig. 3. Requirements of nuclear raw materials (cumulative totals). 1a) Regenerative slow neutron reactor with a reproduction coefficient of 0.85; 1b) regenerative slow neutron reactor with a reproduction coefficient of 1.0; 2) regenerative fast neutron reactor with a reproduction coefficient of 1.4; 3) homogeneous water thermal neutron breeder-reactor with a reproduction coefficient of 1.1; 4) loading of the raw material with the reproducing zone.

to some estimates [2] the proven supplies of these elements (with production costs of approximately 200 dollars/kg) consist of 25 million tons of uranium and 1 million tons of thorium. Taking into account the newness of this enterprise, and, for example, our experience in the production of petroleum, we may note that these estimates are apparently much too low. In future geological prospecting and also an improved technology of extracting uranium and thorium from poor ores will lead to a considerable reevaluation of the reserves of inexpensive ores of uranium and thorium. However, even the resources indicated above are more than sufficient to satisfy all the energy requirements of mankind for the next century.

When regenerative reactors are used with a reproduction coefficient ≤ 1 the extent of burn-out of the uranium, i.e., the degree of its energetic utilization, may be quite high if the uranium is recycled. With a reproduction coefficient equal to 0.8 in accordance with the estimates by Dunworth [7] and by others one may achieve a burn-out of the order of 30 kg/ton if the nuclear fuel is recycled. With a reproduction coefficient close to unity one may achieve burn-out in regenerative reactors which amounts to hundreds of kilograms per ton of uranium. We shall assume in what follows that in regenerative reactors utilizing fuel recycling one may achieve burn-out from 30 to 100 kg/ton.

When breeder reactors are used the attainable degree of burn-out may approach 1000 kg/ton. However, it should be emphasized that the requirements of uranium or thorium for breeder-reactors are considerably larger because of the necessity of introducing nuclear fuel into the reproducing zone. Therefore it turns out that in the early stages of the development of large scale generation of atomic energy, the total requirements of uranium and thorium if breeder reactors are used is even larger than if regenerative reactors are used, and only with time (approximately after 20 years) the breeder reactors will require less nuclear raw material than regenerative ones. This last point may be illustrated by means of graphs given in Lane's article [2].

Fig. 3 gives graphs of the growth in the requirements of nuclear raw material loaded into reactors depending on the type of the latter; it is assumed that the power of atomic electric power stations in the U. S. A. will grow from 500 megawatts in 1960 to 210,000 megawatts in 2000. It is not without interest to note that (according to these graphs) even by 2000 breeder reactors will require quantities of nuclear raw material only 2-4 times less than the requirements of regenerative reactors. Therefore, if one takes into account the low relative magnitude of the fuel component in the cost of atomic electric energy, and the absence, at least today, of any more or less certain expectations of economic advantages of breeder reactors, one can understand why the latter are still not being considered as the most promising type of energy producing reactor for the immediate future.

The world consumption of useful electrical energy in 1952 [8] amounted to approximately 10 billion megawatt-hours (from all sources). By 2000 the consumption of useful energy may reach 84 billion megawatt-hours per annum (approximately 15 billion tons of coal). With a complete utilization of natural uranium, for example in a breeding fuel cycle the burn-out of nuclear fuel in 1952 would amount to (if all the world energy sources were completely replaced by nuclear fuel) approximately 500 tons, and in 2000 to approximately 4000 tons, while contemporary world production of uranium without any doubt approaches several tens of thousands of tons per annum.

As has been mentioned earlier the quantity of uranium or of thorium loaded into breeder reactors considerably exceeds the amount of uranium (or of thorium) burned-out in them. If one assumes an average rate of heat extraction of 100 kw of heat per kg of uranium, then the total load of nuclear fuel will exceed the amount of material burned-out in it in the course of a year by approximately a factor of 50, and will thus amount to approximately 200,000 tons by the year 2000.

TABLE 9

The Expected Increase in the Energy Producing Power Installations in the U. S. A. during the Period from 1955 to 1975*.

Cost of electrical energy in cents per kw-hr	Cumulative total percentage	Billions of kilowatt-hours	Power in megawatts with a load factor of 60%	Total capital expenditures in millions of dollars
0,10	1	9	1 700	300
0,8	4	36	6 800	1 200
0,7	14	118	22 000	3 800
0,6	39	340	65 000	11 000
0,5	67	580	110 000	19 000
0,4	85	740	140 000	25 000
0,3	98	855	163 000	28 000
0,2	100	874	166 000	29 000

* Excluding installations with internal combustion engines.

If the energy requirements were completely met by means of using regenerative nuclear reactors , then with a burn-out of 30 kg per ton the annual consumption of uranium would amount to 15,000 tons in 1952 and 120,000 tons in 2000. The total requirements of uranium in the course of half a century with a 400 fold (or 16% per annum) increase in the use of atomic energy during the period 1960-2000 would amount to approximately 700,000 tons. With a more optimistic estimate of the extent of burn-out up to 100 kg/ton in a single cycle of recycling the annual requirement in the year 2000 will amount to approximately 40,000 tons, and the cumulative requirement for the period 1960-2000 to approximately 250,000 tons.

The Prospects for the Development of the Generation of Atomic Electrical Energy

Attempts are being made to make estimates of the scale of the development of atomic energy industry within the next few decades based on an evaluation of the effectiveness of the use of atomic energy for the production of electrical current.

Up till 1954 many authors expressed the opinion that in the U. S. A. because of the repeatedly noted comparative cheapness of coal there were no prospects for any considerable development in the use of atomic energy. However,in articles published in 1955 this pessimism began to be rapidly replaced by optimism. For this there is the following basis. In the U. S. A. there exists a considerable spread in the cost of electrical energy generated by thermal power stations depending on local conditions. The expected distribution for 1960 of the generation of electrical energy for new electric power stations in the U. S. A. as a function of its cost is shown in Fig. 4.

The possible increase in the power of thermal electric power stations in the U. S. A. in the course of the next 20 years, and the distribution of this power as a function of the cost of electrical energy may be characterized by the data of Table 9 [1].

From this table it follows that if, for example, the cost of atomic electrical energy amounts to 0.7 cents/kw-hr, then atomic electric power stations may by 1975 displace coal powered ones in installations of a total power of 22 million kw, and if the cost of atomic electrical energy will amount to 0.4 cents/kw-hr, then the power of atomic electrical power stations in the U. S. A. may reach 140 million kw by 1975 with a total capital investment amounting to 25 billion dollars.

By the end of 1955 the optimistically inclined experts began to consider that the cost of electrical energy generated by atomic electric power stations may be reduced to 0.4 cents/kw-hr and that therefore atomic energy may account for 5/6 of the total increase in the power of thermal electric power stations in the U. S. A. during the next 20 years.

However, it should be noted that the plans announced up till the present time (which, by the way, have not yet been approved) for the construction of atomic electric power stations in the U. S. A. are very modest, and contemplate the addition of only 800,000 kw of power during the next five years.

In other western countries,where the resources of cheap energy are limited,opinions were expressed even prior to 1955 that the development of atomic energy in these countries may become appreciable even in the next few years.

According to a plan announced by the British government in the course of the next ten years there will be constructed in England 12 atomic electric power stations of 1.5-2 million kw installed power (the power of all the electric power stations in England amounts to 21 million kw). It is possible that during the following decade the power of atomic electric power stations will increase to 10-15 million kw, and will amount to 1/4 of the power of all the electric power stations in England. It should be noted that the atomic electric power stations

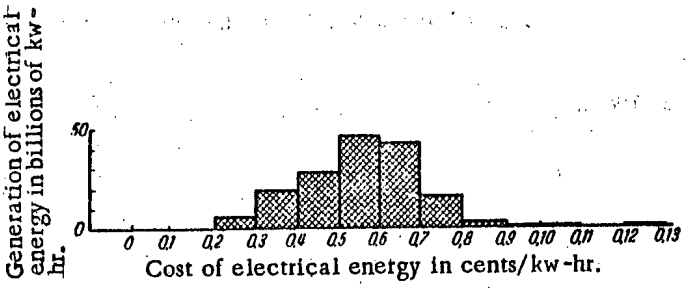

Fig. 4. The distribution of the generation of electrical energy expected for 1960 for new electric power stations in the U. S. A. as a function of its cost.

with gas cooling being built in England belong to the class of extensive installations (i.e., with a low rate of energy extraction per unit weight of uranium) with very large capital investments approaching 200 pounds sterling per kw (560 dollars/kw). In spite of this, because these reactors are being used as dual purpose reactors, i.e., with the plutonium produced being sold to the government at the high prices of the War Ministry, the expected cost of electrical energy is close to the average cost in England. It is not superfluous to remind the Soviet reader that this relative cheapness of atomic electrical energy in England is attained by absorbing a considerable part of its cost into the military budget.

The English journal "The Economist" states, in order to demonstrate the economic justification for the construction of atomic electric power stations [9]:

"After the atomic electric power stations have been put into operation the annual saving of coal will amount to 40 million tons. If it were not for this gradual increase of atomic electric power stations the quantity of coal used by English electric power stations would probably have increased from 37 million to 65 million tons in 1965 and probably would have reached 100 million tons by 1975 It is difficult to imagine how one could attain such an increase in the production of coal, at least at a cost which would be anywhere near acceptable. During the last 20 years the cost of coal in England has risen by 30%, and the cost of coal mined in the least productive mines, or in new mines of greater depth, will increase even faster. This situation is common to all Western Europe, which is suffering not from a direct scarcity of fuel, but from the fact that it is becoming increasingly more difficult to obtain additional quantities of fuel needed to satisfy the ever growing demand for energy.

"There are great regions on earth which are experiencing a more acute need of fuel than England or Western Europe. Among such regions are South America, Africa and all Asia. Atomic electric energy offers them the most favorable opportunity of obtaining a light and easily transportable fuel."

Thus economic evaluations show that already at the present time a wide-spread development of atomic energy is economically attractive.

LITERATURE CITED

[1] J. Lane, The Economics of Nuclear Energy (Reports of foreign scientists at the International Conference on the Peaceful Uses of Atomic Energy) State Technical Press, 1956, pp. 7-34.

[2] J. A. Lane, Nucleonics 12, 6, 12 (1954).

[3] J. Davis and W. B. Lewis, "An Economic Forecast of the Role of Nuclear Power in Canada," Paper No. 11 at the International Conference on the Peaceful Uses of Atomic Energy, 1955.

[4] Energy Producing Nuclear Reactors and the Vitilization of Fission Products, Collection of articles, For. Lit. Press, Moscow, 1955.

[5] R. Murray, Introduction to Nuclear Technology , For. Lit. Press, Moscow, 1955.

[6] The Scientific and Technical Foundations of Nuclear Energy, Vol. II, C. Goodman, Ed., For. Lit. Press, Moscow, 1950.

[7] J. V. Dunworth,"Possible Role of Thorium in Nuclear Energy", Paper No. 867 at the International Conference on the Peaceful Uses of Atomic Energy, 1955.

[8]" World Requirement of Energy, 1975-2000", Paper No. 902 at the International Conference on the Peaceful Uses of Atomic Energy, 1955.

[9] The Economist, July 23 (1955).

ATOMIC SCIENCE NOTES

CONFERENCE OF THE ACADEMY OF SCIENCES OF THE UKRAINIAN S. S. R. ON THE PEACEFUL USES OF ATOMIC ENERGY

In the beginning of March of this year there was held at Kiev a session of the Academy of Sciences of the Ukrainian S. S. R. devoted to the problems of utilizing atomic energy for peaceful purposes. At this conference there was a stock taking of the results of the work of the scientists of Soviet Ukraine in the realm of nuclear physics and of the utilization of radioactive isotopes in science and in technology.

Altogether about 800 persons took part in the work of the session – scientists from the Academy of Sciences of the Ukraine S. S. R., representatives of institutions of higher education, engineering and technical personnel from industry. Approximately 100 reports were presented at this session.

In opening the session the President of the Academy of Sciences of the Ukraine S. S. R. Academician A. V. Palladin spoke of the tremendous problems set before the scientists by the decisions of the XX Congress of the C. P. S. U., and of the appreciation with which the scientists heard the words of thanks directed to them from the Congress rostrum by N. S. Khrushchev in the name of the people and of the party.

The paper "Physical and Technical Foundations of Atomic Energy" presented by the corresponding member of the Academy of Science of the Ukraine S. S. R. professor D. I. Blokhintsev who was the scientific director of the first atomic electric power station in the U. S. S. R. evoked considerable interest among the participants in the session. The report was devoted to a consideration of slow and fast neutron reactors. Scientists of the Soviet Ukraine also had a part in the investigation of nuclear constants and of other characteristics of fissionable and of constructional materials.

The work of the Soviet physicists, and also the investigations carried out by the American scientist Zinn, and by other foreign scientists, showed that in a fast neutron reactor one may obtain more than one new atom of fissionable material for each "burned-out" fissionable atom, i.e. one may realize breeding of nuclear fuel. Therefore the construction of energy producing nuclear reactors operating on fast neutrons seems to be particularly attractive.

The experimental fast neutron reactor built in the U.S.S.R. allowed a number of valuable facts to be learned in regard to the peculiarities of the way in which the chain reaction takes place in reactors of this type.

More than 25 papers on nuclear physics and on questions of the application of tagged atoms in various fields of science and technology were presented at the five sessions of the physical section.

The Kharkov Physico-Technical Institute of the Academy of Science of the Ukraine S. S. R. has achieved considerable successes in the development of linear accelerators. Under the direction of active member of the Academy of Science of the Ukraine S. S. R., K. D. Sinelnikev and of professor A. I. Akhiezer the staff of this Institute made a large contribution to the theory of linear accelerators and built proton and electron accelerators of this type.

A number of papers was devoted to the study of the interaction of fast neutrons with nuclei. The staff of the Kiev Institute of Physics of the Academy of Science of the Ukraine S. S. R. presented results of investigations of inelastic neutron scattering. These investigations showed that at neutron energies up to 4 Mev the periodicity of the properties of the nuclei of the elements makes itself felt. "Magic" nuclei have considerably smaller neutron cross sections than neighboring nuclei. The spectra of the scattered neutrons were also studied. Experiments also showed that at neutron energies up to 3 Mev even in heavy nuclei excited levels produced by neutron

bombardment are separated from one another by considerable intervals. The experimental data obtained for the inelastic scattering of neutrons were compared with theory. It was established that the best fit with the experimental data is given by the model of a semi-transparent nucleus with a smeared-out edge. The model of the semi-transparent nucleus is also supported by the investigation of the angular distribution of elastically scattered neutrons.

The work carried out under the direction of A. K. Valter in the Physico-Technical Institute of the Academy of Science of the Ukraine S. S. R. on the investigation of (d, n) and (d, p) reactions in light nuclei is of considerable interest. Lively interest was evoked by the report of N. A. Vlasov (Acad. Sci. U. S. S. R.) on experiments to discover excitation of α-particles carried out in his laboratory.

This session also made very evident the tremendous possibilities opened up for science and technology by a widespread use of radioactive isotopes. Biology and medicine with their various branches represent a wide open field for their application. The use of radioactive isotopes in biology has marked the beginning of a new stage in its development. This was particularly convincingly brought out in the report of Academician A. V. Palladin on the use of radioactive isotopes for investigations in the field of functional biochemistry of the brain. The use of radioactive isotopes enables one to observe the metabolism in the brain of an animal.

The broad investigations carried out in the Institute of Biochemistry of the Academy of Science of the Ukraine S. S. R. under the direction of Academician A. V. Palladin allowed new data to be obtained of considerable theoretical interest. By means of studying the rate of inclusion of amino acid of methionine containing radioactive sulphur (S^{32}) into the albumens of the various parts of the brain it was established that the greatest rate of albumen renewal is found in the covering of the large hemispheres of the cerebrum and in the cerebellum, i.e., in the functionally youngest parts of the central nervous system; the slowest rate of albumen renewal is found in the spinal cord, i.e., in the functionally least complicated and phylogenetically the oldest part of the central nervous system.

Particularly fruitful turned out to be the use of isotopes for the elucidation of those peculiarities of the metabolism in the cerebrum which are related to its different functional states (retardation or excitation), and also with the phenomena of avitaminosis.

Reports on the use of the method of tagged atoms for the study of metabolism and of other problems of physiology of animals were made by scientists working in other institutes of the Academy of Science of the Ukraine S. S. R., in institutions of the Ministry of Health, and in departments of institutions of higher education.

A large number of reports was devoted to the work carried out under direction of Academician P. A. Vlasyuk in which tagged atoms were used for the study of conditions of plant nutrition.

Isotopes found a wide application in the work of the E. O. Paton Electrical Welding Institute of the Academy of Science of the Ukraine S. S. R. on the study of the chemical inhomogeniety of welded joints, on the testing of welded joints for defects, on the automatic regulation of the liquid metal bath in the case of electric slag welding. The use of tagged atoms made it possible to study the wear of machine parts.

The use of radioactive isotopes in chemistry made it possible to obtain quite new data on the mechanism of chemical reactions (paper by A. I. Brodsky) and on the mechanism of biosynthesis (paper by E. A. Shilov).

Ukrainian scientists show their concern for the health of mankind by carrying out investigations on the biological effects of radioactive radiations.

M. V. Pasechnik

THE FIRST ALL-UNION CONFERENCE ON MEDICAL RADIOLOGY

From January 30 to February 4, 1956 the First All-Union Conference on Medical Radiology took place in Moscow organized by the Ministry of Health of the USSR.

More than a thousand delegates – representatives of 32 special fields – took part in the work of the conference. 232 papers were presented and discussed at the plenary and sessional meetings of the conference which summarized the results of research by Soviet scientists on the action of ionizing radiation on the organism, on the application of atomic energy in biology and medicine, on dosimetry and on hygienic problems of radiology.

A number of papers contained new data on physical and biochemical phenomena which arise in living matter under the action of ionizing radiations.

A. M. Kuzin shows that the radiation energy absorbed by a living system is converted into chemical energy of short-lived free radicals, peroxides, hydroperoxides and excited molecules. The unstable, chemically active substances formed during irradiation bring about slow reactions of depolymerization of substances of high molecular weight which leads to a breakdown in permeability, to a change in the sorptional properties of microstructures and to a breakdown of natural complex compounds.

The members of the conference showed interest in the paper of B. N. Tarusov who made more concrete the concepts of the exact manner in which submicroscopic structures show initial changes on irradiation. As a result of primary photochemical activation the initiation of a reaction of post-action takes places which develops at an accelerating rate and leads to a growth in the physico-chemical changes and to deep damage. The earliest physico-chemical changes of submicroscopic structures appear in lipoid phases (A. P. Polyvoda). The breakdown of normal chemical processes leads to a deep breakdown of the cell function and to their death.

New aspects of the action of ionizing radiation are found and new regularities are observed in the whole animal organism with the complex mechanisms of the integration of functions which are characteristic of it. In the discovery of these regularities Soviet science has undisputed priority. The success of Soviet science in this field is a result of the whole course of development of materialistic natural science. The correct understanding of the role of the nervous system in the regulation of the functions of the organism has for a long time attracted the scientists of our land to the study of the reactions of the nervous system on the effect of ionizing radiation. This division of radiobiology is being developed by Soviet scientists very actively and with great success.

Even though abroad the concept still predominates that the nervous system is insensitive to the action of radiation, nevertheless the papers of L. A. Orbeli, A. V. Lebedinsky, M. N. Livanov and others convincingly demonstrated changes in all the parts of the nervous system and the interrelationship between them. The changes in the higher nervous activity arising under the influence of ionizing radiation may be considered to have been fairly well understood by now. The new technique for the study of bioelectric phenomena in the cerebrum developed by M. N. Livanov and his collaborators, on the basis of using advances of modern electronics, allowed them to observe the most delicate changes which occur in the brain under the influence of irradiation.

At this conference new promising lines of advances have become apparent for the study of the influence of irradiation on the blood system: the elucidation of biochemical and physiological aspects of the reaction of blood-producing organs, the use of the method of labeled atoms and of histochemistry in the study of appropriate delicate mechanisms. New facts have been already obtained along these lines related to a breakdown in the exchange of nucleoproteids in the blood-generating organs, to a change in the activity of adenozin triphosphatase and of other ferments. These directions are being explored on the basis of a wide-spread use of new techniques.

A series of interesting papers (by V. L. Troitsky, I. A. Pigalev, N. N. Klemparskaya, P. N. Kiselev and others) presented results of research on the reactions of immunity under the influence of ionizing radiation, carried out on a broad base of general physiology. These papers contributed much that was new not only from the point of view of elucidating the mechanism of breakdown of immune properties of the organism in radiation sickness, but also from the point of view of understanding the processes of the formation of immunity in general, of the mechanisms of autosensitization.

The paper by P. D. Gorizontov, which summarized a tremendous amount of factual material obtained over a period of years by many methods of investigation, described the modern concept of the mechanism of development (pathogenesis) of radiation damage. P. D. Gorizontov discussed from many points of view the various aspects of the pathological reactions of the organism to irradiation, emphasizing the importance of the toxemic factor, which brings the problem of pathogenesis close to the investigation of the primary mechanisms and gives a foundation for a truly complex study of the problem of radiation damage.

The conference has shown that our research scientists are using isotopes with ever-increasing experimental skill as tracers for the solution of the most diverse problems in physiology and in biochemistry. The work in this field is being extended continuously, and is becoming of great importance. Of the many investigations one might mention the work of I. B. Zbarsky and his collaborators who discovered a breakdown in the synthesis of albumens by the protoplasm and by the nucleus of a cancer cell, the investigations of Ya. G. Uzhansky who showed the existence of an intimate connection between the processes of growth and breakdown of erythrocytes. One should emphasize the importance of tracer methods in physicological investigations on the study of barrier functions of the organism (N. N. Zaiko) and of capillary permeability (I. A. Oivin).

The investigations referred to above are directly connected with the use of radioactive isotopes for diagnostic purposes. An extensive paper by M. N. Fateeva was devoted to this topic as well as the paper of K. N. Badeev on the use of radioactive iodine for the diagnosis of brain tumors etc.

Along with theoretical research devoted to the study of the reactions of the organism to the influence of ionizing radiation there were other papers presented at the conference by clinicians who studied the peculiarities in the progress of radiation sickness on experiments with animals and in the clinic where it arises as a complication of X-ray or radiotherapy. In this connection one should note the interest evoked by the communications of G. A. Zedgenidze, Yu. V. Sebrant and a number of others.

The conference devoted considerable attention to the problem of radiation sickness therapy, and heard the papers of A. A. Bagdasarov and L. S. Rogachev on the treatment of the acute and the chronic forms of radiation sickness, of V. A. Sanotsky on the peculiarities of the therapy of injuries by radioactive substances in the course of an experiment, and others.

The use of radioactive isotopes and of radiation for the treatment of various diseases is one of the principal uses of atomic energy for the benefit of mankind. The papers of A. V. Kozlova, M. P. Domshlak and others were devoted to this question.

The conference adopted a resolution directed toward the further development of the means of treatment of malignant tumors, of skin and of other diseases by methods based on the achievements of modern nuclear physics.

In the directives of the XX Congress of the CPSU with respect to the sixth Five-Year Plan of the development of the economy of the USSR a widespread use of atomic energy for peaceful purposes is contemplated. As a result of this large and varied problems arise before the various branches of the science of hygiene and of its practical applications. 44 Papers were devoted to hygienic problems in radiology and to questions of dosimetry. A. A. Lefavet noted considerable success in the development of basic hygienic norms and prophylactic measures in the work with radioactive substances and radiations, and emphasized the necessity of a further development of work on providing bases for setting maximum permissible levels of irradiation. One should mention here the various means of individual protection in working with radioactive substances which were demonstrated at the meeting of the hygienic session, which permit one to completely shield the respiratory organs and the skin from contact with radioactive substances. The problem of removal and making safe of radioactive wastes described in a review paper by A. N. Marei deserves special notice.

The paper of K. K. Aglintsev devoted to the dosimetric characteristics of radioactive preparations evoked considerable interest. The papers on measuring techniques by N. G. Gusev, F. K. Levochkin and others discussed methods of determining specific β-and γ-activities of extended sources, methods of computing and of measuring doses of β-radiation from applicators, methods of determining radioactive aerosols in air, etc.

The conference noted the need for a further unification of efforts of physicists, chemists, medical men, biologists and other specialists to ensure more rapid progress in the matter of utilization of atomic energy for peaceful purposes.

V. V. Sedov

NEWS OF FOREIGN SCIENCE AND TECHNOLOGY

INVESTIGATIONS INTO THE STRUCTURE OF THE NUCLEUS BY ELECTRON SCATTERING*

Scattering of high-energy electrons by nuclei makes it possible to obtain data on the charge distribution of the nucleus and on the dimensions of the proton. The figure shows an apparatus for the study of electron scattering on nuclei built at Stanford University (USA). An electron beam of 550 Mev energy, coming from a linear accelerator 67 m long and not shown on the figure, enters through tube 1 and strikes the target made of the substance being studied at 2, and passing through it, leaves behind a shielding wall. The angular distribution of the electrons scattered through large angles is studied with the aid of a 55-ton magnetic spectrometer 3, which can be rotated around the target on its platform 4. A scintillation counter located behind a lead shield 5 is used as the recording apparatus of the spectrometer.

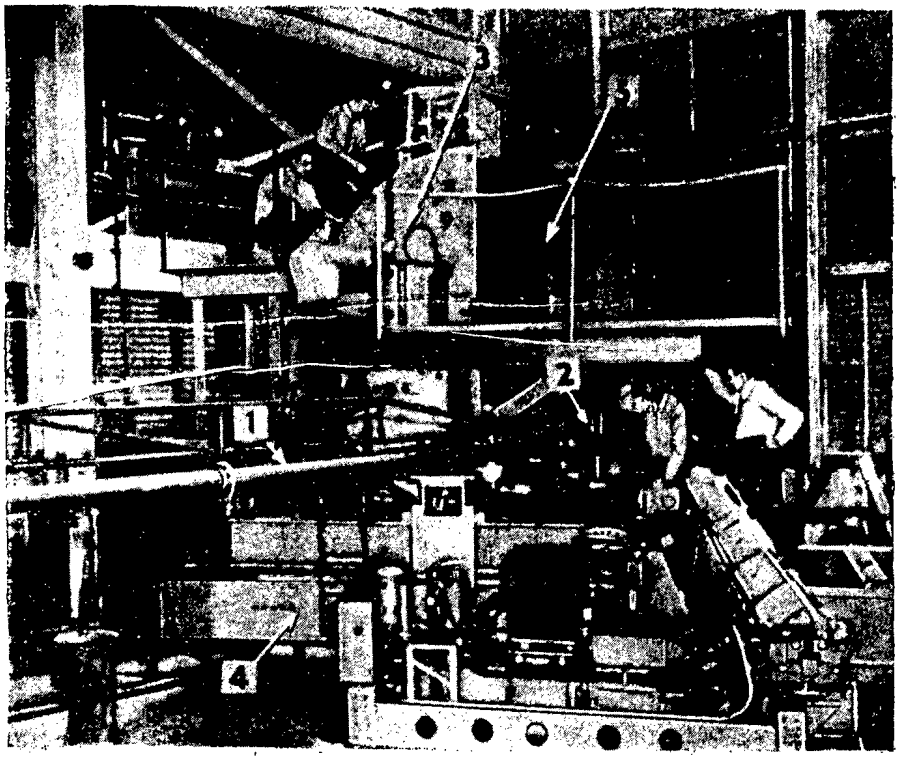

One of the first results of the work is the confirmation of the hypothesis that the density of nuclear matter decreases toward the surface of the nucleus.

* Aviation Week 64, No. 2 (1956).

NEUTRINO AND ANTINEUTRINO

The hypothesis as to the existence of a neutral particle, the neutrino, given off with the electron in β-decay, was made by Pauli in order to avoid the apparent contradiction of the laws of conservation of energy and momentum which are observed in the process of β-decay. A large number of works have been devoted to attempts to observe this particle. Indirect proof of the existence of the neutrino was furnished by experiments on the measurement of the recoil momenta of nuclei and electrons in radioactive decay. It seems that the process of interaction between the neutrino and the nucleus has been observed, namely reverse β-decay. At the present time there are some evaluations of the maximum value of the rest mass of the neutrino ($< \frac{1}{2000}$ electron mass) [1] and of its magnetic moment ($< 10^{-7}$ Bohr magnetons) [2].

The spin of the neutrino is $\frac{1}{2}$, and this particle can be described by the Dirac equation, putting $e = m = 0$. It follows from such a description that the antineutrino exists, in analogy with the case of the electron and positron. On the other hand, the description of the neutrino is possible by a modified equation, proposed by Majorana, which does not assume the existence of an anti-particle. It is possible to formulate β-theory almost equivalently for both cases, and the available data on β-decay does not afford the possibility of choosing between them.

In existing β-theory it is usual to suppose that together with an electron, an antineutrino (ν') is emitted, and that together with a positron, a neutrino (ν). In this case, the processes of β^+-decay, β^--decay, and K-capture can be written

$$n \longrightarrow p + e^- + \nu'; \qquad p \longrightarrow n + e^+ + \nu$$

$$\text{and } p + e^- \longrightarrow n + \nu$$

respectively. In addition the process $p + \nu' \longrightarrow n + e^+$ is possible, which is equivalent to the emission of a neutrino, but the processes

$$p + \nu \longrightarrow n + e^+ \text{ and } n + \nu' \longrightarrow p + e^-$$

are forbidden if the neutrino and antineutrino are not equivalent. This difference in the interaction of ν and ν' with nucleons makes possible the verification of existing theories.

The most direct recently performed experiment [3] consisted of an attempt to record the decay of Ar^{37}, whose occurrence could have been expected as a result of the reaction $Cl^{37}(\nu', e^-)Ar^{37}$ when chlorine is bombarded by the antineutrino current that comes from a reactor as a result of β-decay of the fission fragments. This reaction could take place only for the identity of the neutrino and the antineutrino. The experiment gave a negative result. The author did not find any Ar^{37} in the irradiated samples and evaluated the upper limit of the cross section for the $Cl^{37}(\nu', e^-)Ar^{37}$ reaction, which turned out to be $2 \cdot 10^{-42}$ cm^2/atom.

Another method for confirming the $\nu \equiv \nu'$ identity consists of observing double β-decay. Double β-decay is the process of simultaneous emission of two electrons from the nucleus (or two positrons) which either includes or does not include the emission of two neutrinos. If the neutrino and the antineutrino are not identical, then in double β-decay four particles are emitted: $2n \longrightarrow 2p + 2e^- + 2\nu'$. In this case the energy spectrum of the electrons is continuous, and the half-life is about 10^{21} years for a decay energy of about 2 Mev [4]. If the neutrino and the antineutrino are identical particles, then double β-decay can be considered as a two-stage process in which the neutrino emitted by one nucleon is captured by another:

$$n \longrightarrow p + e^- + \nu; \quad n + \nu \longrightarrow p + e^-.$$

For this type of decay process only two particles are emitted by the nucleus: $2n \longrightarrow 2p + 2e^-$. In this case the total energy of the two electrons is always constant and the half-life for decay is 10^{13}-10^{18} years [4]. Double β-decay is possible for nuclear isobars differing by two units of charge and having a mass difference greater than $2mc^2$. At the present time more than twenty such nuclei have been studied. Most of the experiments were to determine the half-life.

Within the limits of experimental error, no activity corresponding to double β-decay was found. Only the lower limits of the half-lives are quoted. The published results are for measurements on Sn^{124} ($T > 1.5 \cdot 10^{17}$ years); Zr^{96} ($T > 2 \cdot 10^{16}$ years)[5]; U^{238} ($T > 6 \cdot 10^{18}$ years)[6]; Mo^{100} ($T > 3 \cdot 10^{17}$ years); Cd^{116} ($T > 1 \cdot 10^{17}$ years); Cd^{106} ($T > 6 \cdot 10^{16}$ years); Mo^{92} ($T > 4 \cdot 10^{18}$ years) [7]. These results can be reconciled

with one and the other theory, although they favor decay with four emitted particles. A study of minerals whose composition includes Te^{130} was undertaken [8]. The amount of Xe^{130} in them was determined, since its presence could be explained by double β-decay of Te^{130}. The evaluation of the half-life of Te^{130} made in this work gives a value of about 10^{21} years. The resulting half-life cannot be assigned to double β-decay without the emission of a neutrino, since the theoretical calculation for this case gives less than 10^{18} years. On the other hand, it would seem to be impossible to say definitely that double β-decay had taken place in the given case with the emission of four particles, since there is reason to believe that the presence of Xe^{130} in minerals may be a result of ordinary β-decay.

In 1955 an article was published by McCarthy [9] in which, in addition to the determination of the half-life of Ca^{48}, an attempt was made to measure the total energy of the two electrons emitted in the decay of this nucleus.

The author recorded coincidences between particles having a total energy close to 4 Mev, which is in good agreement with the theoretical calculations of the energy of double β-decay of Ca^{48}. The half-life that was found was $1.6 \cdot 10^{17}$ years. This work, if it contains no experimental errors, speaks in favor of the existence of double β-decay without the emission of a neutrino. Recently, however, there has been published a communication on some work in which, essentially, McCarthy's experiment was repeated. With the aid of two scintillation counters of 4π-geometry, the radiation of Ca^{48} and Zr^{96} was recorded. The experiments were performed under conditions of very low background. The work did not verify McCarthy's results. The calculations of the lower limits of the half-lives of Ca^{48} and Zr^{96} that were made in this work are $2 \cdot 10^{18}$ and $0.5 \cdot 10^{18}$ years, respectively. These quantities are difficult to reconcile with the notion that double β-decay is a process taking place without the emission of a neutrino.

Thus the investigations that have taken place up to the present time would seem to indicate the impossibility of double β-decay without the emission of a neutrino, and allow us to reach the preliminary conclusion that the neutrino and the antineutrino are not identical particles.

V. R.

LITERATURE CITED

[1] Langer and Moffat, Phys. Rev. 88, 689 (1952).

[2] Cowan, Reines, Harrison, Phys. Rev. 96, 1294 (1954).

[3] Davis, Phys. Rev. 97, 766 (1955).

[4] Goeppert-Mayer, Phys. Rev. 48, 512 (1935); Primakoff, Phys. Rev. 85, 888 (1952); L. A. Sliv, J. Exptl.-Theoret. Phys. (USSR) 20, 1035 (1950).

[5] McCarthy, Phys. Rev. 90, 853 (1953).

[6] Levine, Ghiorso, Seaborg, Phys. Rev. 77, 296 (1950).

[7] Winter, Phys. Rev. 99, 88 (1955).

[8] Inghram and Reynolds, Phys. Rev. 78, 822 (1950).

[9] McCarthy, Phys. Rev. 97, 1234 (1955).

[10] M. Awschalom, Bull. Am. Phys. Soc. 1, No. 1, 31 (1956).

CYCLOTRONS WITH VARIABLE ENERGY OF THE ACCELERATED IONS

In fixed frequency cyclotrons it is possible to obtain high currents (of the order of a few milliamperes) of ions accelerated to significant energies. Therefore cyclotrons are widely used for the study of nuclear reactions, for obtaining radioactive isotopes, and as sources of fast neutrons. At the present time electrostatic generators, linear accelerators, and nuclear reactors have started to compete with cyclotrons. The cyclotron, however, if it fulfills some special demands, is still of great interest for physicists. Recently the cyclotron has found application as a source of neutron pulses for experiments based on time-of-flight measurements.

One of the basic demands made of the present cyclotron is the possibility of varying the energy of the accelerated ions continuously (or in small jumps). At the Geneva Conference on the Peaceful Uses of Atomic Energy, one of the papers of the USA delegation [1] told of two cyclotrons of variable ion energy, intended for the measurement of fast neutron cross sections. One of the cyclotrons, whose pole-piece diameter is 230 cm, is in the Livermore laboratory, and the second (pole-piece diameter 107 cm) is in the Los Alamos laboratory.

The Livermore cyclotron is intended for obtaining monoenergetic neutrons with energies from 2 to 30 Mev by means of the reactions T(p, n), D(d, n) and H(t, n). In this cyclotron protons can be accelerated to energies of from 2.6 to 14 Mev, deuterons from 5.2 to 12.5 Mev, and tritons from 7.7 to 18.3 Mev. In order to accelerate ions to such energies, the frequency of the electric field in the dees must be varied between the limits of 4.0-9.3 megacycles, and the magnetic field strength from 2600 to 8600 oersteds.

The Los Alamos cyclotron is intended for accelerating protons to from 3.5 to 9 Mev, deuterons from 7 to 17.5 Mev, and tritons from 10.5 to 12 Mev. The range of variation of the electric field frequency is 8.6-14 megacycles. The magnetic field strength changes from 5600 to 18,000 oersteds.

In both cyclotrons the magnetic field strength increases by a factor of more than 3 in going from the lowest energies to the highest.

In the Livermore cyclotron, as a result of the large diameter of the poles of the magnet, the maximum field strength is not very large (no larger than 9000 oersteds), and the curve of the decrease of the field in the whole range of variation changes only slightly, since saturation effects in the poles of the magnet and the covers of the chamber are insignificant. Small changes in the nonuniformity of the magnetic field (of the order of 0.2%) are compensated by the field of some auxiliary coils located on the magnetic pole pieces. The total drop in the field in the final orbits is 1%. As a result of the small diameter of the Los Alamos cyclotron the maximum field strength in it reaches 18,000 oersteds, that is, is in the region where the effects of saturation are strong. Therefore in the range from 5600 to 18,000 oersteds, it is impossible to achieve constant decrease of the magnetic field merely by choosing the correct shape of the pole pieces. The shape of the pole pieces in the Los Alamos cyclotron is chosen so as to obtain the desired drop only for the average values of the magnetic field strength. For large and small values of the field, the required form of the drop is achieved with the aid of correcting coils located inside the chamber. The coils make it possible to increase and decrease the field strength at large distances from the center of the magnet. The coils, consisting of five windings each, are mounted on the covers of the chamber at a distance of 45 cm from its center. The maximum current in the coils is $\pm$ 500 amps. The total drop of the field in the cyclotron is taken as 3.5% for all values of the magnetic field strength.

The Livermore and Los Alamos cyclotrons differ also in their manner of varying the electric field frequency in the dees. In the Livermore cyclotron the whole range of frequencies is covered in jumps of 55 kilocycles (composed of a hundred quartz crystals), as a result of which, the ion energy changes in corresponding steps. The capacity of the dees is regulated continuously within wide limits by the adjustment of grounded panels. The generator of the high-frequency field consists of a master oscillator and a power amplifier. In the Los Alamos cyclotron, the source of the high-frequency field is a self-excited generator. It is possible to change the frequency of this generator, and therefore also the ion energies, continuously.

Both of these cyclotrons are not yet being fully utilized. At the present time tests are being performed on the system for extracting the ion beam. A 60 cm cyclotron with variable ion energy is functioning at Rochester University [1 , 2]. In this cyclotron protons can be accelerated to energies of from 1.5 to 8 Mev, and α-particles and deuterons to 9 and 4.5 Mev, respectively. The proton current at the exit of the analyzing system is several times ten microamperes.

N. F.

LITERATURE CITED

[1] Thornton, Boyer, Peterson, Cyclotrons Intended for the Accurate Measurement of Fast Neutron Cross Sections. Paper No. 584 at the International Conference on the Peaceful Uses of Atomic Energy, Geneva, 1955.

[2] Fulbright, Bromley and Bruner, Phys. Rev. 99, No. 2, 654 (1955).

PLANS FOR A 10 BEV PROTON SYNCHROTRON OF SMALL DIMENSIONS

We note with interest the description of a new type of proton synchrotron, which, according to a communication by the Australian physicist M. L. Oliphant* "should be built in Canberra (Australia) in the course of the next three years", and which "will accelerate protons to energies greater than 10 Bev for relatively small dimensions and cost of the apparatus". The small size of the apparatus is achieved by using a magnet without an iron core, as well as by the possibility of creating a very high magnetic field strength in such a magnet. A homogeneous magnetic field is created inside a toroidal vacuum chamber with the aid of two systems of conductors which carry high currents in opposite directions. The diameter of the torus is 9 meters, and the diameter of the chamber is 22cm. The maximum induced magnetic field is 80,000 gauss, the attainment of which necessitates a current of 1.5 million amps in the windings.

For the achievement of such currents the use of a unipolar generator is proposed, which consists of a system of metal discs rotating in a constant magnetic field. A potential difference is established between the center of each disc and its periphery, under whose influence there arise damped oscillations in the circuit composed of the discs and the windings, causing the kinetic energy of the disc to swing over into the energy of an electromagnetic field and back.

A model was built to study the characteristics of the unipolar generator. A stainless steel disc of 60 cm diameter was rotated at a rate of 6000 rpm in a magnetic field of 18,000 gauss. Currents of 140,000 amps were achieved.

A generator of large dimensions with four discs of diameter about 3.5 meters and weighing 20 tons each is being constructed. The discs will be set into motion by a unipolar motor, that is, by passing a current (of 3000 amps) through the discs. The operating revolution rate, 900 rpm, will be reached in 10 minutes. This time will determine the frequency of repetition of the accelerator pulses.

Preliminary acceleration of the protons to energies of 8 Mev will be performed in a cyclotron with a pole-piece diameter of 65 cm. The accelerating system of the synchrotron will be a toroidal transformer with an iron core, analogous to that used in the Brookhaven cosmotron. The frequency of the accelerating high-frequency field changes in the course of one cycle of acceleration by a factor of eight.

It is hoped that the cost of the project will be comparable to the cost of a synchrocyclotron which can accelerate protons to energies less than 1 Bev. Such an economy became possible because of the sharp decrease in the frequency of repetition of the pulses. The proposal has not yet passed the stage of experimental verification.

P. K.

* Proc. Roy. Soc. (London) 234, 1199, 441 (1956).

THE CONSTRUCTION OF THE SECOND ENGLISH ATOMIC ELECTRIC POWER PLANT

The English program of construction of electric power plants for commercial electric power is based on two fundamental types of nuclear reactors: a thermal neutron reactor with graphite moderator and gas coolant, and a fast neutron reactor.

The first English atomic power plant (being built in Calder Hall) capable of producing 92 megawatts (later to be expanded to 184 megawatts), which is expected to be in operation by the end of 1956, will make use of a reactor with a graphite moderator and a gas coolant.* A few electric power plants of this type are to be built by 1965, with a total power output of 1200-1400 megawatts.

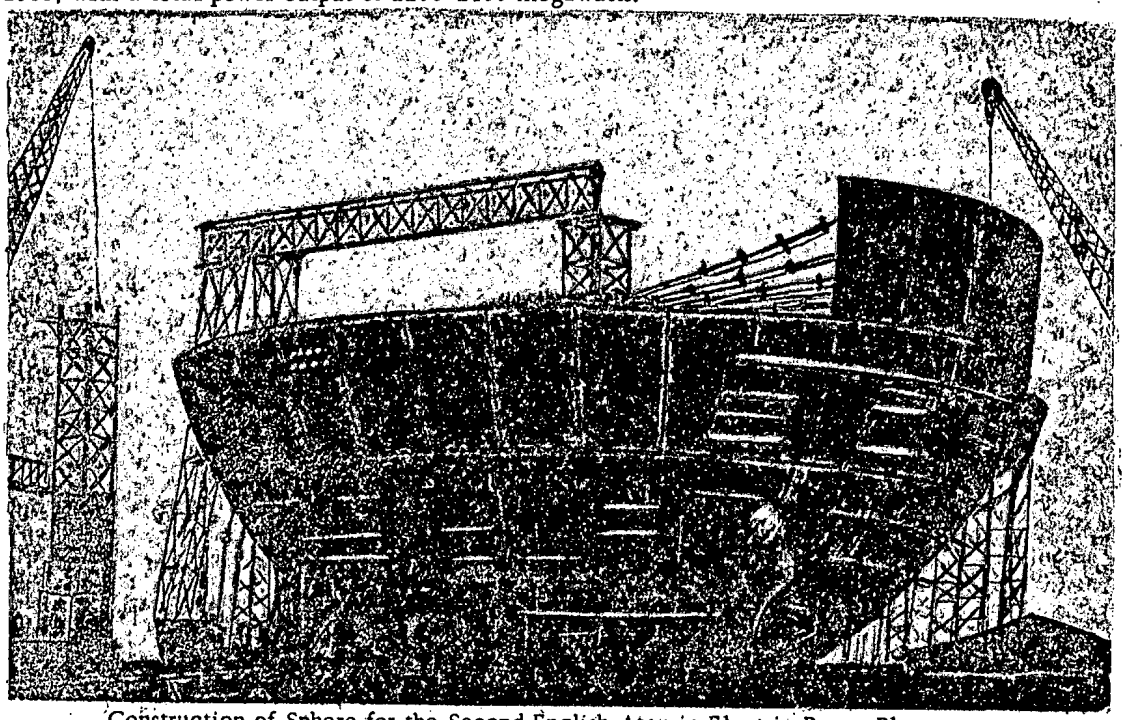

Construction of Sphere for the Second English Atomic Electric Power Plant.

The second English atomic electric power plant with a fast neutron reactor is being built by the United Kingdom Atomic Energy Authority in Downry on the northern coast of Scotland. The construction was begun early in March of 1955.

This power plant is actually an experimental one, and it was therefore designed so that in the process of construction and assembly separate details could be changed.

The projected thermal power of the reactor in Downry is 60 megawatts. There is so far no information regarding its electric power output, but we may assume that it will be of the order of 20 megawatts.

For safety, the reactor will be enclosed in a steel sphere 41.2 meters in diameter, with wall thickness about 2.5 cm. The sphere is calculated for an internal pressure of 1.3 atmospheres, which can arise in the

*See Atomic Energy 1956, No. 1, 106(T.p. 109) (T.p. = Consultants Bureau Translation pagination).

case of cessation of heat extraction from the installation, which in turn can lead to the vaporization of the sodium (used as the coolant) and burning of its vapors.

The sphere is now being assembled. The quality of the welding is being inspected by a radiographic method. Over 1500 meters of seams have already been inspected.

The total cost of the power plant is estimated at several million pounds sterling. It is expected that the cost of the electricity will be about one pence per kilowatt-hour.

In order to accumulate experience in its use, the Atomic Energy Authority is building a small model of the Downry reactor. The plans are to carry out, on this model, investigations of the processes of plutonium production, and to experiment with various coolants and special electromagnetic pumps.

The use of the reactor at Downry will make possible conclusions regarding the principles of the application of fast neutron reactors to the production of electric power on a commercial scale.

I. S.

LITERATURE

[1] Engineering 200, No. 5197, 330 (1955).

[2] Electrical Review 158, No. 1 (1956).

[3] A Programme of Nuclear Power. Her Majesty's Stationery Office, London (1955).

THE FIRST CANADIAN ATOMIC ELECTRIC POWER PLANT

At the Geneva Conference on the Peaceful Uses of Atomic Energy, the Canadian delegation reported on a project for an experimental power reactor (NPD) for an atomic electric power plant, which is to be constructed 150 miles to the northwest of Ottawa. The installation is being designed by the companies "Atomic Energy of Canada, Ltd.," "Canadian General Electric Company, Ltd.," and "Ontario Hydro."

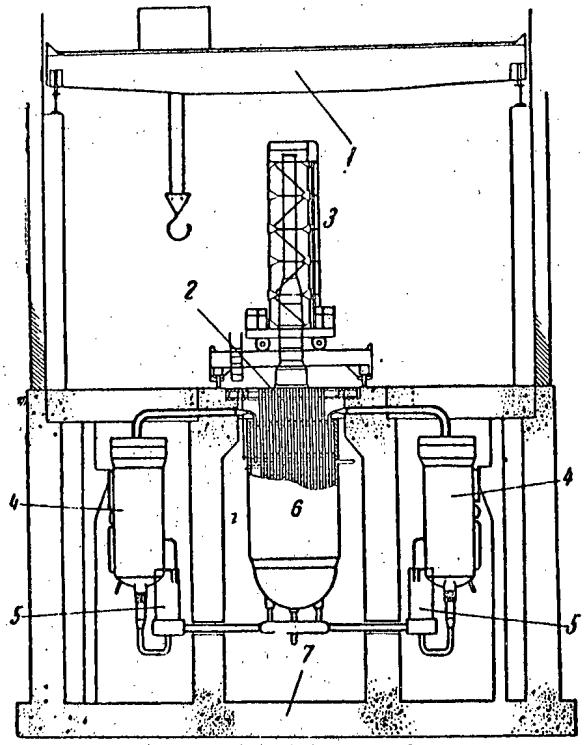

Figure 1. Cross section of the Canadian reactor NPD. 1) Traveling crane; 2) fuel ducts; 3) manipulator; 4) steam generator; 5) heavy water pump; 6) reactor; 7) concrete shielding.

In designing the reactor, a study was made of the economic characteristics of over sixty different types of reactors.

As a result the reactor chosen has the following characteristics:

Power	7.5-20 Mw
Reactor container	Pressure tank
Coolant	Heavy water
Moderator	Heavy water
Average moderator temperature	57°C
Reflector	Ordinary water
Coolant tube wall thickness	0.32 mm
Fuel elements	Tubular type
Thickness of zircalloy cladding	0.08 mm
Maximum heat flow	$1.63 \cdot 10^6$ kcal/m²/hr.
Maximum temperature of the fuel element cladding	288°C
Temperature of the primary coolant:	
at inlet	254°C
at outlet	274°C
Steam	Dry, saturated, at a temperature of 232°C and a pressure of 30 atmospheres.

The area taken up by the power plant has three zones, in which are located the reactor (with the steam generator and pumps), the reprocessing plant, and the turbogenerators. Next to the latter are located the transformers.

The generator is located in a pit which serves in part as the shielding for the steam generators. The reactor is reloaded with the aid of a manipulator. The active zone is enclosed in a cylindrical tank with a hemispherical bottom. The upper cover is composed of parallel tubes welded into steel plates, located one core lattice space apart. The tubes pass through the shielding and are closed at the top by special stoppers. Replacement of the heat producing elements, which are in the form of rods of natural uranium with zircalloy cladding, is performed with the stoppers removed.

The fuel element, located inside a zircalloy tube through which the coolant is intended to flow, is placed inside an aluminum tube outside of which is the moderator. The space between the zircalloy tube and the aluminum one is filled with helium, which functions as insulation between the coolant and the moderator.

The core is surrounded by a reflector of ordinary water. The water in the side reflector is in annular aluminum tubes, and that in the bottom reflector is in an aluminum tank. There is no reflector at the top.

Heavy water is used in the reactor in two circuits: that of the coolant, and that of the moderator. The coolant leaves the reactor and enters the steam generators, where its heat is given up and dry saturated steam is formed. The moderator flows through a special heat exchanger, where it is cooled by ordinary water. In the event of reactor shut-down, residual heat is carried off by natural circulation.

The NPD reactor is planned to operate without control rods. The reactor will be regulated by varying the amount of moderator in the system.

The total cost of the 20 megawatt power installation will be about 11 million dollars. According to the evaluation of Canadian economists, the cost of electric power will be about 0.7 cents per kwh.

Completion of the construction and start of operation of this atomic electric power plant is planned for 1958.

Simultaneously with the construction of this reactor, rough drafts are being suggested for the development of an electric power plant of 100 megawatts.

I. S.

LITERATURE

[1] Canadian Chemical Processing 39, No. 10, 61 (1955)

[2] Engineering Journal 38, No. 12, 1658 (1955).

FRENCH ATOMIC ELECTRIC POWER PLANT PROJECT

At the beginning of January, 1956, in Marcoule (department of Gard), G-1, the first two-purpose reactor in the country, was started. The energetic part of the reactor is to be turned on in July of 1956. The G-1 reactor is similar to the Brookhaven reactor (USA), and has gas cooling. The reactor is fueled by 100 tons of natural uranium, composed of 2700 heat producing rods. The moderator is graphite (1200 tons). The producing capacity of the reactor is about 13 kg of plutonium per year. The thermal power of the reactor is 40 megawatts, and the electric power output of its energetic part is 5 megawatts. The low efficiency of the heat cycle is explained by the relatively low temperature of the gas heat carrier on leaving the reactor (280°C). The reactor is not considered an atomic electric power plant, as the power expended on its own needs (mainly the electric supply to the gas blowers) is 8 megawatts. The experience gained in the design and use of this reactor will be applied to the construction of two more powerful reactors of the same type in Marcoule, intended to be the first French atomic electric power plant.

The atomic electric power plant project is being carried out by the Atomic Energy Commission (actually by its board for reactor study) simultaneously with the reactor facility of the company "Electricite de France" and some commercial concerns (The Alsace Machine Construction Company, the Crezo Company, the Rato Company, and others).

In each of the two reactors of the atomic electric power plant, 100 tons of natural uranium will be used as the fuel. The moderator is graphite, and the heat carrier, carbon dioxide. Standard equipment will be used in the turbogenerator part of the station.

The projected electric power output of the atomic power plant consisting of both reactors is 40,000 kilowatts, though the maximum electric power output from each of the reactors is about 30,000 kilowatts. In addition to electric power, the two reactors will produce about 100 kg of plutonium per year.

The plant is expected to start producing in 1957.

In the city of Cande, at the junction of the rivers Loire and Vienne, a second atomic electric power plant will be constructed, whose power output will be significantly greater than the output of the atomic electric power plant at Marcoule. The construction and exploitation of the new power plant are assigned to the research division of the company "Electricite de France."

I. S.

LITERATURE

[1] Economist No. 5864, 146 (1956).

[2] Machinery Lloyd 28, No. 1A, 82 (1956).

[3] Nucleonics 14, No. 2, 15 (1956).

THE SECOND AMERICAN ATOMIC SUBMARINE

"THE SEA WOLF"

On July 21, 1955, at Groton, Conn., the second American submarine with an atomic power plant, The Sea Wolf, was launched. The construction of this ship was carried out by the firm "Electric Boat Division of the General Dynamics Corporation."

The length of the ship is 97.5 meters, its diameter is 9.15 meters, and its displacement is 3260 tons. The under-water velocity of the ship will be greater than its surface velocity. The energy source is an intermediate velocity neutron reactor, constructed by the "General Electric Company". The fuel in the reactor is enriched uranium. The moderator is graphite, and the heat carrier is sodium. A prototype reactor had been constructed and studied in West Milton.

The US Atomic Energy Commission has made a contract with the firm "Combustion Engineering" for the design, construction, and extensive study of a reactor for a small atomic submarine. The firm of "Combustion Engineering" is the first firm that has been assigned all the work on the construction of a reactor.

The new program for the construction of submarines in the USA specifies the construction of a 4600 ton displacement submarine with two power plants that will be capable of developing a speed of 30 knots; in addition, two submarines with atomic power plants will be constructed of the types established by The Sea Wolf and The Nautilus, as well as three atomic submarines of 2300 tons displacement each.

I. S.

LITERATURE

[1] Engineer No. 5216, 63 (1955); No. 5218, 125 (1956).

[2] Catalogues of American firms issued at the Geneva Conference on the Peaceful Uses of Atomic Energy, 1955.

ATOMIC ENGINES FOR SHIPS

The problem of constructing atomic engines for transportation purposes is more difficult than that of stationary atomic energy installations. These difficulties are mainly connected with the limited weight and dimensions of the reactor shield. But the use of atomic engines for large ships encounters fewer difficulties because the dimensions of the vessels are relatively large.

One of the types of reactor designated for large ships is offered by the English firm of Rolls Royce. The types reactor is cooled by liquid sodium. A closed gas turbine cycle is used for the conversion of nuclear energy into electrical energy. Helium is used as working substance in the cycle, having the following advantages over air: 1) negligibly small neutron capture cross-section, and 2) greater heat conductivity.

The scheme of the cycle is shown in the diagram. Helium at temperature 21°C and pressure 15.4 atmospheres enters a low-pressure compressor and then goes through an intermediate cooler, from which it passes into a high-pressure compressor.

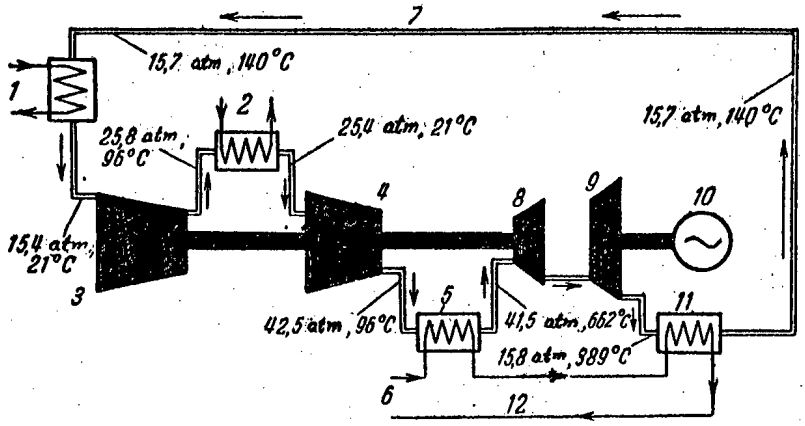

Diagram of working cycle of gas turbine power plant. 1) Preliminary cooling of gas; 2) intermediate cooling of gas; 3) low-pressure compressor; 4) high-pressure compressor; 6) to primary heat exchanger; 7) helium circuit of gas turbine with closed cycle; 8) turbine driving compressor; 9) low-pressure turbine; 10) load; 11) heat recoverer; 12) primary sodium circuit.

Compressed to 42.5 atmospheres at temperature 96°C, the helium is sent into the secondary heat exchanger. The temperature of the helium at the output of the heat exchanger is 662°C and its pressure is 41.6 atmospheres. The heated gas passes successively through two turbines: the turbine driving the compressor and a low-pressure turbine connected to the propellor shaft. 15,000 HP are delivered to the shaft.

The American shipbuilding firm "Newport News Shipbuilding and Dry Dock Company" together with the firm "Westinghouse Electric Corporation" has begun work on the systematic study of the possibility of applying atomic engines in large ships.

One of the projects of this firm is the ship "Atomic Mariner". In the project use is made of the hull and ship fittings of a freighter of type "C4-1A Mariner". The power plant of the ship consists of a turbogenerator of the type generally used in the newest freighters and a nuclear reactor of type "PWR".

The reactor uses enriched uranium in the shape of thin rods covered with zirconium. The system for removing heat consists of two circuits; water under pressure is used as heat transport medium and moderator.

Special attention has been given to the shielding of the reactor and the whole installation. Reduction of the weight of the shielding to a minimum permits an increase of useful load of the ship and makes the power plant more compact.

Calculations have shown that at the present time the installation of an atomic engine on a ship is not economically advantageous.

It may be hoped, however, that in the very near future it will be possible to obtain energy from nuclear engines at a price comparable with that of energy from ordinary engines.

I. S.

LITERATURE CITED

[1] Aeroplane No. 2321, 49 (1956).

[2] Engineer 201, No. 5219, 180 (1956).

[3] Catalogs of American firms.

[4] Engineering 108, No. 4691, 859 (1955).

SEMI-FACTORY INSTALLATION FOR THE EXTRACTION OF PLUTONIUM*

An experimental installation in Chatillon (France), designed for the treatment of heat-developing elements that have been irradiated in a reactor, is constructed in the form of vertically disposed cascades. The technological process of treatment is as follows:

1. The irradiated fuel elements, having first been cut into pieces, are put in a conical container into a tank for removal of their casings. Aluminum casings are treated with a concentrated solution of caustic soda, casings of aluminum-magnesium alloy with cold nitric acid.

2. The container with its contents is transferred into another tank, where the uranium is dissolved in boiling concentrated nitric acid; the oxides of nitrogen liberated here and also the radioactive gases (xenon and krypton) are passed through a cooling column of Raschig rings.

The oxides of nitrogen combine with oxygen and in the presence of water form nitric acid, and the xenon and krypton are caught in a special apparatus.

3. The solution of uranyl nitrate, containing plutonium and fission fragments, is poured into a tank, where by addition of acid and water the concentration is brought to 400 g /liter and that of acid to 1.8-2.0 molar.

4. The prepared solution passes through metering pumps into a set of extracting apparatuses, where it is treated with an organic solvent—tributyl phosphate diluted with kerosene containing paraffin hydrocarbons. In this operation more than 99.5% of the uranium and 99.5% of the plutonium are removed. Only small amounts of fission products get into the solvent: about 0.2% of the β-active and over 1% of the α-active fragments.

5. The uranium and plutonium extracted by the solvent are subjected to reextraction. The plutonium is reextracted by an aqueous solution of a recovering agent, the uranium by sodium carbonate. Of the γ-active products contained in the original solution 1/5 goes into the precipitated uranyl-carbonate complex; the plutonium and 4/5 of the active products remain in the water containing the recovering agent.

After completion of this operation the solvent is returned into the cycle.

6. The fission products contained in the dilute acid solution are subjected to 50-fold concentration by evaporation and are stored in stainless steel tanks. Before the evaporation the residual acidity of the solution is destroyed by adding formaldehyde while heating.

7. To concentrate it, the aqueous solution of plutonium is treated with caustic soda and centrifuged. This precipitates plutonium hydroxide, which is then dissolved in a small volume of nitric acid. By three successive precipitations the concentration of plutonium is increased 30 to 40-fold. The losses of plutonium in the mother liquor are not less than 0.5%.

In the experimental installation it is possible to regenerate 98% of the plutonium contained in the fuel elements. The final regeneration operations are carried out in the laboratory. The plutonium obtained contains not more than 0.2% of the active products.

The control of the work of the installation is achieved by means of a system of taking tests, and by level-meters, manometers, etc., which are observed through periscope arrangements.

V. P.

* Genie Chimique 74, No. 5, 129 (1955).

A NEW AGENT FOR THE ELUTION OF ACTINIDE ELEMENTS*

A new elution agent, ammonium α-hydroxy isobutyrate, makes possible the attaining of considerably more complete separation of the actinide elements than with amonium lactate. A typical curve of the elution of actinides is shown in the figure.

The improvements in the separation of the elements are quite obvious.

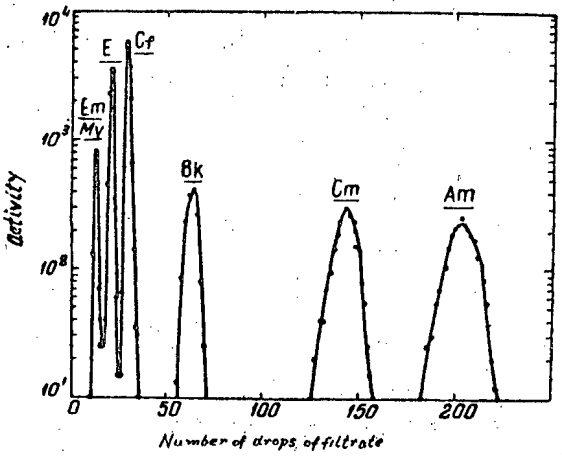

Elution of trivalent actinides from the resin Dowex-50 by a solution of ammonium α-hydroxy isobutyrate.

V. P.

* Journ. of Inorg. and Nuclear Chem. 2, No. 1, 66 (1956).

URANIUM-BEARING CONGLOMERATES OF THE BLIND RIVER REGION IN CANADA

Along the northern shore of Lake Huron, in a large area from Sault Sainte Marie to Sudbury, there are widely spread pre-Cambrian gold-bearing conglomerates. In 1953 it was established that they include uranium ores of commercial grade. The exceptionally favorable economy of the region (the presence of railroads and automobile roads, the nearness of large industrial and cultural centers, etc. encouraged a tremendous rush of prospectors and geological exploring parties of various companies, and the rapid settlement of the region. It is now regarded as one of the most promising uranium-bearing regions of Canada.

The uranium-bearing conglomerates are part of the Mississagi formation of lower proterozoic age, occuring discordantly on an archaic crystalline base. The Mississagi formation is basically made up of arkoses and separate sheets of argillites and conglomerates. Among the conglomerates two varieties are distinguished: the boulder and pebble types. The pebble conglomerates are the bearers of uranium ores; they consist of well-rolled quartz pebbles of diameter 3 to 5 cm and a cement of quartz, sericite, and biotite. The uranium-bearing strata are assigned in age to the lowest part of the formation.

The composition of the uranium ores is extremely complicated and rather unusual—the main uranium mineral is brannerite, but there are also encountered uraninite, pitchblende, thucholite, monazite, and hematite; in small quantities there occur zircon, rutile, magnetite, galena, chalcopyrite, pyrrhotine, and cobaltite; pyrites are widely distributed [3].

The ore-bearing strata have a sloping dip, and their thickness is 3-5 meters. The average uranium oxide content is found to be 0.10-0.14%. The length of the individual ore bodies is from one to two kilometers, and they have been followed along the dip by boring to 3 kilometers. Several beds have been found, the most promising being Pronto, Peach, Quirke Lake, Elliot Lake, and Nordic Lake, located near the town of Algoma.

The complicated composition of the ores has caused great difficulties in the technology of their exploitation. But at the present time there are several (indeed rather complicated) methods available, in particular the method of leaching with heat and pressure, a method of dry extraction by a stratification principle, applications of ultrasonics, and so on.

The explored ore reserves computed for Algoma County [5] amount to 30-50 million tons of ore, i.e., 30-50 thousand tons of uranium, and the total value of the reserves of uranium at Blind River are valued at 3 billion dollars [1]. The discovery of the Blind River uranium deposits was attended with a great clamor and the issuing of obviously exaggerated estimates, dictated by purely speculative considerations [2]. Still the great industrial importance of the deposits is scarcely open to doubt.

The uranium-bearing conglomerates of Blind River in Canada and of the Witwatersrand in South Africa appear to be analogous in many respects. But the Blind River conglomerates excel in the thickness of the ore bodies and the uranium content, while they contain less gold and require more complicated techniques for treating the ore [4].

The uranium ores in the Blind River conglomerates are ascribed by most geologists to the sedimentary (alluvial) type. But there are those who support the idea of a hydrothermal origin of these deposits.

The Blind River region is being strongly developed by industry. From the middle of 1955 more than ten large companies have entered on preparatory operations. Plans have been made for the construction of a number of enriching plants with productions from 2000 to 7000 tons of ore per day [2]. In September 1955 the first mine started operations, and it was proposed to start at once four others with total production 15,000 tons per day [5].

The Canadian government has concluded agreements with several companies that have acquired locations in Blind River, agreeing to purchase the entire production for the next six years. Up to the middle of 1955 the total amount involved in these contracts had reached 250 million dollars [2].

LITERATURE CITED

[1] The Mines Magazine 45, No. 9, 33 (1955).

[2] F. H. Strout, Mining Engineer, No. 5, 462-465 (1955).

[3] R. J. Trail, Canadian Mining Journal 75, No. 4, 63-68 (1954).

[4] P. E. Young, Western Miner and Oil Review 28, No. 11, 35-38 (1955).

[5] F. R. Joubin, Western Miner and Oil Review 28, No. 12, 74-75 (1955).

THE GOLD-URANIUM DEPOSITS IN SOUTH AFRICA

In the American scientific and technical journals much attention is being given to the gold-uranium deposits in South Africa. This interest is explained by the great importance which has during the last ten years, come to be attached to the securing of uranium from the gold mines of the Union of South Africa. The extraction of uranium is already carried on at 17 gold mines and will very soon be begun at 9 more. In the Union of South Africa uranium was obtained in 1953 to the value of 11 million dollars; in 1954 this increased to 41.5 million dollars, and there was a further increase in 1955 [1].

This interest is also due to the fact that the geological structure of the Witwatersrand deposits is very similar to that of the recently discovered large deposits of uranium at Blind River on the north shore of Lake Huron (Canada).

Although exploring work at this location is being carried on at a rapid pace, scientific data are slow in accumulating. Thus it is natural that any data on the geology, mineralogy, and origin of the Witwatersrand deposits that appear in the press are discussed with the most lively interest by American geologists.

During this research attention is given to the possibility of discovering uranium-bearing gold ores of the Witwatersrand type. Such deposits have been found not only in Canada (Blind River), but also in Brazil (Serra de Jacobina) [2].

According to the report of Davidson and Bowie (1951) [3] uraninite, with or without thucholite, is present in all the workable gold-bearing conglomerates of the Rand formation, locally called "reefs". The conglomerates lie in layers from Dominion Reef in the main Witwatersrand system to the upper parts of the Elsburg Reef strata and the Vetersdorp Contact Reef, i.e., over a range of more than 7500 meters. Many reefs unsuitable for exploitation for gold contain considerable amounts of uranium. Although there are still few data for determining the total reserves of uranium in the Witwatersrand basin, they are believed to be greater than in any uranium deposit under exploitation.

The origin of the gold ores of the Rand has long been the object of violent discussions. One group, mostly consisting of the specialists engaged in working the deposits, thinks that the gold and the conglomerates were deposited simultaneously (the theory of alluvial origin). Another group asserts that the gold was precipitated from hot gold-containing solutions that came up from below and deposited the metal in the porous conglomerates of the formation (the theory of hydrothermal origin). Davidson and Bowie (1951) [3] came to the conclusion that the gold and the uranium were deposited simultaneously and that any explanation of the origin of the deposits that can be applied for one of these metals will also be applicable for the other. This conclusion is mainly based on the data of many analyses, which have showed that the content of gold and of uranium varies in the same proportion.

The adherents of the theory of hydrothermal origin of the Witwatersrand deposits bring forward the following arguments to support their position:

—the uranium content in the Rand conglomerates is considerably larger than anywhere else in alluvial gold deposits;

—uraninite is not a mineral characteristic of alluvial deposits;

—it is known that in the vein deposits found in the Belgian Congo, Mexico, and Canada the gold and uraninite were laid down together by precipitation from hot solutions;

—the complex chemical composition of the uranium minerals in the rocks surrounding the Rand basin rules out the possibility of the alluvial introduction of the uranium in the form of uraninite;

—large quantities of pyrites and gold-bearing conglomerates are not characteristic of alluvial deposits;

—the absence from the conglomerates of the "black slick" (i.e., the heavy fraction of minerals, consisting of magnetite, ilmenite, etc.) characteristic of alluvial deposits;

–the relative rareness of gold nuggets; most of the gold in the conglomerates is in the form of grains of size 0.01-0.07 mm;

–the presence in the surrounding rocks of pyrite, galenite, sphalerite, chalcopyrite, chlorite, and sericite, characteristic of hydrothermal activity.

The theory of the alluvial origin of the Witwatersrand deposits received new support in the recently published work of the German geologist P. Ramdor [4]. His conclusions are founded on a careful study of a large number (about 140) of excellently prepared polished sections of specimens of Witwatersrand ore.

In evaluating the facts established by geologists during the study of the Witwatersrand deposit, Ramdor suggests that corrections be made for the influence of "pseudohydrothermal" effects, caused by subsequent magmatic activity, and also for the influence of radioactivity and of the enormous thickness (from 10 to 16 km) of the overlapping sediments.

Ramdor was able to find in the polished sections several types and varieties of pyrites, including alluvial pyrite. He concludes that the gold was alluvial in origin and was accompanied by several minerals typical of alluvial deposits, but was later recrystallized, as indicated by the relative rareness of nuggets. Ramdor has no doubt that the uraninite of the Rand entered the alluvial deposits together with the other components in the form of small rolled grains, which became concentrated in the lower parts of the reefs.

The interest of American geologists in the Witwatersrand is evidenced by the journey made in May 1955 by P. E. Young, manager of the firm "Pronto Uranium Mines" (one of the concerns engaged in the exploration and exploitation of the Blind River deposits) to South Africa, where he spent a month acquainting himself on the spot with geological conditions and the means of working the deposits.

He admits that the South African deposits of gold and uranium, occurring in conglomerates composed of quartz pebbles, are in many respects like the ore layers of the Blind River deposits. But, as Young remarks, the conditions for working the ores at Witwatersrand and at Blind River are dissimilar. The main differences are:

–the depth of mining operations in South Africa reaches 2100-2400 meters, while at Blind River workings are being considered to a depth of 900 meters;

–the average thickness of the ore layers in the Witwatersrand deposits does not exceed 1 meter, while in the Blind River deposits it is more than 2.5 meters, which makes necessary the use of other means of working the latter deposits;

–fifty years' experience in the work at the Witwatersrand makes it possible to establish rather accurately the quality of the ores, the amounts available, etc., by using the results of analyses of the cores from drill borings, distributed at distances about 1.5 km apart. In the Blind River region the borings must be made in a closer network. In the South African mines very powerful ventilation is required because of the enormous extent of the workings (their length reaches 10,000 km) and the high temperatures in the lower levels (for example, at a depth of 1800 meters the temperature reaches 45°C);

–the availability at the South African mines of cheap labor (approximately 1 dollar per day, of which about 50% is withheld for lodgings and food) causes the degree of mechanization of the work in the Witwatersrand mines to be much less than in the Blind River mines, where wages are much higher [1].

The extraction of gold from the Witwatersrand deposits has already been going on for about 70 years, so that many mines have gone out of existence, but the prospects of obtaining uranium has aroused these mines t a "second life" [1].

A. Z., E. G.

LITERATURE CITED

[1] P. E. Young, Western Miner and Oil Review 28, No. 11, 35 (1955).

[2] M. G. White, Uranium Deposits in the Serra de Jacobina (Brazil). Report No. 130 at the International Conference on the Peaceful Uses of Atomic Energy (Geneva, 1955); The Geology of Atomic Raw Materials, page 442, State Tech. Press, Moscow, 1956.

[3] P. F. Kerr, Deposits of Uranium and Thorium. Report No. 1114 at the International Conference on the Peaceful Uses of Atomic Energy (Geneva, 1955); The Geology of Atomic Raw Materials, page 129, State Tech. Press, Moscow, 1956.

[4] H. W. A. Sommerlatte, Mining Magazine 93, No. 3, 142 (1955).

THE APPLICATION OF COMBINED γ-RAY AND ELECTRICAL BORE-HOLE TESTING TO EXPLORATION OF URANIUM DEPOSITS*

The geophysical apparatus and methods used in exploration for oil can be used successfully for the exploration of uranium deposits. One of the variants of their use for seeking uranium is a combined simultaneous γ-ray and electrical resistance bore-hole testing. In the search for uranium on the Colorado Plateau the total length of borings made each year amounts to 1000 km.

The use of the combined test method makes it possible not only appreciably to speed up the testing of the cores, but also to cut the cost of the work by a factor of three or four. The sludge from exploratory borings can be tested by means of ordinary radiometers with scintillation or gas-filled counters, but the hole testing method gives considerably more valuable information about the rocks penetrated.

The curve of apparent resistances of the rocks penetrated, obtained by the electric testing method, makes it possible to compose reliable lithological sections of the bore-holes, contours, and the whole region. The γ-ray testing supplements these lithological data and characterizes the content of uranium and its decay products in the separate levels and strata of the section.

The use of the combined tests makes it possible to obtain maps and define on them the sections most promising for exploration for commercial uranium deposits.

A specially constructed testing outfit is used to carry out the simultaneous measurements. The electrical testing is done with a one-electrode (current) circuit, which assures a sufficiently good differentiation of the strata by the relative values of their apparent resistances.

The electrode current and the pulses from the gas-filled counter are brought from the sound in the bore-hole to the surface telemetrically by a one-strand testing cable. In the sound there are mounted a power pack, a vacuum-tube generator for resistance measurements, a monovibrator, and a Geiger counter; in the lower part of the sound is the current electrode. The circuit of the apparatus is insensitive to leakage and changes of length of the cable.

In the set of apparatus installed on the surface, the signals from the counter and the probe are separated, amplified, and fed to a two-channel register with tape recording. The power supply of the whole outfit is furnished by an engine-driven 110 volt 60 cycle generator. The gamma-radiometer has 10 scaling decades, assuring good linearity in the range 10-10,000 counter per second. According to the results of calibration with a Ra^{226} source, this range corresponds to an intensity of the order of 5000 microroentgens per hour. The radiometer has six time constants (from 0.5 sec to 16 sec), the choice between them being determined by the activity to be measured, the speed at which the test is run, and the stated size of the statistical error. The record on the tape is made to scales 1:10, 1:20, and 1:50. The sensitivity, stability, temperature characteristics, and mechanical durability of the outfit correspond to the requirements of measurements under field conditions. The winch has a cable of length about 600 meters and provides lowering and raising speeds from 0.6 to 30 meters per minute; in case of need the length of the cable can be increased up to 3000 meters. The whole outfit is handled by one operator, performing 6 to 10 test runs per day.

The determination of the U_3O_8 content is not made directly from the measured intensity because of the possible influence on the results of thorium and of disturbances of the Ra-U equilibrium. By the use of special calibrating devices the radiometric determinations of the uranium content can agree with chemical analyses within limits of 15-50%. For the calculation of the U_3O_8 content the true intensity is first determined by the formula

$$I = I_0 \; kd_c,$$

* Geophysics 20, No. 4, 841-859 (1955).

where I is the measured intensity in μr/hr., I_0 is the true intensity in μr/hr., k is a correction coefficient for the thickness of the layer, the speed of the run, and the time constant, and d_c is a correction coefficient for the diameter of the hole.

On the basis of measurements in standardized holes with saturated layers (thickness greater than 75 cm) of known content, a determination is made of the conversion coefficient C, which satisfies the equation

$$U_3O_8\ (\%) = CI_0.$$

Models of standardized holes have to be made from the ore of the given region, whose U_3O_8 content is determined by chemical analysis. For deposits in the state of Colorado a typical value of C is $1.9 \cdot 10^{-4}$ %/μr/hr.

The quantitative interpretation is carried out in the following way.

1. The trace from the register gives the thickness of the active stratum; the value taken is the distance between the points of inflexion of the curve of the anomaly. Strata of thickness less than 15 cm are not resolved, as the counters used in the sound are of this length.

2. The actual activity I_0 is found for the anomaly, and it is translated into μr/hr. by means of a calibration curve.

3. The U_3O_8 content is found, by using a conversion coefficient for the given type of ore.

On the basis of the register traces of resistance and γ-activity one can obtain a rather accurate treatment of the sections of the bore-holes.

From the results of the interpretation of these data there are also constructed maps of the activity and electrical conductivity for various stratigraphic horizons of the state of Utah.

L. P.

EXPLORATORY BORING FOR URANIUM*

The properties of the "Anaconda" company in the vicinity of Granta, New Mexico (USA) have rocks with physical properties suitable for drilling, and the thickness of alluvial deposits is not large; thus very effective drilling surveys for uranium have been possible in the limestone formations at Todilto and the sandstone formations at Entrada.

The exploration of the Morrison sandstone formation was complicated by the necessity of drilling through crevices at 90-120 meters, and because of the great brittleness of the rocks it was impossible to obtain cores from them.

In practice three kinds of drilling were used: diamond bit core-drilling, rotary drilling and impact chipping. The diamond drilling was used to outline the ore bodies and to make a detailed study of the lithological composition of the strata traversed and also of the moisture content. Rotary drilling was conducted in the layers of rocks of low moisture content and was usually accompanied by γ-ray and electrical testing. Chipping was used in limestones, but in places having quartz-bearing rocks this kind of drilling was replaced by the rotary type.

The monthly amount of rotary drilling was about 18,000 meters, and that of diamond-bit drilling was 3000 meters.

Records were made from the holes by choosing 10-50% of the cores from the diamond drilling or the sludge from the rotary drilling.

The use of γ-ray testing made it possible not only to pick out the places with anomalous radioactivity, but also to obtain lithological sections by comparing the γ-ray data with those from diamond-bit drilling.

It turned out in practice, however, that it is insufficient to outline the ore bodies by the γ-ray method alone.

In places where the strata were sloping, the holes were located 15 meters apart along contours traced parallel to each other every 30 meters.

Where the geological structure was more complicated, additional drillings were made along lines intersecting the contours.

In some cases the use of such a network was preceded by "wildcat" exploratory drilling, in which holes were drilled every 180-300 meters. In promising places these distances were reduced to 30-60 meters.

In outlining very short ore bodies in limestones additional holes were drilled near those passing through the ore body, at distances of 3-6 meters.

The results of drillings in promising locations were confirmed by mining operations.

Ore bodies in the form of vertically-placed chimneys filled with brecciated rocks containing ore were explored by drilling inclined holes, for example at Woodrow, Maine.

N. T.

* Mining Congress Journal 41, No. 12, 46-49 (1955).

A COUNTER FOR THE STUDY OF GAMMA-ACTIVITY IN THE HUMAN ORGANISM*

A counter for the measurement of small concentrations of γ-active isotopes in the human organism has been developed at the Los Alamos Laboratory (USA) . The sensitivity for isotopes emitting γ-quanta is $5 \cdot 10^{-10}$ curie for the object, when the mass of the object is of the order of 120 kg. In larger objects a concentration of the order of $3 \cdot 10^{-12}$ curie/kg can be detected. The sensitivity of the counter is high enough so that the natural isotope K^{40} (about 10^{-8} curie) can be measured with accuracy 5% in two minutes of counting.

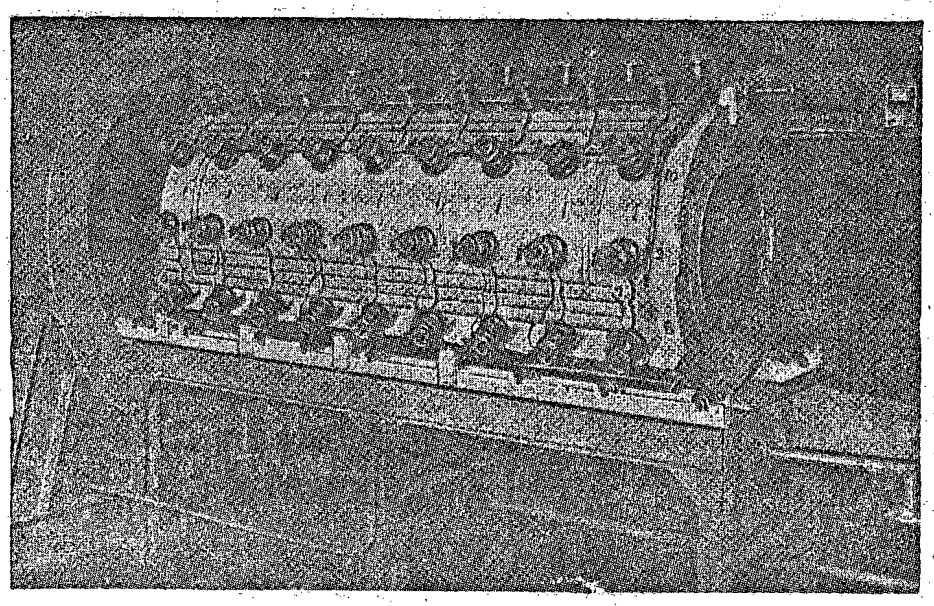

Fig. 1. Outside view of the counter without the lead shield.

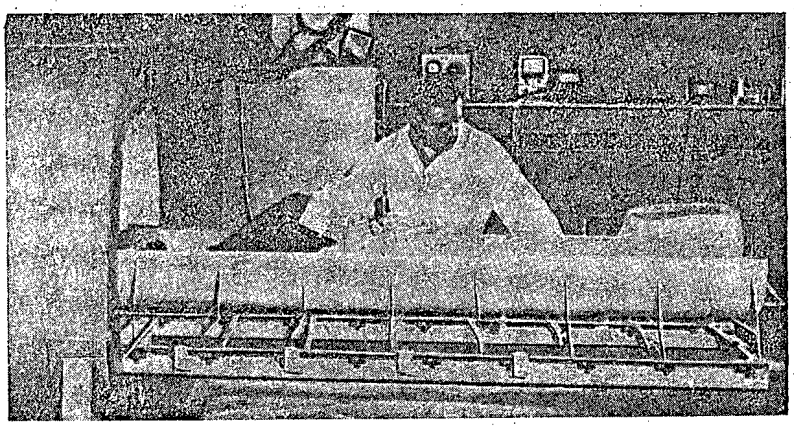

Fig. 2. General view of the counter. This picture shows the lead shield and the trough to hold the object to be tested, which can be moved inside the counter.

* E. C. Anderson, Nucleonics 14, No. 1, 26 (1956).

The counter consists of a cylindrical tank of volume about 500 liters, filled with a liquid scintillator. The scintillations are detected by 108 photomultipliers (12 rows of 9 tubes each). At the axis of the cylinder there is a cavity for the object. On the outside the counter is covered with a massive lead shield. The effective solid angle is close to 4π, and the efficiency does not depend on the position of the object.

The report gives a detailed description of the electrical circuit of the apparatus, and data obtained are presented with a statistical treatment.

A number of studies conducted with this apparatus are described:

1. An investigation of the level of natural radioactivity (K^{40}) of an individual, in relation to sex and age.

2. A study of the artificial radioactivity of the human body after exposure to slow neutrons. The counter makes it possible to detect the artificial activity resulting from the action of 0.3 R. E. P. of slow neutrons.

3. The determination of the contamination of personnel and food by γ-active substances. In the investigation of personnel the variability of the K^{40} content limits the precision of the measurement.

4. Study of the K content of the organism from the point of view of pathological chemistry and pathology.

5. A study of the retention of uranium fission products in the organism.

S. L.

AN UNDERWATER APPARATUS FOR THE HANDLING OF IRRADIATED FUEL ELEMENTS

Reports have appeared in American journals on practical tests of a special outfit for the mechanical handling under water of irradiated fuel elements.

The water assures the shielding of the operating personnel, the cooling of the fuel elements, and the safe removal of the chips from the cutting. A general view of the installation is shown in Fig. 1.

The underwater machine is placed at the bottom of a shaft 7.6 meters deep, constructed at the reactor testing station in Arco (state of Idaho, USA). The loading and unloading of the machine is carried out by means of an electrical travelling crane and manipulator, the control desk for which is seen at the left in the picture. The operator, who is at the other end of the crane bridge over the shaft, can observe the course of operations by means of a periscope, shown at the right in the picture as a column with its lower part of square cross section.

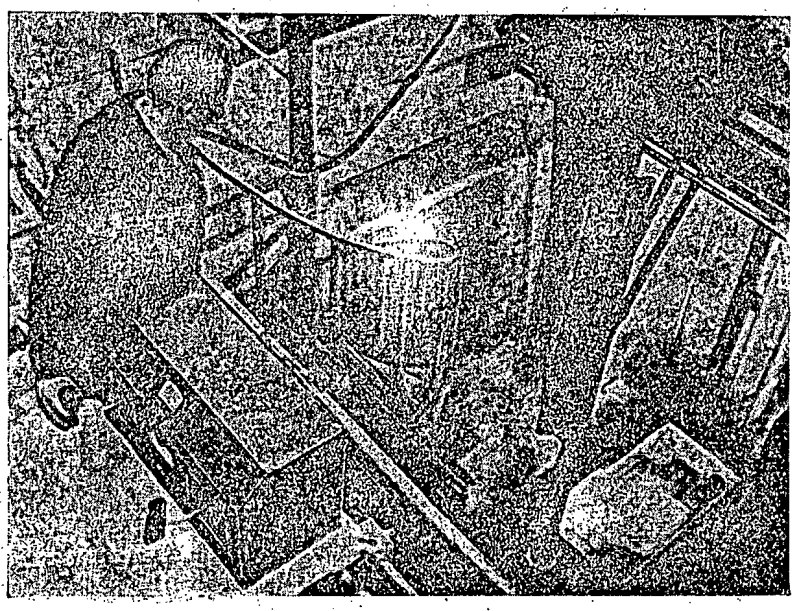

Fig. 1

In Fig. 2 the machine is shown in operation. At the right is the manipulator. The control cables (in center at rear) go to the control desk, which is placed on the floor at the edge of the shaft. By means of these cables one can bring about motions of the material being treated in both vertical and horizontal directions. A shaft driven by a 1.5 horsepower variable-speed motor actuates a worm gear that delivers the fuel elements to the cutter, located below at the right. On the control desk there are devices showing the positions of the fuel elements and the cutter to an accuracy of a few thousandths of a centimeter. Here are also installed the regulators for the length of the cut.

Figure 3 shows the machine without its side and top covers. Alongside the control cables there pass four tubes, two of which deliver water to the hydraulic presses; the other two, of larger diameter, serve to circulate the water removing the chips, at the rate of 760 liters per minute. The water from the jacket around the machine first passes through a screen to catch the chips, and then through a microporous filter which cleans it more thoroughly. After cleaning, the water again enters the machine. Thus there is no intermixing of the water removing the chips with the water in the shaft.

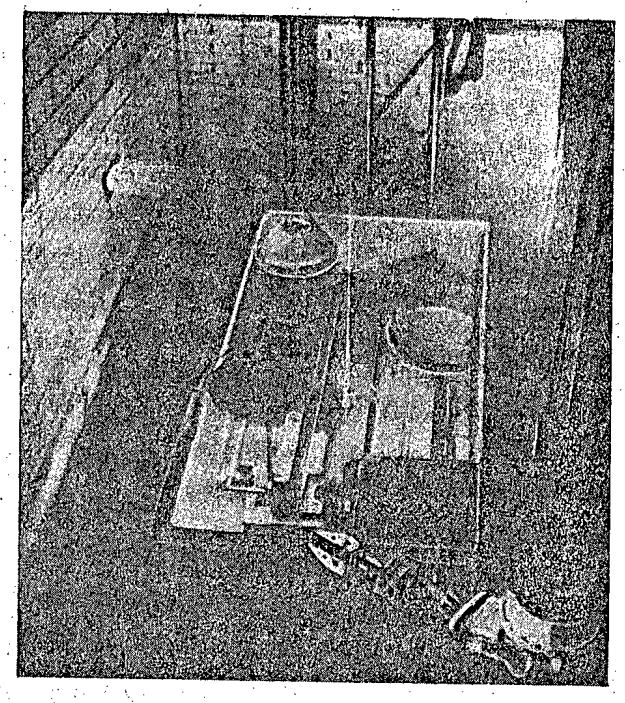

Fig. 2.

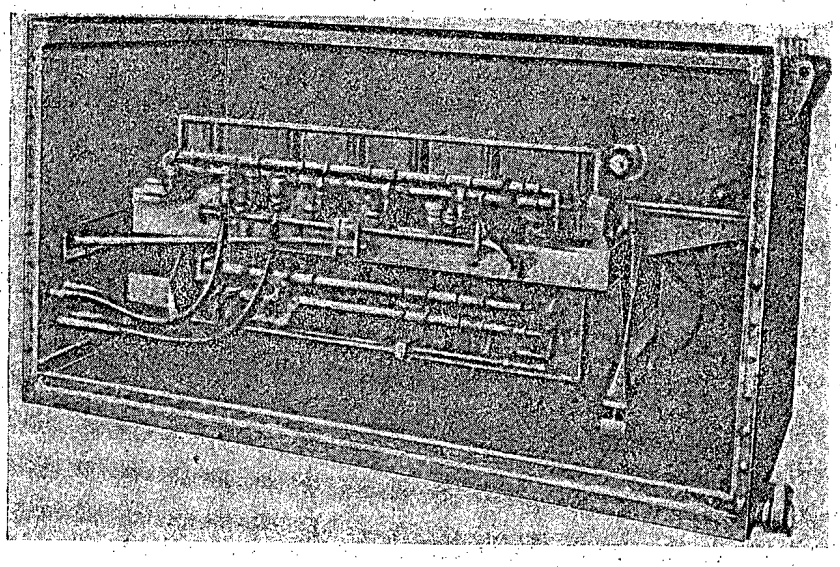

Fig. 3.

During the time that the machine is under water, compressed air is fed into the motor casing to keep water from getting into it.

V. S.-i.

LITERATURE CITED

[1] Electrical Journal 155, No. 6, 460 (1955).

[2] American Machinist 99, No. 17, 110 (1955).

BIBLIOGRAPHY

BOOK REVIEW

I. S. Glazunov, P. D. Gorizontov, D. I. Zakutinsky , I. I. Ivanov, A. A. Kanarevskaya, N. A. Kraevsky, N. A. Kurshakov, A. V. Lebedinsky, V. N. Petyshkov, and Yu. M. Shtukkenberg. Radiation Medicine. A Guide for Physicians and Students. Edited by Corresponding Member of the Academy of Medical Sciences, Professor A. V. Lebedinsky. Medical Press, Moscow, 1955.

In the handbook under consideration there are presented in detail (as far as permitted by the size of the book) current conceptions of the pathogenesis; clinical behavior, diagnostics, and treatment of radiation disease. The pathological anatomy of radiation sickness is fully described, and there are set forth in detail the clinical and laboratory methods for diagnosing the disease which it is necessary for the practicing physician to know. Almost a quarter of the book is devoted to questions of physics: the nature of ionizing radiations, their interaction with matter, and also methods of detecting and measuring radiations (dosimetry). The inclusion in the book of detailed information from the field of physics is extremely valuable, since without a knowledge of physical laws it is impossible either to understand the mechanism of action of radiation on the human organism or to correctly diagnose and treat radiation sickness.

Along with the results of their own investigations the authors of the basic chapters have made rather wide use of the data of Soviet and foreign radiological literature. In their treatment of the pathogenesis of radiation disease the authors have started with the materialistic ideas about the organism as a single whole, a fact that favorably distinguishes the present handbook from analogous works of foreign scholars, where the basic emphasis in the analysis of radiation disease is placed on the study of local processes in the cells and tissues (for example, the many-volume handbook on radiobiology published in the USA in 1954).

At the same time it must be admitted that the handbook "Radiation Medicine" has a number of essential inadequacies.

The basic defect is the absence of a clearly unified plan of presentation of the material. The handbook is too much like a collection of papers of different authors. If some chapters ("The Physics and Dosimetry of Penetrating Radiations", "Pathological Physiology of Radiation Sicknesses", "Radiation Burns", "Pathological Anatomy of Radiation Sickness") give a clear presentation of the subject being discussed, still other chapters, like "Primary Laws of Radiation Disease", "Toxicology of Radioactive Substances" are carelessly written and often leave the reader in a blind alley through the disorderliness and superficiality of the presentation.

Thus, the sections of Chapter IV devoted to the dependence of the action of radioactive substances on their physicochemical properties, ways the substances enter the body, and their distribution in and elimination from the body do not contain many elementary facts about these matters.

In the chapters "Clinical Nature and Treatment of Radiation Sickness" and "Clinico-laboratory Methods of Diagnosis of Radiation Disease" there are many inaccuracies, a number of assertions are made without sufficient basis in the test, and some of the assertions are untrue and disorient the reader.

In Chapter V the definition of radiation disease is given in an extremely rambling fashion. In the description of severe symptoms, such as brain hemorrhages threatening anemia, it is not pointed out that they are observed only in very severe cases of the disease.

In the description of chronic radiation sickness there is no mention of its characteristic peculiarity: its cyclic, wave-like course. Nothing is said about the remote consequences of radiation disease, although there are such data in the literature.

In Chapter VII the author speaks several times about the toxicity of uranium, without mentioning a word about the fact that this toxicity is due to its chemical properties, and not at all to its radioactivity. The inclusion of uranium for its toxic properties in the group of radioactive substances gives rise to misunderstanding.

The lack of a unified plan is also apparent through the occasional ocurrence in chapters written by different authors of contradictions not discussed in the text. Thus, for example, on page 242 we read: "During the period of open manifestations . . . an increase of γ-globulins is observed", which contradicts the data presented on page 108: " . . . after irradiation . . . there occurs . . . an increase of α- and β-globulins; the γ-globulins remain unchanged". A disagreement between data is not rare in science but in a handbook such disagreements must be explained or at least discussed. Furthermore, on page 93 this formulation appears: "As was shown above, the process of ionization of water is of the greatest significance". But in Chapter II, devoted to the primary mechanisms of the biological action, while the author does describe in detail the process of ionization of the aqueous medium of the organism, he still takes as the basic pathogenetic mechanism of radiation disease the direct damage to definite protein structures by the ionizing radiation.

A number of questions are clearly inadequately elucidated in this handbook. As was pointed out above, the chapter on the primary mechanisms of bilogical action of radiation is carelessly written, and the reader gets no distinct conception of the possible courses of realization of the primary effect of ionization in living substance; the chapter ought to be broadened and more illustrations with factual data should be used.

Little is said about the dependence of biological effects on the type of radiation, the dose, and the degree of penetration. The biological classification of doses is not given (maximum allowable, pathogenic, fatal, etc.).

In the chapter "Toxicology of Radioactive Substances" there is no clear statement of the peculiarities of the radiation sickness that arises from the entrance of radioactive substances into the organism, of its resemblance to and differences from the sickness caused by external irradiation.

Quite inexplicable is the absence from the chapter "Clinical Nature and Treatment of Radiation Sickness" of a section devoted to the treatment of chronic radiation sickness. The concluding remark that "treatment must be carried on in accordance with general clinical indications" gives the physician nothing toward an understanding of the principles lying at the basis of the therapy of chronic radiation sickness and of the concrete therapeutic measures necessary in such cases.

In their exposition of the pathogenesis and clinical behavior of radiation disease the authors give great attention to changes in the role of the central nervous system. At the same time, in the description of diagnostic methods not a word is said about the diagnosis of changes of the nervous system.

An extraordinarily serious reproach must be laid at the door of the Medical Press, which has issued a book with a large number of misprints and mistakes, often distorting the meaning of the text. The 64 misprints noted in the text are only an insignificant fraction of what there are.

The inadequacies that have been enumerated undoubtedly decrease the value of a much needed, useful, and correctly conceived first Soviet handbook on medical radiology. It is to be hoped that in a second edition the authors will take into account these critical remarks and eliminate the essential inadequacies that have been allowed to get into the book now reviewed.

S. L.

NEW LITERATURE ON QUESTIONS OF THE PEACEFUL USE OF ATOMIC ENERGY

B O O K S

Academy of Sciences of the Ukrainian SSR, Session devoted to questions of the use of atomic energy for peaceful purposes, 1956, Theses of the reports, Kiev, Acad. Sci. Ukrain. SSR Press, 1956, 195 pp., no price.

All-Union Conference on Medical Radiology, Moscow, 1956, Theses of plenary reports, Board of editors: A. V. Lebedinsky (editor in chief) and others, Medical Press, 1956, 40 pp., no price.

All-Union Industrial Exposition, Moscow, 1956, Exposition on the Uses of Atomic Energy for Peaceful Purposes (exhibits), Moscow, 1956, 106 pp., 4 rubles 50 kopecks.

Application of the Method of Marked Atoms in Chemistry, Collection of shortened translations and surveys of foreign periodical literature, V. G. Vasilyev (ed.), For. Lit. Press, 1955, 372 pp., 17 rubles 55 kopecks.

Balabanov, E. M., Nuclear Reactors, Lecture, "Knowledge" Press, 1955, 40 pp., 60 kopecks.

Beys, A. A., Beryllium, Evaluation of deposits in prospecting and exploring, State Technical Press, 1956, 148 pp., 4 rubles 85 kopecks.

Bibergal, A. V. and others, Protection from Roentgen and Gamma Rays, K. K. Aglintsev (ed.), Medical Press, 1955, 246 pp., 11 rubles 20 kopecks.

Conference on Nuclear Spectroscopy, Theses of the reports of the 6th annual conference on nuclear spectroscopy in Moscow, January 26-30, 1956, Acad. Sci. USSR Press, 1956, 36 pp., no price.

Dyachenko, P. E., Radioactive Isotopes in Machine Construction (Popular Science series), Acad. of Sci. USSR Press, 1956, 52 pp., 80 kopecks.

Dorfman, Ya. G., History of the Rise of Contemporary Nuclear Physics, All-Union Society for the Propagation of Political and Scientific Knowledge, Leningrad section, Leningrad, 1955, 24 pp., 70 kopecks.

Glazunov, I. S. and others, Radiation Medicine, Handbook for Physicians and Students, A. V. Lebedinsky (ed.), Medical Press, 1955, 282 pp., 7 rubles 80 kopecks.

Goldanski, B. I., Nuclear Reactions and Methods for Producing Them, "Knowledge" Press, 1955, 40 pp., 60 kopecks.

Grodzensky, D. E., Radioactive Isotopes in Biology and Medicine, "Knowledge" Press, 1955, 40 pp., 60 kopecks.

Kashin, N. V., Course of Physics, Volume 3, Optics and Atomic Physics, Instructional Press, 1956, 507 pp., 9 rubles 35 kopecks.

Kondratyev, V. N., Scientific Results of the International Conference on the Peaceful Uses of Atomic Energy (Geneva, August 8-20, 1955), Stenographic reports of public lectures, "Knowledge" Press, 1956, 32 pp., 60 kopecks.

Livingston, M., Accelerators, Apparatus for Producing High-energy Charged Particles, Introduction by M. S. Rabinovich (ed.), For. Lit. Press, 1956, 148 pp., 8 rubles 15 kopecks (translation).

Lukyanov, S. Yu., Basic Concepts of Experimental Nuclear Physics, "Knowledge" Press, 1955, 40 pp., 60 kopecks.

Nuclear Theory of the Development of the Earth's Core and Problems of the Geology and Geography of Central Asia, Collection of papers, Editorial board: Active Member of the Academy of Sciences of the Uzbek SSR, Prof. Kh. M. Abdulaev and others, Tashkent, Acad. Sci. Uzbek SSR Press, 1955, 188 pp., 15 rubles 80 kopecks.

The Primary Cosmic Radiation, Its Composition and Variations in Intensity, and the Problems of its Origin, Collection of papers, G. B. Zhdanov and M. I. Fradkin (eds.), For. Lit. Press, 1956, 304 pp., 18 rubles 65 kopecks (translation).

Shcherbakov, L. M., Atomic Energy in the Service of Man, 2nd edition corrected and enlarged, Tula, Book Press, 1956, 56 pp., 90 kopecks.

Starikin, Yu. A., Atomic Energy and Its Application, Novosibirsk, Book Press, 1955, 40 pp., 65 kopecks.

Syrnev, V. P. and Petrov, N. P., Radioactive Radiations and their Measurement, Military Press, 1956, 160 pp., 1 ruble 75 kopecks.

ARTICLES IN JOURNALS

Agishev, E. I. and Ionov, N. I., "A Pulsed Mass Spectroscope," J. Tech. Phys. (USSR) XXV, 1 (1956).

Alpers, V. V., "Nuclear Particles in Photographic Emulsion, Use of pulsed chambers in nuclear investigations," Nature (USSR) 1 (1956).

Badanova, K. A., "Influence of Heavy Water on Plants," Plant Physiol. 3, 1 (1956).

Balashko, Yu. G. and others "Methods of Determining Radium in the Human Organism," Hyg. and Sanit. 1 (1956).

Blazevits, A. and Judson, B., "Purification of Gases Containing Radioactive Aerosols by Fiber-glass Filters," Chemistry and Chemical Technology, (Translations from foreign periodical literature) 2 (1956).

Blok, V., "Microdistillation Apparatus for the Fractionation of Very Small Quantities of Radioactive Liquids, Chemistry and Chemical Technology, (Translations from foreign periodical literature) 2 (1956).

Borisov, V. T. and Golikov, V. M., "On the Theory of the Radiographic Method for Measuring Diffusion Coefficients," Factory Lab. 2 (1956).

Charlesby, A., "Destruction of Celluloses under the Action of Ionizing Radiation," Chemistry and Chemical Technology (Translations from foreign periodical literature) 2 (1956).

Chitkhem, "Application of Rare-Earth Elements in Production," Problems of Contemporary Metallurgy (Collections of surveys and translations) 1, (1956).

Dmitrachenko, V. M., "A Portable Indicator of Radioactive Radiations," Tech. of Meas. 1 (1956).

Dobrolyuskaya, T. S., "Composition of the Center of Luminescence of a Sodium Fluoride Bead Activated by Uranium," J. Anal. Chem. XI, 1 (1956).

"Extraction and Study of Rare-Metals and Their Compounds," (from the foreign literature), Prog. of Chem. XXV, 1 (1956).

Frank, G. M. and others, "The Radiograph—a Universal Nonlinear Integrating Apparatus for Studies During Life by Means of Radioactive Isotopes," Bull. Exptl.-Biol. and Med. 41, 1 (1956).

Gorodinsky, S. M., "Questions of Individual Shielding in Work with Exposed Radioactive Substances," Hyg. and Sanit. 1 (1956).

Goroshko, V. D., "Application of Radioactive Methods in Processes for Enriching Coals," Herald Acad. Sci. USSR 2 (1956).

Gryzin, P. L. and Zemsky, S. V., "Investigation of the Wear of the Refractory Lining of Metallurgical Furnaces by Means of Radioactive Isotopes," Factory Lab. 2 (1956).

Iordan, G. G., "Use of the Radiation of Radioisotopes for the Control of Technological Processes," Apparatus Construction 1 (1956).

Ivanovskaya, I. L. and Novikov, A. G., "A Large Rectangular Wilson Chamber," J. Tech. Phys. (USSR) XXVI, 1 (1956).

Johnson, O., "Germanium and its Compounds," Prog. of Chem. XXV, 1, (1956).

Kornev, Yu. V., "Radioactive Isotopes in Metallurgy," Metallurgist 1 (1956).

Kursanov, A., "Radioactive Elements and the Study of Plant Life," Science and Life 1 (1956).

Lavrenkova, A., "Search and Discovery, On the Finding of the Missing Elements in the Mendeleev Table by Means of Nuclear Reactions," Knowledge Is Power 1 (1956).

Loorts and Beber, "Study of the Melting Process in a Blast Furnace by Means of Radioactive Isotopes," Problems of Contemporary Metallurgy (Collections of surveys and translations) 1 (1956).

Matveev, A. S. and others, "A Radioactive Relay Without Contacts,"Apparatus Construction 1 (1956).

Mikhailov, Ya., "Radioactive Fertilizers," Science and Life 1 (1956).

Obolentsev, R. D. and others "Chromatographic Separation of Isomeric Sulfur-organic Compounds $C_8H_{18}S$ with the Use of Radiosulfur," Doklady Akad. Nauk SSSR 106, 2 (1956).

Proskurnin, M. A., "Radiation Chemistry,"Science and Life 2 (1956).

"Scientific and Technical Conference on the Application of Radioactive Isotopes in the Coal and Mining Industries, Leningrad, January 1956," Coal 2 (1956).

Shifrin, F. Sh., "The Connection Between Electronic Energy Levels and Interatomic Distances in Molecules," Doklady Akad. Nauk. SSSR 106, 2 (1956).

Shteinbok, N. I., "On the Problem of the Principle of Action of Alpha-ionization Gas Analyzers, J. Tech. Phys. (USSR) XXVI, 1 (1956).

Smirnov, V. F., "On Some Possible Applications of Radioactive Isotopes in the Coal Industry," Coal 2 and 3 (1956).

Sulkin, A. G., "Industrial Gamma-ray Apparatus for Radiation Inspection of Materials," Bull. Tech-Econ. Inform. 2 (1956).

Voskresenskaya, N. I. and Grishina, G. S., "On the Question of the Utilization of $C^{14}O_2$ by Plants under Various Conditions of Illumination," Doklady Akad. Nauk. SSSR 106, 3 (1956).

Zhinkin, L. N. and Gracheva, N. D., "Study of the Absorption of P^{32} and S^{35} in the Epithelium of the Tongue and Small Intestine by an Autoradiographic Method," Doklady Akad. Nauk. SSSR 106, 3 (1956).

ERRATA

In the Soviet Journal of Atomic Energy, No. 1, the following typographical mistakes in the original journal were not corrected in the C.B. English translation

Page	Reads	Should read
105 Figure caption	10 kw	100 kw
105 6 lines from top	10 kw	100 kw
105 7 lines from top	100 kw	150 kw
105 7 lines from top	100 mm	500 mm

CONTENTS